Molecular and Neurochemical Effects of Methylphenidate on the Developing Brain

Emmanuel Quansah

January 2017

Department of Pharmacology

School of Pharmacy

De Montfort University

Leicester, LE1 9BH

United Kingdom

Molecular and Neurochemical Effects of Methylphenidate on the Developing Brain

Emmanuel Quansah

Thesis submitted in partial fulfilment of the requirements for the degree of Doctor of Philosophy.

January 2017

Thesis conducted under the supervision of Dr. **Tyra S. C. Zetterström**, first supervisor; and Prof. Bob Chaudhury and Dr. Benjamin S. Gronier, second supervisors.

Department of Pharmacology

School of Pharmacy

De Montfort University

Leicester, LE1 9BH

United Kingdom

ABSTRACT

Attention deficit hyperactivity disorder (ADHD) affects 2.6-4.5% of the worlds population, with affected children often performing poorly at school. The catecholamine hypothesis of ADHD proposes that the disorder results from a hypofunction of the fronto-striato-cerebellar catecholaminergic (i.e. dopaminergic and noradrenergic) system. However, abnormalities in the glutamatergic and GABAergic systems have also been implicated in the symptoms of ADHD. In addition, previous reports indicate that a deviation from the common pattern of cerebral lateralisation also contribute to some of the symptoms of ADHD, with under-activation of the right prefrontal and right parietal cortices observed in ADHD patients. The psychostimulant, methylphenidate (MPH) is the preferred drug for the treatment of the disorder, however the long-term consequences of the drug are not yet established. Here, we have investigated the effects of acute and chronic MPH treatment on monoaminergic protein markers, genes and their corresponding proteins involved in synaptic plasticity, as well as the drug's effect on metabolic pathways. The investigations were conducted on brain regions implicated in the symptoms of ADHD in adolescent rats.

Our data shows in Chapter 3 that MPH increases whole tissue and extracellular dopamine levels in the frontal cortex and striatum. Interestingly, this effect was more prominent in the left sides of these brain areas. Chronic MPH treatment also upregulated dopamine (DAT) and noradrenaline (NET) transporters in the striatum and the nucleus accumbens, an effect that could limit the long-term effectiveness of the drug, as larger doses may be required to reach a functional blockade of the upregulated transporters and achieve clinical efficacy. In addition, chronic MPH but not acute treatment increased protein expression of the: vesicular monoamine transporter (VMAT2),

dopamine D1 receptor, and the catecholamine rate-limiting enzyme tyrosine hydroxylase (TH), in most of the examined brain areas.

By using proton nuclear magnetic resonance (^{1}H-NMR) spectroscopy, this thesis also shows that acute MPH enhances the levels of the large neutral amino acids (LNAAs), tyrosine and phenylalanine in the cerebrum (Chapter 4). In Chapter 5 the thesis further demonstrates that chronic but not acute MPH treatment increases the levels of tyrosine and phenylalanine in the frontal cortex, while also decreasing the levels of these LNAAs in the plasma, suggesting that the drug increases the transport of the these two LNAAs from the plasma into parts of the brain. Given that these two LNAAs are precursors of dopamine synthesis, their enhanced levels following MPH treatment in the frontal cortex but not the striatum (no significant increase of tyrosine or phenylalanine in striatum) this finding might contribute to the elevated cortical levels of dopamine as shown in Chapter 3. This novel finding has resulted in our hypothesis that MPH may alleviate ADHD symptoms in two ways: (1) by a blockade of DAT and NET, and (2) by enhancing the brain pool of tyrosine and phenylalanine. Interestingly, MPH had a similar effect on the energy-related metabolites, lactate and acetate, favouring their transport from the plasma into the frontal cortex and hippocampal areas. In addition, glutamate and GABA levels were also increased by MPH in the frontal cortex and hippocampus. Together, these findings provide support for the contribution of dopaminergic, glutamatergic and energy-related metabolites in the mechanism of action of the anti-ADHD drug, MPH.

Contrasting findings were observed following acute and chronic MPH treatment in the cerebellum (Chapter 6), which were both dose and treatment duration-dependent. Acute treatment decreased cerebellar glutamate, *N*-acetylaspartate and VMAT2, while chronic treatment increased glutamate, tyrosine and VMAT2. However, the chronic MPH-induced increase of tyrosine and

VMAT2 did not correlate with increased cerebellar dopamine, which would suggest that in the cerebellum, the increased tyrosine may elevate the synthesis of noradrenaline rather than dopamine.

In chapter 7, the thesis shows that chronic MPH treatment increases mRNA and protein expression of markers mediating neuroplasticity. Here, chronic MPH increased Arc, IRSp53/58, Cdc42, and Arp2 levels in the: striatum, nucleus accumbens and hippocampus. The MPH-induced increase of these synaptic plasticity-associated markers in these brain regions may induce changes in dendritic spine morphology, as well as in the consolidation of memory strength and drug-seeking behaviour.

In conclusion, the present thesis demonstrates, by applying a wide range of bioanalytical techniques, that the anti-ADHD drug, MPH, has major effects on: catecholaminergic protein markers, metabolic markers, and proteins mediating neuronal plasticity in the adolescent brain. The factors influencing some of these effects were dependent on regional differences, cerebral lateralisation, drug dosage and treatment duration.

ACKNOWLEDGEMENTS

I would like to express my heartfelt appreciation to Dr. Tyra S. C. Zetterström for permitting me to start my research career under her supervision and guidance throughout my MSc and PhD period. I am grateful not only for her help regarding research issues but also regarding personal issues. She has been a real mother to me.

I would also like to thank the rest of my supervisory team, which includes Prof. Bob Chaudhury and Dr. Ben Gronier for their unrelenting support and the advice offered throughout my MSc and PhD research period. In addition, I would like to thank Prof. Martin Grootveld, Dr. Tiziana Sgamma, Dr. Victor Ruiz Rodado, and Dr. Fay Probert for their instrumental contributions to the success of this thesis. I am also grateful to De Montfort University for the 'High Flyers' scholarship, which catered for the tuition fees and the stipend. Without this scholarship, this work would not have been possible.

Special thanks also goes to all my colleagues in neuropharmacology laboratory, including Mathieu Di Miceli, Estabraq Jaddoa and Adesional Omolare for their immense support regarding the animal experiments. Special thanks also goes to the B.S.U. team, which includes Anita O'Donoghue, Mike Storer and Paul Ainsworth, for their efforts in maintaining optimal conditions within the animal unit. Many thanks also goes to all the technicians in room 2.17 of the Hawthorn Building, including David Reeder, Jo Tonkin, Amrat Khorana, Claire West, and Leonie Hough for their technical assistance and the provision of some essential consumables.

Last but not least, I would like to thank my parents John and Gladys, my siblings, friends and loved ones for being there for me in times of need. I am also grateful to my church members and 'little family' here in Leicester, with whom I shared my research challenges and concerns.

PUBLICATIONS

PhD-Related

Quansah, E., Ruiz-Rodado, V., Grootveld, M., Probert, F., Zetterström, T.S.C., 2017. ^{1}H NMR-based metabolomics reveals neurochemical alterations in the brain of adolescent rats following acute methylphenidate administration. Neurochemistry International, S0197-0186(16)30506-X, doi:10.1016/j.neuint.2017.03.003.

Quansah, E., Sgamma, T., Jaddoa, E., Zetterström, T.S.C., Chronic methylphenidate regulates genes and proteins mediating neuroplasticity in the juvenile rat brain. Neuroscience Letters, Accepted.

Quansah, E., Ruiz-Rodado, V., Grootveld, M., Zetterström, T.S.C., 2017. Methylphenidate alters monoaminergic and metabolic pathways in the cerebellum of adolescent rats. Biochemical Pharmacology, submitted.

Quansah, E., Zetterström, T.S.C., 2017. Methylphenidate has prominent effects on catecholamine synthesis and metabolic markers in rat cortex than striatum. Nature Scientific Reports, submitted.

Research Posters

Quansah, E., Zhu, Y., Zetterström, T., 2014. P.7.C.003 Effects of methylphenidate on dopamine targets in the left and right brain hemispheres. European Neuropsychopharmacology 24, Supplement 2, S718–S719.

Quansah, E., Zetterström, T., 2016. Biochemical markers altered in the cerebellum of rats treated with methylphenidate. 10th Federation of European Neurosciences Societies (FENS) Forum of Neuroscience, Copenhagen.

Other Publications

Quansah, E., Karikari, T.K., 2016. Potential role of metabolomics in the improvement of research on traditional African medicine. Phytochemistry Letters 17, 270–277. doi:10.1016/j.phytol.2016.08.004

Quansah, E., Sarpong, E., Karikari, T.K., 2016. Disregard of neurological impairments associated with neglected tropical diseases in Africa. eNeurologicalSci, Neurological Disorders in Africa 3, 11–14. doi:10.1016/j.ensci.2015.11.002

Quansah, E., Karikari, T.K., 2015a. Motor Neuron Diseases in Sub-Saharan Africa: The Need for More Population-Based Studies. Biomed Res Int 2015, 298409. doi:10.1155/2015/298409

Quansah, E., Karikari, T.K., 2015b. Neuroscience-related research in Ghana: a systematic evaluation of direction and capacity. Metab Brain Dis. doi:10.1007/s11011-015-9724-7

Quansah, E., Ohene, L.A., Norman, L., Mireku, M.O., Karikari, T.K., 2016. Social Factors Influencing Child Health in Ghana. PLoS ONE 11, e0145401. doi:10.1371/journal.pone.0145401

Karikari, T.K., **Quansah, E**., 2015. Neurogenomics: Challenges and opportunities for Ghana. Applied & Translational Genomics, Neurogenomics: Coming of Age 5, 11–14. doi:10.1016/j.atg.2015.06.002

Karikari, T.K., **Quansah, E**., Mohamed, W.M.Y., 2015a. Developing expertise in bioinformatics for biomedical research in Africa. Applied & Translational Genomics, What is Translational Bioinformatics 6, 31–34. doi:10.1016/j.atg.2015.10.002

Karikari, T.K., **Quansah, E**., Mohamed, W.M.Y., 2015b. Widening participation would be key in enhancing bioinformatics and genomics research in Africa. Appl Transl Genom 6, 35–41. doi:10.1016/j.atg.2015.09.001

Karikari, T.K., Yawson, N.A., **Quansah, E**., 2016. Developing Science Communication in Africa: Undergraduate and Graduate Students should be Trained and Actively Involved in Outreach Activity Development and Implementation. J Undergrad Neurosci Educ 14, E5-8.

ABBREVIATIONS

^{1}H-MRS	Proton magnetic resonance spectroscopy
^{1}H-NMR	Proton nuclear magnetic resonance spectroscopy
3-MT	3-methoxytyramine
5-HTT/SLC6A4	Serotonin transporter
AAAs	Aromatic amino acids
aCSF	Artificial cerebrospinal fluid
ADHD	Attention deficit hyperactivity disorder
AMPA	Alpha-amino-3-hydroxy-5-methyl-4-isoxazoepropionic acid
Arc	Activity-regulated cytoskeleton-associated gene
Arp2	Actin-related protein 2
ATP	Adenosine triphosphate
BBB	Blood brain barrier
BCAA	Branched-chain amino acid
cAMP	Cyclic adenosine monophosphate
Cdc42	Cell division control protein 42
CNS	Central nervous system
COMT	Catechol-*O*-methyltransferase
COSY	Correlation spectroscopy
D1R and D2Rs	Dopamine receptors
DA	Dopamine
DAT/SLC6A3	Dopamine transporter
DBH	Dopamine beta-hydroxylase
DHPA	3,4-dihydroxyphenylacetaldehyde

DOPAC	3,4-dihydroxyphenylacetic acid
DSM-V	Diagnostic and Statistical Manual of Mental Disorders (V)
EAATs	Excitatory amino acid transporters
EC	Electrochemical detection
ECL	Enhanced chemiluminescence
EMT	Extraneuronal monoamine transporter
GABA	γ-aminobutyric acid
GATs	GABA transporters
GRIN2A	Glutamate receptor
HPLC	High performance liquid chromatography
HSQC	Heteronuclear single quantum correlation
HTR1 and 2	Serotonin receptors
HVA	Homovanillic acid
IRSp53/58	Insulin receptor substrate protein 53/58
L-DOPA	L-3,4-dihydroxyphenylalanine
LAT-1	Large neutral amino acid transporter
LNAA	Large neutral amino acids
MAO	Monoamine oxidase
mGluRs	Metabotropic glutamate receptors
MPH	Methylphenidate
NA	Noradrenaline
NAA	*N*-acetylaspartate
NAD	Nicotinamide adenine dinucleotide
NET/SLC6A2	NA transporter

NMDA	N-methyl-D-aspartate
OPLS-DA	Orthogonal projection to latent structure discriminant analysis
PCA	Principal component analysis
PCR	Polymerase chain reaction
PFC	Prefrontal cortex
PLS-DA	Partial least squares discriminant analysis
ROC	Receiver operating characteristics
RT-qPCR	Real time quantitative polymerase chain reaction
SDS-PAGE	Sodium dodecyl sulphate - polyacrylamide gel electrophoresis
SN	Substantia nigra
SNP	Single nucleotide polymorphism
SSRIs	Selective serotonin reuptake inhibitors
STOCSY	Statistical total correlation spectroscopy
TH	Tyrosine hydroxylase
TOCSY	Total correlation spectroscopy
TPH	Tryptophan hydroxylase
TSP	3-(trimethylsilyl)propionic-2,2,3,3-d4 acid
VMAT2	Vesicular monoamine transporter 2
VNTR	Variable number tandem repeat
VTA	Ventral tegmental area
WHO	World Health Organisation
α_1/α_{2A}	Noradrenergic receptors

TABLE OF CONTENT

LIST OF FIGURES

LIST OF TABLES

CHAPTER 1

1 Introduction

1.1 Attention deficit hyperactivity disorder

1.1.1 Clinical features

Attention deficit hyperactivity disorder (ADHD) is the most prevalent neurobehavioral condition in childhood. Based on the criteria given in the fifth edition of the Diagnostic and Statistical Manual of Mental Disorders (DSM-V), ADHD is characterised by hyperactivity and impulsivity in motor, emotional and social responses, as well as a general lack of inhibition and deficits in sustained attention (American Psychiatric Association 2013). To meet the established criteria for clinical diagnosis, the symptoms should have manifested in at least two different environmental domains (home, social, educational or occupational) for not less than six months, and must have set in before age twelve and cause notable behavioural impairment (American Psychiatric Association 2013). A recent meta-analysis study estimates its global prevalence to be 2.6-4.5% (Polanczyk *et al.* 2015). Other less conservative estimates indicate a prevalence rate of 8-12% among school-aged children (6-12 years), which declines with age but persists into adulthood, affecting 2.5-5.0% of adults (Kessler *et al.* 2006; Valera *et al.* 2007). In the UK, a 6-year longitudinal study has shown a rise in the prevalence of ADHD and its drug prescription from 2003 to 2008 in several age categories. The study demonstrated a rise in prevalence from 4.8% to 9.2% in 6-12 year olds, 3.6% to 7.4% in 13-17 year olds, 0.3% to 1.1% in 18-24 year olds, 0.02% to 0.08% in 25-45 year olds, and 0.01% to 0.02% in adults over 45 years old (McCarthy *et al.* 2012), demonstrating a higher ADHD prevalence among younger individuals than adults. ADHD associated impairments have been observed across lifespan in various areas such as in academic performance, employment, socioeconomic status, and family life (negative parent-child interactions) and worsened mental health status, mostly in relation to higher degree of disruptive behaviours and substance use disorders, as well as oppositional and conduct disorders (Valera *et al.* 2007). In particular, younger children with the disorder demonstrate more overt signs of

agitation, while adolescents may experience internal feeling of restlessness, inability to complete academic work independently, recreational drug taking, and a propensity towards risky behaviours culminating in high accident rates (Brookes *et al.* 2006).

1.1.2 ADHD subtypes

Three behavioural subtypes of ADHD are generally recognised, which are the inattentive (ADHD-I), hyperactive/impulsive (ADHD-H) and the combined (ADHD-C) subtypes (Figure 1.1). While all three disease subtypes may be common in young and adolescent patients, the inattentive subtype is more prevalent in adults with the disorder. In the current categorical clinical view based on DSM-V, these three clinical subtypes belong to the same diagnostic entity (i.e. ADHD). However, there have been previous suggestions that ADHD-I should have a distinct diagnostic category as it shares less in common with ADHD-H and ADHD-C (Milich *et al.* 2001). The subtypes may vary from each other based on inattention symptoms, demographics, comorbid features, and responsiveness to stimulant treatment (Carlson *et al.* 1999). It was also previously postulated that ADHD-H and ADHD-C but not ADHD-I may be associated with deficits in executive functions such as planning, cognition, and working memory (Barkley 1997). However, aspects of this theory has been challenged in some neurophysiological studies which demonstrated that children with ADHD-C did not differ significantly from ADHD-I patients on most of the listed markers of executive functioning (Geurts *et al.* 2005; Pasini *et al.* 2007). Moreover, despite some differences, recent genetic studies have demonstrated that these ADHD subtypes have a lot of genetic features in common (Kuntsi *et al.* 2004; McLoughlin *et al.* 2007).

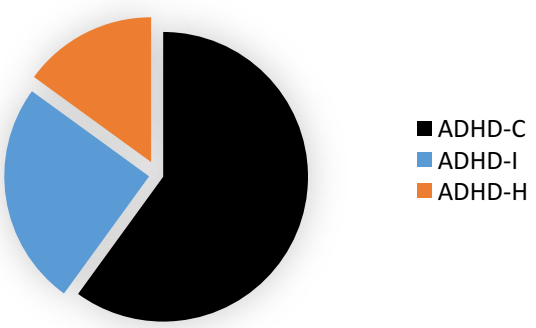

Figure 1.1: General ADHD subtype prevalence across all age categories.
The combined subtype (ADHD-C, dark) remains the most common ADHD subtype globally, followed by the predominantly inattentive subtype (ADHD-I, blue), and the predominantly hyperactive subtype (ADHD-H, orange) (adapted from Miller 2014; Arthur and Terri 2001).

1.1.3 Genetic aetiology

Adoption, twin and family studies have shown the existence of a strong genetic aetiology for ADHD. The disorder often tends to cluster in families with genetic factors explaining up to 76-80% of phenotypic variance (Faraone *et al.* 2005b; Durston *et al.* 2009), making ADHD one of the most heritable brain disorders. In one study, the heritability of the ADHD-H was found to be 88%, with that of ADHD-I being 79% (McLoughlin *et al.* 2007), implying that genetic influence in ADHD dominates the influence of environmental factors. Other studies have observed that the biological relatives (siblings) of hyperactive children were more likely to have hyperactivity than non-biological relatives (e.g. adopted relatives) (Biederman *et al.* 1990; Sprich *et al.* 2000). The estimated sibling risk ratio for broadly defined ADHD (including all subtypes) is reported to be around three- to four-fold higher when compared with population risk (Todd *et al.* 2003). However, the sibling risk ratio for ADHD-C alone is slightly higher, with the estimate being five- to six-fold higher (Todd *et al.* 2003).

A number of genetic linkage studies have also been performed in order to determine regions of certain chromosomes that may be harbouring genes for ADHD. This approach scans several DNA markers across the genome to detect any chromosomal regions that are shared more often than expected within a family that has a history of ADHD. A genome-wide scan of some families from a genetically isolated community in Columbia showed evidence of linkage in several chromosomal regions including, *8q12, 4q13, 11q23, 17p11, 8p23, and 12q23* (Arcos-Burgos *et al.* 2004). In addition, while one study involving 126 American affected pairs of siblings implicated four regions (logarithm of odds {LOD} scores > 1.5): *5p12, 12q23, 10q26,* and *16p13* (Fisher *et al.* 2002). An expanded study involving 164 Dutch affected pairs of siblings observed a strong linkage (LOD > 4) in the *16p13* region, which has also previously been implicated in another brain disorder, i.e. autism (Bakker *et al.* 2003). A recent study on 155 German pairs of siblings also reported a strong linkage for *5p17* but produced only a nominal evidence of linkage for chromosomes *6q, 9q, 11q, 12q, 7p and 17p* (Hebebrand *et al.* 2006). While these data from genetic linkage studies are divergent and remains inconclusive, chromosomes *5p, 12q, 16p, 17p* have often been implicated.

In contrast to the scarcity of genetic linkage studies, several genetic association studies have been conducted. A major advancement in the molecular genetics of ADHD has been the IMAGE (International Multisite ADHD Gene) project, which evaluated 51 genes for association with ADHD. A total of 776 DSM-IV ADHD-C children in Europe, their siblings (n=808) and biological parents (n=1227) were involved in the study (Brookes *et al.* 2006). A high-density single nucleotide polymorphism (SNP) map was created for genes within monoamine neurotransmitter (dopamine, noradrenaline, and serotonin) pathways that are implicated in ADHD. Results from this study, as well as several other genetic association studies, have

indicated some association of ADHD with dopamine transporter (DAT1, SLC6A3) and receptors: D1 (D1R), D2 (D2R), D3 (D3R), D4 (D4R), and D5 (D5R), as well as dopamine β-hydroxylase, monoamine oxidase A, noradrenaline transporter (NET/SLC6A2), noradrenergic receptors (α_{2A}, α_{2C}, α_{1C}), and serotonin transporter (5HTT, SLC6A4). ADHD has also been linked with dysfunctional tryptophan hydroxylase, insulin receptor (IRSp53), and some glutamate receptors such as N-methyl-D-aspartate receptor (NMDAR) and alpha-amino-3-hydroxy-5-methyl-4-isoxazoepropionic acid (AMPAR) (Brookes *et al.* 2006; Faraone and Mick 2010).

1.2 The role of neurotransmitter systems in ADHD

Neurons communicate via an essential process called neurotransmission. Neurotransmission refers to the process by which signalling molecules (i.e. neurotransmitters) are released by a neuron (i.e. transmitting/presynaptic neuron), which binds to and activate the receptors of another neuron (i.e. postsynaptic neuron). Monoaminergic neurotransmitters such as dopamine (DA), noradrenaline (NA) and serotonin when released from presynaptic neurons into the synapse, exert their actions by activating their respective receptors on the postsynaptic neurons. Monoamines have multiple roles in the brain including those implicated in the symptoms of ADHD, e.g. emotion, cognition and arousal. The termination of synaptic transmission occurs via several different mechanisms including: reuptake of monoamines by specific neuronal transporters, degradation of the released monoamine, and desensitisation of target receptors. Overall, these monoamine systems (i.e. DA and NA) have been implicated in ADHD (Biederman 2005) and the mechanism of action of anti-ADHD medications (Del Campo *et al.* 2011).

1.2.1 The dopaminergic system

Initially, DA was only thought to be a precursor in the synthesis of NA and adrenaline, or as a product resulting from tyrosine degradation (Blaschko 1942). However, its prominent role as an

independent catecholamine neurotransmitter was later recognised (Bertler and Rosengren 1959; Sano *et al.* 1959; Hornykiewicz 2002). In neuroscience, DA is particularly important due to its involvement in several common disorders related to impaired brain function, including ADHD, schizophrenia and Parkinson's disease, as well as drug dependence and some endocrine disorders (e.g. hyperprolactinemia). Further, most of the drugs used in treating these disorders target DA transmission (Del Campo *et al.* 2011). Although the distribution of DA in the CNS is more restricted than that of NA, DA controls a wide variety of functions, ranging from coordination of locomotor activity, cognition, emotion, food intake and positive reinforcement (Iversen and Iversen 2007). DA also plays essential roles in the periphery including kidney D1 receptor-mediated renin secretion, pituitary D2 receptor-mediated prolactin secretion, adrenal gland D2 receptor-mediated aldosterone secretion, sympathetic tone regulation, vasodilation, gastrointestinal motility, blood pressure regulation, and renal function regulation mediated by D1, D2 and D4 receptors (Iversen and Iversen 2007; Squire *et al.* 2008).

In ADHD, one of the most robust findings remains that of upregulated DAT density in patients compared to healthy controls (Cheon *et al.* 2003; Dougherty *et al.* 1999; Spencer *et al.* 2005). In support of this, reports show that methylphenidate (MPH; *e.g.* Ritalin^{TM}), which is the main psychostimulant drug used in the treatment of ADHD blocks DAT upon administration, and this may be related to the rapid decline of the clinical symptoms of ADHD (Spencer *et al.* 2005; Vles *et al.* 2003). Blocking DAT has significant biological effects including an elevation of extracellular DA levels (Spencer *et al.* 2005). While moderate extracellular DA levels in the prefrontal cortex (PFC) and striatum may be crucial for cognition, attention and locomotor activity, both abnormally high or too low levels in these brain regions mediate poor cognition and increased locomotor activity in ADHD (Figure 1.2).

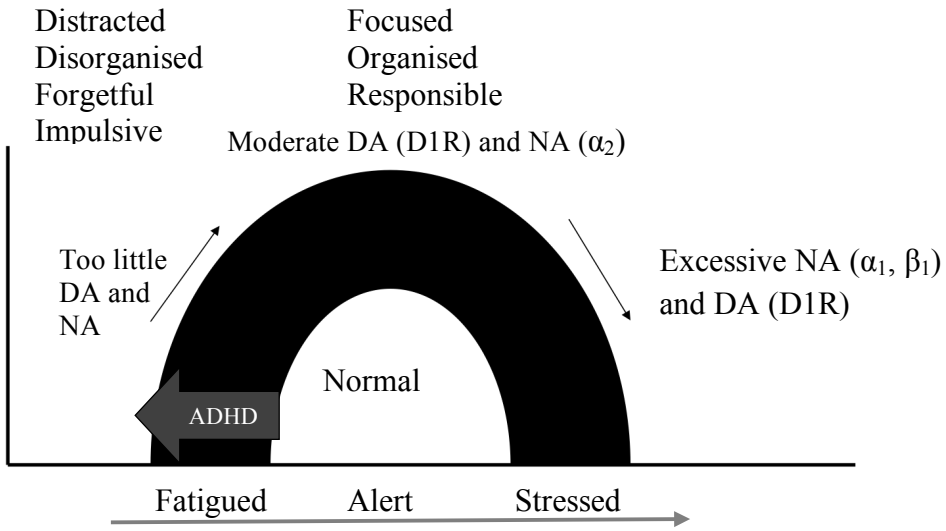

Figure 1.2: The inverted U (dopamine bell) curve and ADHD.
Low levels of dopamine (DA) and noradrenaline (NA) are thought to cause decreased performance in ADHD. The middle of the curve signifies moderate (normal) levels of DA and NA, which causes peak performance by triggering D1 receptors (D1R) and α_2-adrenergic receptors respectively. Elevation of DA and NA above normal as seen after recreational drug taking of cocaine and amphetamine decreases performance via excessive stimulation of D1Rs and α_1/β_1receptors respectively (Arnsten 2009).

1.2.1.1 Dopaminergic pathways

Eight individual dopaminergic nuclei have been identified and classified into individual cell groups designated as A8-A16 (Björklund and Dunnett 2007; Dahlström and Fuxe 1964). DA is synthesised in the nerve terminals originating from the retrorubral field (A8), substantia nigra (A9), and ventral tegmental area (VTA; A10) of the midbrain and projects into several brain regions including the frontal cortex, nucleus accumbens and striatum (Figure 1.3). Also immunoreactive for dopamine is the cell group Aaq in the rostral half of the central grey of the midbrain in primates, as well as the telencephalic group in the rostral forebrain structures including the olfactory tubercle. Dopaminergic dysregulation in these pathways have been associated with ADHD (Faraone *et al.* 2005b; Durston *et al.* 2009). Further, dopaminergic pathways are categorised into the mesolimbic, mesocortical, nigrostriatal, and tuberoinfundibular pathways (Figure 1.3). The mesolimbic and mesocortical pathways are sometimes collectively

referred to as the mesocorticolimbic pathway, which regulates emotional responses, mood, and incentive-based behaviour.

1.2.1.1.1 Mesocorticolimbic pathway

Dopaminergic neurons in the VTA (A10) innervate the amygdala, prefrontal cortex (PFC), hippocampus, ventral pallidum and nucleus accumbens (Figure 1.3) (Björklund and Dunnett 2007; Pierce and Kumaresan 2006). Thus, changes in dopaminergic transmission plays a crucial role in regulating the flow of information through this interconnected limbic circuitry. Projections from the VTA (A10) to the PFC constitute the mesocortical pathway and it is implicated in several cognitive functions including, but not limited to, memory and attention (Squire *et al.* 2008). On the other hand, projections from the VTA to the limbic system via the nucleus accumbens are considered the mesolimbic or "reward/motivation" pathway, since these dopaminergic projections are primarily involved in rewarding behaviours (Squire *et al.* 2008). Therefore, this pathway is hypothesised to play a role in behavioural hyperactivity and the abuse potential of drugs (Pierce and Kumaresan 2006; Wise 2004). Further, the nucleus accumbens is rich in medium spiny (GABAergic) neurons and has a limbic and a motor area known as the shell and the core respectively (Pierce and Kumaresan 2006).

1.2.1.1.2 Nigrostriatal pathway

The nigrostriatal pathway accounts for about 75% of the dopaminergic innervations in the brain and consists of cell bodies located within the substantia nigra (A9) of the ventral midbrain whose axons terminate in the striatum (caudate and putamen), which receive only minor inputs from the VTA (A10), and the A8 cells located caudal to A9 (Figure 1.3). Nerve cells in this pathway send projections either directly to or indirectly through the globus pallidus (external globus pallidus in primates) to the substantia nigra and endopeduncular nucleus (internal globus pallidus in primates) to modulate voluntary movement and goal-oriented behaviour (Money and Stanwood

2013). Due to its role in motor control, this pathway has been one of the main areas of focus of ADHD research, as well as studies into other related disorders. Indeed, loss of DA neurons in this pathway is a key pathological feature of Huntington's chorea and Parkinson's disease (Drui *et al.* 2014).

1.2.1.1.3 Tuberoinfundibular pathway

This pathway is made up by dopaminergic projections in the arcuate (A12) and periventricular (A14) nucleus of the hypothalamus to the pituitary gland (infundibular region), where it regulates the secretion of prolactin (Ben-Jonathan and Hnasko 2001). DA synthesised by neurons in the arcuate nucleus is secreted into the hypophyseal portal system of median eminence that supplies the pituitary gland. In this pathway, DA acts as the neuroendocrine inhibitor of prolactin (Ben-Jonathan and Hnasko 2001). Reports indicate that the normal function of hypothalamic neurons in humans is often preserved in Parkinson's disease (Ben-Jonathan and Hnasko 2001).

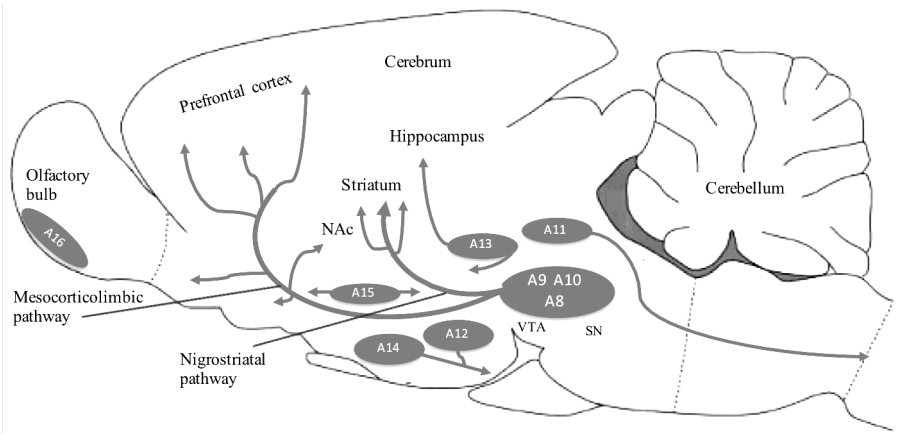

Figure 1.3: Mesocorticolimbic and nigrostriatal dopamine pathways in rat brain.
Dopamine neurons in the mammalian brain are localised in nine distinct cell groups, from the midbrain to the olfactory bulb. The numbering of the dopaminergic cell groups, from A8 to A16, was introduced in the classic study of Dahlström and Fuxe (1964), and is still presently valid. Abbreviations: VTA, ventral tegmental area; SN, substantia nigra; NAc, nucleus accumbens (adapted from Björklund and Dunnett 2007).

1.2.1.2 Dopamine synthesis, storage and release

DA biosynthesis begins with the aromatic amino acid tyrosine. Most of the circulating tyrosine is derived from dietary sources and crosses the blood-brain barrier and enters DA neurons by an energy-dependent uptake process (Fernström 2013; Fernström and Fernström 2007). A number of conditions influence tyrosine transport and may diminish its availability in the brain, affecting DA synthesis. However, in the event of tyrosine deficiency, the enzyme phenylalanine hydroxylase catalyses the hydroxylation of phenylalanine into tyrosine. Tyrosine is then converted into L-3,4-dihydroxyphenylalanine (L-DOPA) by the rate-limiting enzyme, tyrosine hydroxylase (TH). L-DOPA is then converted by DOPA decarboxylase to DA (Meiser *et al.* 2013). TH is the rate-limiting enzyme in DA biosynthesis and tyrosine itself is rarely a limiting factor, especially as TH is saturated at the normal plasma concentrations of tyrosine. Given its importance therefore, TH has become a key target and an endogenous mechanism for regulating the rate of DA synthesis in dopaminergic neurons (Melchitzky and Lewis 2000). Following biosynthesis, DA is transported from the cytoplasm into synaptic vesicles via vesicular monoamine transporter (e.g. VMAT2) for storage. The vesicles perform specific functions including: 1) protecting DA from enzymatic degradation by monoamine oxidase (MAO), 2) minimising constitutive secretion by diffusion from the presynaptic nerve cells, 3) facilitating regulated release, and 4) enabling rapid replenishment of depleted stores. Stored DA is released when action potential raises Ca^{2+} levels in the presynaptic neuron via the activation of voltage-gated Ca^{2+} channels, which causes the vesicles to: 1) target the active zone of the presynaptic membrane, 2) fuse, and 3) release vesicular content (Cartier *et al.* 2010; Meiser *et al.* 2013). The extent of DA release appears to be a function of the rate and pattern of firing. The burst-firing mode causes an enhanced release of DA from dopaminergic nerve terminals. The release of DA

via the Ca^{2+}-dependent exocytosis is also regulated by presynaptic D2/D3 autoreceptors (Ford *et al.* 2010; Sulzer *et al.* 2016).

1.2.1.3 Dopamine receptors

Biochemical and pharmacological studies in the late 1970s revealed that DA binds to two receptors, which became known as D1 and D2 receptors. Much later, it was recognised that D1 receptor was positively coupled to G_S proteins and elevated intracellular cyclic adenosine monophosphate (cAMP) levels, while D2 receptor was coupled to G_i proteins and inhibited cAMP accumulation via adenylyl cyclase (Missale *et al.* 1998). Owing to advancements in gene cloning procedures, both D1 and D2 receptors have been cloned based on sequence homology to known G protein-coupled receptors. At present, three additional DA receptors have been cloned and characterised as D3, D4 and D5 receptors (Beaulieu and Gainetdinov 2011; Butini *et al.* 2016). A number of biochemical, structural and pharmacological studies have pointed out that all the characterised DA receptors belonged to one of the two initially identified receptor groups, and hence were classified into D1-like and D2-like families. The D1-like family includes D1 and D5 receptors, whereas the D2-like family consists of D2, D3 and D4 receptors. DA receptors are members of the G protein coupled receptor superfamily and are made up of single polypeptide chains ranging in size from 387-475 residues (Butini *et al.* 2016). The receptors have 7 transmembrane-spanning domains that form a ring-like hydrophobic pocket surrounded by 3 extracellular and 3 intracellular loops (Figure 1.4). The D1 and D5 receptors are 80% homologous in their transmembrane domains, while D3 and D4 receptors are 75% and 53% homologous with D2 receptor respectively (Beaulieu and Gainetdinov 2011). Functionally, the initial distinction between D1 and D2 receptors also appears to apply to the new members of each receptor subfamily, with both D1 and D5 receptors stimulating adenylyl cyclase and increasing

cAMP, while D3 and D4 receptors both inhibit adenylyl cyclase and decrease cAMP in much the same way as D2 receptor (Sulzer *et al.* 2016; Wahlström *et al.* 2010). Presently, splice variants, leading to short and long forms of D2 receptor and genetic polymorphisms, especially of D4R, have been characterised (Shaw *et al.* 2007; Wang *et al.* 2000).

1.2.1.3.1 D1-like receptors

DA receptors have broad expression, with D1 receptor being expressed at a higher density than all the other receptor types. The D1 receptor is highly expressed on postsynaptic neurons in the nigrostriatal and mesocorticolimbic areas such as striatum, nucleus accumbens, prefrontal cortex, substantia nigra, amygdala, and olfactory bulb, with lower levels in the hippocampus, cerebellum, thalamic and hypothalamic areas (Beaulieu and Gainetdinov 2011; Missale *et al.* 1998). Compared to D1 receptor, D5 receptor is expressed at low levels in pyramidal neurons of the hippocampus, substantia nigra, hypothalamus, dentate gyrus, prefrontal cortex, and other cortical areas. Very low D5 receptor expressions have also been observed in the medium spiny (GABAergic) neurons of the striatum and nucleus accumbens (Beaulieu and Gainetdinov 2011; Butini *et al.* 2016).

Both D1 and D5 receptors have been shown to stimulate adenylyl cyclase (Missale *et al.* 1998). It is generally thought that the activation of adenylyl cyclase by D1-like receptors is predominantly mediated by the $G_S\alpha$ subunit of G-proteins. However, $G_{olf}\alpha$ an isoform of $G_S\alpha$ that also stimulate adenylyl cyclase is expressed at higher levels than $G_S\alpha$ in the striatum, nucleus accumbens and olfactory bulb, suggesting that D1-like receptors may couple to adenylyl cyclase through multiple mechanisms (Hervé 2011). Indeed, in the striatum of mice lacking $G_{olf}\alpha$ gene, adenylyl cyclase activation in response to D1-like receptor stimulation is absent, indicating that D1-like receptors act through the $G_{olf}\alpha$ protein to stimulate the production of cAMP (Corvol *et al.* 2001). In

addition, D1 receptor stimulation can induce neuroplastic changes in the brain via the activation of protein kinase A and CREB (cAMP response element binding protein) leading to an increased activity of glutamate receptors (e.g. NMDAR), and an increased expression of plasticity related genes such as activity-regulated cytoskeleton-associated (*Arc*) gene, and the brain-derived neurotrophic factor (BDNF) gene (Monsma *et al.* 1990; Konradi *et al.* 1996; Dudman *et al.* 2003).

1.2.1.3.2 D2-like receptors

D2 receptors have the highest expression in this subgroup and are mostly found in the striatum, nucleus accumbens, and olfactory tubercle. D2 receptors are also expressed at significant levels in the VTA, substantia nigra, cortical areas, hippocampus, hypothalamus, septum, and amygdala (Butini *et al.* 2016). D3 receptors have a more limited pattern of distribution, with the highest density being in the limbic areas, such as in the shell of nucleus accumbens, the islands of Calleja and the olfactory tubercle (Missale *et al.* 1998). Compared to D2 receptors, D3 receptors are detectable at lower levels in the striatum, hippocampus, VTA, substantia nigra, septum and various cortical areas. However, relative to D2 and D3 receptors, the D4 receptor has the lowest level of expression in the brain, with some level of expression in the prefrontal cortex, hippocampus, amygdala, hypothalamus, substantia nigra, thalamus and globus pallidus (Missale *et al.* 1998). In addition, while D1, D2, and D4 receptors have also been observed in the retina, all receptor subtypes have been detected at varying levels in peripheral nerves in the heart, kidney, adrenal glands, gastrointestinal tracts, and blood vessels (Butini *et al.* 2016).

The original classification of D2 receptor was based on its ability to inhibit adenylyl cyclase in the CNS. Although less apparent, both D3 and D4 receptors have also been shown to inhibit adenylyl cyclase. Initially, D3 receptor was reported not to inhibit adenylyl cyclase in cell lines

and appeared not to couple to G-proteins as indicated by the lack guanine nucleotide shift in agonist binding curves (Sokoloff *et al.* 1990). Later studies, however, revealed that D3 receptor actually inhibit adenylyl cyclase in some cells lines, albeit less strong relative to that elicited by D2 receptor (Chio *et al.* 1994). Moreover, D4 receptors have been shown to inhibit adenylyl cyclase activity and cAMP accumulation in the retina via the G_i subunit of G-proteins (Cohen *et al.* 1992). Thus, confirming adenylyl cyclase inhibition as a consistent feature of D2-like receptors.

In addition to postsynaptic D2 receptors, there is also presynaptic localisation of D2-autoreceptors. Presynaptic autoreceptors exist on most dopaminergic cells including dendrites, soma and nerve terminals (Butini *et al.* 2016; Wolf and Roth 1990). Presynaptic autoreceptors provide important negative feedback mechanism, which adjust the rate of neuronal firing, synthesis and release of neurotransmitter in response to changes in synaptic levels (Wolf and Roth 1990). Generally, activation of presynaptic D2-autoreceptors in the somatodendritic region causes a decline in the firing rate of DA neurons, while the activation of autoreceptors on DA nerve terminals inhibit DA synthesis and release (Wolf and Roth 1990; Missale *et al.* 1998). Although the full identities of D2-autoreceptors are still somewhat unclear, evidence points towards distinct pharmacology of autoreceptors relative to postsynaptic D2 receptors. For instance, D2-autoreceptors are preferentially activated by lower concentrations of DA agonists (Beaulieu and Gainetdinov 2011).

1.2.1.3.3 Function of brain dopamine receptors

The role of DA in the nigrostriatal pathway and on locomotor activity has been studied extensively. The activation of D1 and D2 receptors, expressed on postsynaptic neurons, has a moderate stimulatory effect on locomotor activity (Tran *et al.* 2005). In contrast, activation of

D2-class autoreceptors causes a reduction in DA release, resulting in decreased locomotor activity (Missale *et al.* 1998). Since D2-autoreceptors are often activated by lower DA agonist concentrations than required to stimulate postsynaptic receptors, the same DA agonist can have a biphasic effect, resulting in reduced activity at low doses and behavioural activation at higher doses (Beaulieu and Gainetdinov 2011). Interestingly, the long and short D2 receptor splice variants (Wang *et al.* 2000), appear to have different neuronal localisations, with the short variant being predominantly presynaptic and the long being postsynaptic. Thus, the differing roles of presynaptic and postsynaptic D2 receptors may be determined by the varying contributions of these D2 receptor isoforms (De Mei *et al.* 2009). D3 receptors seem to have moderate inhibitory effect on locomotion, while D4 and D5 receptors exert minimal action on the control of movement, perhaps due to their limited expression pattern in the primary motor areas of the brain (Missale *et al.* 1998). At the same time, synergistic interaction between D1 and D2 receptors are essential for maximal locomotor activity (White *et al.* 1988).

The mesocorticolimbic pathway is implicated in reward and reinforcement mechanisms, with stimulants and drugs of abuse eliciting an enhancement of DA release in this pathway, and their withdrawal causing significant reductions in dopaminergic transmission. Several pharmacological studies have shown that D1, D2, and to a lesser extent, D3 receptors are critically involved in reward and reinforcement mechanisms and play significant roles in mediating the reinforcing properties of drugs of abuse (Sulzer *et al.* 2016). Moreover, both D1 and D2 receptors appear to be critical for learning and memory mechanisms, particularly in the PFC (Beaulieu and Gainetdinov 2011; Goldman-Rakic *et al.* 2004). At the same time, D3, D4, and perhaps D5 receptors, appear to have minor modulatory impact on specific aspects of cognition, mediated by areas in the hippocampus (Missale *et al.* 1998). Other functions mediated in part by the

dopaminergic receptor subtypes in the CNS include: attention, decision-making, impulse control, motor learning, reproductive behaviours, regulation of food intake and sleep (Butini *et al.* 2016; Iversen and Iversen 2007).

1.2.1.4 Dopamine reuptake

Reuptake is the means through which the released neurotransmitter is carried back into the presynaptic nerve terminals via DA transporters (high affinity neuronal uptake) or the means by which the released transmitter is taken up by surrounding glial cells (non-neuronal uptake). Reuptake represents the major mechanism through which cytosolic MAO and COMT terminate the action of released DA (Westerink 1985). Such tight regulation helps in limiting the duration and magnitude of the effect of the released DA, hence establishing a spatial and temporal constraint on excessive DA signalling in the brain. In addition, reuptake also permits the recycling of DA and saves the energy costs of biosynthesis (Sulzer *et al.* 2016).

DAT plays a crucial role in regulating the intensity of DA neurotransmission in the brain by mediating DA reuptake. DAT transports released DA from the extracellular to the intracellular milieu. Inhibition or removal of DAT prolongs the lifetime of extracellular DA by several folds (Jones *et al.* 1998). Following uptake, VMAT regulates the accumulated DA in the cytoplasm. In particular, VMAT2 reloads the intracellular DA into presynaptic vesicles (Narendran *et al.* 2015). On the other hand, the extraneuronal monoamine transporter, belonging to a large and widely distributed family of organic cationic transporters, also performs extraneuronal reuptake of DA and other catecholamines, albeit it has a low affinity for these neurotransmitters. Overall, these transporter systems vary not only in structure but also in cellular localisation, substrate specificity, energy requirements and antagonist selectivity (Figure 1.4).

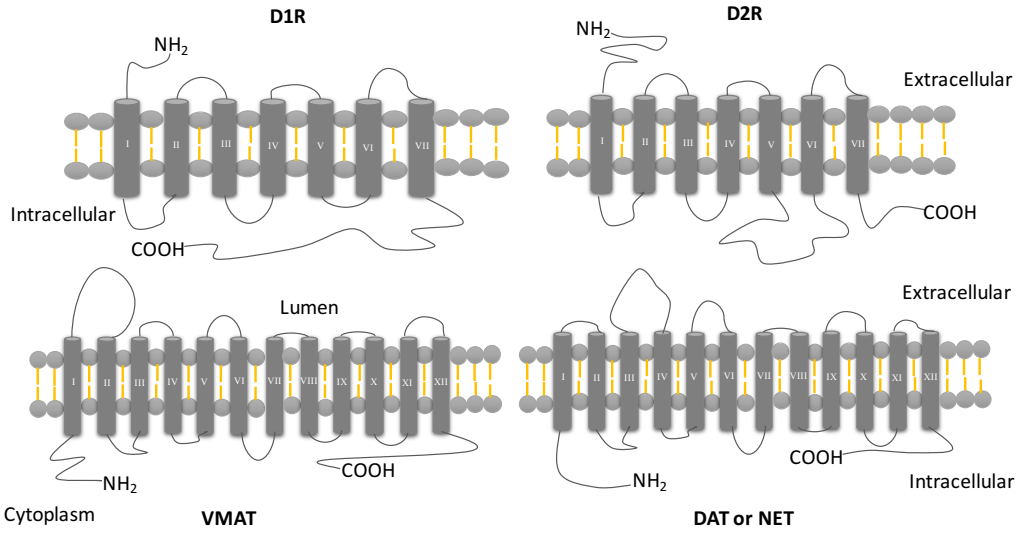

Figure 1.4: Structure of dopamine receptors and catecholamine transporters.
D1 (D1R) and D2 (D2R) receptors belong to the superfamily of 7 transmembrane domains G protein-coupled receptors. D1Rs have a longer cytoplasmic carboxyl terminus, whereas D2Rs have a larger third intracellular loop. Transporters DAT (or NET) and VMAT have 12 transmembrane domains but little primary sequence homology. In contrast to the receptors, the transporters have both the N- and C-termini at the cytoplasmic side of the membrane. VMAT has a large intraluminal loop between transmembrane domains 1 and 2, while DAT has an extracellular loop between transmembrane domains 3 and 4 (Ben-Jonathan and Hnasko 2001).

Regardless of some structural differences, all monoamine transporters including DAT and NET (as well as serotonin transporter, 5HTT or SERT) are Na^+/Cl^- dependent and therefore act as co-transporters of Na^+/Cl^- and DA (as well as NA and serotonin as is the case of NET and 5HTT), utilising the electrochemical gradient for Na^+ as the driving force. The process of reuptake by DAT has a stoichiometry of 2 Na^+: 1 Cl^-: 1 DA (Ben-Jonathan and Hnasko 2001). VMAT, on the other hand, is driven by the proton gradient existing between the cytosol and the vesicle content (Wahlström *et al.* 2010). VMAT recharges the intracellular vesicles with the neurotransmitter via an electrochemical gradient generated by vacoular ATP-dependent H+ pump (V-ATPase), a pump that maintains intravesicular acidic environment and permits the uptake of the transmitter against its concentration gradient. DAT and NET are relatively selective for DA and NA respectively, with high affinity but low maximum rate of reuptake, and are important in ensuring

the maintenance of releasable stores of DA and NA. Extraneuronal monoamine transporter, however, has low affinity but higher transport capacity than DAT and NET for all types of catecholamines (Sulzer *et al.* 2016).

In situ hybridisation and immunohistochemistry studies have revealed that DAT is expressed in the CNS (Björklund and Dunnett 2007). The transporter co-localize with TH in the CNS and serves as a marker of dopaminergic neurons, especially as it is limited to these neurons and are not found in the locus coeruleus (the origin of NA in the CNS) or on adrenergic and noradrenergic nerve terminals (Björklund and Dunnett 2007). The highest expression of DAT is in the soma (perikarya), dendrites and axonal processes of substantia nigra and VTA. Thus, DAT has a significant presence in the mesocorticolimbic and nigrostriatal pathways, with limited expression in the hypothalamic dopaminergic neurons. However, electron microscopy has revealed that the DAT protein is found predominantly in the extra-synaptic area instead of the active zone of the synapse, indicating that DAT may have a role in limiting diffusion of DA following its release (Meiser *et al.* 2013).

1.2.1.5 Dopamine catabolism

Catabolism is one of the effective means of DA inactivation. DA may be enzymatically inactivated via different breakdown pathways: 1) oxidative deamination by MAO (isoforms A and B), and 2) *O*-methylation by catechol-*O*-methyltransferase (COMT). In the striatum of rats, DA catabolism often begins with oxidative deamination by MAO, yielding the intermediate product 3,4-dihydroxyphenylacetaldehyde (DHPA) (Figure 1.5). This aldehyde is inactivated either by rapid oxidation to the corresponding carboxylic acid, 3,4-dihydroxyphenylacetic acid (DOPAC), by acetyl aldehyde dehydrogenase. In the synaptic cleft, DA may be taken up by surrounding glial cells, which degrade DA via both MAO and COMT. 3-*O*-methylation of

DOPAC by COMT results in the formation of homovanillic acid (HVA), one of the major degradation products of DA (Laatikainen *et al.* 2013). Alternatively, DA inactivation may begin with COMT, giving rise to 3-methoxytyramine (3-MT), which is later converted to 3-methoxy-4-hydroxyphenylacetaldehyde (MHPA) and HVA by MAO and aldehyde dehydrogenase respectively. Given that tissue levels of the extracellular metabolite, 3-MT are generally quite low, it is possible that this compound is deaminated quite rapidly (Laatikainen *et al.* 2013).

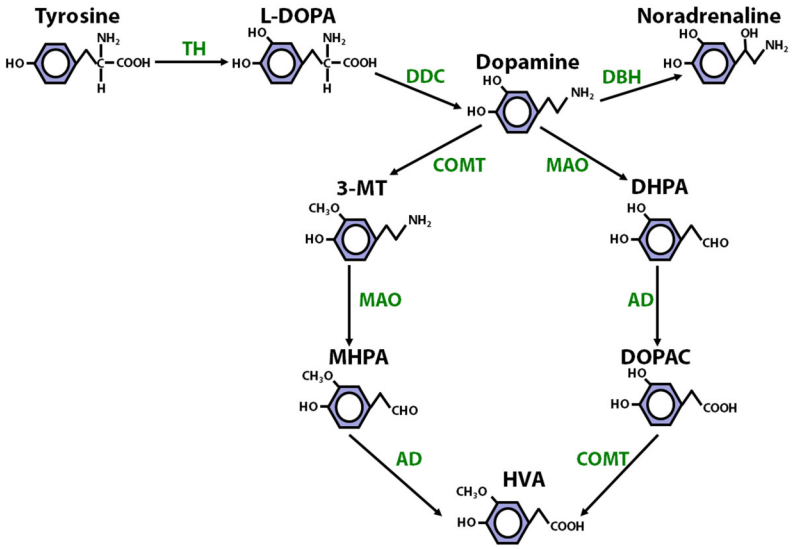

Figure 1.5: Catecholamine synthesis and catabolism.
DA is synthesised from tyrosine via L-DOPA (rate-limiting step, mediated by tyrosine hydroxylase). DA may either be converted to NA (catalysed by DA β-hydroxylase) or catabolised by the actions of monoamine oxidase (MAO), by catechol-o-methyltransferase (COMT) and aldehyde dehydrogenase (AD). Abbreviations: 3-MT, 3-methoxytyramine; DHPA, 3,4-dihydroxyphenylacetaldehyde; MHPA, 3-methoxy-4-hydroxyphenylacetaldehyde; HVA, homovanillic acid; (Laatikainen *et al.* 2013).

In rodents, DOPAC and HVA are quantitatively the most prominent DA metabolites. Indeed, DOPAC is considered as an index of MAO mediated DA catabolism. This stems from the observation that reserpine, which induces neuronal catecholamine breakdown by blocking vesicular storage, increases striatal DOPAC levels (Fekete *et al.* 1980; Fornstedt and Carlsson 1989; Westerink 1985). Reserpine also increases HVA, albeit transiently, which is to be expected

as most HVA is generated from DOPAC. Elevated DOPAC levels following reserpine treatment therefore signify a reduction in DA levels, reduction in vesicular storage and hence increased catabolism.

1.2.2 The noradrenergic system

Noradrenergic projections originate predominantly from neurons in the brainstem nucleus, locus coeruleus and project into multiple regions, including hippocampus and prefrontal cortex, which have critical roles in affective processes and high-level cognitive functions such as working memory and inhibitory response control, that are often impaired in ADHD (Robbins and Arnsten 2009). However, noradrenergic innervations in the striatum are sparse, suggesting that its modulation of the striatum may be limited (Del Campo *et al.* 2011). In noradrenergic neurons, dopamine-beta-hydroxylase converts DA into NA. However, DA-beta-hydroxylase is localised to the vesicles rather than cytosol, implying that conversion of DA to NA only occurs after DA has been packaged into vesicles (Xing *et al.* 2016). The vesicular storage of dopamine-beta-hydroxylase also means that it can be released into the synaptic cleft along with both DA and NA. By acting on presynaptic receptors, NA can regulate its own release (the so-called autoinhibitory feedback mechanism). This inhibitory feedback mechanism operates via α_2-adrenergic receptors, which inhibit adenylyl cyclase and prevent the opening of Ca^{2+} channels. At the post synaptic site, NA binds to two main G-protein-coupled receptor types, the α-adrenergic (α_1 and α_2) and β-adrenergic (β_1, β_2, and β_3) receptors (Arnsten 2011). Generally, the α_1 receptors are coupled to G_q proteins and therefore activate phospholipase C and inositol 1,4,5-triphosphate intracellular signalling, leading to the release of intracellular Ca^{2+}. NA has lower affinity for α_1 receptors compared to α_2 receptors. The α_2 receptors stimulate G_i proteins that are negatively coupled to adenylyl cyclase, leading to a decrease in cAMP formation as well as inhibiting Ca^{2+}

channels. In comparison, the β-receptors have the lowest affinity to NA and are coupled to G_s proteins that stimulate adenylyl cyclase and activate cAMP signalling (Xing *et al.* 2016).

Reuptake of released NA by NET is the main mechanism for the termination of NA transmission in the CNS (Seneca *et al.* 2006). Interestingly, most of the drugs effective in the treatment of ADHD such as MPH and amphetamine have important effects on NA along with DA transmission. In addition, the selective NA inhibitor (NET blocker), atomoxetine has shown clinical effectiveness and is approved for the treatment of ADHD (Faraone *et al.* 2005a). In rodents, atomoxetine increases cortical NA and DA levels by several-folds when administered systemically, without any significant effects on the subcortical DA system (Bymaster *et al.* 2002). It is the subcortical (particularly the nucleus accumbens) DA effects that are suggested to underlie the abuse potential of psychostimulant treatments (Volkow 2006). The approval of NA modulating drugs for use in ADHD, stem from their beneficial effects on cognition (Del Campo *et al.* 2011). Some studies have shown that moderate increase of NA may improve cognition and impulse control mainly through effects on α_2 receptors, while elevated NA levels such as during extreme stress, impair cognition via α_1 receptors (Arnsten and Li 2005).

Another line of evidence implicating brain noradrenergic pathways in ADHD emanates from findings in candidate gene and genome-wide association studies. Findings from some of these studies have not only indicated that some SNPs (single nucleotide polymorphisms) such as *rs36021* (Thakur *et al.* 2012) within the *SLC6A2* gene (this gene codes for NET) may be associated with ADHD, but have also shown that other SNPs (such as rs3785143) may be associated with improved patient responses to atomoxetine and other ADHD medications (Yang *et al.* 2013). Overall, these findings demonstrate the important role of the noradrenergic system in the neurobiology of ADHD.

1.2.3 The serotonergic system

Evidence of the involvement of the serotonin (5-HT) system in ADHD (although not as strong as the evidence for DA and NA) comes from genetic and neurochemical studies investigating 5-HT, its transporter (5-HTT) and receptor levels, as well as pharmacological studies in ADHD patients and animal models of the disease (Banerjee and Nandagopal 2015; Gadow *et al.* 2013). Neuroanatomical evidence suggests that 5-HT may regulate behavioural domains of hyperactivity and impulsivity in ADHD through the orbitofronto-striatal circuitry (Banerjee and Nandagopal 2015). Moreover, the prefrontal cortex, which regulates attention, emotion, motivation and cognitive control, contains a large density of both inhibitory and excitatory 5-HT receptors (Arnsten and Rubia 2012). The orbitofrontal cortex is particularly dependent on 5-HT, and a depletion of 5-HT from this region significantly impairs orbitofrontal cortex mediated regulation of emotion, inhibition and learning (Clarke *et al.* 2007). A chronic deficit of 5-HT at the synapse of these cortical areas is therefore hypothesised to trigger some of the symptoms of ADHD (Quist and Kennedy 2001). In line with this, deficits in blood 5-HT levels have been recorded in hyperactive and severely affected ADHD children (Banerjee and Nandagopal 2015; Spivak *et al.* 1999).

In addition, 5-HTT knockout rodents have increased extracellular 5-HT levels and improvements in performance on cognitive tasks (Brigman *et al.* 2010; Nonkes *et al.* 2012). Moreover, the 5-HT receptor 1B knockout mice also exhibit significant hyperactivity and are considered as models of motor impulsivity (Brunner and Hen 1997). Thus, these animal models provide a 'face-validity' for the involvement of the serotonergic system in ADHD. Interestingly, other reports have suggested that although deficits in 5-HT levels could cause hyperactivity, psychostimulants such

as MPH and amphetamine may act by balancing the monoaminergic tone, which includes balancing DA, NA, and 5-HT levels (Berger 1999; Borycz *et al.* 2008).

1.2.4 Glutamatergic and GABAergic systems

Currently existing evidence favour the 'DA and NA hypothesis' of ADHD, especially as drugs enhancing catecholamine levels such as MPH and amphetamine have displayed substantial efficacy in relieving the symptoms of the condition (Del Campo *et al.* 2011). However, although stimulants have shown clinical effectiveness in improving ADHD symptoms in the short term, they are not effective in all cases. For instance, stimulants produce complete remission in about 30% of cases, have substantial but partial remission in another 40%, but have little or no benefit in 30% of cases (Steele *et al.* 2006). Thus, deficient DA or NA transmission seems unlikely to be responsible for all cases of this heterogeneous disorder. In order to fully understand the disorder and develop effective medications, therefore, it has become crucial to look beyond DA and NA (Maltezos *et al.* 2014). Emerging evidence points to impaired neuronal and glial energy metabolites, glutamate and gamma-aminobutyric acid (GABA) signalling, as well as altered membrane phospholipids as possible underlying abnormalities in some cases of ADHD, thus some of these targets are being considered as possible future therapeutic targets for ADHD (Adler *et al.* 2012; Russell *et al.* 2006).

Glutamate is the principal excitatory neurotransmitter in the CNS, while GABA is a major inhibitory neurotransmitter. Neural activity in general is constituted, to a large extent, by excitatory and inhibitory balance and this must be tightly regulated to ensure proper neuronal signalling (Duncan *et al.* 2014). Preliminary evidence suggests glutamatergic involvement in the pathophysiology of ADHD. For example genetic studies have reported an association between ADHD and the genes of some glutamate receptors (e.g. NMDARs) (Dorval *et al.* 2007). Using

proton magnetic resonance spectroscopy (^{1}H-MRS), some researchers have also recently shown that glutamate and glutamine are significantly altered in the corticostriatal circuitry of ADHD patients (i.e. increased levels in the cerebrum but decreased levels in the cerebellum) (Perlov *et al.* 2007; Perlov *et al.* 2010; Carrey *et al.* 2002; Carrey *et al.* 2003). In comparison with DA, glutamate is more widely expressed in the brain. Indeed, glutamate projections originating in the PFC extend into the striatum, nucleus accumbens, ventral tegmental area and the midbrain (Figure 1.6). Glutamate is produced in the nerve terminals of these projections via two routes: 1) glutamine transported from glial cells, and 2) the Krebs cycle (Rowley *et al.* 2012). Once glutamate is produced, it is transported into vesicles via vesicular glutamate transporter. Glutamate stored in vesicles within the presynaptic neurons are released into the synapse when a presynaptic action potential stimulates Ca^{2+}-dependent exocytosis. In addition, a reversal of the cysteine/glutamate exchangers can sometimes cause release of non-vesicular glutamate to the extracellular space (Rowley *et al.* 2012).

Maintenance of extracellular glutamate and GABA concentrations is facilitated via reuptake by high-affinity sodium dependent excitatory amino acid transporters embedded in plasma membranes of neurons and astrocytes (such as EAAT1/GLAST, EAAT2/GLT-1, EAAT3/EAAC1, EAAT4, and EAAT5 for transporting glutamate; and GATs for transporting GABA) (Rowley *et al.* 2012; Danbolt 2001). Dysfunction of glutamate transporters are known to cause neuronal cell death due to glutamate-induced excitotoxicity (Rowley *et al.* 2012). The glutamate taken up by the transporters (i.e. the EAATs) embedded on glial cells is converted into glutamine by glutamine synthetase and transported out of the glial cells by system N-transporter and is subsequently taken up by system A-transporter on presynaptic neurons to help restore glutamate levels through the mitochondrial enzyme glutaminase. Glutamate taken up by

presynaptic neurons may also be metabolised into GABA by glutamate decarboxylase. Glutamate acts on two major synaptic glutamate receptor types: 1) ionotropic [alpha-amino-3-hydroxy-5-methyl-4-isoxazoepropionic acid (AMPA) and N-methyl-D-aspartate (NMDA)] and kainate receptors, and 2) metabotropic receptors including excitatory mGluRs 1 and 5 and inhibitory mGluRs 2, 3, 4, 6, 7, and 8 (Danbolt 2001; Purves *et al.* 2001). When glutamate binds to AMPA and kainate receptors, a conformational change occurs making them permeable to sodium, and this allows Na^{2+} influx into the postsynaptic neuron causing depolarisation. Conversely, NMDA receptors require the binding of glutamate and glycine, as well as depolarisation to release/dislodge Mg^{2+} from blocking the pores of NMDA calcium channels, thereby allowing Ca^{2+} influx into the postsynaptic neuron (Danbolt 2001; Purves *et al.* 2001).

On the other hand, mGluRs are G-protein coupled receptors that make use of second messenger systems for signal transduction and may therefore be slower in comparison with ionotropic receptors (Niswender and Conn 2010). Importantly, there seem to be an interaction between DA and glutamate systems, an aberration of which is not only implicated in ADHD but also in schizophrenia, Parkinson's disease, Alzheimer's disease, mood disorders and drug addiction (Rowley *et al.* 2012). It is hypothesised that glutamate modulate DA release in fronto-striatal pathways (Karreman and Moghaddam 1996).

1.2.5 Neurotransmitter interactions

Cortical and midbrain DA systems play crucial roles in schizophrenia, addiction, depression and Parkinson's disease, as well as in ADHD (Wallace *et al.* 2014; Arnsten 2011). Midbrain DA regions such as the ventral tegmental area and substantia nigra (A10 and A9 cell groups) that form the origin of the nigrostriatal and mesocorticolimbic DA pathways receive glutamatergic,

GABAergic, serotonergic and noradrenergic innervations which influence DA activity (Caravaggio *et al.* 2016).

Glutamate and DA interact in the prefrontal cortex and the basal ganglia (e.g. striatum), intimately modulating each other's function and release (Figure 1.6). The classical basal ganglia model developed in the 1980s predicts that striatal DA loss would reduce extracellular glutamate levels in the striatum and the cortex (Albin *et al.* 1995; Albin *et al.* 1989; Jones 2011). It also predicts that increased striatal DA would increase striatal and cortical glutamate levels (Caravaggio *et al.* 2016). Indeed, it is now well established that glutamate influences DA release in the prefrontal cortex (Feenstra *et al.* 1995), nucleus accumbens (Del Arco and Mora 2005), and midbrain DA neurons, by regulating *in vivo* firing activity, especially burst activity (Charlety *et al.* 1991). Administration of both metabotropic and ionotropic glutamate receptor agonists have also been shown to produce excitatory response in midbrain DA neurons (Chergui *et al.* 1993; Shen and Johnson 1997). The hypomonoaminergic theory of ADHD suggests that decreased DA and/or NA levels cause the inattentive and hyperactive behaviours associated with the disorder (Figure 1.2). While elevated DAT may underlie the decreased DA levels in ADHD (Cheon *et al.* 2003; Dougherty *et al.* 1999; Spencer *et al.* 2005), glutamate has also been shown to be decreased in the cerebral regions in ADHD patients, which could also contribute to the reduction of striatal and cortical DA levels in adult ADHD (Maltezos *et al.* 2014; Dramsdahl *et al.* 2011; Perlov *et al.* 2007). However, this classical model of the basal ganglia fails to take into account the influence of other neurotransmitter systems such as the cholinergic system that also excite midbrain DA neurons via nicotinic receptors (Obeso *et al.* 2008).

GABAergic inputs into midbrain DA neurons originate in the striatum and pallidum, and from intrinsic GABAergic interneurons of the midbrain (Mora *et al.* 2008). Administration of GABA

onto DA neurons induces hyperpolarisation, which results in an inhibitory response of DA neurons (Belousov and Pol 1997; Georges and Aston-Jones 2002). Moreover, extracellular GABA and DA levels are both increased by local infusions of both AMPA and NMDA glutamate receptor agonists in the basal ganglia (Cano-Cebrián *et al.* 2003; Hernández *et al.* 2003; Kendrick *et al.* 1996).

Noradrenergic afferents originating from the locus coeruleus provide excitatory inputs onto midbrain DA neurons via α_1-adrenergic receptors (Grenhoff *et al.* 1993; Grenhoff and Svensson 1993; Williams *et al.* 2014). However, serotonergic afferent inputs from the raphe nuclei induce inhibitory response of midbrain DA neurons (Kapur and Remington 1996).

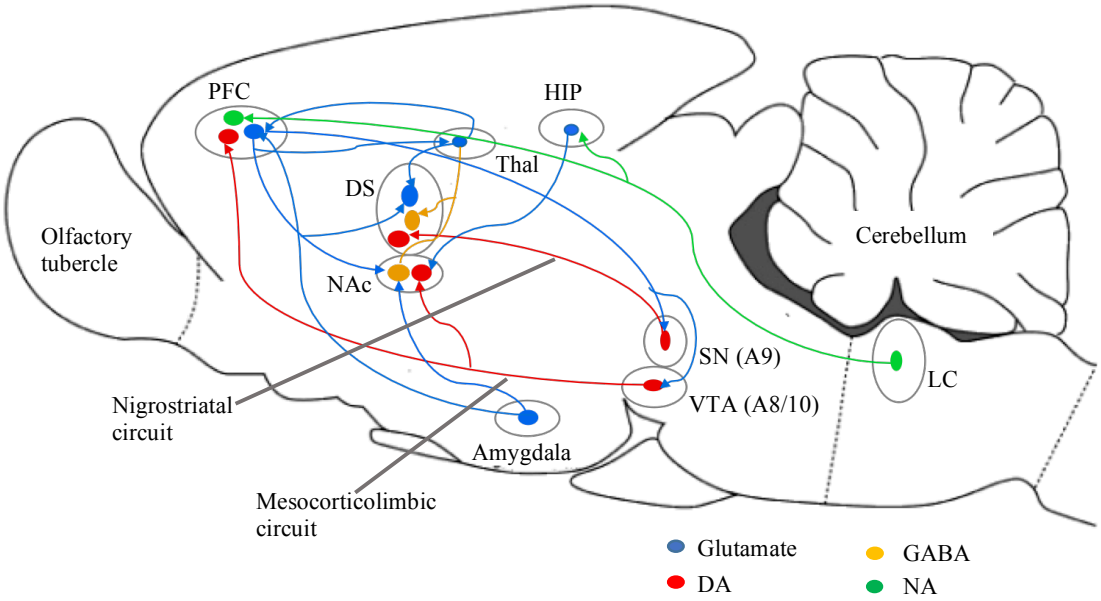

Figure 1.6: Neurotransmitter interactions in the mesocorticolimbic and nigrostriatal pathways.
Modulatory dopaminergic neurons (red) arising from the substantia nigra (SN, A9) project to the striatum (DS), and those arising from the ventral tegmental area (VTA, A10) also project to the nucleus accumbens (NAc) and prefrontal cortex (PFC). The locus coeruleus (LC) projects ascending noradrenergic axons (green) to the PFC and hippocampus (HIP). From the DS inhibitory GABAergic neurons (gold) extend to multiple sites including thalamus (Thal), with reciprocal glutamate connections (blue) to the DS, as well as connections to the PFC. PFC efferent glutamatergic neurons extend to the NAc, DS, SN, and VTA (adapted from Russo and Nestler 2013).

1.3 Neuroenergetics and ADHD

Some researchers have suggested that some forms of brain conditions including ADHD could be considered as cortical energy-deficit syndromes, in addition to the hypofunctionality of catecholamine systems (such as DA and NA) that regulate neuronal and astrocytic glucose and glycogen metabolism (Todd and Botteron 2001). The brain has a high energy demand and it utilises approximately 25% of total glucose produced in the body (Killeen *et al.* 2013). Astrocytes carry glucose from capillaries, store it as glycogen and convert it to lactate, which serves as the primary fuel for rapidly firing neurons (Killeen *et al.* 2013). It has been hypothesised that some of the ADHD symptoms may arise as a result of impaired lactate production by astrocytes that is insufficient to meet the brain's energy demands (Russell *et al.* 2006). This subsequently impairs performance in some high-energy demanding motor and cognitive tasks (Killeen *et al.* 2013; Russell *et al.* 2006). This hypoenergetics theory of ADHD seems to be supported by several strands of emerging evidence related to ADHD. For instance, ADHD patients are reported to have deficiencies in enzymes associated with energy supply and therefore require more energy than healthy controls, possibly because they have not sufficiently developed energy-efficient neural networks, including limited fully myelinated axons (Fair *et al.* 2010; Killeen *et al.* 2013; Nagel *et al.* 2011).

The recent finding of decreased *N*-acetylaspartate (NAA) levels in ADHD lends more support to the energy-deficiency hypothesis in ADHD and other related brain disorders (Soliva *et al.* 2010; Yang *et al.* 2010; Perlov *et al.* 2009). Not only is NAA a marker of neuronal integrity (McLoughlin *et al.* 2007), it is also a neuron-specific storage form of acetyl coenzyme A, an important component of energy production in Krebs cycle (Ariyannur *et al.* 2010). Clinical treatment with MPH elicits improvements in the reduced NAA levels seen in the cortex and other

brain areas of ADHD patients (Wiguna *et al.* 2012; Kronenberg *et al.* 2008). In addition to energy metabolism, NAA plays other crucial roles in the brain including: (a) lipid biosynthesis, which is required for myelin sheath formation, and (b) osmoregulation – whereby NAA acts as a constituent of a molecular water pump, facilitating the removal of intracellular water from myelinated neurons (Baslow 2002). Myelin sheaths are known to make neurotransmission faster and more energy efficient, thus their plausible alteration in ADHD (Nagel *et al.* 2011). This implies that transmission of information along axons is more energy consuming in ADHD patients, possibly causing the slow and variable reaction times in energy-demanding tasks associated with ADHD pathology (Harris and Attwell 2012; Russell *et al.* 2006; Killeen *et al.* 2013).

1.4 Synaptic plasticity

In most vertebrates, the brains communicate and store information by altering the CNS through an important process referred to as synaptic plasticity. This involves several mechanisms, such as changing existing synapses or substituting aged synapses with new ones (Kasai *et al.* 2003). These alterations involve dendritic spines, which are tiny, specialised, semi-autonomous, knob-like structures protruding from the main dendritic shaft and are often responsible for excitatory postsynaptic input (Soria Fregozo and Pérez Vega 2012). Depending on stimulus, cellular environment and location, dendritic spines can have rapid rearrangement capabilities and undergo constant turnover throughout life, playing an essential role in the processing of information in the mammalian CNS, particularly for excitatory synaptic transmission (Maiti *et al.* 2015). Given that they are highly plastic in nature and variations in their number and morphology determines the strength and stability of a synapse, dendritic spines are considered the “hot spot” of synaptic plasticity (Maiti *et al.* 2015). Interestingly, while most spines are stable in mature neurons, under conditions such as sensory input, stress, environmental enrichment, learning, social interactions,

prolonged exposure to addictive drugs (e.g. psychostimulants), and other behavioural paradigms, spines are often remodelled to appropriately sub-serve specific functions, such as memory (Kasai *et al.* 2003). In addition, rearrangement of the structures and functions of most dendritic spines influences synaptic connectivity and neuronal plasticity, which could control our memory, learning, motor coordination and behaviour (Maiti *et al.* 2015; Soria Fregozo and Pérez Vega 2012). Aberrations in spine formation and density are therefore often associated with several brain disorders including ADHD.

On the basis of their functions, the main signalling proteins, hormones, and growth factors identified in dendritic spines are categorised as: 1) actin binding and cytoskeletal proteins, 2) receptor tyrosine kinases and other kinases, 3) cell surface receptor adhesion molecules, 4) small GTPase associated proteins, 5) microRNA such as mRNA binding proteins and transcription factors, and 6) postsynaptic scaffolding proteins and adaptor proteins (Sala and Segal 2014). In ADHD, some of these plasticity-related proteins are known to be associated with the action of psychostimulants (e.g. MPH), while others are actually aberrant in the disorder. Some of the aberrant proteins in ADHD include brain-derived neurotrophic factor (BDNF), synaptosomal-associated protein 25 kDa (SNAP25), and activity-regulated cytoskeleton-associated protein (Arc) (Amiri *et al.* 2013; Barr *et al.* 2000; Corominas-Roso *et al.* 2013). Moreover, the implication of glutamatergic and GABAergic signalling in ADHD (Perlov *et al.* 2007; Perlov *et al.* 2010), indicates that postsynaptic scaffolding or adaptor proteins that are key regulators of multiple members within the glutamatergic and GABAergic pathway have become particularly important in ADHD (Lesch *et al.* 2013). Such scaffolding proteins that have attracted interest in ADHD include glutamate receptors (AMPA/NMDA/mGlu etc.) and $GABA_A$ receptor ($GABA_AR$), which are mainly localised in the spine head and play significant roles in synaptic

plasticity (Lesch *et al.* 2013). Similarly, other kinases involved in regulating spine structure and dynamics, such as cyclin dependent kinase 5 (Cdk5), have also been linked with ADHD, with animal models lacking Cdk5 showing increased locomotor activity that is corrected by psychostimulants (Krapacher *et al.* 2010). Interestingly, recent evidence also shows an association of the postsynaptic scaffolding/adaptor protein IRSp53 (insulin receptor substrate protein 53 kDa) with ADHD (Liu *et al.* 2013; Ribasés *et al.* 2009). The IRSp53 is a key player in cytoskeletal dynamics (discussed in detail in Chapter 7), which may be involved in NMDA receptor-linked synaptic plasticity through protein kinase C signalling (Hori *et al.* 2005). It may also be involved in cerebral asymmetry and confers risk for Autism spectrum disorders, which share some genetic risk factors in common with ADHD (Toma *et al.* 2011).

1.5 Involvement of some brain regions in the symptoms of ADHD

The well-established role of DA and NA in the frontal cortex, striatum, nucleus accumbens, and hippocampus, in varying behaviours, has recently been extended by findings showing that these brain regions operate together with the cerebellum to execute goal-directed behaviours, although it is through functionally distinct neural networks (Del Campo *et al.* 2011).

1.5.1 The frontal and parietal cortices

The frontal cortex, and to an extent, the parietal cortex, regulate attention, cognitive behaviour and reasoning, collectively referred to as 'executive functions'. These executive functions are necessary for planning and organisation. The frontal cortex regulates attention and motor responses through its connections with the sensory and motor cortices, the striatum and the cerebellum. Conversely, the frontal cortex regulates emotions through connections with the nucleus accumbens, amygdala and other midbrain regions mediating arousal response (Arnsten 2009). The right frontal and right parietal cortices are particularly important for the regulation of

attention and motor behaviour (Arnsten 2011). Functional imaging studies in humans have shown that the right frontal and right parietal cortices are less-activated when patients perform poorly on attentional tasks (Rubia *et al.* 1999; Vance *et al.* 2007). In contrast, these regions are active when patients perform better on such tasks and also when they successfully inhibit or stop movements (Arnsten 2009). Lesions to the right frontal cortex in monkeys induce impulsivity and hyperactivity (Kennard *et al.* 1941), which are among the major symptoms associated with ADHD. The catecholamines DA and NA are of major importance for this network and in the functions of the frontal cortex. Indeed, DA and NA dysfunctions are associated deficits in prefrontally-mediated cognitive functions, which are associated with several brain disorders, including ADHD (Wallace *et al.* 2014; Arnsten 2011). A moderate stimulation of D1 receptors by DA improves frontal cortex mediated working memory and attentional functions by suppressing inputs to neurons that are irrelevant to current demands (i.e. it decreases 'noise'). Stimulation of postsynaptic α_{2A}-receptors by NA also enhances the functionality of the frontal cortex by strengthening the appropriate network connections and permitting networks to maintain their firing for extended periods (i.e. increasing 'signals') (Arnsten 2009; Arnsten 2011).

1.5.2 The striatum and nucleus accumbens

The human striatum is organised into the dorsal striatum (which is referred to as 'striatum' in this thesis and it is involved in cognition and motor function) and ventral striatum (also referred to as 'nucleus accumbens'). The interest in the striatum is related to the fact that striatal DAT is the main target for stimulants (e.g. MPH) that are the preferred drugs for the treatment of ADHD. In fact, MPH has been shown to block up to 70% of DAT in the striatum, resulting in an enhanced striatal DA availability (Dougherty *et al.* 1999; Volkow *et al.* 2001). There are suggestions that this increased extracellular DA levels following striatal DAT blockade by MPH decreases background firing rates (i.e. decreases 'noise'), while increasing the signal of striatal neuronal

cells, which consequently improves attention and minimises distractibility (Volkow *et al.* 2001). On the other hand, the nucleus accumbens is suggested to mediate motivation, emotion and reward-related behaviour. It has been reported that stimulating the accumbens in rodents increases cocaine and amphetamine self-administration, and selective lesions to DA terminals in the accumbens attenuates the self-administration of these drugs (Moghaddam and Bunney 1989; Pettit *et al.* 1984). Indeed, evidence indicates that DA systems in the accumbens are particularly important for drug-related reinforcement behaviours such as drug self-administration and place preference (Moghaddam and Bunney 1989; Pettit *et al.* 1984).

1.5.3 The hippocampus

The hippocampus, which lies within the limbic system is an important structure playing crucial roles in the consolidation of information from short-term memory to long-term memory and spatial navigation (Milner and Klein 2016). Damage to the hippocampus results in memory loss and disorientation. Indeed, extensive bilateral hippocampal damage results in an inability to form and retain new memories (Milner and Klein 2016). Individuals with ADHD tend to have attentional and memory deficits, which may be related to abnormalities in the hippocampus. Indeed, a recent study found significantly reduced hippocampal volume in young medication naïve ADHD patients compared to matched controls (Posner *et al.* 2014).

1.5.4 The cerebellum

The cerebellum was initially only considered to play a significant role in motor control (Strick *et al.* 2009; Middleton and Strick 1994). However, it is now also suggested to be important to higher cognitive functions such as working memory, learning, emotion, and visuo-spatial processing, emphasising its importance in ADHD (Strick *et al.* 2009; Middleton and Strick 1994). There appears to be a strong interconnection between the cerebellum, frontal cortex and

the striatal structures, with some studies also suggesting that the cerebellum is capable of undergoing morphological plasticity much like hippocampus and some other cerebral areas (Strick *et al.* 2009; Middleton and Strick 1994).

With the strong interconnections displayed by multiple brain regions in the regulation of cognitive and motor behaviour, it is suggested that abnormalities related to the functions of monoamines (i.e. related to dopaminergic and noradrenergic functions), especially in the frontal cortex, parietal cortex, striatum, hippocampus, and cerebellum could contribute to the dysfunctions seen in several clinical syndromes including ADHD. Given this background, these brain regions were ideal targets for our investigations in the adolescent brain regarding the partly unknown mechanism of action of MPH, which remains the drug of choice for ADHD treatment.

1.6 Brain lateralisation and ADHD

Hemispheric asymmetries are evident in the anatomy, cytoarchitecture and neurochemistry of the vertebrate brain. Decades of research have shown that a number of cognitive abilities rely heavily on lateralised processing in the human brain, with the most widely investigated being language and visuo-spatial processing (Corballis 2009). As an example, for most right-handed individuals, being attentive to language-based stimuli results from an increased brain activity lateralised to the left hemisphere, while being attentive to visuo-spatial processing-based stimuli results from increased brain activity in the right hemisphere (Nielsen *et al.* 2013; Toga and Thompson 2003). Other cognitive domains relying on lateralised brain functionality include: emotional processing (Onal-Hartmann *et al.* 2012), fine motor skills (Arning *et al.* 2013), and memory (Habib *et al.* 2003), as well as face and body perception (Thoma *et al.* 2014) (see Figure 1.7). Case-control studies have shown that anatomical and functional asymmetries underlie brain functions as well as several brain disorders (Altarelli *et al.* 2014; Toga and Thompson 2003; Wang *et al.* 2015). A

recent study on dyslexic patients and matched controls suggested that an altered pattern of cortical asymmetry (e.g. within the planum temporale region of the cortex), preferring the right hemisphere might underlie dyslexia (Altarelli *et al.* 2014). Abnormal structural asymmetries have also been reported in Parkinson's disease, schizophrenia, and Alzheimer's disease (Derflinger *et al.* 2011; Wang *et al.* 2015). Although structural and functional asymmetries in the brain were previously thought to be unique to humans, both structural and functional asymmetries have been identified in non-human primates and other species including rats (Glick and Ross 1981; Toga and Thompson 2003; Lister *et al.* 2006; Kristofiková *et al.* 2010). For example, Japanese macaques have a right-ear advantage for processing auditory stimuli, while Passerine birds produce songs under the control of the left-hemisphere (Petersen *et al.* 1978; Nottebohm 1971; Toga and Thompson 2003). In male Sprague Dawley rats (the rat type used in this thesis), significant asymmetries have been found in the hippocampus, with the right hemisphere containing fewer neurons compared to the left hemisphere (Lister *et al.* 2006).

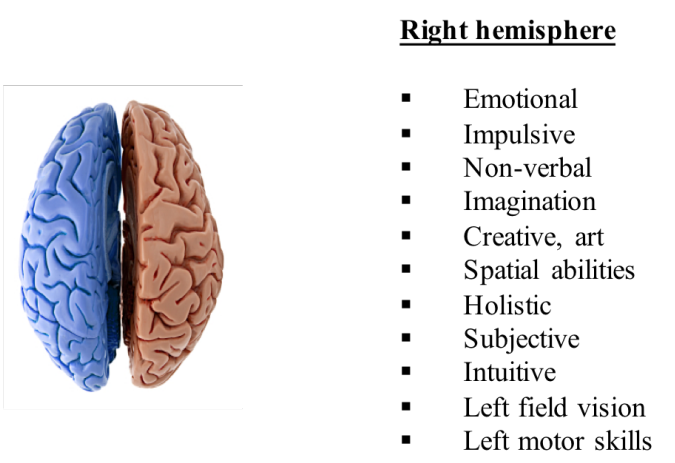

Figure 1.7: Lateralised functions of the brain.
Structural and functional asymmetries described in the vertebrate brain.

Cortical right-hemisphere dysfunctions are thought to have some roles in ADHD (Casey *et al.* 1997; García-Sánchez *et al.* 1997). The existence of such dysfunctions leads to expectations of

differences in lateralisation between ADHD patients and healthy individuals. In this regard, a number of studies have confirmed such expectations with a higher than expected rate of non-right-handed (ambidextrous and left-handed) individuals being observed in the ADHD population (Shaw and Brown 1991; Yamamoto and Hatta 1982). Converging evidence from imaging studies also suggest a reversed brain asymmetry in ADHD, with ADHD patients having a right-greater-than-left cortical asymmetry compared to controls (Filipek *et al.* 1997; Hynd *et al.* 1993; Semrud-Clikeman *et al.* 2000). Indeed, an abnormal pattern of brain lateralisation is suggested to contribute to aspects of the inattention and impulsivity symptoms of ADHD, with some patients showing asymmetrical performance deficits on visuospatial attention mostly for endogenous cuing on card sorting tasks (Semrud-Clikeman *et al.* 2000; Nigg *et al.* 1997; Carter *et al.* 1995).

1.7 Management of ADHD

Different treatment paradigms are available for the management of ADHD. There are both pharmacological and non-pharmacological treatment options. While environmental and behavioural psychotherapy are thought to be successful alone, in some cases, they may be more effective when used in conjunction with anti-ADHD drugs.

1.7.1 Pharmacological treatment options

Several pharmacological treatment options are available for ADHD treatment. These are categorised as: 1) stimulants e.g. MPH, amphetamine, 2) non-stimulants e.g. atomoxetine, clonidine and guanfacine, 3) tricyclic antidepressants e.g. desipramine, imipramine, clomipramine, amitriptyline, and nortriptyline, 4) MAO inhibitors e.g. selegiline, phenelzine, and, 5) Others e.g. bupropion and modafinil. Among these, the two main treatment options for ADHD are the stimulant and non-stimulant drugs (Biederman and Faraone 2005).

1.7.1.1 Stimulant drugs for ADHD treatment

The medications of choice in ADHD treatment are stimulants, and in most cases represent the first-line therapeutic option. MPH and amphetamine, which are known to enhance DA and NA neurotransmission, are the two main stimulants prescribed for ADHD treatment. While the stimulants MPH and amphetamine have similar clinical efficacy, they differ in duration of action, dosing, and adverse effect profiles in individual patients.

1.7.1.2 Non-stimulant drugs for ADHD treatment

An important development in ADHD treatment has been the use of the non-stimulant, atomoxetine. Atomoxetine blocks NET, which then attenuates ADHD symptoms by elevating NA in the synapse, mostly in the prefrontal cortex (Del Campo *et al.* 2011). While atomoxetine has measurable effects on improving ADHD symptoms and even represents the first-line drug in patients that do not respond to stimulant medication, it could have some hepatotoxic effects and therefore has limited use among patients with jaundice, pruritis, dark urine, or unexplained flu-like symptoms (Biederman and Faraone 2005). The two α_2-agonists, guanfacine and clonidine, are also used in the treatment of ADHD but due to the sparse efficacy data and side effects, they are rarely prescribed. However, a meta-analysis study reported that clonidine appears to be quite effective against ADHD (Connor *et al.* 1999). There are also indications that clonidine may be useful as an adjunct to stimulant medications, particularly when hyperactive, impulsive and aggressive symptoms are not well controlled, or when tics and sleep difficulties are present (Biederman and Faraone 2005). Guanfacine may also be moderately effective in treating ADHD symptoms and may also alleviate tic disorders. Common side effects of these α_2-agonists include sedation, depression and drowsiness (Biederman and Faraone 2005).

1.7.2 MPH - the main stimulant drug for ADHD treatment

Among the stimulant medications currently available for ADHD treatment, MPH remains the most commonly prescribed (Abbas *et al.* 2016; Lakhan and Kirchgessner 2012). MPH is sold under varying trade names, with Ritalin™ being one of the most familiar trade names.

1.7.2.1 Physico-chemical properties of MPH

MPH is a benzylpiperidine and a phenethylamine derivative that shares aspects of its basic structure with catecholamines. Given that MPH (methyl 2-phenyl-2-(piperidin-2-yl)acetate) has two chiral centers, four isomers of the drug are possible, with a pair each of erythro- and threo-isomers being distinguished. The threo-isomers are preferred, with only the d-threo-isomer exhibiting pharmacologically desired effects in ADHD (Figure 1.8) (Heal and Pierce 2006).

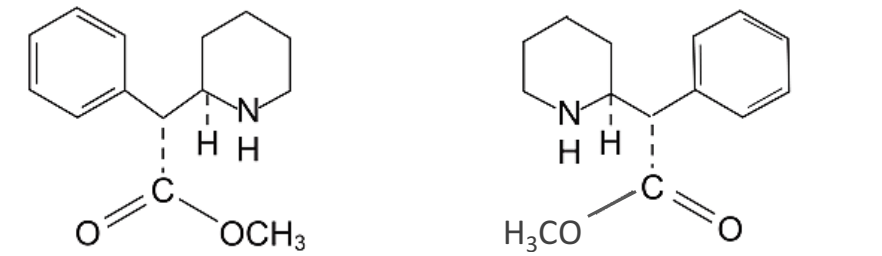

Methyl (2R)-2-phenyl-2-[(2R)-piperidin-2-yl]acetate
(also known as d-threo-MPH)

Methyl (2S)-2-phenyl-2-[(2S)-piperidin-2-yl]acetate
(also known as l-threo-MPH)

Figure 1.8: Chemical stuctures of d-threo- and l-threo-methylphenidate.
The d-threo- and l-threo isomers are mirror images of each other (enantiomers). The d-threo-isomer exhibits the desired pharmacological effects in treating ADHD.

1.7.2.2 Indications

When taken orally, MPH has a bioavailability of ~30% (range: 11-52%), with peak plasma concentration attained at approximately 2-4 hours for the short-acting (e.g. Ritalin), 3-8 hours for intermediate (e.g. Ritalin SR), and 8-12 hours for the long-acting (e.g. Concerta) type. MPH has a half-life of 2-3 hours, depending on the individual. MPH is contraindicated for individuals using monoamine oxidase inhibitors such as phenelzine (as hypertensive crisis may result), or those

with marked agitation, tension and anxiety (as the drug may aggravate these symptoms), as well as those with tics, glaucoma, Tourette's syndrome or hypersensitivity to any MPH ingredient, as it can worsen these conditions (Lu *et al.* 2006). The effect of the drug on unborn babies is not fully understood, hence pregnant women need counselling prior to MPH intake.

By increasing extracellular neurotransmitter (e.g. DA and NA) activity in the brain, MPH improves ADHD symptoms. The drug is reported to be effective in about 70% of users (Engert and Pruessner 2008; Greenhill *et al.* 2002). MPH medicated ADHD children generally exhibit improved relationships with family members and peers, and perform better at school, have longer attention spans and are less distractible and less impulsive (Greenhill *et al.* 2002). Therapeutic doses of MPH are known to enhance cognitive functioning, including working and episodic memory, as well as inhibitory control in both healthy individuals and ADHD patients (Engert and Pruessner 2008; Spencer *et al.* 2015). MPH is also known to improve task saliency and increase arousal (Volkow *et al.* 2005). The drug is a CNS stimulant and aside ADHD, it is indicated for the treatment of the sleep disorder, narcolepsy (Biederman and Faraone 2005). The drug's effective action against narcolepsy (excessive daytime drowsiness and sudden need for sleep), is due to its ability to increase wakefulness, vigilance and performance (Fry 1998).

1.7.2.3 Mechanism of action

MPH was approved for clinical use in 1955 and has been used in treating ADHD since the 1960s. However, there are still uncertainties regarding its mechanism of action. Neurochemically, MPH is known to influence DA and NA neurotransmission, playing a crucial role in cognition and motor activity. MPH binds to and blocks DAT, which is responsible for the removal of DA from the synapse and hence the termination of DA function. MPH-induced blockade of DAT, therefore increases DA concentration in the synaptic cleft and extracellular space (Volkow *et al.* 2005).

Therapeutic doses (0.3-0.6 mg/kg) of oral MPH has been shown to occupy more than 50% of DAT (Volkow *et al.* 1998). The highest specific MPH binding are often detected in the terminal regions of the nigrostriatal and mesocorticolimbic pathways (including striatum, accumbens, and prefrontal cortex) (Volkow *et al.* 1998; Volkow *et al.* 2005). Following the delivery of therapeutic MPH doses, the moderately increased extracellular levels of DA in the prefrontal cortex primarily stimulates D1 receptor and improve working memory functioning by suppressing inputs to cells not required for improving memory (i.e. reduces 'signal/noise' ratio) (Arnsten 2011).

Beyond the DA-specific effect, MPH also increases extracellular levels of NA by blocking its re-uptake by NET. In line with this, a rat-based microdialysis study, has shown that MPH increases both NA and DA efflux in the prefrontal cortex (Berridge *et al.* 2006). Although both NA and DA have crucial influence on cognitive functions under the control of prefrontal cortex, compared to NET there are relatively low levels of DAT present in the prefrontal cortex, which emphasise the potential significance of NA in the action of MPH in the prefrontal cortex (Arnsten 2009). Therapeutic MPH doses results in moderate increases of NA in the prefrontal cortex, which then engages α_2 adrenergic receptors, particularly the postsynaptic α_{2A}-receptor. The stimulation of the α_{2A}-receptor improves prefrontal cortex regulation of attention, emotion and behaviour by strengthening network connections between neurons and allowing networks to maintain their firing for long periods (increasing 'signal') (Arnsten 2011). Indeed, blocking of α_{2A}-receptors in the prefrontal cortex of non-human primates using yohimbine induces locomotor hyperactivity and impulsivity and impairs working memory, similar to what is seen in ADHD (Ma *et al.* 2005). Thus, currently existing data are consistent with the hypothesis that clinical MPH doses improve cognition, attention, and performance by increasing both DA and NA

availability, which in turn activate D1-like and α_2-adrenergic receptors, mostly within the prefrontal cortex (Engert and Pruessner 2008).

In the striatum, it is hypothesised that when DAT is blocked in the presence of a therapeutic MPH dose, extracellular or resting state DA level is elevated by about six-fold (moderate enhancement) (Engert and Pruessner 2008; Seeman and Madras 2002; Seeman and Madras 1998). The moderately elevated DA level then acts preferentially on pre-synaptic D2-like autoreceptors, decreasing impulse-triggered DA release. This decreased extracellular DA level would therefore result in limited activation of postsynaptic D1- and D2-like receptors, leading to reduced psychomotor activity, hence normalising striatum-mediated hyperactive symptoms of ADHD (Engert and Pruessner 2008; Seeman and Madras 2002; Seeman and Madras 1998). In line with this hypothesis, clinically relevant MPH doses have been shown to suppress locomotor activity in hyperactive rats (Kuczenski and Segal 2002). Higher MPH doses, however, markedly raise the magnitude of DA release and extracellular DA levels, overriding the presynaptic inhibitory mechanism, causing widespread activation of postsynaptic DA receptors, and triggering a generalised CNS stimulation (see Figure 1.2) (Engert and Pruessner 2008; Seeman and Madras 2002; Seeman and Madras 1998).

Emerging evidence suggests that MPH also exert significant effects on the inhibitory neurotransmitter GABA and the excitatory neurotansmitter, glutamate and its receptors, particularly NMDAR (Carrey *et al.* 2002; Cheng *et al.* 2014; Di Miceli and Gronier 2015). Other reports demonstrate effects of the drug on brain glucose, lactate and NAA levels, as well as other water-soluble brain metabolites (Tafazoli *et al.* 2013; Volkow *et al.* 2008). However, the extent and mechanisms by which MPH influence the glutamatergic and GABAergic systems, as well as

amino acids and other brain metabolites remains to be clarified, and hence addressed in this thesis by using proton nuclear magnetic resonance spectroscopy (^{1}H-NMR) (see Chapters 4, 5 and 6).

1.7.2.4 Adverse effects

Although MPH is generally well tolerated, there are some commonly observed adverse effects ranging from gastrointestinal, cardiac, and opthalmologic to CNS-based effects. Predominant CNS adverse effects include akathisia (restlessness/agitation), lethargy (drowsiness/fatigue), and irritability. The opthalmologic effects may be blurred vision and dry eyes, with some sparse reports of mydriasis (pupil dilation) and diplopia (double vision) (Jaanus 1992). The important gastrointestinal side effects are abdominal pain and weight loss. Cardiac adverse effects may also include mild changes in blood pressure and heart rate, palpitations, and tachycardia (rapid resting state heart beat rate). Other adverse effects include emotional liability, confusion, bruxism (grinding of the teeth), depression, hypersensitivity (skin rash, fever, urticaria), and rare cases of chest pain. Less serious but often reported side effects include nausea, appetite loss, hyperhidrosis (increased sweating), anxiety or nervousness, and insomnia (Kolar *et al.* 2008; Wilens *et al.* 2004).

There are some reports of mild reductions of growth rate following prolonged MPH intake, but causal relationships are yet to be established (Cortese *et al.* 2013). Importantly, MPH could worsen psychosis in psychotic patients, and in a few instances, it has been associated with the emergence of new psychotic symptoms (Kraemer *et al.* 2010). Additionally, in bipolar patients, the drug also has a potential of inducing mania (Wingo and Ghaemi 2008). Libido disorders, hallucinations, and disorientation are also reported, albeit rarely.

1.7.2.5 Recreational use and abuse liability

Although the therapeutic effects, safety, and efficacy of MPH in paediatric and adult ADHD are well documented, there are persisting concerns regarding its misuse, abuse and addiction potential. Indeed, the last few decades have seen a rapid rise in ADHD diagnoses and MPH-prescriptions. According to the estimates by the World Health Organisation (WHO), MPH consumption increased rapidly (~269%), from 4.66 to 17.9 defined daily doses per 1000 population, between 1995 and 2006 (Gahr *et al.* 2014). Interestingly, the number of MPH consumed worldwide, far exceeded the relative increase in the number of MPH prescriptions per year, from 15,044,359 to 30,137,136 (100%). This, has therefore fuelled debates about possible illicit MPH use for pharmacologic neuroenhancement or recreational purposes (Gahr *et al.* 2014; Dietz *et al.* 2013).

Given that MPH can improve performance on difficult and boring tasks, it is used by some students' as a study aid (Gahr *et al.* 2014; Dietz *et al.* 2013). The drug is also used by some athletes to enhance their performance (Lakhan and Kirchgessner 2012). Moreover, since only the symptoms of ADHD are treatable, young and adolescent patients rely on MPH over a prolonged period, raising concerns over possible drug dependence/addiction and potential long term effects on the developing brain (Wang *et al.* 2013; Zhu *et al.* 2011). A manifestation of these concerns is the Schedule II status assigned to MPH in the US Drug Enforcement Administration's scheduling scheme, with the drug placed in the same schedule/class as morphine and cocaine (Zhu *et al.* 2011). It is thought that the dose and duration of MPH administered is critical for eliciting therapeutic response and for any potential drug dependence issues. It is known that while therapeutic MPH doses improve working memory and learning, excessive doses beyond therapeutic range, could adversely affect cognitive control and working memory (see Figure 1.2)

(Arnsten 2009). Excessive stimulation of D1 receptor in the prefrontal cortex due to excessive stimulant medication or during stress, impairs cortical functioning by weakening several network connections and suppressing all neuronal firing (Arnsten 2009). Similarly, excessively high levels of extracellular NA in the prefrontal cortex following high MPH doses, engage lower affinity α_1- and β-receptors (rather than α_2- receptors), thus impairing cortical function by suppressing cortical cell firing (Arnsten 2009; Birnbaum *et al.* 2004).

1.7.3 Non-pharmacological treatment options

A number of non-pharmacological ADHD interventions have emerged, mostly due to concerns about the long-term safety of medications used in treating the disorder. Non-pharmacological interventions may be psychosocial or dietary in nature. The dietary interventions include: 1) restricted elimination diets, which involves the elimination of artificial colours or diets that provoke behavioural problems, and 2) free fatty acid supplementation, which involves supplementing diets of affected individuals with free fatty acids, particularly omega-3 and omega-6 supplements (Bélanger *et al.* 2009; Boris and Mandel 1994; Sonuga-Barke *et al.* 2013); this is vital as ADHD is thought to be secondary to essential fatty acid deficiency (Colquhoun and Bunday 1981). On the other hand, the psychosocial interventions include: 1) Cognitive training, which involves the use of computer-based systems to improve working memory, 2) neurofeedback (electroencephalogram), which involves teaching patients to produce brain-wave patterns consistent with 'focus', by allowing patients to see their own brain wave patterns when they are focused on a particular task and when they are not. Thus, patients are trained to keep their brain active while concentrating or performing certain tasks, and 3) parent education and classroom management, which involves improving parents' and teachers' understanding of the child's behaviour and equipping them with strategies to improve functioning and communication,

while discouraging unwanted behaviour (Bakhshayesh *et al.* 2011; Sonuga-Barke *et al.* 2013; Steiner *et al.* 2011).

1.8 Genetically unmodified *vs.* genetic models of ADHD

Although animals cannot be used in studying complex human behaviour such as language, they have similar basic behavioural, genetic and developmental processes (Andersen and Navalta 2011). Despite some obvious limitations, experimenting on rodents (non-modified) offer valuable data on: (a) neurobiological basis of abnormal behaviours associated with disorders like ADHD, (b) the normalisation of abnormal behaviour after drug treatment, and in (c) identifying therapeutic targets (Andersen and Navalta 2011). In general, preclinical studies on rodents offer the following advantages:

- Controlled means of investigating a drug's effect independent of drug-drug interactions (i.e. the medication history of animals used in experiments are known and controlled).
- Allows the researcher to get better control over confounding factors such as environment, diet, and learning history.
- Efficient and more realistic means of evaluating the chronic effects of a drug.
- An avenue for studying a drug's effect irrespective of the underlying disease state.
- A good means of investigating the mechanism of action of specific medications at various stages of neurodevelopment.

Interestingly, several animal models of ADHD have been proposed ranging from chemically-induced and environmentally-induced models to genetically modified models. The genetic models include spontaneously hypertensive rat (SHR), Naples High Excitability rat, mice expressing human mutant thyroid hormone receptor, DAT knockout mice, SNAP-25 deficient mutant coloboma mouse, tachykinin-1 receptor knockout mouse, and a nicotinic receptor knockout mouse. The chemically induced models of ADHD include pre- or early post-natal animals exposed to nicotine, ethanol, polychlorinated biphenyls, or 6-hydroxydopamine. The

environmentally induced models available include neonatal anoxia and rat pups reared in social isolation. While most of these animal models have abnormalities in the monoaminergic systems, several of them do not satisfy the established criteria for animal models of ADHD (Russell *et al.* 2005). The working list of criteria for an optimal animal model of ADHD suggests that the model should have; (i) face-validity – implying that it should mimic the fundamental behavioural characteristics of the disorder such as impulsiveness and hyperactivity (these must be absent in a novel non-threatening environment and should develop gradually over time), as well as sustained attention deficit (this must be demonstrated only when stimuli are well spaced in time), (ii) construct-validity – i.e. the model must conform to a theoretical rationale for ADHD, implying that the model should demonstrate altered reinforcement of novel behaviour, as well as deficient extinction of previously reinforced behaviour, (iii) predictive-validity – i.e. the model must predict novel aspects of ADHD-related behaviour, genetics, and neurobiology, (iv) the model should be neurodevelopmental, preferably a genetic model (Sagvolden *et al.* 2005).

Among the existing animal models, the SHR rats and DAT-knockout mice are commonly used. While these animal models provide useful information regarding various aspects of ADHD, none of these models can truly reflect this human neurodevelopmental disorder. For instance, the DAT-knockout mouse model lacks the gene encoding DAT, therefore this model exhibit hyperactivity and shows deficiencies in learning and memory tasks (Russell *et al.* 2005). However, among other factors, the DAT-knockout mouse models have non-functional striatal D2 autoreceptors, with postsynaptic striatal D1 and D2 receptors being down-regulated by approximately 50% (Gainetdinov *et al.* 1999). In reality, this magnitude of striatal D1 and D2 receptor down-regulation does not appear to exist in ADHD patients, hence limiting the usage of this model as accurate ADHD models (Gainetdinov *et al.* 1999). In a similar vein, although SHR

rats are probably the most established ADHD models, hypertension remains a major confounding factor in this model. The development of hypertension in the SHR models is reported to be due to a repeatedly increased release of NA from the sympathetic nerve terminals (Russell *et al.* 2005). Variability in response to stimulants has also been reported in the SHR model. In this regard, some inter-species differences in relation to genetics, behaviour and responses to ADHD medications (such as amphetamine) have been reported between SHR rats and the WKY rats that are commonly considered as the controls for SHR. For instance, some blood group antigens and isozymic markers of the major histocompatibility complex in SHR and WKY rats is reported to be different (H'Doubler *et al.* 1991). Thus, such differences could introduce confounding factors when using this model.

Given the variations in human ADHD and existing animal models of the disorder, and the difficulty associated with obtaining a model that perfectly satisfies all the criteria for an ideal animal model, we used genetically unmodified animals in this thesis. This ensures that an important foundation is laid for the development of a more radical treatment paradigm, which will be preventive and curative but not just symptom ameliorative (Andersen and Navalta 2011). Moreover, using non-genetically modified animals in this thesis ensured that only drug-specific changes are observed and reported independent of underlying disease state, which is something that remains difficult to tease apart in clinical studies (Andersen and Navalta 2011).

1.9 Project aims

The aim of this thesis is three-fold: 1) to examine the treatment duration and region-specific effects of MPH on monoaminergic targets, 2) to use the ^{1}H-NMR approach to examine previously unexplored effects of MPH on water-soluble metabolites in the brain, and 3) to

compare the acute and chronic effects of MPH treatment on DA and neuroplasticity-related targets, as well as metabolic pathways in the developing brain.

1.9.1 Specific aims

- To establish the treatment-duration and region-specific effects of MPH on protein targets in the cortico-striato-cerebellar pathways.
- To evaluate the acute, chronic and lateralised effects of the drug on brain neurochemistry and metabolic markers.
- To use a broad range of methodologies to examine the importance of the cerebellum in the mechanism of action of MPH.
- To investigate the action of MPH on neuroplasticity-related genes and their corresponding proteins.

CHAPTER 2

2 Materials and methods

2.1 Animals and treatment

2.1.1 Housing and environmental conditions

Young (20-25 days old; 80-100 g) to adolescent (35-40 days old; 180-220 g) male Sprague-Dawley rats were used for the experiments in this thesis and were purchased from Charles River (UK). All animals were housed six per cage under controlled conditions of light (12/12 h light-dark cycle) and temperature (22-25°C, 45% humidity), with free access to food and water. After five days of acclimatisation, the rats were used for the experiments. All animal experiments in this study were carried out in strict accordance with the UK Home Office guidelines and the Animal Scientific Procedures Act (1986).

2.1.2 Drug treatment

The animals were randomly assigned to treatment (MPH) or control (saline) groups within the acute and chronic treatment groups, with 6, 12 or 18 animals being in a group, depending on the experimental design and technique used. The rats were weighed, and those in the control groups received either a single 1.0 ml/kg saline injection (acute group) intraperitoneally (i.p) or twice-daily saline injections for 15 days (chronic group). The rats in the MPH groups were injected with either a single 2.0 mg/kg MPH dose or a 5.0 mg/kg MPH dose (acute groups) and those in the chronic groups received a twice-daily 2.0 mg/kg MPH dose i.p for 15 days (chronic treatment) at 9 am and 5 pm each day. Considering the high metabolic rate in rats compared to humans, doses of MPH used in this study have previously been shown to achieve clinically relevant therapeutic doses (8-40 ng/ml) (Balcioglu *et al.* 2009; Kuczenski and Segal 2005; Kuczenski and Segal 2002). In addition, similar doses have been reported to alter brain transmitters including DA and NA, as well as the expression of plasticity-related genes and proteins (Banerjee *et al.* 2009; Réus *et al.* 2014; Wagner *et al.* 2009). The rats in the acute groups were 35-40 days old on the day of experiment (180-220 g). However, the rats in the chronic

groups were 20-25 days old at the start of the experiments, while they were 35-40 days old at the end of the experiments (180-220 g). Overall, the weights of the animals receiving saline treatment (controls) and MPH treatment were not statistically different (p = 0.78; n=144 rats) on the day they were sacrificed (Figure 2.1).

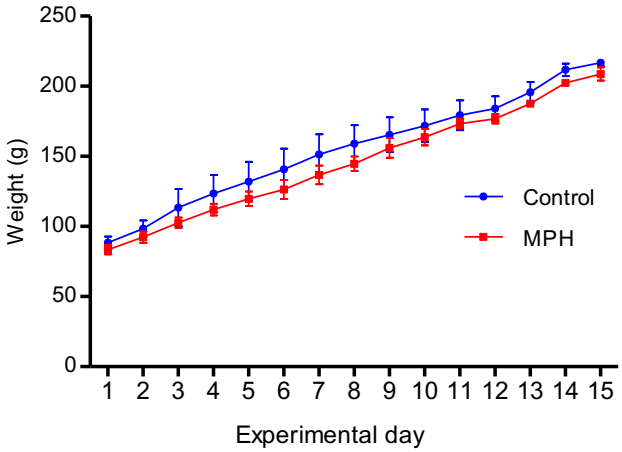

Figure 2.1: Weight of animals across experimental days 1 to 15.
A total of 144 animals were used in this thesis, with 72 animals each receiving either saline (control group) or MPH treatment (MPH-treated group). In general, the animals in the control groups (average weight = 215.6 g) weighed slightly more than the animals receiving MPH treatment (average weight = 210.7 g) on experimental day 15 but this difference was not statistically significant ($p > 0.05$).

2.1.3 Dissection of brain tissues

On the day of experiment, the animals were sacrificed by rapid cervical dislocation 1 h after last injection for experiments on brain neurochemistry, and 24 h after the last injection for protein and gene expression analyses experiments (Schaefer *et al.* 2006). Using a fine scalpel and the Paxinos and Watson rat brain atlas as a guide (Paxinos and Watson 2006), the left and right brain hemispheres were separated by a midline cut and the brain regions corresponding to the frontal cortex, striatum, nucleus accumbens, hippocampus, parietal cortex, and cerebellum in the left and right sides of the brain were dissected out (see Figures 2.2 and 2.3). In some experiments, the left and right cerebral hemispheres were also dissected out for neurochemical analyses. Following

dissection, the brain regions were snap frozen in isopentane, before being weighed and stored at -80ºC prior to analysis.

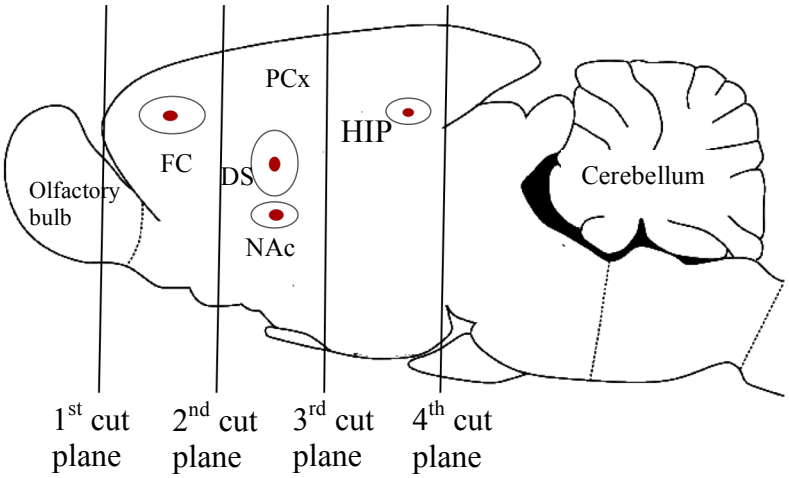

Figure 2.2: Central neuronal pathways containing DA in the rat brain.
There were four cut planes: 1st cut plane, was at the connection of the olfactory bulb and the frontal cortex (FC); 2nd cut plane, was anterior to the corpus callosum; 3rd cut plane, was anterior to the fornix; and 4th cut plane, was anterior to the midbrain substructures. Abbreviations: DS, striatum; NAc, nucleus accumbens; PCx, parietal cortex; HIP, hippocampus.

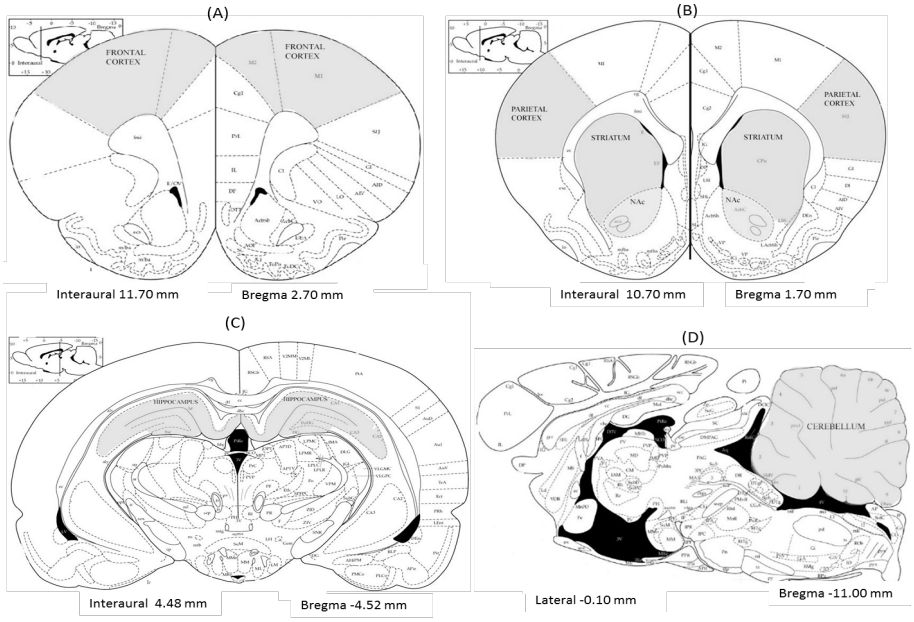

Figure 2.3: Representation of the examined brain regions.
(A) frontal cortex; (B) parietal cortex, striatum, and nucleus accumbens (NAc); (C) hippocampus; and (D) cerebellum, based on Paxinos and Watson rat brain atlas (Paxinos and Watson 2006).

2.2 ^{1}H-NMR metabolomics

Metabolomics refers to the comprehensive profiling of multiple metabolite concentrations and their changes in response to drugs, genetic modulations, environment, and diet, in order to identify the beneficial and adverse effects of such interactions (Beckonert *et al.* 2007). High resolution ^{1}H-NMR is a quantitative technique that gives detailed information regarding the features (i.e. atomic nuclei properties and interactions) of solution-state molecules (Beckonert *et al.* 2007). In a typical NMR experiment, a solution of a biological sample in a 5.0 mm glass tube is placed between the poles of a powerful external magnet (a 400 MHz external magnet was used throughout this thesis) (Figure 2.4). A radiofrequency pulse is then applied, via the Fourier transformation method (Gallagher *et al.* 2008), to 'excite' all the proton nuclei in the samples at the same time. Excited nuclei resonate or flip from one energy state to another e.g. from low energy state to a high-energy state (Figure 2.5). As the 'excited' nuclei 'relax' back to the equilibrium (or low energy state), complex radio wave frequency resonances are emitted (i.e. free induction decays), which is analysed computationally and transformed to produce the typical NMR spectra. The obtained NMR spectra can then be analysed using available statistical packages.

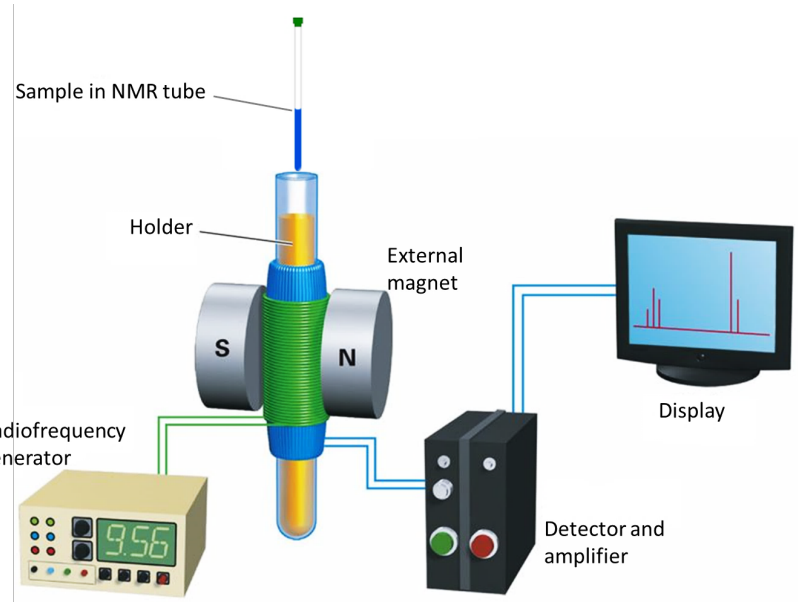

Figure 2.4: Schematic operation of a simple NMR spectrometer.

In principle, NMR is concerned with the magnetic properties of the nucleus of an atom, particularly the ability of the nuclei to spin i.e. nuclear spin (I). The net spin of a nucleus is dependent on the nucleon composition (i.e. the number of neutrons and protons). For example, if the number of neutrons and protons are both even, the nucleus has no spin (i.e. I = 0; e.g. ^{12}C, ^{16}O, ^{32}S) but if the number of neutrons plus protons is odd, the nucleus has a half-integer spin (i.e. I = 1/2, 3/2 or 5/2; e.g. ^{1}H, ^{13}C, ^{19}F, ^{31}P). Atoms with I = ½ nuclei (e.g. ^{1}H, ^{13}C, ^{31}P) are particularly measurable in NMR spectroscopy. When a nucleus with I = ½ is placed in an external magnetic field, it can either align itself with the direction of the magnetic field (low energy state) or against it (higher energy state). If radio waves are applied it is possible for the nuclei in the lower energy state to absorb the applied energy and 'flip' to the higher energy state (Figure 2.5). The absorption of the energy or the subsequent release of the energy (i.e. energy difference between low energy and high energy states) can be observed as the nucleus 'relaxes' back to the lower energy state. The radio waves are applied by scanning each individual nucleus slowly through a range of radio wave frequencies (this is called continuous wave) or by using a

more recent method, the Fourier Transformation method, where one big broad pulse of radio wave is applied to excite all nuclei. The resultant 'free induction decays' (FIDs) or resonances are transformed into the NMR spectrum we know (see Chapter 4, Figure 4.2).

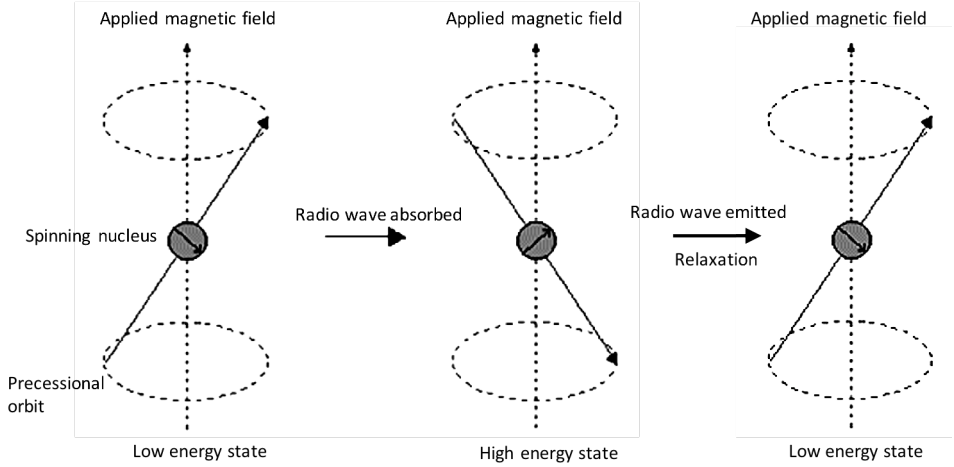

Figure 2.5: Excitation and relaxation of a nucleus.
When a low energy state ½ spin nuclei is excited following the absorption of a radio wave, it flips the magnetic moment so that its spin direction opposes the applied magnetic field (high energy state). When the radio wave is emitted, the ½ spin nuclei returns to equilibrium (low energy state). This produces resonant signals that are transformed into the typical NMR spectra. Nuclei in an NMR experiment are held in a sample. The sample containing the nuclei is called the lattice. The nuclei in the lattice are in a vibrational and rotational motion, creating a magnetic field called the lattice field. This lattice field has many components that can interact with the nuclei in the higher energy state causing them to lose energy (and returning to the low energy state). The average lifetime of nuclei in the higher energy state is referred to as the relaxation time (T_1) or relaxation delay. Another relaxation mechanism called the transverse or spin-spin relaxation is characterised by a relaxation time T_2.

The description in Figure 2.5 applies to isolated nuclei (or isolated protons). However, in a real molecule, there are electrons surrounding the nuclei (or protons in the nuclei). These electrons move in response to the applied external magnetic field and 'shield' the protons by generating local magnetic fields to oppose the stronger external magnetic fields applied (i.e. nuclear shielding). The external magnetic fields must therefore be increased in order to achieve resonance or 'flipping' (i.e. absorption of the radio wave frequency). The increments are quite small, often in parts per million (ppm). The differing electronic environment around each nucleus (i.e.

differing nuclear shielding) means that each ½ spin nucleus would not give resonant signals at the same frequency values. In this regard, compounds with increased nuclear shielding produce resonant signals at the higher field (closer to the zero point) of the NMR spectrum and the vice versa, which results in a (^{1}H-NMR) spectrum with resonant signals from individual atomic nuclei that are spread over a 0 ppm to 10 ppm range. It is convenient to reference the resonant signal frequencies to a standard (e.g. TSP, trimethylsilylpropanoic acid), which produces a resonant signal at the zero point and can therefore be used as a reference signal. The difference (in ppm) of each resonant signal from this zero point is referred to as the chemical shift (δ).

In general, the main stages of NMR-based metabolomics include sample preparation, data acquisition, data processing, metabolite identification, and data analysis and interpretation (Figure 2.6) (Quansah and Karikari 2016).

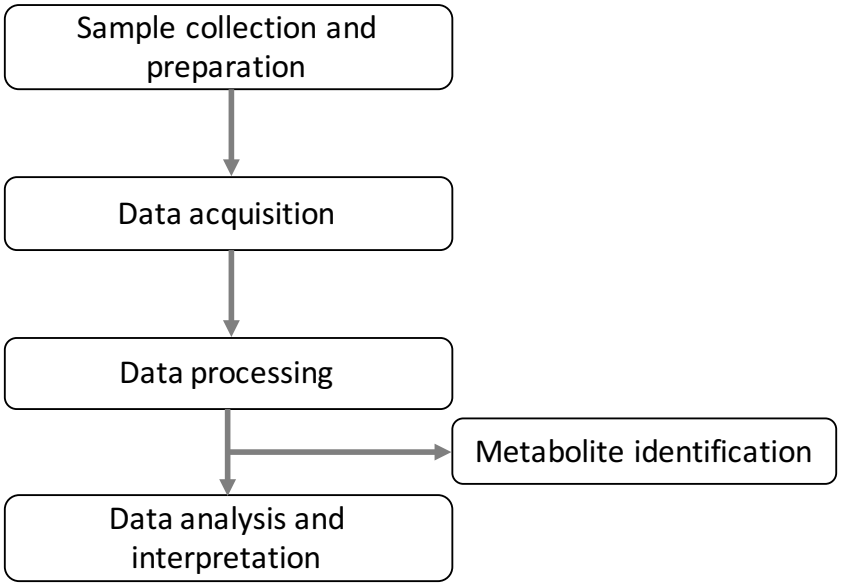

Figure 2.6: Typical ^{1}H-NMR metabolomics workflow.

The sample preparation is an important step and requires the use of suitable solvents that have no hydrogen (e.g. CCl_4 - carbon tetrachloride) to prevent the introduction of interfering resonant

signals. However, as CCl_4 is a poor compound for many polar solvents, deuterium labelled compounds (e.g. D_2O) are now preferred since deuterium has a different spin (i.e. spin 1) that is not visible in a spectrometer focused on protons (Quansah and Karikari 2016). At present, NMR spectral data is acquired using powerful external magnets (100 – 900 MHz) and Fourier Transformation methods. Free data processing tools such as ACD Labs (http://www.acdlabs.com/) are available for obtaining integral values from the obtained sample spectra. The spectral data can then be analysed statistically (multivariate and univariate data analysis) using online resources such as *MetaboAnalyst* (http://www.metaboanalyst.ca/). A major challenge associated with ^{1}H-NMR spectroscopy has to do with overlapping/co-resonances, where different metabolites may have resonant signals in the same region of the spectrum. However, this challenge can be overcomed by performing further NMR experiments – two dimensional (2D) experiments, such as HSQC (Heteronuclear Single Quantum Correlation), COSY (COrrelation SpectroscopY), TOCSY (TOtal Correlation SpectroscopY) and STOCSY (Statistical TOtal Correlation SpectroscopY). These 2D experiments operate by correlating the chemical shifts of hydrogen nuclei with other nuclei (e.g. ^{13}C nuclei or even another hydrogen nuclei). In addition, the identities of resonant signals are verified using ^{1}H-NMR and 2D spectral information available from online resources such as the human metabolome database (HMDB; http://www.hmdb.ca/). The NMR metabolomics stages employed in this thesis are discussed in greater detail below.

2.2.1 Preparation of brain extracts for NMR analysis

The frozen brain samples were retrieved and extracted using acetonitrile. The extraction procedure used was based on that described by Waters *et al.* (2002), but with some minor modifications. In brief, the frozen tissue samples were weighed before being homogenised in an equal measure (1:1 dilution) of acetonitrile (Fisher Scientific, UK) and HPLC-grade water (4 ml

per gram of tissue). Homogenates were kept on ice for 30 mins, and then centrifuged at 10,000 x *g* for 10 mins at 4°C (Sorvall Legend Micro 17R, Thermo Scientific, UK). The upper aqueous phase of each sample was extracted and lyophilised (freeze-dried). The residue for each sample was reconstituted with 50 µl of 1 M sodium phosphate buffer (pH 7.0) and 550 µl of deuterium oxide (D_2O) containing 0.9 mM of TSP (Sigma Aldrich, UK). While the D_2O provided the deuterium lock signal for the NMR spectrometer, the TSP provided the chemical shift reference (δ 0.00 ppm). Following centrifugation at 10,000 x *g* for 5 mins, the supernatant of each sample was transferred into a 5.0 mm NMR tube (Norell, UK) for ^{1}H-NMR spectroscopy.

2.2.2 Plasma preparation for NMR analysis

Trunk blood from MPH-treated and control animals were collected into BD Vacutainer lithium heparin blood collection tubes (BD, USA). Blood samples were then centrifuged at 13000 x *g* for 15 mins. Following centrifugation, 500 µl of blood plasma from the blood samples were dispensed into fresh Eppendorf tubes. 50 µl of D_2O without TSP (Fisher Scientific, UK) was then added to the plasma samples to provide deuterium lock signal for the NMR spectrometer. The mixture was centrifuged at 10000 x *g* at 4°C for 5 mins. The supernatants were then transferred into 5.0 mm NMR tubes (Norell, UK) for ^{1}H-NMR spectroscopy.

2.2.3 ^{1}H-NMR experiments

All the ^{1}H-NMR experiments were done using a Bruker Avance AM-400 spectrometer (Leicester School of Pharmacy facility, DMU, Leicester, UK) operating at a frequency of 399.94 MHz and a probe temperature of 298 K (25°C). The spectra were acquired using the *noesygppr1d* (TOPSPIN version 3.0, Bruker Biospin) pulse sequence for water suppression. The number of scans was 128, with a relaxation delay of 3 s, a spectral width of 4,800 Hz and a time domain of 32 K points. An exponential line broadening of 0.3 Hz was applied to the free induction decays (FIDs) prior to Fourier transformation. A major consideration when acquiring ^{1}H-NMR metabolomic

data is that, for some biofluids such as plasma that are not pre-treated, the samples often contain large molecular weight molecules such as lipoproteins and triglycerides that give rise to broad signals in the resultant spectra. Such broad signals may obscure the narrow signals from lower molecular weight molecules such as amino acids and sugars. To enable the observation of narrower signals, the one dimensional ^{1}H-CPMG (Carr-Purcell-Meiboom-Gill) pulse sequence was applied. The CPMG procedure employs T_2 spectral editing (i.e. spin-spin relaxation) that attenuates the contribution of large biomolecules.

2.2.4 Pre-processing of NMR Spectra

The ^{1}H-NMR spectra were corrected manually for phase and baseline using ACD/NMR processor (academic edition; Ontario, Canada) software before data analysis. All the ^{1}H-NMR spectra of the brain tissue samples were referenced to the TSP resonance at δ = 0.00 ppm, while the ^{1}H-NMR spectra of the plasma samples were referenced to the lactate resonance (1.26-1.33 ppm). An 'Intelligent-Bucketing' method was employed for dividing the spectrum into integral segments, ranging from 0.50 to 9.00 ppm, with all the integral values for brain being normalised to the TSP peak (δ, 0.00 ppm). The region from 4.60 to 5.10 ppm (representing H_2O/HDO peaks) in the brain sample was removed prior to the bucketing procedure. Generally, datasets of about 20 - 80 rows (samples) x 110 - 150 columns (variables) were obtained after removing regions containing 'noise' signals (no peak areas).

2.2.5 Multivariate and Univariate Statistical Analysis

Univariate and multivariate statistical analysis were performed on the TSP-normalised integral values. Both Principal Component Analysis (PCA) and Partial Least Squares Discriminant Analysis (PLS-DA) were performed using *MetaboAnalyst 3.0* (Xia *et al.* 2015), a web based metabolomics data analysis resource. PCA was carried out to ascertain inherent similarities of the spectral profiles and to detect any potential outliers (abnormal data points) in the datasets, while

PLS-DA was conducted for class discrimination and biomarker identification. Spectral data were further analysed using Orthogonal Projection to Latent Structure Discriminant Analysis (OPLS-DA), to remove any confounding variation and focus solely on the effect of drug treatment. Thus, OPLS-DA maximises the class (metabolite) selection between the control and drug-treated classes. The default 10-fold cross validation was applied in order to guard against model over-fitting. Prior to any univariate and multivariate analysis, the dataset was cube root transformed and Pareto scaled in order to satisfy assumptions of normality and homoscedasticity (i.e. assumption that variance around the regression line is the same for all values of a predictor variable), conditions necessary for the parametric tests further performed. To explore the performance of the different subsets and combination of discriminatory metabolites previously selected by PLS-DA or OPLS-DA, ROC (Receiver Operating Characteristic) curve analysis (see Figure 4.3, Chapter 4) was conducted using the option available in *MetaboAnalyst 3.0*.

Univariate analysis was also carried out using an ANOVA model (conducted with the corresponding function in R 3.1.2 statistical software) in which 2 factors and 3 primary sources of variation were incorporated (for samples involving the left and right hemispheres): (1) 'treatment status' (MPH-treated *vs.* control rats) (T_i); (2) 'brain hemisphere' (left *vs.* right) (H_j) and (3) 'treatment status' x 'brain hemisphere' (TH_{ij}) combined effect. This experimental design is represented by equation 1, in which Y_{ij} represents the (univariate) response variable values observed, μ its overall population mean value in the absence of any significant sources of variation, and e_{ij} the unexplained error (residual) contribution.

$$Y_{ij} = \mu + T_i + H_j + TH_{ij} + e_{ij} \qquad (1)$$

This univariate analysis model (equation 1) was used to further test the effect of 'treatment status' (MPH-treated *vs.* control samples) or 'brain hemisphere' (left bain *vs.* right brain), in order to

confirm the changes observed following the multivariate analysis. In addition, in samples where multivariate analysis was not statistically significant, the univariate analysis was performed to determine which individual variables (metabolites) are statistically significant. In such cases, Bonferroni correction [where p = (0.05/total number of buckets for each sample)] was further applied in order to guard against type I error (false positives).

2.2.6 Metabolite Identification

^{1}H-NMR resonance signals for brain and plasma samples were assigned on the basis of literature values (Govindaraju *et al.* 2000; Gao *et al.* 2012; Liu *et al.* 2014), information available in databases such as the Human Metabolome Database [HMDB] (Wishart *et al.* 2013), and by the consideration of chemical shift values, coupling patterns and coupling constants. The two-dimensional NMR techniques ^{13}C-^{1}H HSQC (Heteronuclear Single Quantum Correlation), ^{1}H-^{1}H COSY (COrrelation SpectroscopY), TOCSY (TOtal Correlation SpectroscopY) and STOCSY (Statistical TOtal Correlation SpectroscopY) were employed in order to confirm these assignments.

2.2.6.1 ^{13}C-^{1}H HSQC

The 2D Heteronuclear Single Quantum Correlation experiment operates by correlating the chemical shifts of hydrogen's with those of carbon-13 nuclei to which they are directly attached through one-bond ^{13}C-^{1}H coupling constants ($^{1}J_{C,H}$). HSQC, therefore introduces new and orthogonal dimension (available from the C-13 chemical shift), beyond the normal ^{1}H-NMR, thus yielding more information on the structure of metabolites (Dona *et al.* 2016). HSQC also provides much more sensitive response to minor changes in metabolite structure than ^{1}H-NMR, as the C-13 chemical shift has a higher range (mostly 220 ppm) than ^{1}H-NMR chemical shift (mostly 10.0 ppm). The HSQC spectra were acquired on the Bruker Avance AM-400 spectrometer (Leicester School of Pharmacy facility, DMU, Leicester, UK). The HSQC spectral

acquisition was done using the *hsqcedetgpsp.3* pulse sequence (TOPSPIN version 3.0, Bruker Biospin), 128 scans for 128 increments were acquired for each spectrum. Spectra were collected with 2048 points in t_2 and 256 points in t_1 over a sweep width of 66,000 Hz and 4800 Hz and in F1 and F2, respectively. A 2D ^{13}C-^{1}H HSQC spectrum for creatine has been shown in Figure 2.7.

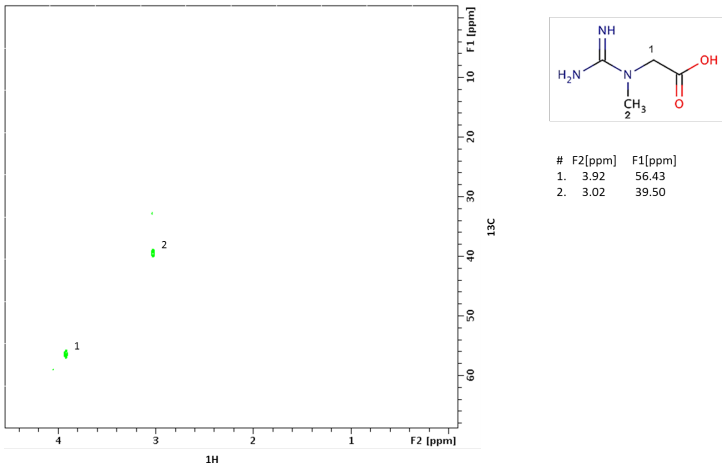

Figure 2.7: 2D ^{13}C-^{1}H HSQC spectrum (correlation of a ^{13}C spectrum and a ^{1}H spectrum). Obtained from a creatine standard revealing the exact locations of the creatine resonant signals in a two-dimensional (x and y) plane.

2.2.6.2 Two-dimensional ^{1}H-^{1}H COSY and TOCSY

The 2D correlation spectroscopy (COSY) and total correlation spectroscopy (TOCSY) NMR experiments were performed to elucidate further structural information on the small molecules of interest. Both COSY and TOCSY provide similar information regarding the directly coupled hydrogen's, but TOCSY provides further structural information by detecting larger, interconnected groups of spin-coupled hydrogen's (Dona *et al.* 2016). The 2D COSY and TOCSY experiments were carried out at 27°C on the Bruker AV-400 MHz (DMU, UK). COSY spectra were acquired using the *cosygpprqf* pulse sequence (TOPSPIN version 3.0, Bruker Biospin), with presaturation during relaxation delay utilising gradient pulses for selection. The spectral width for the F1 and F2 axes was 4800 Hz, with 2048 data points being collected in F2. While the total acquisition time was 7 h, the relaxation delay was 4.5 s. A sine function was

applied in both time domains, prior to the Fourier transformation. Representative 2D ^{1}H-^{1}H TOCSY spectra from a creatine standard and rat cerebellum are shown in Figures 2.8 and 2.9 respectively.

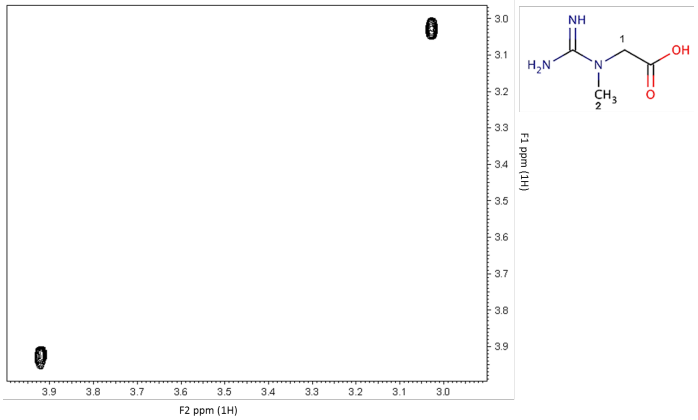

Figure 2.8: 2D ^{1}H-^{1}H TOCSY spectra (correlation of two ^{1}H-^{1}H spectra).
Obtained from a creatine standard revealing the exact locations of the creatine resonant signals in a two-dimensional (x and y) plane.

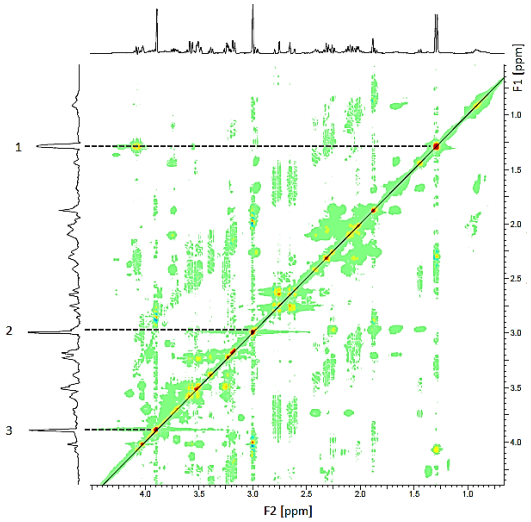

Figure 2.9: 2D Cerebellar ^{1}H-^{1}H TOCSY spectra (correlation of two ^{1}H-^{1}H spectra).
Obtained from rat cerebellum revealing the exact locations of the observed resonant signals in a two-dimensional (x and y) plane. The resonant signal labelled 1 corresponds to lactate, while signals 2 and 3 correspond to creatine).

2.2.6.3 STOCSY

Statistical Correlation Spectroscopy takes advantage of the inherently linear relationship existing between intensity variables of the same molecule in an NMR spectrum. STOCSY assess the

covariance of variables in a spectral set and produces a correlation matrix that reveals the degree of correlation between each individual variable in the spectrum. Strongly correlated variables may belong to the same molecule, while weakly correlated molecules may belong to the same pathway. STOCSY was applied for the resolution of some brain resonance signals such as inosine and hypoxanthine using the option available in the MUMA R package (Cloarec *et al.* 2005; Gaude *et al.* 2013).

2.2.7 Metabolite set enrichment and metabolic pathway analysis

Detailed analysis of the most relevant cerebral metabolic pathways and networks invoked as respondents to MPH treatment was performed by the *MetaboAnalyst 3.0* tool (Xia *et al.* 2015). This web-based facility employs high-quality Kyoto Encyclopedia of Genes and Genomes (KEGG) metabolic pathways as the structured back-end knowledge base, and integrates a series of now well-established methods (i.e., univariate and over-representation analyses), together with novel algorithms and concepts (i.e., Global Test, Global-ANCOVA and Network Topology Analysis) with pathway analysis. For all datasets, the Global ANCOVA and Relative-Betweeness Centrality algorithm for metabolic pathway and topological analyses were employed, the latter serving as a key measure indicating the importance of a graph node when expressed relative to that of the others (Aittokallio and Schwikowski 2006). For the pathway topology analysis performed, the *Rattus norvegicus* (rat) mammalian pathway library was selected. This approach was also utilised to provide estimates of pathway impact and false discovery rate (FDR)-adjusted *p* values.

2.3 *In vivo* microdialysis

In vivo microdialysis is a technique widely used in neuropharmacology research for the sampling and quantitation of extracellular transmitter levels, which serves as an index of transmitter release (albeit not always the case). The microdialysis technique was established by Ungerstedt and colleagues during the late 1970s and early 1980s at the Karolinska Institute in Sweden (Ungerstedt *et al.* 1982; Zetterström *et al.* 1988). In this thesis, the microdialysis technique was employed to investigate the extracellular levels of striatal DA and its main metabolite, DOPAC. The technique involves the implantation of a probe that contains a semi-permeable membrane. The implanted probe is perfused with a medium having ionic composition similar to that found in endogenous cerebrospinal fluid, hence referred to as artificial cerebrospinal fluid (aCSF). A perfusion pump at an optimum rate, usually 1.0 – 5.0 µl/min, pumps the aCSF medium into the probe. The perfusion pump is connected to the probe's inlet tubing (see Figure 2.10). Once the probe is inserted (e.g. into the brain) and the perfusion medium (aCSF) is pumped into the probe, molecules (e.g. neurotransmitters) on the outside of the microdialysis membrane (i.e. in the extracellular space) diffuse through the semi-permeable membrane along their concentration gradient into the probe and are collected at the probe's outlet either manually or by using a fraction collector (Chefer *et al.* 2009). The dialysates (dialysis samples) can be collected at regular time intervals (e.g. every 20 min) and the neurotransmitter contents can then be analysed using an analytical technique such as high performance liquid chromatography coupled with electrochemical detection (HPLC-EC). Given the large number of neuroactive substances (e.g. transmitters, amino acids, proteins, peptides etc.) present in the brain and other tissues, probes with different pore sizes have been developed to screen the substances entering the probe's semi-permeable membrane. In this thesis, a probe of 6 kDa was used, hence only molecules smaller than this size could cross the membrane.

A key benefit to the use of the microdialysis technique is that the semi-permeable membrane is only present at the tip of the probe (see Figure 2.10), thus dialysis occurs only at the desired discrete brain area. Crucially, probes with different membrane sizes are currently available to suit different research purposes. In general, the small size of the dialysis probe (smaller than devices used for push-pull or cortical cup perfusion) means that it displaces a smaller area of tissue and therefore does less damage to tissues when compared to the push-pull technique (Chefer *et al.* 2009; Darvesh *et al.* 2011). A major disadvantage of the technique, however, is that the sample collection stage takes a longer time (typically 20 min collection periods are employed), as opposed to other techniques such as *in vivo* voltammetry (Chefer *et al.* 2009). However, continuous improvements in the detection limits of analytical devices coupled to the microdialysis technique may help in reducing this time limitation. In addition, the dialysis process can create an area around the probe in which solutes capable of crossing the probe's membrane are all depleted. Such changes in the neurochemical milieu could affect basal levels and perhaps pharmacological responsiveness. However, reports indicate that basal levels of DA in the striatum is relatively unaffected by variations in the amount of non-DA solutes depleted around the probe (Sam and Justice, 1996).

2.3.1 Probe design

The microdialysis experiments were conducted using AT 9 probes (AGNTHOS, Sweden), having 3.0 mm polyethersulphone (PES) membranes with a 6 kDa cut-off. The probes had the typical Y-like skeleton, with the inlet/outlet made with thermoplastic polyimide polyetheretherketone (Figure 2.10) tubing (non-metallic), while the shafts were made from polyimide tubing and fused silica and was 14 mm long.

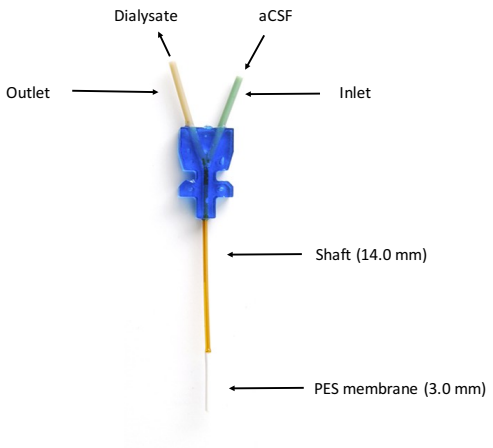

Figure 2.10: A schematic diagram of a microdialysis probe used in extracting dialysates from the striatum of the adolescent rats.

2.3.2 Surgical Procedure and probe implantation

Male Sprague Dawley rats (weight: 180 - 220 g) were anaesthetised with urethane (10.0 mg/kg, i.p. over the entire duration of the procedure) and placed in a stereotaxic frame (David Kopf Instruments, USA). The incisor bar was set at 3.3 mm below the interaural line (flat skull position) and the animals body temperature maintained at ~37°C via a thermostatically controlled heating blanket coupled with a rectal probe (Havard Apparatus Ltd, UK). A longitudinal incision made in the scalp exposing the surface of the skull and the bregma position was marked with a small pencil dot. A trephine hole was drilled in the skull in one hemisphere of the striatum (2.5 mm anterior and 1.5 mm lateral) with the duramater (dura) remaining intact.

The microdialysis probe mounted on a probe holder was connected to a UNIVENTOR 801 perfusion pump (AGNTHOS, Sweden) using polyethylene portex tubing (1.09 mm OD, 0.38 mm ID; Sims Portex Ltd, UK), and perfused at 2 μl/min flow rate with artificial cerebrospinal fluid (aCSF). The microdialysis probes were attached to a stereotaxic manipulator and positioned at the desired anterior and medio-lateral stereotaxic coordinates relative to bregma (2.5 mm anterior and 1.5 mm lateral) and then slowly implanted into the brain tissue (6.5 mm below the dura) after

a sterile needle had been used to pierce the exposed dura. Throughout the duration of the experiment, the anaesthesia levels were checked every hour and maintained using additional i.p injections of 0.5 ml of 100% (w/v) urethane as a top up.

2.3.3 Sample collection

To collect the dialysis samples, 0.2 ml microtubes (Sigma Aldrich, UK) containing 10 µl of 0.2 M perchloric acid were placed upside down on the outlet of the dialysis probe. Perchloric acid was added to protect the dialysates, particularly DA from degradation (i.e. from rapid oxidation). The dialysates were collected every 20 min (2 µl/min), yielding 50 µl samples. The collected samples were immediately placed on ice and then quickly analysed using high performance liquid chromatography coupled with electrochemical detection (HPLC-EC), as described below.

2.3.4 Perfusion medium

The microdialysis probes were perfused using artificial cerebrospinal fluid (aCSF) containing:

- NaCl 140 mM
- KCl 3.0 mM
- $MgCl_2$ 1.0 mM
- NaH_2PO_4 0.27 mM
- Na_2HPO_4 1.20 mM
- Glucose 7.2 mM
- $CaCl_2$ 2.4 mM
- pH adjusted to 7.4

A fresh aCSF stock solution was prepared each week and filtered using Whatman filter discs (Whatman, UK) before use in any experiment.

2.3.5 Location of implanted probe

At the end of the experiment, the animals were given an overdose of urethane i.p. and the brains were removed, snap frozen and stored in -20°C for probe placement analysis. Probe placement was verified by examination of the striatal brain sections. Striatal brain sections were cut on a cryostat to a thickness of 30 µm (Bright Instruments Ltd, UK) and then mounted on chromalum gelatin subbed microscope slides. The brain sections were examined using a microscope and then compared to the brain atlas (Paxinos and Watson 2006). To further aid identification, the slides were hydrated in decreasing solutions of isopropanol and subsequently stained with haematoxylin (Mayer's) and 1% eosin stain, and then a DPX mountant (Sigma Aldrich, UK) added following dehydration to aid microscopy. Figure 2.11 gives the typical positions of the microdialysis probes inserted into the striatum.

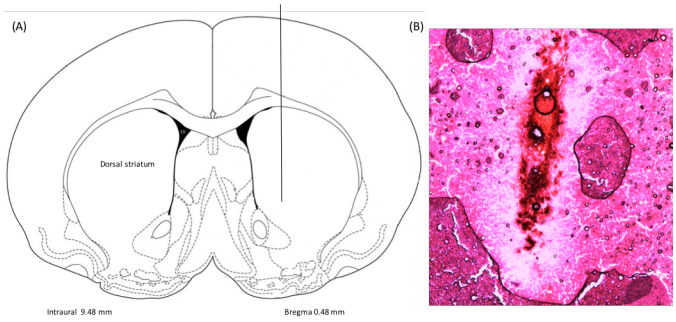

Figure 2.11: Typical position of the microdialysis probes inserted into the striatum of rats. (A) Shows the site of probe placement in the striatum, (B) Probe inserted in the rat striatum, the image was obtained after haematoxylin and eosin staining.

2.4 High performance liquid chromatography-electrochemical detection

HPLC coupled with electrochemical detection (HPLC-EC) is an important method for the analysis of brain monoamine levels. HPLC and carbon-based electrochemical detection offers a highly selective and sensitive means for the detection of compounds having a catechol or indole core. In this thesis, HPLC was employed to analyse DA and its metabolite (DOPAC and HVA) levels in whole tissues (from the frontal cortex, striatum, and cerebellum) and in the striatal dialysates obtained from the microdialysis experiment. A typical setup of the HPLC-EC system is shown in Figure 2.12. The HPLC-EC system (Waters Ltd, UK) used in the present study consisted of:

- HPLC pump – Waters 1515 Isocratic HPLC pump
- Injector – Rheodyne model 7725i (manual injector), fitted with 50 μL loop.
- HPLC Column - C18 column (5 μm Spherisorb ODS2, 4.6 x 250 mm; Waters Ltd, UK)
- Detector – Waters 2465 electrochemical detector (Waters Ltd, UK).
- Flow cell (working, reference and auxillary electrodes) – Waters model 282065
- Recorder/Integration software – Breeze 2 software (Waters Ltd, UK).

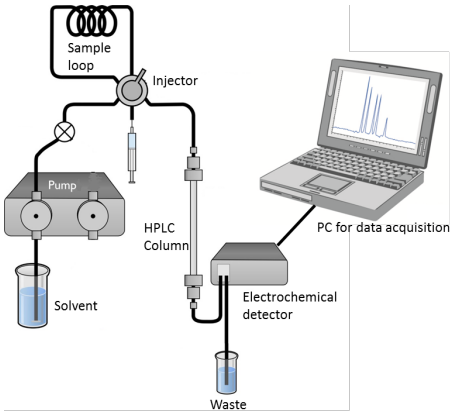

Figure 2.12: Isocratic HPLC system and electrochemical detection setup.

In an HPLC-EC system, a high-pressure pump is used to generate and circulate a specified flow rate of solvent (i.e. mobile phase) typically in millilitres per minute. A sample (in a Hamilton

syringe) to be analysed can be introduced by manually injecting it into the injection valve (injector), which introduces the sample into the continuously flowing stream of mobile phase (polar mobile phase used in this thesis) that carries the sample into the HPLC column. The column has chromatographic packing material (called stationary phase) required to effect the separation. In this thesis, the Spherisorb ODS2 (reverse phase C18 column, 5 μm particle size and 25 mm long; Waters, UK) was used. This column has a silica-based packing material that has 18 carbons added to make it non-polar (non-polar stationary phase) and this interacts with non-polar compounds in the injected sample making them pass through the column slowly (greater attraction), while the polar compounds pass through the C18 column more rapidly (less attraction). This means that some compounds in the injected sample (or analyte) exit the column faster than others (chromatographic separation).

As the separated analyte exit the column, it passes through the electrochemical cell, where it undergoes either oxidation or reduction. The electrochemical cell has three electrodes: (1) working electrode – where oxidation and reduction occur, (2) auxillary electrode – which acts as a counter electrode, (3) reference electrode – for stabilisation of the set-up. For oxidation or reduction to occur in the working electrode, a controller (potentiostat) maintains the potential of the working electrode (relative to the reference electrode) at value (set at 0.65V in this thesis) that causes the analyte to eletrolyse (i.e. oxidise or reduce). As an example, the oxidation/reduction reaction of DA is shown in Figure 2.13.

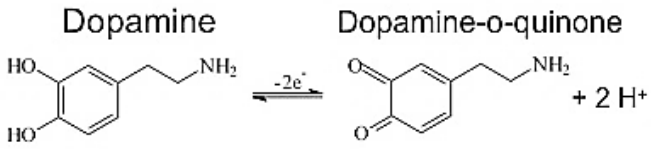

Figure 2.13: Oxidation and reduction of dopamine.
When the cell potential increases, dopamine is oxidised to dopamine-o-quinone but when the potential decreases, the dopamine-o-quinone is reduced back to dopamine.

The electrolysis current (electrical signal) resulting from the oxidation (or reduction) of the analyte is then measured by the cell and then transmitted to a computer data station. The electric signal arising from the analyte (injected sample) is then plotted as electric signal (y-axis) with respect to time (x-axis), producing peaks corresponding to the compounds in the injected sample (see Figures 2.14, 2.15 and 2.16). The area of resultant peaks from the injected analyte have a linear correlation with the concentration of the compounds in that sample (Schaefer *et al.* 2006). Each chromatographic peak is then identified and the area under each signal (integral data) analysed using statistical packages.

2.4.1 Mobile phase

In HPLC-EC analysis, the composition of the mobile phase depends on the sort of compounds the system is set-up to measure. In this thesis, the mobile phase prepared for detecting DA, DOPAC and HVA consisted of:

- Sodium dihydrogen orthophosphate dihydrate 1.2 M
- Disodium ethylenediamine tetracetate 10% (v/v)
- Octanesulfonic acid sodium salt 0.5 mM
- Methanol 15% (v/v)
- pH 4.0

The mobile phase was filtered using Whatman filter discs (Whatman, UK) and degassed for 20 mins before use. The mobile phase was pumped at a flow rate of 1.0 ml/min.

2.4.2 Extraction procedure for whole tissue experiments

The extraction procedure for the brain tissues used is similar to that described by Schaefer *et al.* (2006) but with some minor modifications. In brief, the tissues from striatum, frontal cortex, and cerebellum were homogenised in 0.2 M perchloric acid (4 ml per gram of tissue) and centrifuged

for 5 min at 10,000 *g*. 50 µl aliquots were injected using the Rheodyne manual injection valve into a 50 µl loop and then pumped onto the C18 column (5 µm Spherisorb ODS2, 4.6 x 250 mm; Waters Ltd, UK) placed in a column oven maintained at a 35°C (Waters Ltd, UK). The column was protected from any possible contaminants by a pre-column filter of pore size 0.5 µm (Waters Ltd, UK).

2.4.3 Analysis of microdialysates

The microdialysates were analysed similar to the whole tissue samples. Here, 50 µl dialysates were injected manually into the 50 µl loop and then pumped onto the C18 column (5 µm Spherisorb ODS2, 4.6 x 250 mm; Waters Ltd, UK), as already described (see section 2.4.2).

2.4.4 Determination of concentrations

The concentrations of the analytes [DA; 3,4-dihydroxyphenylacetic acid (DOPAC); and homovanillic acid (HVA)] were determined using their peak area with reference to external standards (see Figure 2.14) assayed daily in 0.2 M perchloric acid from stock solutions of each compound.

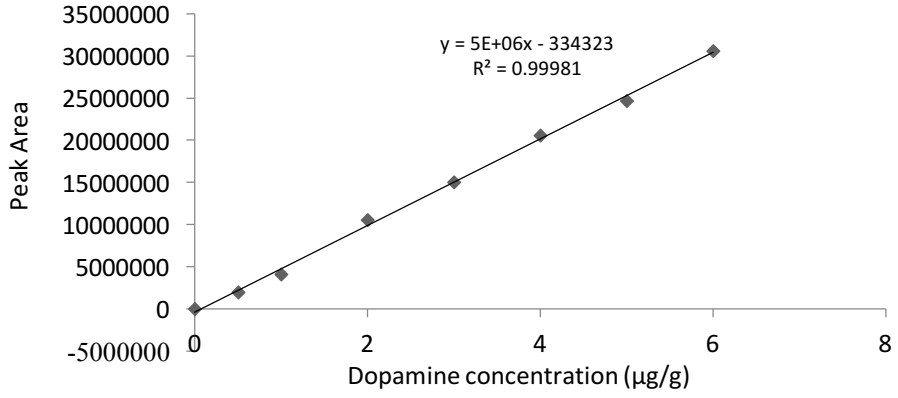

Figure 2.14: Typical standard (calibration) curve used in the determining the concentration of dopamine in the rat brain samples.

The identity of each peak was confirmed by running the individual standard compounds and also by spiking brain samples with each standard compound in trial experiments. The standard measurements of the peak area have been previously reported to be linear to the concentration of compounds (Schaefer *et al.* 2006). Typically, the retention times for DA, DOPAC and HVA standards were approximately 5.5, 7.5, and 19 min respectively (see Figure 2.15). Figure 2.16 also shows the retention times within the rat brain samples.

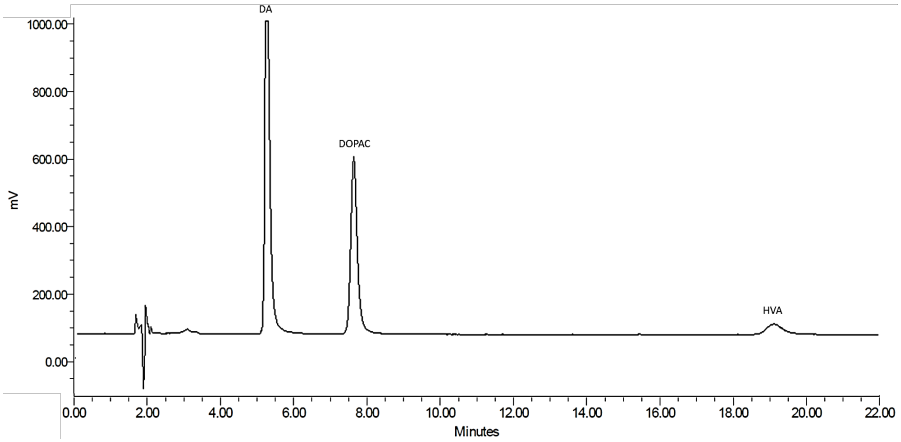

Figure 2.15: Chromatogram of DA, DOPAC and HVA standards of 0.2 µg/g concentration (i.e. 10^{-6} M dilution).

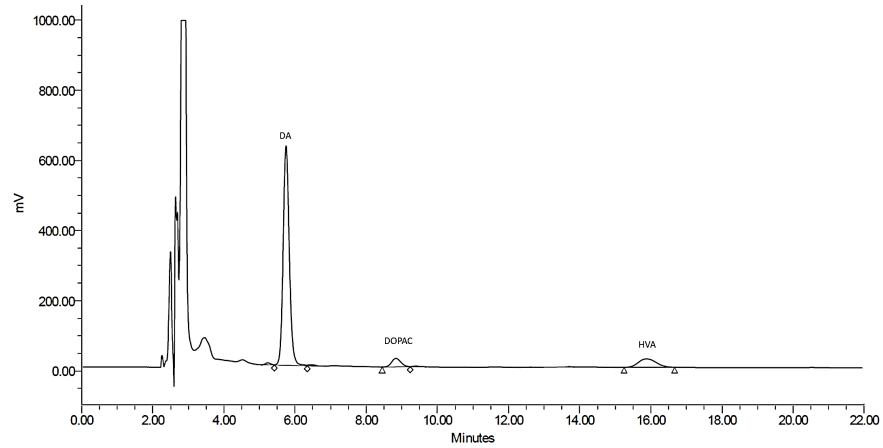

Figure 2.16: Chromatogram of DA, DOPAC and HVA peaks in a rat striatal sample (i.e. whole tissue levels).

2.5 Western blotting

The Western blot technique is used for the detection of specific protein molecules from among a complex mixture of proteins. This mixture may include all the proteins associated with a particular cell type or tissue. Western blots are used in evaluating protein expression or for assessing the size of a protein of interest (Kurien and Scofield 2006; Mahmood and Yang 2012). In this thesis, the Western blot technique was employed to evaluate the expression of proteins involved in the monoaminergic system and those associated with synaptic plasticity following MPH treatment relative to non-drug treated controls.

The first major step in a Western blot is sample preparation, where samples are mixed with a detergent, usually sodium dodecyl sulphate (SDS), which unfolds the proteins in the sample into linear strands and then coats them with a net negative charge (Kurien and Scofield 2006; Mahmood and Yang 2012). The protein molecules are then separated according to their sizes via gel electrophoresis. After separation, the proteins on the gel are transferred onto a blotting membrane (e.g. nitrocellulose membrane). Following a successful protein transfer, the nitrocellulose membrane would carry all of the protein bands originally seen on the gels. The membrane then goes through a treatment process called 'blocking' (carried out using non-fat dry milk or bovine serum albumin), which prevents the occurrence of any non-specific reactions. To detect a specific protein from the protein mixture on the membrane, the membrane is incubated with a primary antibody that specifically binds to the target protein. After primary antibody incubation, any unbound antibody is washed off with a buffer (e.g. using a tris buffered saline with tween i.e. TBST buffer). The membrane is incubated again but this time with a secondary antibody that recognises and binds specifically to the primary antibody (Figure 2.17). The secondary antibody used in this thesis was linked with a reporter enzyme (e.g. HRP i.e. horse

radish peroxidase) that produces colour or light, permitting it to be detected, imaged and quantified (Kurien and Scofield 2006; Mahmood and Yang 2012). Through these processes, therefore, the Western blot technique allows the detection and quantification of target proteins from among a complex mixture of proteins.

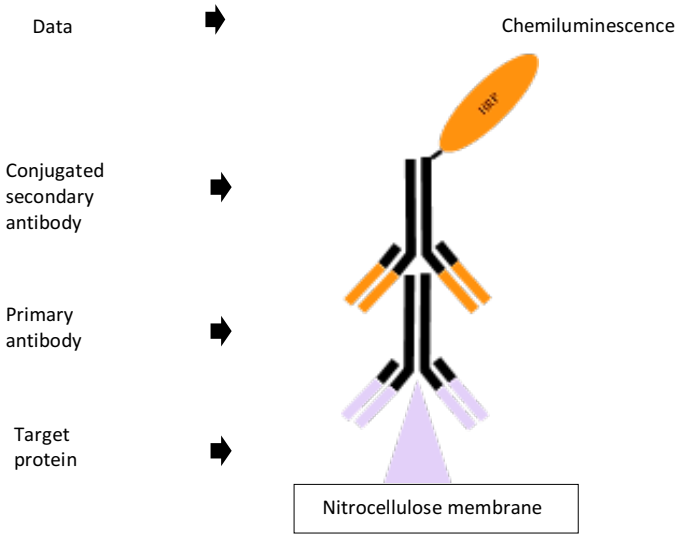

Figure 2.17: The primary and secondary antibody complex in Western blotting.
The primary antibody binds to the target protein and then a secondary antibody linked with a reporter enzyme (e.g. HRP – horse radish peroxidase) then binds to the primary antibody. This enzymatic complex can then be detected upon addition of chemiluminescence substrates.

Regardless of the great utility of Western blots, there are several known limitations. Western blots are manually intensive and time consuming, requiring long hours when taking into account the gel preparation, sample separation, electro-blotting, and the multiple incubation periods. Sensitivity is often in the nanogram and microgram range making them incompatible with sample-limited analysis. In addition, analysis of large proteins is hindered by difficulties in transferring them from slab gels. However, the ability to refine protein separation by altering a number of important components, including buffer constituents, pH, gel concentration, and effective pore sizes of gels, means that the SDS-PAGE stage can be highly specialised to suit each individual protein and each experiment. Film-based visualisation of bands remains the most

widely used detection technique for chemiluminescent blots. However, oversaturation is a major challenge associated with this detection technique, as blots can get easily saturated (Kurien and Scofield 2006; Mahmood and Yang 2012). Moreover, it is sometimes not obvious when oversaturation has occurred. To prevent effects of saturation, the films can be characterised to identify its linear dynamic range for detection of a specific antibody under relevant testing conditions (as performed in this thesis by first exploring and deciding on the best exposure time). Despite the outlined limitations, the selective protein detection ability of the technique following antibody binding coupled with the ability to tailor experimental procedures to maximise protein signals, makes Western blot a suitable technique for examining the effect of MPH on the monoaminergic and plasticity-related proteins. The steps used in this thesis are detailed below.

2.5.1 Preparation of brain samples

A 1:1000 dilution of protease inhibitor and RIPA lysis buffer (Cocktail SIGMA) mixture was prepared. 500 µl of this mixture was added to each of the dissected brain regions: nucleus accumbens, frontal cortex, parietal cortex, striatum, hippocampus and cerebellum for the left and right sides. The tissue samples were then homogenised using Polytron PT318 (Kinematica, Switzerland) and then centrifuged for 10 mins at 13,000 g and 4°C using a bench top temperature-regulated centrifuge (Sorvall Legend Micro 17R, Thermo Scientific, UK). The supernatant was extracted and 100 µl of the extract added to 100 µl of 2x electrophoresis buffer (5% β-2-mercaptoethanol, 20% glycerol, 0.5 M Tris-HCl of pH 6.8, 0.006% w/v bromophenol blue and 10% sodium dodecyl sulphate). The resultant mixture was heated at 90°C for about 3 mins and then stored at -80°C for later use. The remaining supernatants were used in estimating the concentrations of the total proteins using Bradford assay kit (Sigma Aldrich, UK), which allowed for equal protein concentrations (20 µg/µl) of the brain samples to be loaded.

2.5.2 Estimation of brain tissue protein concentration

A standard protein curve was generated from the Bradford assay by diluting 1.0 mg/ml of bovine serum albumin (BSA) in distilled water to yield a range of concentrations from 0 - 1 mg/ml at intervals of 0.1 mg/ml. The protein standards were made in duplicate. From the 1.0 mg/ml BSA stock, the standards were prepared as shown below:

- BSA stock (100 µl) 1.0 mg/ml
- 90 µl stock + 10 µl diluent 0.9 mg/ml
- 80 µl stock + 20 µl diluent 0.8 mg/ml
- 70 µl stock + 30 µl diluent 0.7 mg/ml
- 60 µl stock + 40 µl diluent 0.6 mg/ml
- 50 µl stock + 50 µl diluent 0.5 mg/ml
- 40 µl stock + 60 µl diluent 0.4 mg/ml
- 30 µl stock + 70 µl diluent 0.3 mg/ml
- 20 µl stock + 80 µl diluent 0.2 mg/ml
- 10 µl stock + 90 µl diluent 0.1 mg/ml
- 0 µl stock + 100 µl diluent 0.0 mg/ml

Along with the protein standards, tissue homogenates were also diluted 1 in 8 in distilled water and loaded into a 96-well plate (Multiwell plate, polystyrene 96-well, Fisher Scientific, UK). 200 µl of Bradford reagent (Sigma Aldrich, UK) was then added to each well. The 96-well plate was mixed gently, covered with a foil and incubated at 37°C for 30 mins. Following incubation, the plate was allowed to cool for 10 mins, mixed gently and the foil removed before being placed in a micro-plate reader (uQuant^{TM}, BioTek, USA) set at 595 nm. Prior to the calculation of the concentration (µg/µl) of protein in each sample, the standard curves were checked for outliers.

2.5.3 SDS-PAGE electrophoresis

Sodium dodecyl sulphate - polyacrylamide gel electrophoresis (SDS-PAGE) was performed using the BIO-RAD Mini-Protean system. Glass plates (0.75 mm) along with its spacer plates (BIO-RAD, UK) were mounted in support cassettes. Before sealing the cassettes, the lower borders of both the glass plates and their spacers were checked to ensure correct alignment. The gel cassettes were then clamped against a casting frame, which allowed a level pouring of gels. To maximise the resolution of protein molecules, a discontinuous SDS-PAGE system was employed. Both the stacking and the separation (resolving) gels were prepared with standard acrylamide gel reagents using concentrations estimated from the Chang Bioscience website (http://www.changbioscience.com/calculator/sdspage.html). A 10 ml of 12% separation gel (for 10 – 200 kDa proteins) was prepared as follows:

- 30% Polyacrylamide 4.0 ml
- 1.5 M Tris-base (pH 8.8) 2.5 ml
- 10% Ammonium persulphate 0.1 ml
- 10% SDS 0.1 ml
- TEMED (tetramethylethylenediamine) 0.004 ml
- Distilled water 3.3 ml

A 5 ml of 5% stacking gel was also prepared as follows:

- 30% Polyacrylamide 0.85 ml
- 1.0 M Tris-base (pH 6.8) 0.63 ml
- 10% Ammonium persulphate 0.05 ml
- 10% SDS 0.05 ml
- TEMED 0.005 ml
- Distilled water 3.4 ml

The prepared separating gel solution were gently inverted two or three times and then dispensed into the space between the mounted glass plate and the spacer plate of the gel cassettes. To ensure a smooth surface, a small layer of isopropanol was placed at the top of the separating gel and left for 30 mins to polymerise. After polymerisation, the isopropanol was decanted and the stacking gel solution was prepared and poured on top of the separating gel. A 15 well comb (3 mm x 10 mm, BIO-RAD, UK) was then inserted gently in the gel, refilled and left for an hour to polymerise. Subsequently, the wells were thoroughly rinsed with distilled water to remove excess polymerised acrylamide. The gels were then connected to the electrophoresis tank and then filled with 1x running buffer prepared from a 10x stock. A litre of the 10x running buffer stock was prepared as follows:

• Tris-base	30.3 g	25 mM
• Glycine	144 g	250 mM
• SDS	10 g	1%
• Distilled water	up to 1000 ml	

Equal concentrations (20 µg/µl) of each tissue sample were loaded into the wells. The first and the last wells contained 2 µl of all blue precision protein standard (BIO-RAD, UK) and 2 µl of 2x electrophoresis buffer (negative control), respectively. The standard protein aided in the later estimation of the molecular weight range of the proteins of interest. Prior to loading, all the samples were denatured at 90°C for 3 mins. The samples were initially run at 120 V for 15 mins to allow sample passage through the stacking gel followed by 100 V for 45 mins. The bromophenol blue tracking dye present in the electrophoresis (loading) buffer and/or the all blue standard protein marker allowed the visualisation of protein movement in the gel.

2.5.4 Protein transfer

The separated proteins were transferred from the gels onto a Protran™ nitrocellulose membrane (GE Healthcare, UK) via a transfer sandwich and an electroblotter. The transfer sandwich consisted of two pieces of white scotchbrite pads (200 mm x 160 mm, BIO-RAD, UK), two pieces of 3 mm Whatman filter papers (Fisher Scientific, UK) and a piece of nitrocellulose membrane. The transfer sandwich was arranged as follows:

- Scotchbrite pad
- Whatman filter paper
- Gel
- Nitrocellulose membrane
- Whatman filter paper
- Scotchbrite pad

The black side of the transfer cassette was placed on the workbench and each element in the transfer sandwich was soaked in a transfer buffer, and then stacked on the cassette with air bubbles being dispelled at each stage by rolling sterile glass pipette over the sandwich. The cassette was then sealed and inserted into a Mini trans-blot tank (BIO-RAD, UK), while taking note of the colour codes (red for red). The transfer tank was filled with cold (4°C) transfer buffer. One litre of 1x transfer buffer (pH 9.2) was prepared as follows:

• Tris-base	5.82 g	48 mM
• Glycine	2.93 g	39 mM
• Methanol	200 ml	20%
• Distilled water	up to 1000 ml	

The transfer set up was then run at 100 V for 1 h. Following the transfer procedure, the nitrocellulose membranes were stained a Ponceau S dye to allow an estimation of transfer efficiency. The nitrocellulose membranes were immersed in the Ponceau S dye and left on a shaker for 5 mins. After staining, the nitrocellulose membranes were placed in a destaining solution (5% glacial acetic acid) and left on the shaker for 5 mins. The destaining solution was changed 3-5 times until clear bands with almost no pink background were obtained. A 0.1% (x/v) Ponceau S dye in 1% (v/v) acetic acid was made as follows:

- Ponceau S dye 0.033 g
- Glacial acetic acid 0.3 ml
- Distilled water up to 30 ml

Dissolving 5 ml of the 100% glacial ascetic acid in 95 ml distilled water also yielded a 100 ml of 5% glacial ascetic acid.

2.5.5 Immunoblotting

Following Ponceau staining, a 10x TBS stock was (24 g Tris-base, 88 g NaCl, distilled water up to 1000 ml, pH 7.6) prepared. The membranes were blocked with 3% (w/v) non-fat dried milk in 1x TBST (0.1% Tween 20 in 1x TBST; blocking buffer) for 30 mins at room temperature to prevent non-specific antibody binding. The 3% non-fat dried milk blocking buffer was observed to produce better quality bands with less background compared to 5% non-fat dried milk buffer. Primary antibodies were incubated overnight at 4°C in blocking buffer. While 1:2000 dilutions were used for the secondary antibodies, the primary antibody dilutions varied as shown in table 2.1.

Table 2.1: Primary antibody dilutions for Western blotting

Primary antibody (source)	Dilution	Final concentration (μg/ml)	Secondary antibody
Goat anti-DAT polyclonal IgG	1:1000	0.2	Anti-goat IgG-HRP
Anti-DA D1R rabbit pAb	1:1000	0.2	Anti-rabbit IgG-HRP
Anti-SLC18A2 rabbit polyclonal IgG (VMAT2)	1:1000	0.2	Anti-rabbit IgG-HRP
Rabbit polyclonal anti-NA transporter (NET)	1:1000	0.2	Anti-rabbit IgG-HRP
Rabbit polyclonal anti-Tyrosine Hydroxylase IgG (TH)	1:1000	1.0	Anti-rabbit IgG-HRP
Goat anti-BAIAP2 polyclonal IgG (IRSp53/58)	1:2000	0.25	Anti-goat IgG-HRP
Rabbit polyclonal anti-*Arc* IgG)	1:1000	0.2	Anti-rabbit IgG-HRP
Mouse monoclonal anti-Cdc42 IgG_3	1:1000	0.2	Anti-mouse IgG-HRP
Rabbit polyclonal anti-Arp2 IgG	1:1000	0.2	Anti-rabbit IgG-HRP
Mouse anti-β-actin monoclonal IgG_1	1:2000	0.1	Anti-mouse IgG-HRP

DAT, Cdc42, Arp2, *Arc*, β-actin and the secondary antibodies (anti-mouse IgG, anti-rabbit IgG and anti-goat IgG) were purchased from Santa Cruz Biotechnology, while D1R was from Millipore. VMAT2, NET and IRSp53 were also from Origene, with TH being purchased from Abcam (Cambridge, UK).

Following overnight exposure to the appropriate primary antibodies, the membranes were washed three times with 1x TBST for 5 mins each time, in order to wash off unbound antibody. The membranes were then incubated with the relevant secondary antibody in blocking buffer. In accordance with the enhanced chemiluminescence (ECL) system (Amersham Biosciences, UK), all secondary antibodies used were linked to the detection enzyme, horseradish peroxidase (HRP). After secondary antibody binding, the membranes were again washed three times with 1x TBST for 5 mins each. Following the last wash, the membranes were developed via the ECL plus detection kit (Amersham Biosciences, UK), which allows the emission of light produced in a multistep reaction in which peroxidase catalyses the oxidation of luminol. In this procedure, the nitrocellulose membranes were incubated with ECL reagent A (luminol) and reagent B

(peroxide) for 5 mins (1:1 dilution). After the 5 mins exposure, excess ECL reagents were poured off and the membrane was sealed in a plastic wrap (Saran™ film). In a dark room, the wrapped membranes were gently smoothened to remove air bubbles and then placed in a film cassette. Subsequently, a sheet of autoradiography film (Kodak^{TM}, UK) was placed on top and the cassette was closed for 40 s (exposure time). The sheets were then dipped in a developer solution (135 ml water, 50 ml developer) followed by a fixer solution (135 ml water, 50 ml fixer) and then dried under red light.

2.5.6 Image analysis

Membrane images were captured using MCID^{TM} core digital imaging system (MCID, UK), consisting of a video camera coupled to a computer. MCID^{TM} image analysis software (version 7.0) was used for post image acquisition analysis and quantification of immunoreactive bands. The MCID^{TM} software assigns each protein band with an optical density value, which is the sum of the pixel values for each individual band. The background values were also obtained by calculating the fringe pixel density around each band of interest and then deducted from the corresponding protein band.

2.5.7 Membrane stripping and reprobing

For all experiments, the nitrocellulose membranes were stripped following film development. Stripping allowed for the removal of the primary and secondary antibodies from the membranes. The membranes were then re-probed with the mouse anti-β-actin monoclonal IgG_1 primary antibody. The β-actin protein was used as a control for the amount of protein loaded into each well. A mild stripping buffer (containing 15 g glycine, 1 g SDS, 10 ml Tween20, distilled water up to 1000 ml, pH 2.2) was prepared. The membranes were washed twice with stripping buffer for 10 mins each at room temperature. The membranes were then washed twice with 1x PBS for

10 mins each, followed by a 5 mins wash with TBST. A 10x PBS stock solution was prepared as follows:

- NaCl 80.0 g
- KCl 2.0 g
- KH_2PO_4 2.4 g
- Na_2HPO_4 14.4 g
- Distilled water up to 1 L
- pH 7.4

The membranes were then blocked for 1 h with 3% non-fat dried milk blocking buffer, after which the immunoblotting protocol was repeated with anti-β-actin primary antibody and an anti-mouse secondary antibody.

2.6 Polymerase chain reaction

Polymerase chain reaction (PCR) is a molecular/genomic technique used to make multiple copies of a section of a gene (or DNA), which allows for the detection and/or identification of gene sequences. The PCR technology was developed by Kary Mullis in the 1980s (Mullis 1990). PCR can be performed using DNA from a variety of biological samples including tissues (e.g. from brain, skin, etc.), fluids (e.g. blood, saliva), and hair.

Each PCR reaction is facilitated by polymerase enzymes. DNA polymerase is a crucial enzyme in the PCR process as this enzyme links complimentary deoxynucleotides (adenine, thymine, guanine, and cytosine i.e. A, T, G, C) to an existing DNA template (i.e. a short DNA strand). Smaller pieces of DNA, usually between 20-30 nucleotides long, called primers are used as starting points for the DNA polymerase enzyme to add nucleotides (VanGuilder *et al.* 2008; Garibyan and Avashia 2013). For a PCR reaction to occur, therefore, the following are required: template DNA or complementary DNA (cDNA), DNA polymerase, deoxynucleotides, and primers. These components, together with an appropriate Buffer and Magnesium source, is placed in a thermal cycler that allows repeated cycles of DNA amplification to occur through three steps: denaturation, hybridisation/annealing, and elongation (VanGuilder *et al.* 2008; Garibyan and Avashia 2013). The thermal cycler is programmed to heat up at a high temperature of 90-95°C, to allow the double stranded DNA to split into two single stranded DNAs (denaturation). The temperature is then reduced to a primer specific temperature (approximately between 50-60°C) for the primers to bind to the complementary sequence of the single stranded DNA (annealing). Following primer annealing, the temperature is increased (to usually 72°C), permitting the DNA polymerase enzyme to add the deoxynucleotides to the primer, thereby extending the DNA (Garibyan and Avashia 2013). By repeating these steps, the number of

amplified DNA molecules doubles. To obtain enough copies of the target gene for analysis, these three steps are typically repeated 30-40 times.

For verification of the integrity of the amplified DNA and for visualisation and analyses of the PCR products, agarose gel electrophoresis is often conducted. Agarose gel electrophoresis separates the DNA products according to their size. This allows for the determination of the presence and size of the amplified PCR products. Figure 2.18 shows the PCR products of the target genes investigated in this thesis.

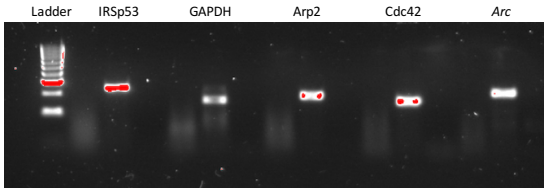

Figure 2.18: Visualisation of the PCR products via agarose gel electrophoresis.
The first lane corresponds to a ladder (standard marker), followed by the PCR products of the housekeeping gene and genes of interest (i.e. IRSp53, GAPDH, Arp2, Cdc42, and *Arc*). In the lane preceding each cDNA of interest was loaded the RNA product of that gene (which produced no visible bands).

Standard PCR is used for quality control. To quantify a product, real time quantitative PCR (RT-qPCR) is usually used. RT-qPCR can be used for both the detection and the quantification of the target DNA in real time, while it is being synthesised. The steps and necessary components in RT-qPCR are the same as already described for the standard PCR. However, in addition, each RT-qPCR reaction has a fluorescence reporter molecule. The fluorescence reporter molecule produces increased fluorescence with an increasing amount of amplicon product (VanGuilder *et al.* 2008; Garibyan and Avashia 2013). Either double stranded DNA binding dyes or fluorescently-labelled sequence specific probes may be used as the fluorescence-labelling method. A light source in the RT-qPCR instrument excites the fluorescence and a camera captures the fluorescent signals. As the amplification proceeds, the fluorescence accumulated is

captured by the instrument after every cycle and translated into an RT-qPCR graph (see Figure 2.19).

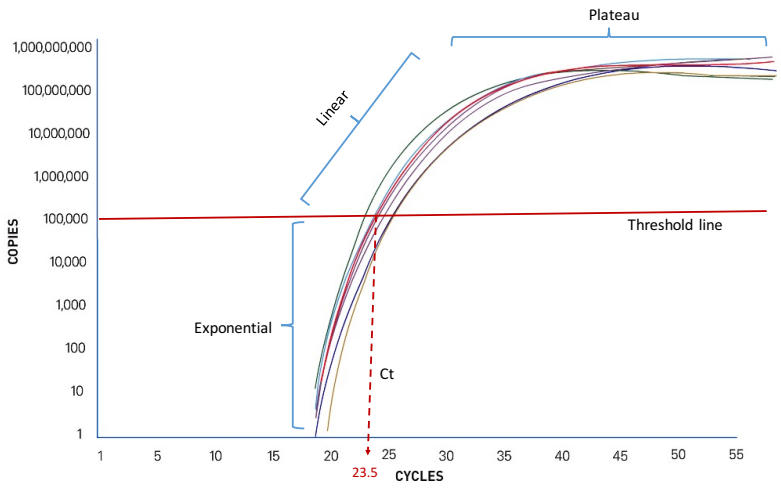

Figure 2.19: Typical real-time PCR amplification curve.
This displays the three phases of real-time PCR amplification including exponential, linear, and plateau phases. The cycle threshold (Ct) value, which represents the cycle at which the sample reaches the threshold line, can be compared to that of a standard curve to estimate the concentration of the sample.

Real-time PCR amplification curves can be divided in three phases: the exponential phase where the reagents are in abundance and PCR product doubles in every cycle, the linear phase where the reagents begin to run out and the PCR reaction slows down, and the plateau phase where the reagents are depleted and the reaction stops. Real-time PCR amplification results focus on the exponential phase as this phase provides the most precise data for quantitation. Within the exponential phase two values are calculated: (a) the threshold line which is the point at which a reaction reaches a fluorescent intensity above background, and (b) Cycle threshold (Ct) which is the PCR cycle at which the sample reaches the threshold line (this Ct value is used in quantitation; see Figures 2.19 and 2.20). By comparing the Ct value of samples to that of a standard curve, the concentration of the samples can be established.

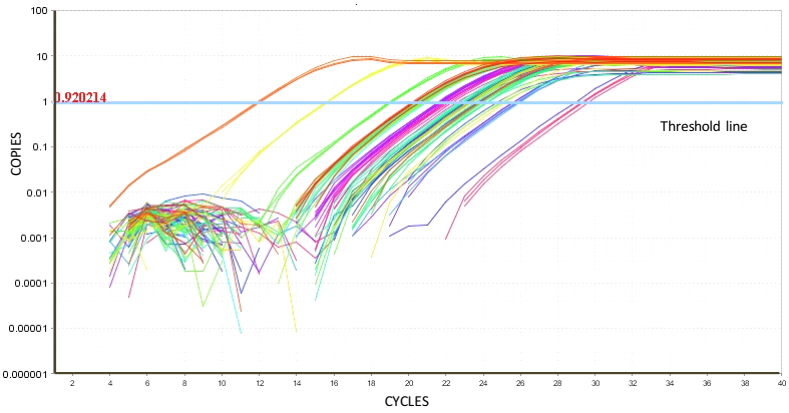

Figure 2.20: Amplification curve from the PCR products of the IRSp53/58 gene in all the analysed brain samples.

In general, RT-qPCR can be combined with reverse transcription, which permits messenger RNA to be converted into cDNA (complementary DNA), after which quantification of the cDNA may be performed with RT-qPCR. In this thesis, RNA was extracted from rat brain regions (such as frontal cortex, parietal cortex, striatum, and cerebellum) and reverse transcribed into cDNA. Prior to RT-qPCR, regular PCR was performed followed by agarose gel electrophoresis to ensure the integrity of the amplified genes of interest. The genes of interest investigated here included the insulin receptor substrate protein (IRSp53/58; BAIAP2), activity-regulated cytoskeleton-associated protein (*Arc*), cell division control protein 42 (Cdc42), and actin-related protein 2 (Arp2) that are associated with synaptic plasticity and actin dynamics.

Despite the numerous advantages associated with PCR, in practice the technique can fail for various reasons. Indeed, due to the high sensitivity of the technique, it is prone to contamination from extraneous DNA, resulting in the amplification of spurious DNA products. Contamination with extraneous DNA can, however, be addressed with laboratory procedures that separate pre-PCR mixtures from any potential source of DNA contaminants. Such laboratory measures may involve spatial separation of PCR set-up areas from areas used for purification or analysis of PCR products, as well as thorough cleaning of the working area between reaction setups. Primer

design techniques are also essential in improving the yield of PCR products and in avoiding the formation of spurious PCR products. Other critical issues defining the reliability of real time quantitative PCR data are the choice of housekeeping (reference) genes and the sample preparation methods. An ideal housekeeping gene should always have the same level of expression. However, not all currently available housekeeping genes fulfil this prerequisite. As such, the constant expression of the chosen reference gene must be tested and verified for reliable data to be obtained. Alternatively, as done in this thesis, two or more reference genes can be used in the experimental setup for data analysis.

2.6.1 Primer selection, design, and verification

A total of four actin-binding genes of interest and two reference genes were selected based on previously published papers associating these genes with ADHD (Liu *et al.* 2013; Ribasés *et al.* 2009; Banerjee *et al.* 2009). The actin-binding genes of interest selected were, IRSp53/58 (also known as BAIAP2), *Arc*, Cdc42, and Arp2. The two selected reference genes commonly used in previous studies were glyceraldehyde 3-phosphate dehydrogenase (GAPDH) and beta-actin (β-actin) (Miao *et al.* 2009; Ning *et al.* 2011). The nucleotide sequence of each of the targeted genes specific for *rattus norvegicus* was retrieved from GenBank (https://www.ncbi.nlm.nih.gov/gen-bank/) (Table 2.2) and a blast search conducted for verification. The coding sequence of the matching contigs for each gene of interest was used in designing the primers using Primer3Plus (http://www.bioinformatics.nl/cgi-bin/primer3plus/primer3plus.cgi/) (Sgamma *et al.* 2016). To select the ideal primer pair, different factors were taken in consideration and set as parameters e.g. annealing temperature (60-67°C), GC content (40-60%), an optimum primer length of 20-24 base pairs and a maximum product size of 230 base pairs (see Table 2.2). Secondary structures of each amplicon were examined via Mfold (http://unafold.rna.albany.edu/?q=mfold/rna-folding-

form). Primer dimers and non-specific amplifications were observed post-PCR, if any, by analysing the melting curve data.

Table 2.2: Target primers and their annealing temperatures

Gene (GenBank accession number)	Primer Sequence	Ta	Ta used for PCR analysis	Product size
*Arc** (XM_008765590.1)	F: GGGAGTTCAAACAGGGCTCGGT	65	65	199
	R: TCCTCCTCCTCAGCGTCCACAT	65		
IRSp53* (AY037934)	F: GACCAAGATGCGGGGCTGGT	61	62	152
	R: AGTCAGGAGGAGGGAGGGCC	63		
Cdc42* (XM_008764287.1)	F: GCAGGGCAAGAGGATTATGACAG	65	64	179
	R: TCAATTTGGGTCCCGACAAGCAA	63		
Arp2* (FQ219838.1)	F: GTGGCGCAGTCCTAGCAGACAT	65	68	147
	R: TTAGAGGCGTGATGGGGACAAGCC	71		
Beta-actin^{+} (NM_031144.3)	F: TCCGTAAAGACCTCTATGCC	55	57	230
	R: GGACTCATCGTACTCCTGCTT	59		
GAPDH^{+} (NG_028301.2)	F: AAACCCATCACCATCTTCCA	53	55	156
	R: GGCGGAGATGATGACCCTTT	57		

F, Forward primer; R, Reverse primer; Ta, Annealing temperature; (*), Gene of interest; (+), Control.

2.6.2 RNA extraction

Twenty milligram of the frozen tissue samples corresponding to nucleus accumbens, frontal cortex, striatum, and cerebellum were dissected out on ice for total RNA extraction using RNeasy® Mini Kit (Qiagen, UK). Each 20 mg tissue was homogenised using 350 µl buffer RLT (lysis buffer) and the supernatant was carefully removed. 350 µl of 70% ethanol was added to the lysate and thoroughly mixed by pipetting. 700 µl from each sample, including precipitate, was transferred into an RNA mini spin column placed in a 2 ml collection tube and centrifuged for 15

s at 10,000 *g*, with the flow through subsequently discarded. Then 700 µl of Buffer RW1 (washing buffer) was added to the RNeasy spin column and centrifuged for 15 s at 10,000 *g,* with the flow through subsequently discarded. The samples were then mildly washed by adding 500 µl of buffer RPE (mild washing buffer) to the RNeasy spin column and centrifuging for 15 s at 10,000 *g,* and the flow through discarded. Further, the samples were mildly washed twice by adding 500 µl of Buffer RPE to the RNeasy spin column and centrifuging for 2 min at 10,000 *g*. The RNeasy spin column was then changed and centrifuged for 1 min at 10,000 *g* in order to dry the membrane. Finally, the RNeasy spin column was placed in a new 2 ml collection tube and 30 µl of RNase-free water was added directly to the spin column membrane and centrifuged for 2 min at 10,000 *g*. In order to obtain a high RNA yield (> 30 µg), the final step was repeated. The sample was then transferred into an Eppendorf tube and kept on ice.

2.6.3 DNA digestion

The TURBO DNA-free™ DNase treatment kit (Ambion Inc, USA) was used to remove genomic DNA contamination following the manufacturer's guidelines. The concentration and quality of the RNA sample was then verified by spectrometry using A260/280 ratios, with a Nanodrop Lite Spectrophotometer (Thermo Scientific, UK). This was achieved by placing 1 µl of the RNA sample on the Nanodrop Lite Spectrophotometer. PCR was performed, as described in section 2.6.5 (see below), to prove the lack of DNA contamination using the primers listed in Table 2.2. The integrity of the RNA sample was also evaluated by running 2 µg of total RNA (PCR product) on 2% agarose gels.

2.6.4 cDNA synthesis

cDNA was synthesised using 1.0 µg of the cleaned total RNA from each brain sample using iScript™ cDNA synthesis kit (Bio-Rad, UK) following the manufacturers instructions. In brief, a reaction mix was prepared comprising: 4 µl 5x iScript mix, 1 µl iScript reverse transcriptase, 1.0

µg RNA template, and nuclease-free water adjusted to give a total volume of 20 µl. The reaction mix was then incubated in a thermal cycler (PTC-200 Peltier Thermal Cycler) with the following parameters: priming for 5 min at 25°C, reverse transcription for 20 min at 46°C, reverse transcription inactivation for 1 min at 95°C, and a final incubation step for 5 min at 4°C. The samples were subsequently treated with 1 µl RNAse H (ThermoFisher Scientific, UK) for 20 min at 37°C in order to digest any remaining RNA. The cDNA samples were then kept at -20°C.

2.6.5 PCR amplification and gel electrophoresis

To verify the integrity of the synthesised cDNA and to test the primer conditions prior to real-time quantitative PCR (RT-qPCR), regular PCR amplifications were run and the products analysed via gel electrophoresis. MyTaq red master mix (Bioline, UK) was prepared as follows: 5 µl of MyTaq red (containing Taq polymerase), 0.5 µM of each forward and reverse primer, 4.1 µl nuclease-free water, and then either 1 µl cDNA or 1 µl RNA, or 1 µl nuclease-free water. The PCR reactions were run at an initial denaturation temperature of 95°C for 15 s, primer specific annealing temperature (see Table 2.2) for 15 s, extension/elongation 72°C for 10 s for 35 cycles.

The PCR products (including the test sample/PCR products, RNA and negative control/blank) were run on a 2% agarose (ThermoFisher Scientific, UK) gel prepared with 1x Tris/Borate/EDTA buffer (TBE buffer) and 0.2 µg/ml of SYBR™ Safe DNA Gel Stain (Invitrogen Ltd, USA). Electrophoresis was carried out in tanks filled with 1x TBE buffer at 90 V for 30 min and visualised on a Gel Doc™ EZ Imager (Bio-Rad, UK). HyperLadder™ 100 bp DNA ladder (Bioline, UK) was run alongside the samples in gels.

2.6.6 Real-time quantitative polymerase chain reaction

The RT-qPCR analysis was carried out using StepOnePlus™ Real-Time PCR system (AB Applied Biosystems, UK). Each reaction contained 5 µl SensiFAST™ SYBR Hi-ROX Mix

(Bioline, UK), 0.5 µl cDNA, 0.5 µM of each of the forward and reverse primers, in a total volume of 10 µl made up with sterile distilled water. The amplification conditions were as follows: 95°C for 2 min followed by 40 cycles of 5 s at 95°C and 30 s at the primers specific annealing temperature (see Table 2.2). To obtain the melting curve, the amplified template was melted from 65°C to 95°C increasing the temperature by 0.5°C per cycle. Three technical replicates were used for each sample. The amplification efficiencies for all pairs of primers were evaluated via tenfold serial dilutions of pooled cDNA.

2.6.7 Relative quantification and statistical analysis

Relative quantification, which is based on internal reference genes to determine fold differences in the expression of the target genes, was performed in this study. To do this, the qBASE+ software (Qbase, UK) was used for preprocessing of the data. The qBASE+ relative quantification takes into consideration the Ct values obtained from the RT-qPCR experiments, along with the PCR efficiencies in each experiment. The data was then normalised to two genes, GAPDH and β-actin. Also, to control for differences arising from running samples in the different 96-well plates, an inter-run calibration was performed using standard samples that were included in all plates. After performing the relative quantification, the two treatment groups (chronic MPH-treated vs. saline control) were tested for their statistical significance. The data was entered into GraphPad Prism (version 5.0, GraphPad software Inc., La Jolla, CA) and a Students t-test was applied to compare the two treatments.

CHAPTER 3

3 Effect of methylphenidate on dopamine transmission and protein targets

3.1 Introduction

The monoamine (e.g. DA, NA and 5HT) hypothesis of ADHD proposes that hypofunction of the fronto-striatal monoamine circuit result in the inattention, hyperactivity and impulsivity symptoms associated with the disorder (Del Campo *et al.* 2011). Administration of MPH, which is the first-line drug for ADHD reduces the symptoms of the disorder in about 70% of affected children (Fusar-Poli *et al.* 2012; Vles *et al.* 2003). MPH blocks both DAT and NET, increasing extracellular DA and NA levels in both rodents and humans (Berridge *et al.* 2006; Moghaddam *et al.* 1993; Volkow *et al.* 2005; Kuczenski and Segal 2005). However, despite decades of clinical, biochemical, genetic, and neuroimaging research, the exact neurobiological mechanism underlying ADHD and its psychostimulant drug treatment is not fully understood.

The hypo-functional DA hypothesis in ADHD emerged from initial molecular imaging studies that focused on the role of DAT and found increased DAT density in ADHD patients (Cheon *et al.* 2003; Dougherty *et al.* 1999; Spencer *et al.* 2005). An overexpressed DAT implies that extracellular DA may be quickly taken up by the transporter into the presynaptic neuron, thus limiting the synaptic availability and activity of DA (Del Campo *et al.* 2011). However, this idea of an overexpressed DAT in ADHD has been challenged recently by a series of case-control PET studies in adult never medicated ADHD patients, which found ADHD to be associated with a decrease of DAT and D2/D3 receptor availability in the left striatum, accumbens and the midbrain (Volkow *et al.* 2009; Volkow *et al.* 2007b; Volkow *et al.* 2007a). Possible reasons that may be underlying these discrepancies in findings on DAT could be the medication history and the different ages of the patients used in these studies. This may emphasise the importance of prior drug treatment and its influence on DAT expression. It also underscore the need to delineate

the effect of drugs (e.g. MPH) from the underlying disease pathology by examining the effect of the drug on normal drug naïve rodents.

Altered DA activity in ADHD could be due to a direct defect in the function of dopaminergic cells (i.e. regarding DA synthesis, cell firing, DA autoreceptors, DAT, TH, and VMAT2) or it could be as a result of indirect effects (i.e. dysregulation of glutamatergic cortical inputs to dopaminergic cells) (Volkow *et al.* 2009; Volkow *et al.* 2007b; Volkow *et al.* 2007a). DA is synthesised from tyrosine and subsequently serve as a precursor for the synthesis of NA. The rate-limiting enzyme, TH is responsible for catalysing the conversion of L-tyrosine to L-DOPA, which is then converted into DA. The synthesised DA is sequestered into vesicles by the integral membrane transporter, VMAT2 (Calipari *et al.* 2014). The vesicles fuse with the plasma membrane in an action potential dependent manner, releasing DA into the synaptic cleft (i.e. exocytosis). DA released from dopaminergic neurons regulate cortical, striatal, and hippocampal pathways through the activation of two distinct families of receptors, the D1-like (D1 and D5 receptors) and the D2-like (D2, D3 and D4 receptors) families (Missale *et al.* 1998). On the other hand, the action of DA at the synapse is terminated by its uptake back into the nerve terminal via DAT. If DAT is impaired it has significant effect on synaptic DA levels, making DAT a crucial regulator of synaptic DA action. Similarly, NET functions as a key regulator of synaptic NA levels. The deficits in DA and NA activity reported in ADHD (Volkow *et al.* 2007b), highlights the focus on the expression of proteins such as DAT, NET, TH, VMAT2, and D1 receptor within the dopaminergic circuitry of ADHD patients and in the mechanism of action of MPH and other anti-ADHD medications (Calipari *et al.* 2014; Del Campo *et al.* 2011; Narendran *et al.* 2015).

The human brain is well-known to show cerebral lateralisation (see Chapter 1, section, 1.6), similarly lateralisation of cerebral function has been documented in the brain of several animals

species, including rats (Glick and Ross 1981; Toga and Thompson 2003; Lister *et al.* 2006; Kristofiková *et al.* 2010). A deviation from the common pattern of cerebral lateralisation is suggested to be involved in the various impairments observed in ADHD patients, including the core symptoms of impulsivity, inattention and executive function deficits (Liu *et al.* 2013; Ribasés *et al.* 2009). Indeed, the development of human cerebral asymmetry is reported to have a key importance in cognition, handedness and language (Liu *et al.* 2013). Non-right-handedness, particularly mixed-handedness is suggested to be a potential risk factor for the symptom severity of inattention in ADHD (Liu *et al.* 2013; Rodriguez *et al.* 2010). Brain asymmetry has also been reported in several brain disorders including Alzheimer's disease, schizophrenia, autism and Parkinson's disease (Morris *et al.* 1994; Ricciardi *et al.* 2015). The dysfunctional right hemisphere hypothesis of ADHD is based mainly on abnormal right-sided frontostriatal activity in patients (Castellanos *et al.* 1996; Heilman *et al.* 1986; Heilman and Van Den Abell 1980; Vance *et al.* 2007). In support of this, a number of structural magnetic resonance imaging (MRI) studies have shown that ADHD patients have reductions in right caudate and right cerebral cortex (Valera *et al.* 2007), and thinner right frontal and parietal cortices (Makris *et al.* 2007). Further, delayed maturation of the cortical thickness and cortical surface area, also more prominent in the right hemisphere, have also been reported (Shaw *et al.* 2007; Shaw *et al.* 2009). In fact, some researchers have suggested that the level of rightward volumetric asymmetry might be an indicator of the severity of the inattentive symptom of ADHD (Schrimsher *et al.* 2002). In addition, hemisphere-specific findings have also been observed in functional MRI studies on ADHD patients, including an under-activation of the right parietal cortex (Vance *et al.* 2007), and right PFC (Rubia *et al.* 1999) during motor and attentional tasks.

Despite the growing evidence suggesting an abnormal right-sided frontostriatal activity in ADHD, information is still lacking regarding any lateralised action of drugs used in the treatment of ADHD, including MPH.

3.1.1 Aims

The aim of this study was to investigate the effects of MPH on protein markers associated with dopaminergic and noradrenergic function after acute and chronic treatment. In addition, the study evaluates the hemisphere-specific effects of acute and chronic MPH treatment on whole tissue and *in vivo* extracellular levels of DA, and its metabolites DOPAC and HVA. Specifically the effects of MPH on the following were examined:

- Proteins associated with pre- and post-synaptic dopaminergic and noradrenergic function in the frontal cortex, parietal cortex, striatum, nucleus accumbens, and hippocampus using Western blotting.
- *Ex vivo* whole tissue DA and its metabolite levels in the left and right frontal cortex and striatum following acute and chronic MPH treatment, using HPLC-EC.
- Extracellular DA and DOPAC levels in the left and right striatum following acute MPH administration to anaesthetised animals, using *in vivo* microdialysis coupled with HPLC-EC.

3.2 Methods

3.2.1 MPH Treatment

For a detailed description of the MPH treatment procedures see Chapter 2, section 2.1. In brief, the animals were assigned to two treatment groups i.e. acute and chronic groups. The adolescent animals in the acute groups (35-40 days old) received either a single i.p injection of 1.0 ml/kg saline (controls) or a 2.0 mg/kg MPH dose (drug-treated group). On the other hand, the animals

in the chronic groups either received a twice daily 1.0 ml/kg saline injection (control group) or 2.0 mg/kg MPH injection (treatment group) for 15 days (from post natal day 25 to post natal day 40) at 9 am and 5 pm each day. For the *in vivo* microdialysis study, to ensure an effect sufficiently strong for the occurrence of a lateralised action, adolescent animals (35-40 days old) were given a single i.p. injection of 5.0 mg/kg MPH dose. For all treatment groups, MPH was freshly prepared in saline on the day of the experiment.

3.2.2 Acute and chronic effects of MPH on monoaminergic markers

The Western blot technique was employed to examine the acute and chronic effects of MPH treatment on DAT (1:1000 dilution; Santa Cruz, USA), NET (1:1000 dilution; OriGene, USA), TH (1:1000 dilution; Abcam, UK), VMAT2 (SLC18A2; 1:1000 dilution; OriGene, USA), and D1R (1:1000 dilution, Millipore, UK) protein expression in the frontal cortex, parietal cortex, striatum, nucleus accumbens, and hippocampus (as previously described in Chapter 2, section 2.5). In these experiments, β-actin (1:2000 dilution; Santa Cruz, USA) was used as the reference protein. There were six animals in each treatment group (treatment and controls). The animals were sacrificed 24 h after the last drug treatment and the brains removed, snap-frozen and then stored at -80°C until analysis (as previously described in Chapter 2, section 2.1).

3.2.3 *In vivo* microdialysis and whole tissue DA analysis

A 10^{-3} M stock solution of DA, DOPAC and HVA standards (Sigma, UK) were prepared weekly in 1.0 M perchloric acid and stored at 4°C in the dark. From these stock solutions, serial dilutions of the standards were prepared daily using 0.2 M perchloric acid to obtain 10^{-5} - 10^{-9} M dilutions for the microdialysis and whole tissue experiments. For the *in vivo* microdialysis technique, 1.5 mg/ml solutions of urethane were prepared daily and stored at 4°C for use in anaesthetising the animals.

3.2.4 Probe implantation

Microdialysis probes were implanted into the striatum using stereotaxic coordinates relative to bregma (2.5 mm anterior, 1.5 mm lateral and 6.5 mm below the dura) (Paxinos and Watson 2006), and then perfused with artificial CSF (see Chapter 2, section 2.3.4). DA and its main metabolite (i.e. DOPAC) were then measured using HPLC-EC, with perfusates being collected every 20 mins (2 μl/min) over a 2 h period or until the dialysate DA levels had reached a steady state (see Chapter 2, section 2.3).

3.2.5 Acute MPH effects on extracellular DA and its metabolites

The *in vivo* microdialysis technique was employed on the urethane anaesthetised rats to measure the effects of acute MPH treatment on extracellular levels of DA and its main metabolite (i.e. DOPAC) in the striatum of adolescent male Sprague Dawley rats (approximately 35-40 days old, 180 - 220 g; n=6 rats/group). To investigate the effect of drug treatment in the left and right striatum, dialysates were taken from the left (n=3 rats/group) and right (n=3 rats/group) sides of the MPH-treated animals and their corresponding controls. The animals were anaesthetised with urethane (10.0 mg/kg, i.p.) over the entire duration of the procedure.

3.2.6 Effects of MPH treatment on whole tissue levels of dopamine and its metabolites

The effects of both acute and chronic MPH treatment on the whole tissue levels of DA, DOPAC and HVA levels were examined using HPLC-EC (Chapter 2, section 2.4). Following MPH treatment (2.0 mg/kg MPH dose) or 1.0 ml/kg saline injection (controls), brain regions corresponding to the frontal cortex and striatum (left and right sides) were quickly dissected out and homogenised in 0.2 M perchloric acid. Following HPLC-EC analysis, whole tissue levels of DA, DOPAC, HVA, and the turnover ratios, DOPAC/DA were calculated for each sample.

3.2.7 Statistical analysis

Data from the whole tissue DA, DOPAC, and HVA study were calculated as μg/g for each treatment group. These datasets were analysed using SPSS (version 22, IBM Statistics, Illinois, USA) and GraphPad Prism (version 5.30, GraphPad Software Inc., La Jolla, CA). Separate two- and three-way ANOVAs [with the factors, 'drug' (MPH, saline), 'hemisphere' (left, right), and 'duration' (acute, chronic)] and all interactions were carried out on the concentration levels of DA, DOPAC, and HVA, and the two ratios DOPAC/DA and HVA/DA. On the other hand, significant effects of 'drug' and 'duration' on the monoaminergic protein markers (DAT, NET, TH, VMAT2, and D1 receptor) were tested using two-way ANOVA. The data on the monoaminergic protein markers represent percentage of controls ± S.E.M. All significant main effects or interactions were further analysed using multiple comparison Bonferroni *post-hoc* analyses, with a $p < 0.05$ considered statistically significant.

Data from the *in vivo* microdialysis study were plotted as mean ± S.E.M for each treatment group. Data analysis was performed using GraphPad Prism (version 5.30). Striatal DA and DOPAC (% of baseline levels at time 0 min) were analysed among treatment groups using two-way mixed design ANOVA with 'time' as a repeated measure. Two-way repeated ANOVA was used to determine the significant effect of 'time' on the MPH-treated and saline-treated groups, with Bonferroni *post-hoc* tests for multiple comparisons against the baseline (0 min) used to detect, which time points differed significantly. Significant effects and interactions between 'drug' (MPH *vs.* control) and 'time' were also followed up with Bonferroni *post-hoc* tests.

3.3 Results

3.3.1 MPH induces an overexpression of DAT and NET

The present study shows that MPH alters the expression of DAT and NET transporters in several brain regions in a 'treatment duration' dependent manner. In this experiment, DAT was reliably detected and measured in the striatum and nucleus accumbens. Here, the influence of two variables (factors) were tested i.e. 'drug' (MPH *vs.* saline) and 'duration' (acute *vs.* chronic). The two-way ANOVA (drug x duration) indicated no significant interaction between these two variables and no significant effect of 'duration' but a statistically significant effect of 'drug' on DAT levels in the nucleus accumbens ($F_{(1,44)} = 19.1$, $p < 0.00001$). The Bonferroni *post-hoc* analysis showed that both acute ($p < 0.05$) and chronic ($p < 0.01$) MPH treatment significantly enhanced DAT density in the accumbens (Figure 3.1). In contrast, there was a significant effect of both 'drug' ($F_{(1,44)} = 14.8$, $p = 0.0002$) and 'duration' ($F_{(1,44)} = 22.5$, $p = 0.00004$) influencing DAT levels in the striatum. In this region, there was a contrasting effect of MPH on DAT, whereby acute MPH treatment had no significant effect on DAT (marginal decrease) but chronic treatment significantly up-regulated DAT ($p < 0.05$) (Figure 3.1).

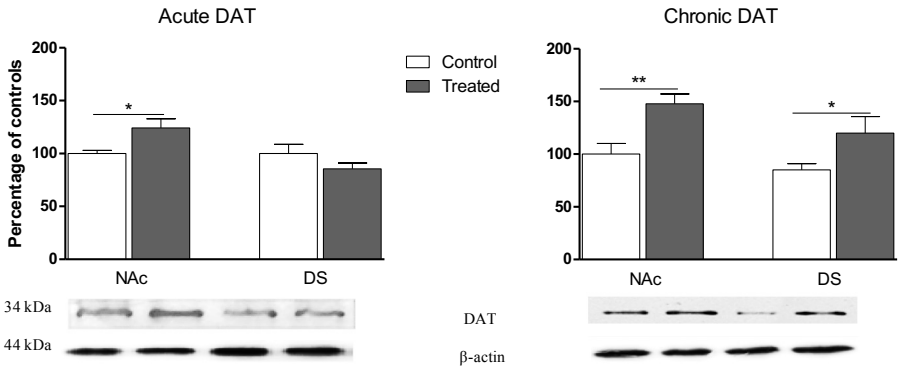

Figure 3.1: Effect of (A) acute, and (B) chronic MPH treatment on DAT protein density. DAT density was reliably measured in the nucleus accumbens (NAc) and striatum (DS) of adolescent rats. Values represent percentage ± S.E.M (n=6 rats/group but two data points from the left and right sides of each brain region). *$p < 0.05$, **$p < 0.01$ (two-way ANOVA).

Unlike DAT, which was only reliably detected and measured in the accumbens and striatum, the expression of NET was reliably measured in the frontal cortex, parietal cortex, striatum, nucleus accumbens, and hippocampus. The two-way ANOVA revealed significant interaction effect between 'drug' x 'duration' ($F_{(1,44)}$ = 14.4, p = 0.0008) and a significant effect of both 'drug' ($F_{(1,44)}$ = 10.1, p = 0.006) and 'duration' ($F_{(1,44)}$ = 16.9, p = 0.0007) in the nucleus accumbens and parietal cortex (main effect of drug: $F_{(1,44)}$ = 18.4, p = 0.0006; main effect of duration: p = 0.003; duration x drug interaction: p < 0.00001). The *post-hoc* analysis indicated that chronic MPH treatment (but not acute) significantly increased NET density in the accumbens (p < 0.05) and parietal cortex (p < 0.05) (Figure 3.2).

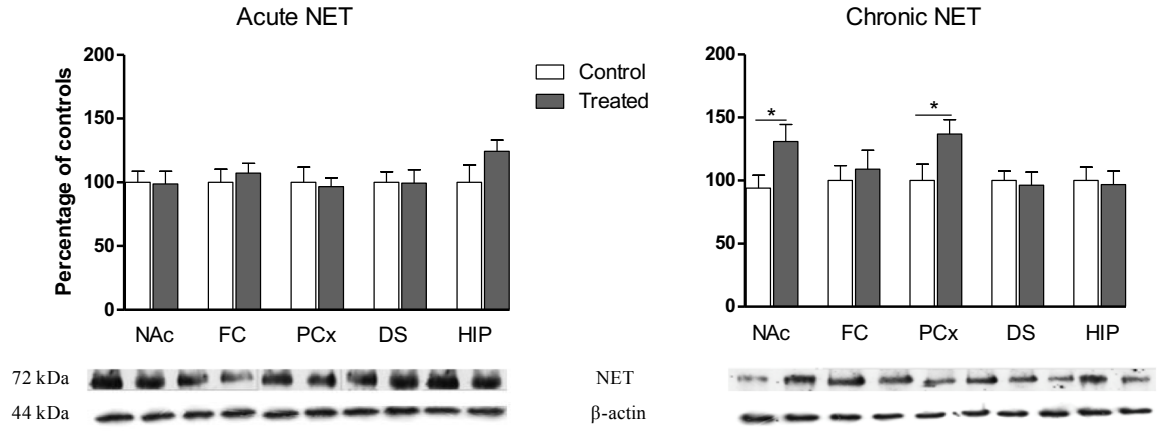

Figure 3.2: Effect of (A) acute, and (B) chronic MPH treatment on NET protein density. NET density was measured in the nucleus accumbens (NAc), frontal cortex (FC), parietal cortex (PCx), striatum (DS), and hippocampus (HIP) of adolescent rats. Values represent percentage ± S.E.M (n=6 rats/group but two data points from the left and right sides of each brain region). *p < 0.05 (two-way ANOVA).

3.3.2 MPH elevates TH and VMAT2 densities

TH and VMAT2 play key roles in the synthesis and vesicular storage of catecholamines such as DA and NA. Acute MPH treatment did not significantly alter TH density in any of the examined brain regions (Figure 3.3). However, chronic MPH treatment showed significant effect in the

nucleus accumbens ($F_{(1,44)}$ = 6.6, p = 0.001), with the density of TH being significantly upregulated in this region ($p < 0.05$) (Figure 3.3). In the parietal cortex, there was a significant 'drug' x 'duration' interaction effect ($F_{(1,44)}$ = 7.2, p = 0.02) and a significant effect of 'drug' ($F_{(1,44)}$ = 4.5, p = 0.04) and 'duration' ($F_{(1,44)}$ = 9.1, p = 0.008) and the *post-hoc* analysis revealed MPH-induced increase of TH levels following chronic treatment ($p < 0.01$) (Figure 3.3).

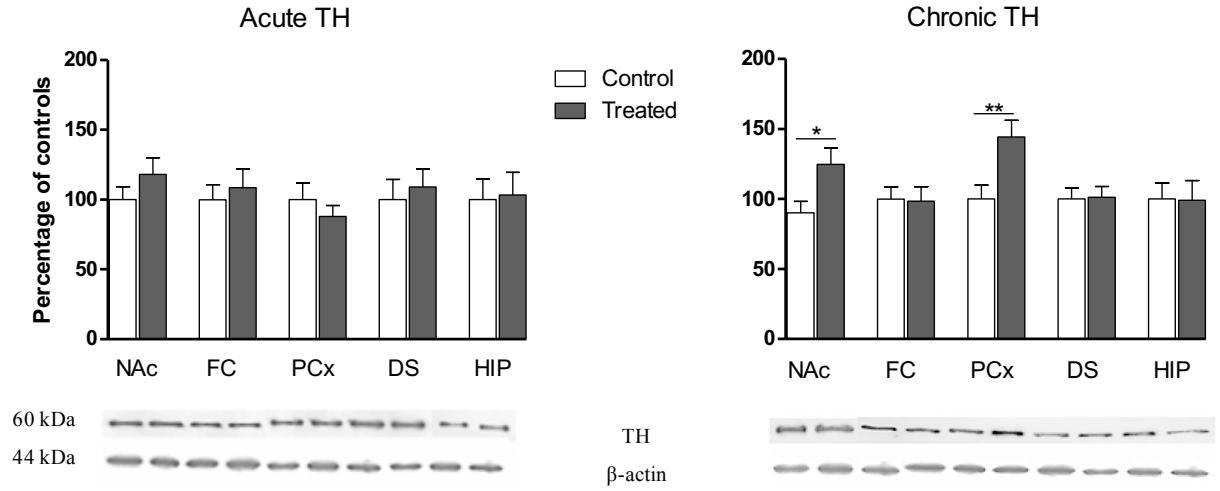

Figure 3.3: Effect of (A) acute, and (B) chronic MPH treatment on TH protein density. TH density was measured in the nucleus accumbens (NAc), frontal cortex (FC), parietal cortex (PCx), striatum (DS), and hippocampus (HIP) of adolescent rats. Values represent percentage ± S.E.M (n=6 rats/group but two data points from the left and right sides of each brain region). *$p < 0.05$, **$p < 0.01$ (two-way ANOVA).

Similar to the effect of MPH on TH expression, acute MPH treatment had no significant effect on VMAT2 expression in any of the investigated regions (Figure 3.4). The two-way ANOVA indicated a significant 'drug' x 'duration' interaction effect ($F_{(1,44)}$ = 8.7, p = 0.005), and a significant effect of both 'drug' ($F_{(1,44)}$ = 8.2, p = 0.02) and 'duration' ($F_{(1,44)}$ = 8.7, p = 0.005) in the parietal cortex. The *post-hoc* analysis indicated that MPH increased VMAT2 protein expression in the parietal cortex following chronic treatment ($p < 0.01$) (Figure 3.4). In contrast, there was only a significant effect of 'drug' in the accumbens ($F_{(1,43)}$ = 3.5, p = 0.02) and frontal cortex ($F_{(1,44)}$ = 3.7, p = 0.01). Here, the *post-hoc* analysis showed that MPH significantly

increased VMAT2 expression in the accumbens ($p < 0.05$) and frontal cortex ($p < 0.05$) following chronic treatment (Figure 3.4).

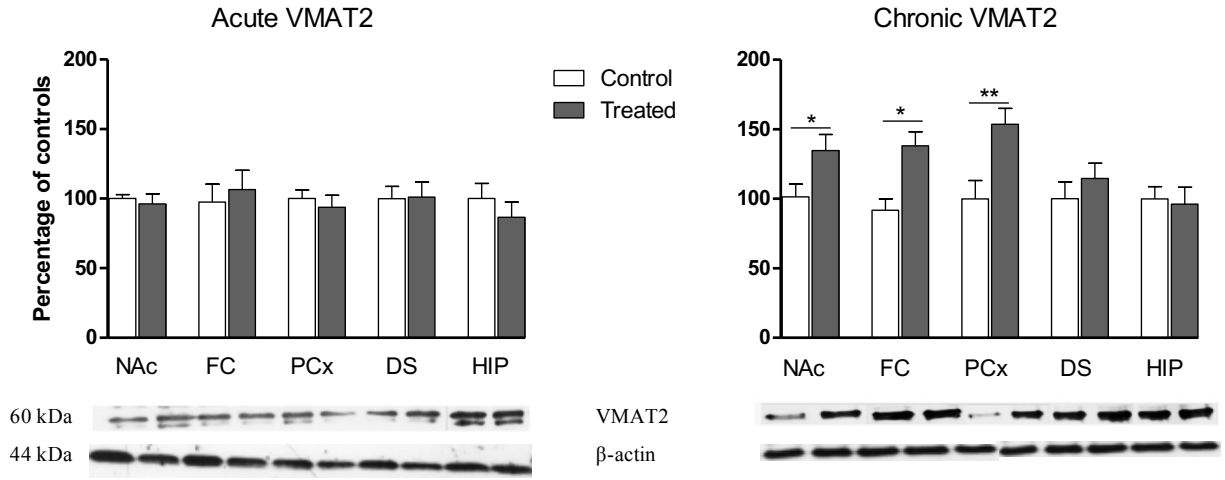

Figure 3.4: Effect of (A) acute, and (B) chronic MPH treatment on VMAT2 protein density. VMAT2 density was measured in the nucleus accumbens (NAc), frontal cortex (FC), parietal cortex (PCx), striatum (DS), and hippocampus (HIP) of adolescent rats. Values represent percentage ± S.E.M (n=6 rats/group but two data points from the left and right sides of each brain region). *$p < 0.05$, **$p < 0.01$ (two-way ANOVA).

3.3.3 MPH and D1 receptor expression

Consistent with the previous findings obtained in this study (i.e. findings on NET, TH and VMAT2 expression), acute 2.0 mg/kg MPH treatment had no significant effect on D1 receptor expression. However, there was a significant interaction between 'drug' x 'duration' ($F_{(1,44)} = 6.5$, $p = 0.01$) and a significant effect of both 'drug' ($F_{(1,44)} = 2.9$, $p = 0.02$) and 'duration' ($F_{(1,44)} = 4.6$, $p = 0.04$) in the parietal cortex, with MPH increasing D1 receptor expression in this region following chronic treatment ($p < 0.05$) (Figure 3.5). Moreover, there was a significant effect of 'drug' ($F_{(1,44)} = 4.9$, $p = 0.03$) in the accumbens, with chronic MPH treatment increasing D1 receptor density ($p < 0.05$) (Figure 3.5).

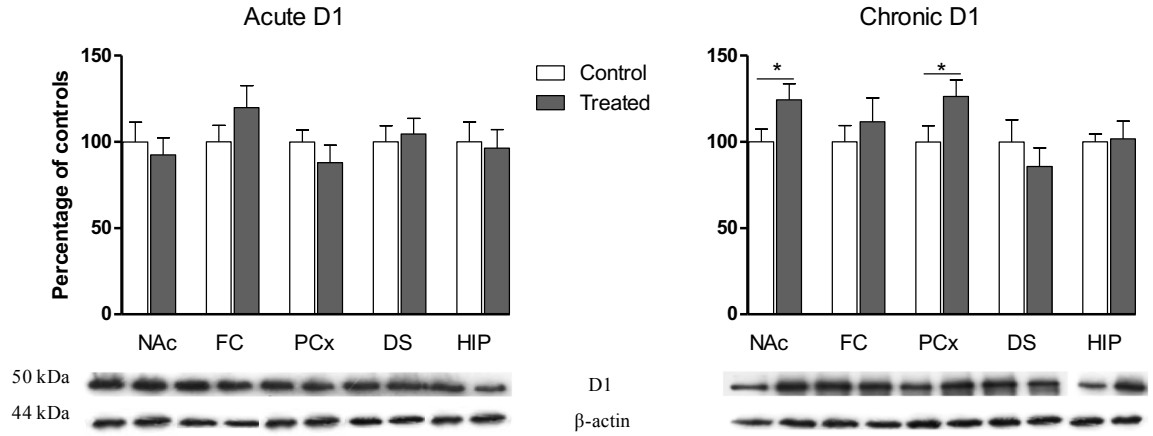

Figure 3.5: Effect of (A) acute and (B) chronic MPH treatment on D1 protein density.
D1 receptor (D1) density was measured in the nucleus accumbens (NAc), frontal cortex (FC), parietal cortex (PCx), striatum (DS), and hippocampus (HIP) of adolescent rats. Values represent percentage ± S.E.M (n=6 rats/group but two data points from the left and right sides of each brain region). *$p < 0.05$ (two-way ANOVA).

3.3.4 Effects of MPH on whole tissue levels of DA and its metabolites in the striatum and frontal cortex

3.3.4.1 MPH-induced modulation of DA and its metabolites in the striatum

Here, the lateralised effect of both acute and chronic MPH administration on DA and its metabolite (DOPAC and HVA) levels were investigated and analysed using three- and two-way ANOVAs. In the striatum, acute MPH treatment did not significantly alter the whole tissue levels of DA in the left and right sides compared to their corresponding controls but DA concentration in the MPH-treated rats was significantly higher ($F_{(1,20)} = 20.7$, $p < 0.001$) in the left compared to the right side (i.e. 'hemisphere effect'; Figure 3.6). In comparison, DA levels were significantly increased by chronic MPH treatment ($F_{(1,20)} = 4.85$, $p = 0.03$) in the left striatum compared to controls (Figure 3.6). Comparison of the acute and chronic MPH-treated samples revealed a significant effect of 'duration' ($F_{(1,20)} = 11.7$, $p < 0.001$), resulting from the potent drug effect on the chronic samples relative to the acute samples. The concentrations of DA, its metabolites and the turnover ratios in the striatum are presented in Table 3.1.

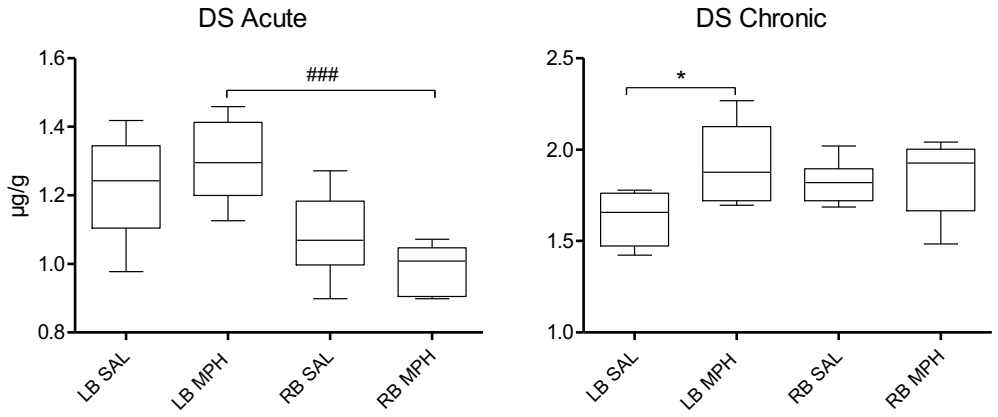

Figure 3.6: DA concentration in the left (LB) and right (RB) hemispheres of the striatum. Box plots showing DA concentration in the striatum (DS) was measured following (A) acute, and (B) chronic MPH treatment using HPLC-EC. Each box shows the 25th and 75th percentiles, the 'whiskers' show the 10th and 90th percentile, while the solid line inside the box shows the median. ###$p < 0.001$ (significant hemisphere effect i.e. left MPH-treated *vs.* right MPH-treated group), *$p < 0.05$ (MPH-treated *vs.* control).

Unlike DA, no significant effects of 'drug' and 'hemisphere' were observed on DOPAC and HVA levels. However, while no significant changes were observed in the acute group, in the chronic group DA turnover, i.e. DOPAC/DA ratio was significantly influenced by 'hemisphere' ($F_{(1,20)} = 7.11$, $p = 0.01$), with the ratio being higher in left striatum of the control group than the right ($p < 0.05$). A significant effect of 'hemisphere' ($F_{(1,20)} = 5.86$, $p = 0.02$) on HVA/DA ratio was also recorded following acute treatment with no changes observed after chronic treatment. Pairwise comparisons indicate a higher HVA/DA turnover ratio in the right acute MPH-treated group compared to the left side of the striatum ($p < 0.05$).

Table 3.1: DA and its metabolite levels in the striatum following acute and chronic MPH treatment

Striatum	Brain region	Acute		Chronic	
		Control	MPH	Control	MPH
DA (μg/g)	Left	1.22 ± 0.06	1.30 ± 0.05#	1.62 ± 0.06	1.92 ± 0.08*
	Right	1.08 ± 0.05	0.99 ± 0.03	1.82 ± 0.05	1.85 ± 0.09
DOPAC (μg/g)	Left	0.10 ± 0.01	0.12 ± 0.02	0.13 ± 0.007	0.14 ± 0.01
	Right	0.11 ± 0.01	0.09 ± 0.01	0.13 ± 0.007	0.13 ± 0.009
HVA (μg/g)	Left	0.045 ± 0.004	0.051 ± 0.006	0.040 ± 0.003	0.037 ± 0.006
	Right	0.049 ± 0.004	0.052 ± 0.004	0.042 ± 0.003	0.044 ± 0.002
DOPAC/DA	Left	0.0846 ± 0.005	0.09295 ± 0.01	0.0797 ± 0.004#	0.0732 ± 0.002
	Right	0.0997 ± 0.003	0.0974 ± 0.008	0.0686 ± 0.002	0.0680 ± 0.001
HVA/DA	Left	0.0370 ± 0.003	0.0392 ± 0.005	0.0227 ± 0.001	0.0195 ± 0.003
	Right	0.0453 ± 0.004	0.0537 ± 0.005#	0.0231 ± 0.001	0.0242 ± 0.001

Values (mean ± SEM, n=6 rats/group) were determined using HPLC-EC. *$p < 0.05$ (significant effect of 'drug' i.e. MPH *vs.* control), #$p < 0.05$ (significant 'hemisphere effect' i.e. left *vs.* right hemisphere).

3.3.4.2 MPH-induced modulation of DA and its metabolites in the frontal cortex

In the frontal cortex, there was a significant 'drug' x 'hemisphere' interaction ($F_{(1,20)} = 4.64$, $p = 0.04$) and significant effects of both 'drug' ($F_{(1,20)} = 15.5$, $p < 0.001$) and 'hemisphere' ($F_{(1,20)} = 17.7$ $p < 0.001$) influencing DA levels following acute MPH treatment. The *post-hoc* comparisons indicated that MPH induced a significant increase of DA levels in both the left ($p < 0.001$) and right ($p < 0.05$) sides following acute MPH administration in comparison to the controls (Figure 3.7). After chronic MPH treatment, significant effects of 'drug' ($F_{(1,20)} = 11.1$, $p = 0.003$) and 'hemisphere' ($F_{(1,20)} = 3.64$, $p = 0.05$) were observed to be influencing DA levels, with the levels being significantly increased by MPH in the left side ($p < 0.01$) but not the right side (Figure 3.7). The concentrations of DA, its metabolites and the turnover ratios in the frontal cortex are presented in Table 3.2.

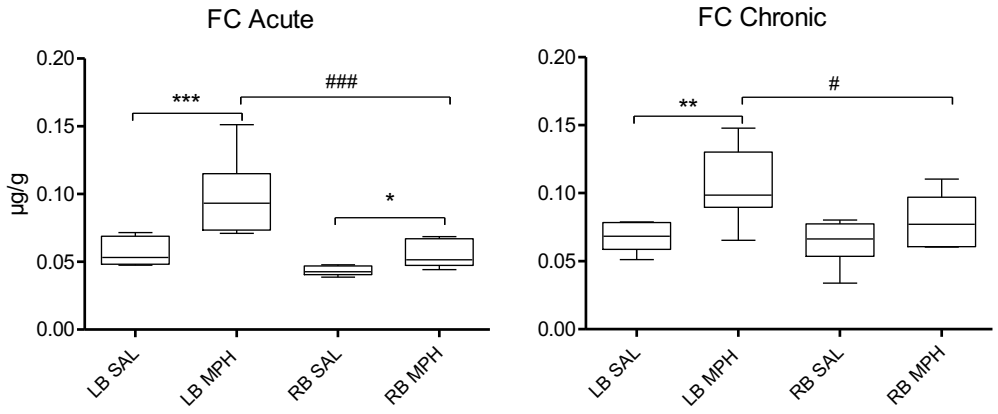

Figure 3.7: DA concentration in the left (LB) and right (RB) hemispheres of frontal cortex. Box plots showing DA concentration in the frontal cortex (FC) was measured following (A) acute, and (B) chronic MPH treatment using HPLC-EC. Each box shows the 25th and 75th percentiles, the 'whiskers' show the 10th and 90th percentile, while the solid line inside the box shows the median. #$p < 0.05$, ###$p < 0.001$ (significant 'hemisphere effect' i.e. left MPH-treated *vs.* right MPH-treated group), *$p < 0.05$, **$p < 0.01$, ***$p < 0.001$ (MPH-treated *vs.* control).

With regards to DOPAC levels in the frontal cortex, there was a significant effect of 'drug' ($F_{(1,20)} = 15.9$, $p < 0.001$) after acute treatment, with the levels being increased in both the left ($p < 0.01$) and right ($p < 0.05$) sides of the MPH-treated groups relative to the controls (Table 3.2). In the chronic samples, a significant effect of 'hemisphere' ($F_{(1,20)} = 3.64$, $p = 0.04$) was observed, with the levels being higher in the left hemisphere relative to the right ($p < 0.05$) of the control groups. Moreover, a 'drug' x 'duration' ANOVA analysis showed a significant effect of 'duration' ($F_{(1,20)} = 6.61$, $p = 0.018$) to be influencing cortical DOPAC levels. In addition, a significant 'drug' ($F_{(1,20)} = 22.7$, $p < 0.001$) and 'hemisphere' ($F_{(1,20)} = 16.09$, $p < 0.001$) effect on cortical HVA levels were also observed following acute treatment but not chronic treatment. The *post-hoc* analysis revealed high cortical HVA levels in the left ($p < 0.05$) and right ($p < 0.05$) MPH-treated groups compared to the controls (Table 3.2). Also, chronic MPH treatment significantly decreased ($F_{(1,20)} = 5.69$, $p = 0.027$) DA turnover as measured by DOPAC/DA ratio, in the left cortical hemisphere ($p < 0.05$). Similarly, both acute ($F_{(1,20)} = 50.5$, $p < 0.001$) and chronic ($F_{(1,20)}$

= 4.84, $p = 0.039$) MPH treatment significantly decreased HVA/DA ratio in the left side of both control and drug-treated groups ($p < 0.01$) relative to the right side (i.e. 'hemisphere effect').

Table 3.2: DA and its metabolite levels in in the frontal cortex following acute and chronic MPH treatment

		Acute		Chronic	
Frontal cortex	Brain region	Control	MPH	Control	MPH
DA (μg/g)	Left	0.057 ± 0.004	0.098 ± 0.01***	0.068 ± 0.004	0.105 ± 0.01**
	Right	0.043 ± 0.001	0.055 ± 0.004*	0.064 ± 0.006	0.079 ± 0.007#
DOPAC (μg/g)	Left	0.004 ± 0.0001	0.010 ± 0.001**	0.0124 ± 0.004#	0.0124 ± 0.008
	Right	0.004 ± 0.0004	0.006 ± 0.0004*	0.0082 ± 0.0008	0.0084 ± 0.0007
HVA (μg/g)	Left	0.023 ± 0.0002	0.029 ± 0.001*	0.0276 ± 0.001	0.0298 ± 0.001
	Right	0.029 ± 0.0005	0.036 ± 0.002*	0.0284 ± 0.002	0.0319 ± 0.001
DOPAC/DA	Left	0.076 ± 0.05	0.115 ± 0.02	0.175 ± 0.01	0.124 ± 0.01*
	Right	0.097 ± 0.01	0.113 ± 0.01	0.142 ± 0.02	0.109 ± 0.01
HVA/DA	Left	0.428 ± 0.03	0.324 ± 0.03	0.328 ± 0.07	0.308 ± 0.05
	Right	0.666 ± 0.03##	0.674 ± 0.05##	0.472 ± 0.05##	0.425 ± 0.05##

Values (mean ± SEM, n=6 rats/group) were determined using HPLC-EC. *$p < 0.05$, **$p < 0.01$, ***$p < 0.001$ (significant effect of 'drug' i.e. MPH *vs.* control); #$p < 0.05$, ##$p < 0.05$ (significant 'hemisphere effect' i.e. left *vs.* right hemisphere).

3.3.5 Effects of MPH on extracellular DA and DOPAC levels in the striatum

3.3.5.1 Baseline extracellular DA levels

The baseline levels (i.e. levels before MPH injection) of DA in dialysates collected from the striatum did not differ significantly ($p = 0.312$; Students t-test) between saline (1.79 ± 0.41 ng/ml) and MPH-treated (1.78 ± 0.76 ng/ml) animals. The basal level of DA in striatal samples reported in this study is comparable, albeit slightly higher (1.79 ng/ml in this study *vs.* 1.09 ng/ml in the study by Sharp *et al.* 1986) to previously reported striatal DA levels in adult rats. This difference could be attributed to several factors including the different types of dialysis probes, the anaesthesia used, or the age of the rats used (i.e. adolescent rats used in the present study *vs.* the adult rats used by Sharp *et al.* 1986).

3.3.5.2 Drug-induced extracellular DA and DOPAC levels

Dialysates collected from the 5.0 mg/kg MPH-treated animals (n=6 rats/group) showed increased levels of DA, compared to the samples collected from the corresponding saline-treated controls (Figure 3.8), with a maximum level post-MPH treatment average of 3.99 ± 1.1 ng/ml at 20 min after the injection. The two-way repeated ANOVA revealed significant 'drug' x 'time' interaction ($F_{(8, 80)} = 3.108$, $p = 0.004$) and significant effect of 'drug' ($F_{(1, 80)} = 5.197$, $p = 0.002$) on DA levels. The Bonferroni *post-hoc* test showed this difference to be at time points, 20 min ($p < 0.01$) and 40 min ($p < 0.02$) after drug injection (Figure 3.8A). In contrast, there was no significant effect of MPH treatment on DOPAC levels in striatal dialysates, although there appeared to be a trend towards decreased DOPAC levels after drug treatment (Figure 3.8B).

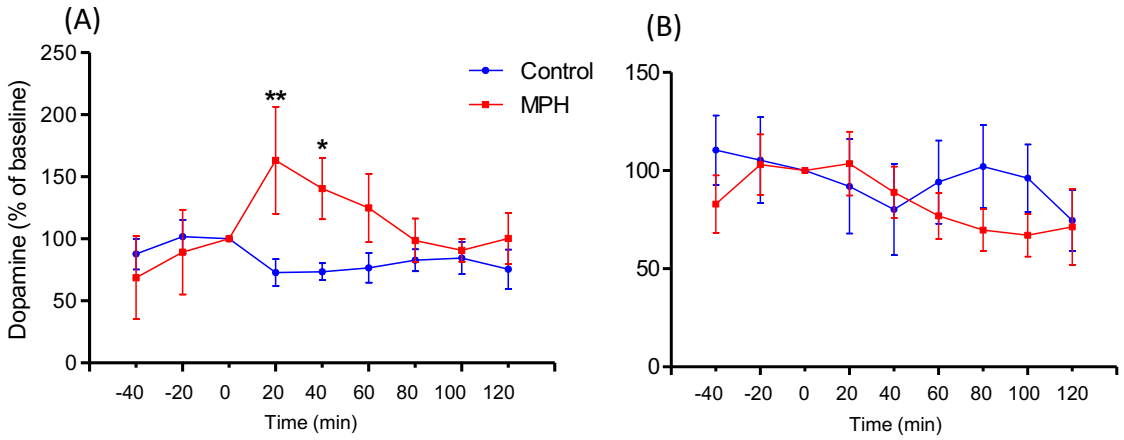

Figure 3.8: (A) DA, and (B) DOPAC concentrations in the striatum.
DA and DOPAC concentrations were measured following acute 5.0 mg/kg MPH or saline treatment. Values represent percentage of baseline values (i.e. time point 0; representing 100%) ± S.E.M (n=6 rats/group). *$p < 0.05$, **$p < 0.01$ (MPH-treated *vs.* control).

3.3.5.3 Hemisphere-specific effects of MPH on extracellular DA and DOPAC in the striatum

The two-way repeated ANOVA of 'drug' x 'time' revealed a significant effect of 'drug' treatment at the time point 40 min ($F_{(1, 8)} = 6.017$, $p = 0.039$) on striatal DA concentration in the left striatum (i.e. MPH increased striatal DA 40 min after injection in the left side; n=3) (see

Figure 3.9A). Conversely, there were no significant changes observed in the right striatum (Figure 3.9B). Also, there was no significant effect of 'drug' treatment on DOPAC levels in both the left and right hemispheres.

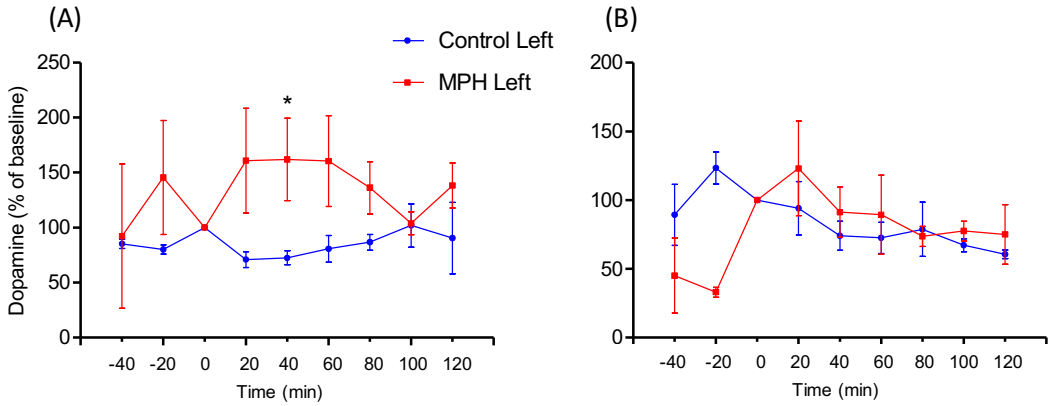

Figure 3.9: DA levels in the (A) left, and (B) right striatum.
DA levels were measured following saline or acute MPH treatment. Values represent percentage of baseline values (i.e. time point 0; representing 100%) ± SEM (n=3 rats/group). *$p < 0.05$ (MPH-treated *vs.* control); statistical power = 0.943 (G*Power, version 3.1).

3.4 Discussion

3.4.1 Principal findings and MPH dosing

The present chapter describes the effects of acute and chronic MPH treatment on the expression of protein targets involved in monoamine synthesis and release (i.e. TH and VMAT2), DA and NA uptake (i.e. DAT and NET) and the DA D1 receptor. These measurements were done in brain regions implicated in the symptoms of ADHD including: the nucleus accumbens, frontal cortex, parietal cortex, striatum, and hippocampus. In addition, this chapter examined the acute and chronic effect of MPH on whole tissue levels of DA and its metabolites DOPAC and HVA, as well as its acute effect on extracellular levels of striatal DA and DOPAC using *in vivo* microdialysis.

The study shows that MPH induced upregulations of DAT, NET, TH, VMAT2, and D1 receptor in the investigated brain regions in a 'treatment duration' dependent manner. Apart from DAT which was upregulated in the nucleus accumbens after both acute and chronic treatment, the significant protein upregulations were all recorded following chronic treatment but not acute treatment. There were also marked regional variations (i.e. brain region-specific effects) associated with the enhanced protein expressions recorded in the examined brain regions. Significant upregulations of all the examined monoaminergic protein targets were found in the nucleus accumbens, while the hippocampus failed to show any significant changes. Data from these studies also revealed that acute MPH treatment increased whole tissue levels of DA in the frontal cortex, while chronic treatment increased whole tissue levels of DA in both the frontal cortex and striatum, with the changes being more prominent in the left sides of these brain regions. Further, extracellular DA levels were increased by acute MPH treatment in the striatum, with the increase also being more prominent in the left side. This dominating effects of MPH on the left sides of these brain regions appear to be consistent with another study on humans suggesting that MPH may have more pronounced effects on neurochemicals in the left sides of the brain (Ben Amor 2014).

In these sets of experiments, 2.0 mg/kg and 5.0 mg/kg MPH doses were used. High doses of psychostimulants (e.g. 10.0 mg/kg) are reported to impair cognition and induce prominent reinforcing and locomotor-activating functions (Arnsten 2009). In contrast, at low and clinically relevant doses, these drugs are without the locomotor-activating effects and rather reduce movement (hyperactivity) and impulsivity, while improving cognitive functions such as working memory and sustained attention (Solanto 1998). MPH doses (i.e. 2.0 mg/kg and 5.0 mg/kg) used in the current studies have been previously estimated to yield peak plasma levels (8-40 ng/ml)

that are associated with clinical efficacy in humans (Berridge *et al.* 2006; Kuczenski and Segal 2002; Swanson and Volkow 2003). While 5.0 mg/kg i.p MPH treatment may seem moderately high, in rodents it has been shown to maintain drug levels within the therapeutic range over a longer period (> 30 minutes) compared to much lower doses (Kuczenski and Segal 2005). Overall, these doses improve sustained attention and working memory in rats (Berridge *et al.* 2006; Kuczenski and Segal 2002).

3.4.2 Effect of MPH on dopamine and noradrenaline transporters

There appears to be some support for the hypothesis that catecholamine dysregulation in the frontostriatal circuit is the main factor underlying ADHD symptoms (Spencer *et al.* 2005; Volkow *et al.* 1998; Volkow *et al.* 2009). The catecholamines, DA and NA play central roles in executive functioning, reward-seeking behaviour and motor activity. DAT and NET are key regulators of DA and NA function respectively, making them critical targets in studies on ADHD. Here, the effects of acute and chronic MPH treatment on these transporters have been assessed.

3.4.3 MPH induced DAT overexpression

DAT remains a major target for stimulant medications and has therefore been the focus of several neuroimaging studies in ADHD patients. Despite being the focus of several ADHD studies, however, findings on DAT have been inconsistent. While some initial studies observed elevated striatal DAT in ADHD patients (Cheon *et al.* 2003; Dougherty *et al.* 1999; Spencer *et al.* 2005), other recent studies have reported significant decreases of the transporter in some medication naïve patients (Volkow *et al.* 2009; Volkow *et al.* 2007b; Volkow *et al.* 2007a). The DAT hypothesis in ADHD stems from the fact that administering DAT blockers such as amphetamine (also a DA releasing agent) and MPH ensures an increase in extracellular DA levels in some

brain regions (e.g. frontal cortex and striatum), resulting in the enhancement of the brain's executive functions, which is underactive in ADHD patients (Del Campo *et al.* 2011).

In this study, we report that while acute MPH treatment showed a trend towards decreased DAT levels in the striatum, there was a significant increase of DAT in the nucleus accumbens (Figure 3.1). Following chronic 2.0 mg/kg MPH treatment, however, DAT density in both the striatum and accumbens was significantly elevated (Figure 3.1). These findings emphasise the importance of the accumbens and striatum in the mechanism of action of MPH, especially as these regions are reported to have abnormal DAT levels in ADHD patients (Spencer *et al.* 2005). Abnormalities in the striatum and accumbens are linked with cognitive/motor dysfunctions and altered reward-seeking behaviour in both humans and rodents. Indeed, a previous MRI study demonstrated improper striatal activation in ADHD patients (Vaidya *et al.* 2005).

The present finding of elevated DAT in the accumbens following MPH treatment is supported by a recent clinical study which also observed DAT upregulation in the accumbens following long-term MPH therapy (Wang *et al.* 2013). In line with the present findings, clinical studies on other psychostimulants such as cocaine (a DAT blocking drug) have also reported upregulated striatal DAT expression in chronic users of the drug compared with controls (Little *et al.* 1999). MPH is known to block DAT, which increases the extracellular levels of DA. However, presynaptic DAT levels are in turn regulated by extracellular DA levels, with DAT levels decreasing when extracellular DA levels are low and increasing when extracellular levels are high (Zahniser and Sorkin 2004). In ADHD, it is hypothesised that elevated DAT could be a 'trait' or a 'state' (Spencer *et al.* 2007). A 'trait' could be as result of 'hypertrophy' of dopaminergic neurons or dendritic trees arising from abnormalities in the DAT gene or inadequate pruning during neurodevelopment. A 'state', on the other hand, may arise from neuroadaptive processes to

compensate for altered DA transmission (Spencer *et al.* 2007). Based on the present findings and emerging findings from literature therefore, it is possible that the increased DAT density observed in the accumbens and striatum reflect an adaptational response to prolonged stimulant (i.e. chronic MPH) treatment. Thus, it is hypothesised that the upregulated DAT observed in the present study could be a response to elevated extracellular DA levels. In support of this hypothesis, the present study also shows increased extracellular levels of DA in the striatum following acute MPH treatment (Figure 3.8). Additional support for this hypothesis comes from previous studies that have shown that both acute and chronic MPH treatment increase extracellular DA levels in the striatum and accumbens, as well as in other brain regions such as the cortex and midbrain (e.g. VTA and SN) of rats (Calipari *et al.* 2014; Calipari and Jones 2014; Koda *et al.* 2010; Wagner *et al.* 2009). This idea of a neuroadaptative increase of DAT is consistent with previous studies that have shown that MPH is effective in the short-term but that its long-term clinical effectiveness may be limited, as larger doses may be required to ensure clinical effectiveness, and the long-term effectiveness waning after years of medication i.e. increased DAT levels require higher drug doses to reach functional blockade of DAT (Hazell 2011; Wang *et al.* 2013).

3.4.4 MPH induced NET overexpression

Beside DAT, MPH has also been shown to block NET. Reports from several studies indicate that clinical doses of MPH significantly block NET in the cortex, increasing extracellular levels of NA (Berridge *et al.* 2006; Hannestad *et al.* 2010). Clinical doses of MPH have also been shown to preferentially increase extracellular DA and NA levels in the cortex relative to the subcortical areas (Berridge *et al.* 2006; Kuczenski and Segal 2002). Moderate extracellular levels of NA in

the cortex stimulate α_2–adrenergic receptors and improves attention, while extracellular DA acts on D1 receptors to regulate working memory, attention, and behaviour (Arnsten 2009).

In the present study, while acute MPH treatment had no significant effects on NET density in the investigated brain regions, chronic MPH treatment increased NET density in the accumbens and parietal cortex (Figure 3.2). This finding is in line with existing studies highlighting the importance of NET and the noradrenergic system in the mechanism of action of MPH. While no studies have, to our knowledge, examined the effects of chronic MPH treatment on NET density, studies on the transporter following chronic cocaine (which is also a DAT and NET blocker) administration have revealed significant upregulations of the transporter in the thalamic area (Beveridge *et al.* 2005; Macey *et al.* 2003). It is conceivable that similar to DAT, the levels of NET could vary as a function of its substrate, NA. Therefore, the increased NET density in the parietal cortex and accumbens provides an additional support that repeated MPH treatment elevates transporter levels (i.e. DAT and NET), thereby regulating the extracellular levels of catecholamines. Indeed, NET blockade by MPH has been shown to increase extracellular NA (Berridge *et al.* 2006; Kuczenski and Segal 2002). Thus, an upregulation of both NET and DAT, emphasise the idea that the long-term efficacy of MPH may be limited. However, further clinical studies are required to confirm this finding on NET.

3.4.5 Effect of MPH on tyrosine hydroxylase and the vesicular transporter

Catecholamines such as DA and NA are synthesised from tyrosine. TH catalyses the rate-limiting step in the synthesis of these catecholamines. Specifically, TH catalyses the hydroxylation of L-tyrosine to dihidroxyphenylalanine (L-DOPA) (Fossbakk *et al.* 2014). Given that the activity of TH is the slowest in the catecholamine synthesis pathway (i.e. rate-limiting), this enzyme is of major interest in ADHD research and its treatment. VMAT2 is also an important regulator of

intraneuronal catecholamine concentrations, as this protein transports the synthesised DA into synaptic vesicles, thereby preventing the cytoplasmic breakdown of DA by monoamine oxidase and therefore contributes to the amount of this neurotransmitter that is stored and subsequently released via exocytosis.

3.4.6 MPH induces an overexpression of TH

When catecholamine levels are low in the catecholaminergic synapse (e.g. during excessive uptake via DAT and NET), autoreceptor mediated feedback inhibition of catecholamine synthesis is reduced and TH is activated to produce more DOPA, which is then decarboxylated into DA and transferred into synaptic vesicles by VMAT2 (Daubner *et al.* 2011). An influx of Ca^{2+} into the presynaptic terminal results in the emptying of the content of the vesicles into the synaptic cleft (Daubner *et al.* 2011). We initially postulated that if MPH elevates whole tissue and extracellular levels of DA, the changes might be explained by alterations in TH expression.

In the present study, we report that acute MPH treatment does not alter TH levels significantly in any of the investigated brain regions. However, chronic MPH treatment significantly elevates TH expression in the nucleus accumbens and the parietal cortex (Figure 3.3). This finding is in line with a recent study reported increased TH densities in the core and shell of the nucleus accumbens following chronic MPH exposure to young rats (Lepelletier *et al.* 2015). That TH levels in the striatum and the other brain regions were not significantly altered is also consistent with a previous study that found no changes in either the mRNA or the protein levels of TH in the striatum and some other brain regions (e.g. VTA) following chronic MPH treatment in rats (Calipari *et al.* 2014). Given that MPH treatment failed to enhance TH expression in striatum and frontal cortex, it is unlikely that the measured increase of whole tissue levels of DA by MPH treatment in these brain regions is related to increased TH expression (see Figures 3.6 and 3.7).

3.4.7 MPH induced VMAT2 overexpression

VMAT2 has historically been considered as one of the markers of monoaminergic (including dopaminergic and noradrenergic) neuronal integrity. This has particularly been the case in disorders that result in the loss dopaminergic neurons such as Parkinson's disease. In this disorder VMAT2 levels are significantly lower compared to healthy volunteers (Pifl *et al.* 2014). Studies on transgenic VMAT2 knockout mice have demonstrated that impulse-dependent DA release is significantly lower compared to wild type mice, while VMAT2 over-expressing mice show increased intracellular DA concentration and DA release relative to controls (Lohr *et al.* 2014). Furthermore, psychostimulant (e.g. amphetamine) induced increases of extracellular DA is significantly dampened in VMAT2 knockout animals relative to controls (Patel *et al.* 2003). Given the MPH-induced increase of TH in the accumbens and parietal cortex following chronic MPH treatment, it was hypothesised that such increases in TH may be associated with a corresponding increase of VMAT2 in these brain regions.

In this study, we report that acute MPH treatment does not significantly alter VMAT2 density in any of the brain regions investigated. In comparison, chronic MPH treatment (2.0 mg/kg) induced a significant increase of VMAT2 in the nucleus accumbens, frontal cortex and parietal cortex (Figure 3.4). Thus, these findings point to 'treatment duration-dependent' differences in the mechanism of action of MPH regarding this transporter. Elevated VMAT2 density in the parietal cortex and nucleus accumbens following chronic MPH treatment correspond with our finding of increased TH density in these brain regions. Overall, this provides more support for a potential enhancement of DA synthesis, requiring increased vesicular storage capacity, which would be aided by the enhanced VMAT2 expression. In addition, like TH, no significant changes in VMAT2 density was recorded in the striatum, and this appears to be in line with a previous study

in SHR rats that also showed that chronic MPH treatment failed to alter striatal VMAT2 protein expression (Simchon *et al.* 2010). However, in contrast to our findings in the striatum following acute treatment, a previous study has reported an increase in striatal VMAT2 density following acute MPH treatment (Sandoval *et al.* 2002). The difference in findings could be related to the difference in response to MPH treatment by animals of different ages (180-220 g animals were used in the present study *vs.* 280-340 g used in the study by Sandoval *et al.* 2002), as well as the differences in dosing regimen (2.0 mg/kg in this study *vs.* 1.0 mg/kg in their study).

In general, two types of presynaptic vesicles have been described: a membrane associated fraction and a cytoplasmic fraction (Sandoval *et al.* 2002). Interestingly, some researchers have proposed that MPH treatment redistributes VMAT2 protein from the membrane associated vesicle fraction to the cytoplasmic vesicle fraction, leading to an increase in VMAT2 density and an increase in vesicular DA content in the cytoplasmic fraction (Fleckenstein *et al.* 2009). The data reported in this study would suggest that any increase in DA (both whole tissue and extracellular DA) induced by chronic MPH treatment might be related to the enhanced expression of VMAT2, particularly in the cortices and the nucleus accumbens (as TH is also increased in these regions). Alternatively, increased VMAT2 density could be due to an increased reuptake of DA and NA. In this context, the present study shows that chronic MPH upregulates DAT and NET in the nucleus accumbens and parietal cortex respectively, an effect that coincided with the increased levels of both VMAT2 and TH. Taken together, an upregulation of these two reuptake transporter proteins (i.e. DAT and NET), as well as TH could lead to enhanced cytoplasmic catecholamine levels (albeit not measured in the present study for the accumbens and parietal cortex), and hence would require enhanced VMAT2 protein expression for transporting the neurotransmitters into the vesicles.

3.4.8 MPH induced D1 receptor overexpression

MPH has been shown to improve working memory in both ADHD patients and healthy volunteers. As previously mentioned, MPH acts as a DAT and NET blocker, increasing extracellular levels of both DA and NA. The increased synaptic levels of these catecholamines stimulate postsynaptic receptors. In particular, DA stimulates D1-like and D2-like receptors, resulting in behavioural changes such as improved attention and concentration (Arnsten 2009; Arnsten 2011).

In this study, while acute MPH treatment does not significantly alter D1 receptor expression in the examined brain regions, chronic MPH treatment significantly elevates the density of this receptor in the nucleus accumbens and the parietal cortex (Figure 3.5). This finding may support the role of this brain region in attention and memory. Although MPH is thought to have more effect on NA than DA in the cortex, it has long been known that DA is essential to the working memory functions of the cortex. Recent findings obtained from studies on monkeys indicated that MPH improves attention and working memory performance in the cortex by indirectly enhancing D1 and α_{2A} receptor actions (Gamo *et al.* 2010). Other studies on rodents have shown that moderately enhanced stimulation of D1 receptors has beneficial outcomes on working memory (Arnsten 2009; Arnsten 2011).

Moderate stimulation of D1 receptor enhances spatial memory by selectively suppressing firing to non-preferred inputs i.e. decreases 'noise' (Arnsten 2009; Arnsten 2011). Modest stimulation of D1 receptor occurs with clinically relevant doses of MPH (as used in the present study), however when extremely high doses of MPH (e.g. 10.0 mg/kg dose) or when other D1 receptor agonists are administered it suppresses all neuronal firing, impairing working memory (Arnsten 2009; Arnsten 2011). Given that previous studies have shown increased DA release and increased

extracellular DA in the cortex and other brain regions following both acute and chronic MPH exposure (Calipari *et al.* 2014; Calipari and Jones 2014; Koda *et al.* 2010; Wagner *et al.* 2009), it is hypothesised that the increased extracellular DA in the cortex could activate the upregulated cortical D1 receptor (observed in the present study) and its signalling pathway in the cortex and possibly improve working memory (Gamo *et al.* 2010). Activation of the upregulated D1 receptor and its signalling pathway in the nucleus accumbens by extracellular DA could, on the other hand, have effects on drug-seeking behaviour and drug-induced long-term plasticity (Fricks-Gleason and Marshall 2011; Gong *et al.* 1999).

3.4.9 Lateralised effect of MPH on DA and its metabolites

Similar to a previous report, analysis of the data on whole tissue levels of striatal DA following acute (2.0 mg/kg) MPH treatment revealed no significant effect of MPH (Schaefer *et al.* 2006). However, there was a trend towards an increased whole tissue DA level in the left striatum (Figure 3.6). Further evaluation of the effect of acute MPH administration in the striatum examined via *in vivo* microdialysis (single 5.0 mg/kg MPH) revealed significantly elevated extracellular DA levels in the striatum, but not its main metabolite DOPAC (Figure 3.8). This increase in extracellular DA was more pronounced in the left side of the striatum (albeit a small sample size, n=3 rats/hemisphere). Similar enhancements of DA levels following acute MPH treatment has consistently been reported in both preclinical and clinical studies (Berridge *et al.* 2006; Kuczenski and Segal 2002; Swanson and Volkow 2003). Indeed, a number of studies have suggested a role for striatal DA in the stimulant treatment of ADHD (Volkow *et al.* 2001; Wang *et al.* 2013). Other studies have also observed a significant increase of DA in the mesocorticolimbic pathway following acute MPH administration to rats (Kuczenski and Segal 2002) and adult human volunteers (Volkow *et al.* 2001). In the present study, acute MPH

treatment induced significant increases in extracellular DA levels 20 min and 40 min after drug administration (Figure 3.8). This finding is consistent with other studies using similar MPH doses that also observed increases in extracellular DA levels at these time points in the striatum, accumbens and other regions in the mesocorticolimbic pathway (Kuczenski and Segal 2002; Schiffer *et al.* 2006).

On the other hand, after chronic MPH treatment, whole tissue levels of DA were significantly elevated in the left but not the right striatum (Figure 3.6). This elevated whole tissue levels of striatal DA is unlikely to be driven by altered TH, as striatal TH was not increased by chronic MPH administration in this region. However, DAT was increased by chronic MPH treatment in the striatum suggesting an enhanced reuptake of DA back into DA nerve terminal. The DOPAC/DA and HVA/DA ratios are frequently used as indicators of dopaminergic activity (Lavielle *et al.* 1979). In addition to the elevated whole tissue levels of DA in the striatum, there was a significant increase in the DOPAC/DA ratio in the left striatum ('hemisphere effect') but not in the right side (Table 3.1), further suggesting an enhanced dopaminergic activity in the left striatal area. The increase of whole tissue DA levels in the striatum of genetically unmodified (i.e. normal) animals following chronic MPH treatment in the present study is not consistent with findings from a previous study on 'Naples High excitability rats' that showed decreased whole tissue striatal DA and DOPAC levels following chronic drug treatment (Ruocco *et al.* 2010). The differences in findings could be due to the type of rats used, as the 'Naples High excitability rats' have been shown to have abnormal mesocortical dopamine function (due to abnormal levels of DAT, TH, and D1 receptor) and are not hyperactive or impulsive and are therefore not considered to satisfy the criteria for animal models of ADHD (Russell *et al.* 2005). In addition, although the extracellular levels of striatal DA after chronic treatment was not measured in the present study,

several studies have previously found increased extracellular DA concentrations in the striatum, accumbens, and other brain regions following repeated MPH treatment (Calipari *et al.* 2014; Calipari and Jones 2014; Koda *et al.* 2010; Wagner *et al.* 2009).

A dysfunction of the left striatum is considered to be a core abnormality in ADHD (Vaidya *et al.* 2005). In particular, while some studies have shown improper activation of the striatum in ADHD patients, other studies have reported that individuals suffering from left striatal lesions have deficits in attention and executive function (Vaidya *et al.* 2005; Benke *et al.* 2003). Therefore, an MPH-induced increase of DA levels in the left striatum may be critical to the normalisation of striatal functions. In addition, the non-significant changes to the levels of DOPAC and HVA by MPH in the present study is comparable to findings from some previous studies (Panos *et al.* 2014; Nielsen *et al.* 1983).

Unlike the changes in the striatum, both acute and chronic MPH treatment increased the whole tissue levels of DA and its metabolites (DOPAC and HVA) in the frontal cortex (Table 3.2). Further evaluation showed that although the increase in cortical DA occured in both the left and right sides, the left cortical DA increase was more pronounced (Figure 3.7). The frontal cortex is suggested to play important roles in the processes that have been implicated in ADHD (Kuczenski and Segal 2002; Arnsten 2009). For instance, functional imaging studies have found an under-activation of several areas of the cortex including the frontal and parietal areas in ADHD patients during tasks related to attention and motor activity (Dickstein *et al.* 2006; Rubia *et al.* 1999; Vance *et al.* 2007). This under-activation is suggested to be particularly prominent in the right cortex (Rubia *et al.* 1999; Vance *et al.* 2007). However, in the present study, although both acute and chronic MPH treatment increased whole tissue levels of DA in the frontal cortex, the increase was much more prominent in the left side. The present finding is consistent with a

previous clinical study which has also shown that MPH may have a more pronounced effect on neurochemicals in the left frontal cortex and left striatum (Ben Amor 2014). The increase of whole tissue levels of DA in the frontal cortex is unlikely to be related to TH density, as both acute and chronic MPH treatment did not significantly alter TH levels. Catecholamines (including DA and NA) exert pronounced modulatory actions on cortical neuronal activity and cortex-dependent behaviour, including attention and working memory (Arnsten 2009). Although the extracellular levels of DA in the frontal cortex following acute and chronic MPH treatment were not measured in the present study, previous studies have reported increased extracellular DA in this region following MPH treatment (Berridge *et al.* 2006; Kuczenski and Segal 2002). If the present finding of elevated whole tissue levels of DA in the frontal cortex correlates with an increased extracellular DA (as shown previously by other researchers), it would activate the enhanced cortical D1 receptor density and aid in the improvement of working memory and sustained attention (Berridge *et al.* 2006; Kuczenski and Segal 2002).

3.5 Conclusion

The current study shows that both acute and chronic MPH treatment increases whole tissue levels of DA in the frontal cortex and the striatum, with the effect being more pronounced in the left side of both regions. Further evaluation revealed increased extracellular DA in the striatum after acute MPH treatment, also more prominent in the left side. These changes in DA levels, particularly in the frontal cortex, coincided with increased D1 receptor levels recorded in the cortex (both frontal and parietal). Further evaluation of the protein markers showed increased expression of TH and VMAT2 in the frontal and parietal cortex, and nucleus accumbens after chronic but not acute MPH treatment. Interestingly, chronic MPH treatment increased the density of DAT in the nucleus accumbens and striatum and increased NET density in the nucleus

accumbens and parietal cortex. Given that DAT and NET increase DA and NA reuptake respectively, the increase of these two protein targets by chronic MPH treatment indicates that the long-term effects of the drug could be limited, as larger doses may be required to block the overexpressed DAT and NET in order to achieve clinical effectiveness. In addition, although ADHD is suggested to be a right hemisphere disorder due to studies showing right cortical (frontal and parietal) under-activation in patients (Rubia *et al.* 1999; Vance *et al.* 2007), the present findings indicate that MPH may have more pronounced effect on DA systems in the left frontal cortex as opposed to the right side. Further investigations may establish the clinical relevance of these findings.

CHAPTER 4

4 Neurochemicals and brain metabolites altered by methylphenidate in rat cerebral hemispheres

4.1 Introduction

Along with the dysfunctional dopaminergic and noradrenergic systems postulated to be underlying the pathophysiology of ADHD, there are neurochemical theories suggesting that alterations to more global brain biomolecules such as glutamate, glutamine, GABA and creatine may also be associated with ADHD (Jin *et al.* 2001; Moore *et al.* 2006; Carrey *et al.* 2007; Perlov *et al.* 2009). However, despite these observed metabolic changes in ADHD patients, the impact of MPH treatment on most of these biochemicals in the brain remains to be determined.

Anatomical theories of ADHD indicate a reduced size of the corpus callosum, which leads to insufficient transmission between the two cerebral hemispheres. Some studies also suggest a right hemisphere dysfunction amongst ADHD children (Waldie and Hausmann 2010). This hypothesis is supported by the fact that the symptoms of ADHD are similar to those observed in patients with right parietal lobe lesions (Voeller and Heilman 1988). More recent brain imaging studies also link the behavioural symptoms of ADHD to the smaller and less activated anterior regions of the right cerebral hemisphere relative to the left hemisphere (Stefanatos and Wasserstein 2001). Therefore, in order to identify any potential hemisphere-specific differences involved in the mechanism of action of MPH, samples from both the left and right cerebral hemispheres were investigated in the present study.

The symptoms of ADHD are successfully treated with the psychostimulant MPH, which blocks the re-uptake of transporter proteins for both dopamine and noradrenaline, thereby increasing the transmission of these neurotransmitters in the synaptic cleft (Volkow *et al.* 1998; Kuczenski and Segal 2002). With an increasing rate of ADHD diagnosis worldwide, a sharp rise in the number of prescriptions of MPH to young children and adolescents has been recorded (Rabiner 2013), despite an incomplete understanding of the drug's effects on the adolescent brain. Non-stimulant

alternative treatments, such as the noradrenaline re-uptake inhibitor atomoxetine, are also often prescribed (Warrer *et al.* 2016), and more recently, administration of the aromatic amino acid, tyrosine, a precursor of dopamine and noradrenaline, has also been tested and shown to be effective (Hinz *et al.* 2011). Alternatively, the use of exercise as a non-drug treatment paradigm is also recently gaining increasing support, both alone and in combination with MPH (Choi *et al.* 2015).

In humans, metabolomics-type studies employing proton magnetic resonance spectroscopy (^{1}H-MRS) is increasingly used for the study of psychiatric disorders and their treatments, including schizophrenia (Marsman *et al.* 2014) and bi-polar disorders (Brambilla *et al.* 2005), together with ADHD (Perlov *et al.* 2007). However, ^{1}H nuclear magnetic resonance (^{1}H-NMR) spectroscopic analysis of biofluids and tissues, although related to ^{1}H-MRS, offers higher spectral resolution, in addition to more accurate quantification and greater sensitivity, allowing the detection of less abundant metabolites, including the neurotransmitter GABA (Du *et al.* 2015). Indeed, ^{1}H-NMR spectroscopy has already been successfully applied to study alterations in human metabolite levels in post-mortem tissue and cerebrospinal fluid collected from patients diagnosed with various psychiatric and neurological disorders (Prabakaran *et al.* 2004; Holmes *et al.* 2006; Lan *et al.* 2008). Notwithstanding, surprisingly few studies have explored drug-inducible metabolic changes in human or animal brain tissue using high-resolution ^{1}H-NMR analysis. Drugs already investigated using this ^{1}H-NMR-linked metabolomics strategy include lithium ions (Li^{+}), antipsychotic drugs and methamphetamine (McLoughlin *et al.* 2009; Bu *et al.* 2013). However, to the best of our knowledge, this approach has not yet been applied to determine the effects of MPH on the brain metabolome.

In this study, we have employed, for the first time, a ^{1}H-NMR-based metabolomics approach in order to simultaneously explore the effects of MPH on a wide range of brain metabolites in adolescent rats. We also sought to determine if MPH influences brain metabolites differently in the left and right cerebral hemispheres. The biochemical, therapeutic and physiological significance of the research work performed is discussed in detail.

4.1.1 Aims

This study was aimed at evaluating the effect of acute MPH treatment on cerebral neurochemistry and levels of metabolic markers. The experiment tests the hypothesis that acute MPH treatment elevates cerebral metabolites and precursors within the catecholamine synthesis pathway. Specifically, the experiment was to assess the effect of the drug on:

- Large neutral amino acids such as tyrosine and phenylalanine that are involved in catecholamine synthesis.
- Excitatory and inhibitory amino acid transmitter levels.
- Amino acids and biomolecules associated with energy and membrane metabolic pathways.
- The hypothetical presence of a differential effect on brain metabolites and neurochemicals in the left and right cerebral hemispheres.

4.2 Methods

4.2.1 Drug treatment and brain dissection

For a detailed description of the animal housing and MPH treatment procedures see Chapter 2. In brief, the animals were assigned to two treatment groups i.e. saline-treated control group and drug-treated group. The animals in the saline-treated control group received a single 1.0 ml/kg

saline dose, while the animals in the drug-treated group received a single 5.0 mg/kg MPH dose intraperitoneally. One hour after the last treatment, the animals were killed via a rapid dislocation of the neck and the left and right cerebral hemispheres were dissected out on ice, snap-frozen in isopentane on dry ice and stored at -80°C until required for ^{1}H-NMR analysis.

4.2.2 Preparation of brain extracts and ^{1}H-NMR experiments

The brain sample preparation and ^{1}H-NMR experiments were performed as described in Chapter 2, section 2.2.1 and 2.2.3.

4.2.3 Pre-processing of NMR spectra

The ^{1}H-NMR spectra acquired were phase and baseline-corrected using ACD/NMR processor (academic edition; Ontario, Canada) software prior to the univariate and multivariate data analysis. Subsequently, the 'intelligent-bucketing' procedure was applied, giving a full dataset of 71 rows (samples) and 301 columns (variables). The resulting intelligently-selected bucket (ISB) integral intensity values were normalised to the TSP signal (*s*, δ = 0.00 ppm). Spectral regions that did not contain any resonances (i.e., noise regions) were edited and removed, so that a final dataset of 71 (samples/rows) x 113 (potential predictor ISB variables/columns) was obtained for further analysis. The intense δ = 4.65-5.16 ppm residual H_2O/HOD signal region was also removed from all the ^{1}H-NMR profiles acquired prior to the univariate and multivariate data analysis strategies.

4.2.4 Multivariate and univariate analysis of rat cerebral data

Multivariate and univariate statistical analyses were performed on the TSP-normalised integral values as described in Chapter 2, section 2.2.5. Following the multivariate analysis, the performance of the different subsets and combination of discriminatory metabolites selected by PLS-DA (as described in section 2.2.5) was further explored using a ROC curve analysis. The

ROC curve analysis was conducted using the *Biomarker Analysis* option available in *MetaboAnalyst 3.0*. The univariate statistical analysis was then carried out in R statistical package based on equation 1.

$$Y_{ij} = \mu + T_i + H_j + TH_{ij} + e_{ij} \qquad (1)$$

In addition, to explore the effect of MPH on the left and right cerebral hemispheres, simultaneous multivariate evaluation of the main experimental factors i.e. 'treatment status' (i.e. MPH *vs.* control) and 'brain hemisphere' (i.e. left *vs.* right side) was conducted using ANOVA simultaneous component analysis (ASCA) via the two-factor independent samples option of *MetaboAnalyst 3.0* (which is based on equation 1) to detect any significant major metabolic patterns arising from each experimental factor, including the multivariate TH_{ij} interaction component of variance. The significance of each of these multivariate variance components was determined via associated permutation testing with 2,000 permutations.

4.2.5 Retrospective multivariate power analysis of the rat cerebral data

The minimum sample sizes required to achieve multivariate statistical significance between the MPH-treated and saline-treated control groups were retrospectively determined by applying the 'Power Analysis' option of *MetaboAnalyst 3.0* to a dataset consisting of the 13 key biomarker variables discovered via PLS-DA analysis (i.e., GABA, alanine, aspartate, phosphocreatine, phosphocholine, hypoxanthine, *myo*-inositol, glutamate, lysine, taurine, valine, phenylalanine and tyrosine; Table 4.1). With an FDR-adjusted *p*-value of 0.005, predicted multivariate test powers of 0.61, 0.86, 0.96, 0.99 and 1.00 were calculated for sample sizes of 3, 6, 10, 16, and 24 per group (Figure 4.1), and this clearly confirms that the sample sizes selected for a biomarker variable-optimised NMR-linked metabolomics study would indeed be more than sufficient (i.e. n=18 rats per group).

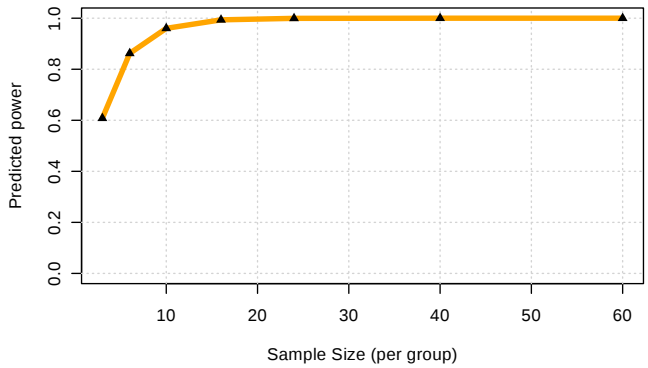

Figure 4.1: Retrospective multivariate power calculations.
This was performed for a model incorporating 13 key cerebral biomarker variables for MPH treatment status (alanine, aspartate, phosphocreatine, phosphocholine, hypoxanthine, *myo*-inositol, GABA, glutamate, lysine, taurine, valine, phenylalanine and tyrosine).

4.2.6 Metabolic pathway analysis of the cerebral dataset

Analysis of the most relevant cerebral metabolic pathways altered following MPH treatment was performed using the *MetaboAnalyst 3.0* tool, as described in Chapter 2, section 2.2.7.

4.3 Results

4.3.1 ^{1}H-NMR profiles of rat brain extracts

Representative, mean ^{1}H-NMR spectrum acquired on an aqueous cerebral extract from saline-treated controls and MPH-treated rats spanning spectral regions (a) 0.80-4.50 ppm, and (b) 5.6-8.9 ppm, are shown in Figure 4.2. These spectra contained a large number of prominent resonances assignable to a wide range of low-molecular-mass metabolites, including amino acids (e.g., alanine, aspartate, GABA, lysine, tyrosine and phenylalanine), organic acid anions (acetate, formate, lactate, etc.), as well as creatine, phosphocreatine, and *myo*-inositol, together with purines and pyrimidines, and their nucleoside adducts (hypoxanthine, inosine, etc.).

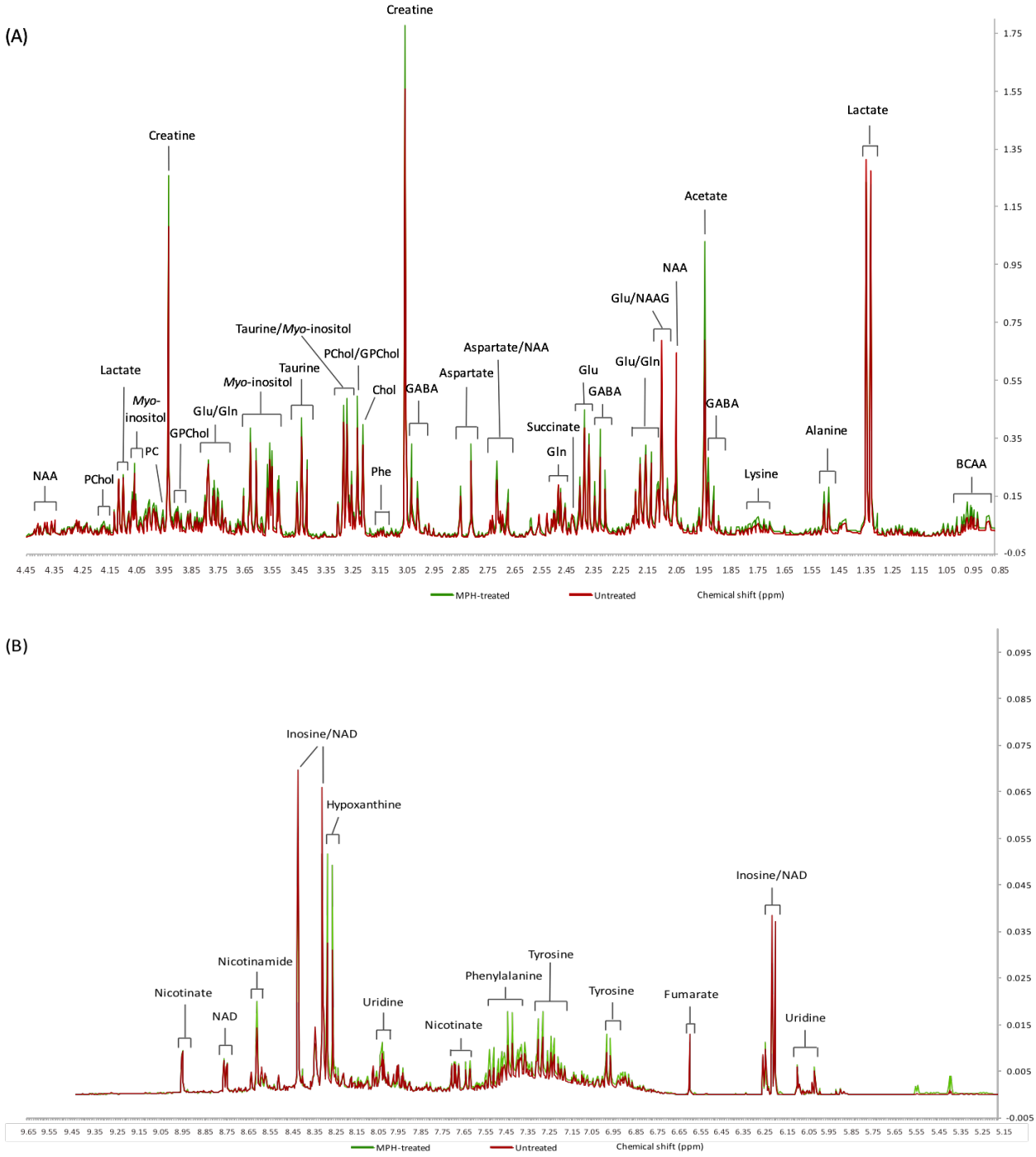

Figure 4.2: Average 400 MHz ^{1}H-NMR spectra of the cerebral extracts.

The spectra were obtained from the saline-treated controls (red) and MPH-treated rats (green) (A) 0.8 to 4.5 ppm, and (B) 5.6-8.9 ppm (resonance intensity amplitude enhanced 20-fold of that of (A)] spectral region. Abbreviations: BCAA, branched chain amino acids (valine, isoleucine, leucine); GABA, γ-amino butyric acid; NAA, *N*-acetylaspartate; NAAG, *N*-acetylaspartylglutamate; Glu, glutamate; Gln, glutamine; PCr, Phosphocreatine; Chol, choline; PChol/PC, phosphocholine; GPChol, glycerol-phosphocholine; Phe, phenylalanine; NAD, nicotinamide adenine dinucleotide.

4.3.2 Classification of the ^{1}H-NMR profiles according to their treatment status

Of the 113 'intelligently-selected' buckets variables investigated, 103 variables had higher mean values for the MPH-treated group relative to the saline-treated control group, while 10 variables had higher mean values for the saline-treated control group relative to the MPH-treated group (i.e. MPH treatment resulted in 103 positive and 10 negative fold-changes). Primarily, PLS-DA was employed to analyse the ^{1}H-NMR dataset in order to classify the samples according to their treatment status. The 3D scores plot for the first three components showed that the MPH-treated cerebral regions can be clearly distinguished from the saline-treated controls (Figure 4.3A). Indeed, a 10-fold cross-validation procedure was also applied to the PLS-DA analysis in order to evaluate the performance of the classification when checked with an independent subset from the original dataset. This strategy achieved a maximum accuracy of 0.87 with a total of 5 components, and a Q^2 value of 0.50, which were the maximum values achieved using this parameter ($Q^2 \geq 0.3$ was considered statistically significant) (McLoughlin *et al.* 2009; Worley and Powers 2013). To evaluate the performance of class discrimination, a permutation test was conducted with 2,000 permutations, where the ratio of the between-sum-of-squares to the within-sum-of-squares (B/W-ratio) for the class assignment prediction of each model was computed, and this yielded a *p*-value of 5.0×10^{-4}, indicating a strong discrimination between the MPH-treated and saline-treated control groups. PCA analysis of the dataset also revealed a variable loadings plot of PC1 *vs.* PC2, the former representing the component most responsible for these discrimination observed between the two classifications (see Appendix 1; Figure A1).

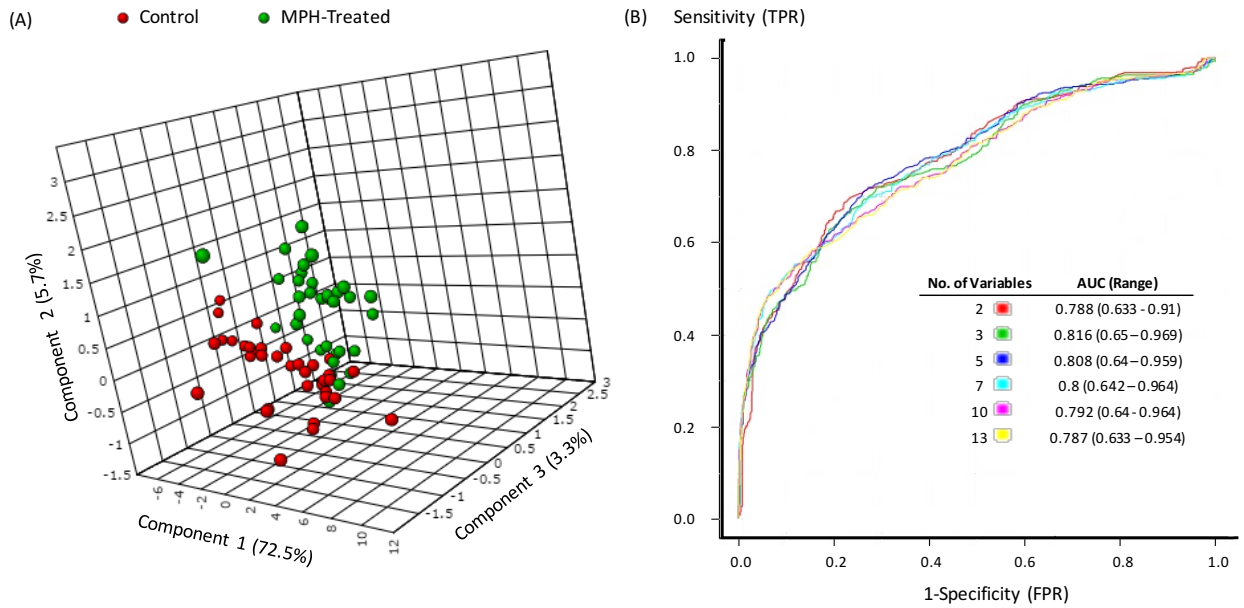

Figure 4.3: PLS-DA scores plot and ROC analysis curve of the cerebral samples.
(A) PLS-DA scores plot demonstrating a clear separation between the MPH-treated and control groups (the contribution of each PLS-DA component to the total variance is provided in brackets), and (B) ROC (receiver operating characteristic) curve for the 13 selected metabolites by PLS-DA and their respective AUROC (area under ROC) values for biomarker models with increasing numbers of predictor (X) variables.

4.3.3 MPH-induced metabolic alterations in brain samples

Treatment of experimental animals with MPH was found to significantly alter the metabolic profiles of rat cerebrum (Figure 4.3). Indeed, metabolites identified as significantly different in the MPH-treated rats when compared to the controls were all elevated in the MPH-treated group. The top 22 discriminating metabolites identified by PLS-DA based on their VIP (variable importance in projection) scores, together with their *p*-values obtained from the ANOVA model depicted in equation 1, are shown in Table 4.1. This table also lists the assignments for the discriminatory 'intelligently-selected' buckets, the multiplicity, coupling constants, and fold-changes. Positive fold-change values indicate an increased level of the specified metabolite in the MPH-treated group when expressed relative to the controls.

Table 4.1: Top 22 discriminatory variables for the MPH-treated and control cerebral extracts selected by PLS-DA based on their VIP scores.

Variable Ranking	ISB	Assignment	Multiplicity (*j*, Hz)	Raw ANOVA *p*-values for 'between treatment status' factor	Fold-change
1	1.85-1.95	GABA-C3-CH_2	*q* (7.47, 7.48)	4.53 x 10^{-4}	+1.49
2	2.99-3.03	GABA-C2-CH_2	*d* (2.95)	6.06 x 10^{-4}	+1.45
3	2.25-2.33	GABA-C4-CH_2	*t* (7.31)	9.25 x 10^{-4}	+1.39
4	0.91-1.00	Valine-C4-CH_3	*m* (3.85, 4.25)	1.42 x 10^{-3}	+1.51
5	3.51-3.58	*Myo*-inositol-C3-CH_2	*dd* (2.96, 2.81)	3.21 x 10^{-3}	+1.29
6	1.45-1.53	Alanine-C3-CH_3	*d* (7.39)	2.44 x 10^{-3}	+1.43
7	1.66-1.75	Lysine-C5-CH_2	*m* (1.66, 1.57)	4.07 x 10^{-3}	+1.43
8	1.00-1.08	Valine-C4'-CH_3	*d* (7.24)	3.57 x 10^{-3}	+1.53
9	8.21-8.23	Hypoxanthine-C7-CH	*s*	7.64 x 10^{-6}	+1.76
10	8.17-8.21	Hypoxanthine-C2-CH	*s*	1.16 x 10^{-5}	+1.68
11	3.58-3.66	*Myo*-inositol-C4-CH	*t* (3.70)	6.75 x 10^{-3}	+1.26
12	3.21-3.25	Phosphocholine/Glycerol-phosphocholine-$N(CH_3)_3$	*s*	5.22 x 10^{-3}	+1.29
13	2.73-2.81	Aspartate-C3-CH_{2a}	*d* (4.58)	8.56 x 10^{-3}	+1.31
14	3.08-3.13	Phenylalanine-β-CH_2	*dd* (4.88, 6.51)	2.96 x 10^{-3}	+1.48
15	7.40-7.48	Phenylalanine-C2-CH	*m* (7.38, 6.89)	3.51 x 10^{-4}	+1.85
16	3.39-3.48	Taurine-C1-CH_2	*t* (3.39)	8.86 x 10^{-3}	+1.26
17	3.25-3.33	*Myo*-inositol-C5-CH	*t* (6.36)	1.53 x 10^{-2}	+1.23
18	4.03-4.08	*Myo*-inositol-C2-CH	*t* (4.06)	7.83 x 10^{-3}	+1.26
19	2.33-2.39	Glutamate-C4-CH_2	*m* (6.90, 7.14)	4.07 x 10^{-2}	+1.20
20	7.16-7.23	Tyrosine-C6-CH	*m* (7.87, 6.89)	4.66 x 10^{-3}	+1.41
21	2.81-2.88	Aspartate-C3-CH_{2b}	*d* (4.44)	6.29 x 10^{-3}	+1.34
22	3.94-3.96	Phosphocreatine-C2-CH_2	*s*	2.94 x 10^{-3}	+1.44

4.3.4 ROC curve analysis

ROC (receiver operating characteristic) curve analysis provides a graphical view of the degree to which the discriminant metabolites are successfully classified into one of the two groups explored, based on their treatment status (i.e. either MPH or control group). Here, a maximum of 13 discriminant metabolites selected from the top 22 ISB variables listed in Table 4.1 were employed for this ROC curve analysis. Selection was based on variable rankings, and therefore in cases where two or more resonances arising from the same metabolite were selected as discriminatory features, only the highest ranked ISB variable was included in the analysis. The 13 variables included in the ROC curve analysis were GABA-C3-CH_2 (1.85-1.95 ppm), valine-C4-

CH_3 (0.91-1.00 ppm), *myo*-inositol-C3-CH_2 (3.51-3.58 ppm), alanine-C3-CH_3 (1.45-1.53 ppm), lysine-C5-CH_2 (1.66-1.75 ppm), hypoxanthine-C7-CH (8.21-8.23 ppm), phosphorocholine/glycero-phosphorocholine-$N^+(CH_3)_3$ (3.21-3.25 ppm), aspartate-C3-CH_{2a} (2.73-2.81 ppm), phenylalanine-β-CH_2 (3.08-3.13 ppm), taurine-C1-CH_2 (3.39-3.48 ppm), glutamate-C4-CH_2 (2.33-2.39 ppm), tyrosine-C6-CH (7.16-7.23 ppm), and phosphocreatine (3.92-3.96 ppm). The ROC curve in Figure 4.3(B) shows the AUROC range values for the metabolites included. Overall, this analysis indicates a good separation between the MPH-treated and control groups (mean AUROC value > 0.8), which provides further evidence that the two treatment groups differed significantly in terms of their ^{1}H-NMR metabolic profiles.

4.3.5 Multifactorial multivariate ASCA analysis

The 'treatment status' and 'between-cerebral hemispheres' variance components were simultaneously explored using an ASCA (ANOVA-spontaneous component analysis) two-factor independent sample analysis option. No significant differences were observed for the 'between-cerebral hemispheres' factor after performing this analysis (i.e. $p > 0.05$). Furthermore, the 'treatment status x brain hemisphere' interaction component of variance was also found not to be significant for the first two (major) principal components explored ($p > 0.05$). However, as expected, the 'treatment status' factor was indeed significant ($p = 0.006$).

4.3.6 Exploration of differences between right and left cerebral hemispheres

The paired option PLS-DA analysis performed on the dataset using 'brain hemisphere' as a response variable showed no significant differences between the left and right cerebral hemispheres for both the MPH-treated and the control rats. In both cases, the maximum accuracy value was 0.54 for a model containing 3 components and the Q^2 values obtained were below 0.1. Additionally, the *p*-value obtained from the permutation test (2,000 permutations) was non-

significant (p = 0.44). The ANOVA analysis performed also did not reveal any significant differences the two brain (i.e. cerebral) hemispheres and the 'brain hemisphere x treatment status' interaction effect was also not significant. Similarly, as noted above, the ASCA strategy performed on the complete ISB variable dataset failed to detect any differences between the two brain hemispheres and their interaction with the 'treatment status' factor.

4.3.7 Quantitative network metabolic pathway analysis

Quantitative network pathway analysis (involving pathway enrichment analysis and pathway impact from pathway topology) (Xia *et al.* 2015; Xia *et al.* 2012) revealed statistically-significant MPH-induced modulations to a series of metabolic pathways (Table 4.2). Those with the greatest metabolic impact were: tyrosine biosynthesis > alanine, aspartate and glutamate metabolism > taurine and hypotaurine metabolism > phenylalanine metabolism > tyrosine metabolism > arginine and proline metabolism. Pathway impact indices, together with false discovery rate (FDR)-adjusted p-values (computed from a quantitative comparison of the MPH-treated and control groups performed on the full dataset), are also listed in Table 4.2.

Table 4.2. Quantitative network pathway analysis involving pathway enrichment analysis and pathway impact from pathway topology

Metabolic Pathway	Total Compounds	Hits	FDR p value	Pathway Impact
Tyrosine biosynthesis	4	2	0.006692	1
Phenylalanine metabolism	9	2	0.006692	0.41
Alanine, aspartate and glutamate metabolism	24	4	0.008495	0.57
Tyrosine metabolism	42	1	0.008821	0.14
Arginine and proline metabolism	44	4	0.012328	0.11
Taurine and hypotaurine metabolism	8	1	0.11743	0.43

NB: Hits – refers to the number of metabolites in the specified pathway that were impacted by drug treatment e.g. 2 out of 4 metabolites in the 'tyrosine biosynthesis' pathway (i.e. phenylalanine and tyrosine) were impacted by MPH treatment in this study. The '**pathway impact**' values give an indication of how crucial changes to the 'hit' metabolites are in their respective networks/pathways (i.e. scores for each hit). This implies that hit metabolites that have key positions/roles and hence have severe impact on a network when altered are assigned higher impact values, with the maximum impact being 1.0).

4.4 Discussion

4.4.1 Principal findings

The psychostimulant drug MPH is increasingly used for the treatment of ADHD symptoms in children, despite the availability of only a limited amount of knowledge regarding its effects on the developing brain. Here, we provide some novel insights into the biochemical and metabolic mechanism of action of MPH on the adolescent brain. For this purpose, a ^{1}H-NMR-linked metabolomics approach was employed to analyse the left and right cerebral hemispheres of rats that have not been genetically manipulated. Non-genetically modified animals were used in this study as no currently existing ADHD animal model adequately reflect the neurobiological basis of the disorder (Andersen and Navalta 2011). Moreover, the use of non-modified animals also ensured that only drug-specific changes are observed independent of underlying disease state, which is something that still remains quite difficult to tease apart in clinical studies (Andersen and Navalta 2011). Our data indicate that MPH significantly elevates amino-acid transmitters (e.g. GABA, glutamate, and aspartate), large neutral amino-acids (e.g. phenylalanine, tyrosine, and valine), energy metabolites (e.g. phosphocreatine), and purine metabolism (e.g. hypoxanthine), as well as metabolites associated with membrane dynamics (e.g. phosphocholine, *myo*-inositol, and taurine), among others.

4.4.2 MPH increases amino-acid neurotransmitter levels

One major finding in the present study is the increased level of GABA in cerebral extracts of the adolescent rats treated with MPH compared to those of the corresponding saline-treated controls (Table 4.1). Compared to the high number of clinical and preclinical studies addressing the involvement of monoamines (in particular dopamine) in the symptoms and treatment of ADHD, previous investigations of the primary brain inhibitory neurotransmitter GABA in ADHD are

limited and inconsistent. A previous study using magnetic resonance spectroscopy (MRS) reported diminished GABA concentrations in sensorimotor cortex of children diagnosed with ADHD (Edden *et al.* 2012). However, a more recent study which explored different parts of the brain (including the sub-cortical regions) demonstrated developmental changes in GABA levels in ADHD individuals, with an increase in adults and no changes in children (Bollmann *et al.* 2015). The enhancement of GABA levels following MPH treatment observed in this study is likely to indicate a general enhancement of inhibitory neurotransmission and supports an earlier electrophysiological study which demonstrated that MPH increases GABAergic neurotransmission in the sensory thalamic nuclei of rat cerebrum (Goitia *et al.* 2013). Given that MPH's ability to block monoamine transporters including DAT and NET (a process leading to increased extracellular levels of DA and NA) is well established, the link between this effect and increased whole tissue levels of GABA remains somewhat unclear. The upregulated GABA levels are, however, not unique to MPH, since previous animal studies using high-resolution ^{1}H-NMR analysis have detected similar effects following both single and repeated injections of the anti-manic drugs lithium (Li^{+}) and carbamazepine (McLoughlin *et al.* 2009; Lan *et al.* 2008). Importantly, the Li^{+}-induced enhancement of GABA levels was replicated in human brain tissues (Lan *et al.* 2008). In contrast, a range of antipsychotic drugs failed to increase rat brain levels of GABA, an observation indicating that this effect does not appear to be a general one observed with all brain-active amphiphilic drugs (McLoughlin *et al.* 2009).

This study also detected enhanced levels of glutamate in brain samples from MPH-treated rats when compared to those of the saline-treated control group (Table 4.1). Since it is well known that GABA is generated from glutamate in GABAergic neurons via glutamic acid decarboxylase, it is possible that elevated glutamate levels may indeed be related to our finding of MPH-induced

enhancement of GABA levels. Consistent with this postulate, a corresponding PCA revealed that the ISBs containing all 3 of GABA's ^{1}H-NMR resonances (see Table 4.1) were found to strongly and positively load (loading scores 0.89-0.96) on the same principal component as that of the glutamate's C4-CH_2 signal (loading score 0.88). In addition, glutamatergic abnormalities have also been implicated in the pathophysiology of ADHD (Moore *et al.* 2006), and anti-ADHD drugs such as MPH modulate glutamate neurotransmission in animal models, including glutamate receptor function, long-term potentiation and cognition (Chen *et al.* 2015; Schmitz *et al.* 2016; Rozas *et al.* 2015; Di Miceli and Gronier 2015). Given that glutamate is stored in both neuronal and glial cells, it is unclear if the MPH-induced enhancement of whole tissue levels of glutamate in this study is related to an enhanced level of excitatory neuronal transmission.

Brain levels of aspartate and taurine were also enhanced by MPH in this study. The non-essential amino acid aspartate, like glutamate, is stored in both glia cells and neurons. Indeed, some studies have suggested vesicular co-storage of glutamate and aspartate (Patneau and Mayer 1990; Morland *et al.* 2013). Based on the fact that aspartate acts as a full agonist on the glutamatergic NMDA (N-methyl-D-aspartate) receptors, it has been proposed that aspartate also acts as a co-transmitter with glutamate in excitatory synapses (Patneau and Mayer 1990; Morland *et al.* 2013). Such a role for aspartate has, however, recently been contested (Herring *et al.* 2015). The enhancement of taurine in brain samples of rats treated with MPH could also be of much neurochemical importance. Taurine is one of the most abundant amino acids in the brain, and it's involved in a variety of brain functions including cytoprotection and brain development (Ripps and Shen 2012). The chemical structure of taurine is similar to GABA, and it acts as an agonist on $GABA_B$ (Kontro and Oja 1990), as well as on the glycine site of the NMDA receptors (Chan *et al.* 2014). MPH is known to enhance monoamine function, and this effect is implicated in the

drug's promotion of long-term potentiation at excitatory synapses (Jenson *et al.* 2015). In this regard, it is interesting to note that previous studies have found that taurine affects dopamine release, and together with D1 receptor activation, it promotes long-term potentiation, an NMDA receptor-dependent mechanism (Salimäki *et al.* 2003; Suárez *et al.* 2014). Hence, it is possible that the MPH-induced upregulation of brain tissue levels of both taurine and aspartate observed here is involved in MPH-induced long-term potentiation (Jenson *et al.* 2015).

4.4.3 MPH increases brain levels of large neutral amino acids

The present study also demonstrated significant MPH-induced upregulations of some large neutral amino acids (LNAA), including the aromatic amino acids (AAAs) tyrosine and phenylalanine, in addition to the branched-chain amino acid (BCAA) valine. However, these LNAAs are all polar compounds and cannot pass across the blood-brain barrier (BBB) freely. In order to enter the brain from blood plasma, they alternatively utilise an active transport system, the large neutral amino acid transporter LAT-1 (Fernström 2013). Different types of LNAAs compete with each other for transport from the plasma to the brain via the LAT-1 system, and it cannot be excluded that MPH may indeed modify the physiological balance of LNAAs in the plasma, a process that may favour the entry of some of these LNAAs into the brain over others (Fernström and Fernström 2007). In this study, adolescent rats were treated with a moderate dose of MPH (5.0 mg/kg, i.p.), which gives rise to pronounced behavioural activation including increased locomotion, sniffing and rearing. It may therefore be speculated that such an MPH-induced increase in motor activity enhances the plasma to brain transport of selected LNAAs, including tyrosine and its precursor phenylalanine. In support of this, rats exposed to treadmill running show increased brain levels of tyrosine (Acworth *et al.* 1986). Similar to our findings on MPH in this study, another psychostimulant, d-amphetamine, which is also used in the treatment

of ADHD, has been shown to increase rat brain levels of LNAAs, including tyrosine (Fernando and Curzon 1978). A possible contributing factor for a psychostimulant-induced upregulation of brain levels of LNAAs may also include their known body temperature rising action (as increasing body temperature increases metabolism), observed in both animals and humans (Fernando and Curzon 1978; Hetzler *et al.* 2014).

Dysfunctional neurotransmission of the DA and NA systems are implicated in the symptoms of ADHD, and these catecholamines play important roles in the control of motor activity and executive brain function (Del Campo *et al.* 2011). Further, both animal and clinical studies clearly demonstrate that MPH blocks the presynaptic DAT and NET, and thereby increase extracellular levels of these catecholamines (Berridge *et al.* 2006; Kuczenski and Segal 2002; Volkow *et al.* 1998). Here, we have demonstrated that MPH significantly increased levels of the AAA tyrosine and its precursor phenylalanine in the brain of MPH-treated adolescent rats over those of the corresponding saline-treated rats (Table 4.1). Tyrosine functions as a precursor for both DA and NA in the brain. Unlike almost all other neurotransmitter biosynthetic pathways, the rates of synthesis of DA and NA are sensitive to local substrate concentrations, particularly in the ranges normally found *in vivo.* Consequently, *ex vivo* factors such as diet and exercise that enhance the brain pool of tyrosine also increase the rate of conversion to DA and NA in their respective nerve terminals, ultimately elevating their synaptic concentrations (Fernström and Fernström 2007). In contrast, when tyrosine transport into the brain is suppressed by the administration of a tyrosine/phenylalanine-free LNAA mixture, the physiological- and amphetamine-evoked release of DA in animal models is impaired (Le Masurier *et al.* 2013; McTavish *et al.* 2001). Similarly, in humans dietary tyrosine/phenylalanine depletion attenuates reward-related behaviour, which is driven by DA (Bjork *et al.* 2014).

The MPH induced increase of brain tyrosine levels may indeed be relevant to recent neuropsychological studies reporting that tyrosine-free amino acid mixtures disrupt performance in a range of behavioural and cognitive tasks that are dependent on DA and NA (Coull *et al.* 2012). Also of interest to this study is a recent clinical finding which demonstrates that administration of a tyrosine-rich amino acid mixture effectively reduces ADHD symptoms in some children (Hinz *et al.* 2011). Therefore, it is possible that MPH alleviates ADHD symptoms in two ways: (1) via blockage of DAT and NET, and (2) by enhancing the brain pool of tyrosine and phenylalanine as demonstrated here.

In addition, brain levels of the non-essential amino acid alanine were significantly higher in brain samples from MPH-treated rats when compared to those of the corresponding controls. Alanine is involved in glucose generation, and can be manufactured in the body from the BCAA valine, which as noted above was also upregulated by MPH in this investigation. Although the brain is normally not associated with glycogenesis some previous data suggest that this might indeed be the case; however, it might be at a much less efficiency in the brain than that occuring hepatically (Bhattacharya and Datta 1993). Moreover, brain levels of the essential amino acid lysine were also found to be significantly elevated in MPH-treated rats. Although the direct functional impact of this effect is not yet clear, lysine has been reported to block serotonin receptors, and a reduced lysine intake is associated with anxiety, a symptom occasionally coinciding with ADHD (Smriga *et al.* 2002; Mulraney *et al.* 2016).

4.4.4 MPH alters energy metabolism

Previous studies have suggested that MPH alters brain energy metabolism. Specifically, it has been shown to alter cerebral glucose utilisation (Porrino and Lucignani 1987), and serves to increase uptake of this molecule in the brain of young and adult rats (Réus *et al.* 2015). In the

present study, we detected a significant MPH-induced upregulation of phosphocreatine levels in the cerebrum (Table 4.1). Indeed, it is possible that this finding is related to an earlier study showing that MPH (2.0-10.0 mg/kg) increases creatine kinase activity in several regions of rat cerebrum, including the prefrontal cortex, hippocampus and striatum, all of which are implicated in the mechanisms of action of MPH (Scaini *et al.* 2008). Creatine kinase catalyses the transfer of a phosphoryl group from adenosine triphosphate (ATP) to creatine, producing phosphocreatine and adenosine diphosphate, and our results indicate an imbalance in this transfer, with brain phosphocreatine levels being upregulated in the MPH-treated group when compared to that of the corresponding saline-treated control group. This reaction is, of course, reversible, and hence creatine kinase may play an important role in the rapid regeneration of ATP in high energy-consuming tissues such as the cerebrum. Furthermore, MPH is known to elevate neuronal activity, as evident from its ability to increase the transcription of several activity-dependent genes, together with their corresponding proteins (Yano and Steiner 2007; Banerjee *et al.* 2009; Gronier *et al.* 2010), and it is likely that this effect is dependent on a local elevated level of ATP metabolism. Although it is not possible to establish the precise mechanism behind the MPH-induced elevation of phosphocreatine levels in this study, it is likely that this effect is related to the known blockade of DAT by MPH, which increases synaptic DA levels and hence DA receptor stimulation. In support of this, antipsychotic drugs known to block DA receptors reduce creatine kinase activity and creatine levels in the brains of rats and humans respectively (Assis *et al.* 2007; Sarramea Crespo *et al.* 2008).

In addition to the creatine/phosphocreatine cycle, purine metabolism is also closely linked to ATP production and utilisation. Here, we found that the purine derivative hypoxanthine was significantly enhanced in the cerebrum of the MPH-treated rats compared to the controls (Table

4.1). This could give rise to increased levels of the final metabolite of purine catabolism, urate. Indeed, like MPH, d-amphetamine, which also increases synaptic levels of DA, and is also used in the treatment of ADHD, has been shown to increase brain levels of this metabolic product (Miele *et al.* 2000).

4.4.5 MPH and metabolites affecting cell membranes

Brain levels of *myo*-inositol were also significantly increased following MPH administration (Table 4.1). *Myo*-inositol is abundant in both neurons and glial cells, and it is known to be a marker of membrane turnover as well as glial integrity (Brand *et al.* 1993). In contrast to the present findings, other psychoactive drugs, including antipsychotic drugs, Li^+ and valproate have been found to reduce brain levels of *myo*-inositol in both animal and human studies (McLoughlin *et al.* 2009; Lan *et al.* 2008).

Phosphocholine is a known precursor to various membrane phospholipids in both glial cells and neurons (Paoletti *et al.* 2011). Significantly increased concentrations of this metabolite were also observed in the MPH-treated brain samples, and this may indicate that altered lipid turnover may be involved in the mechanism of action of the drug. Taken together, the enhancement of phosphocholine and *myo*-inositol by MPH could indicate that the drug acutely alters the dynamics of brain cell membranes.

4.4.6 Comparison of the left and right cerebral hemispheres

Some studies have previously suggested that ADHD may be a right hemisphere dysfunction (Waldie and Hausmann 2010). Consequently, here we also sought to establish if MPH influences brain metabolites differentially in the right and left cerebral hemispheres. However, both the univariate and paired multivariate analysis approaches employed for this purpose failed to detect any significant metabolic differences between these two cerebral hemispheric groups.

4.5 Conclusions

This study was aimed at detecting MPH-induced alterations of multiple cerebral metabolites in order to improve our understanding of the mechanisms of action of this drug in the adolescent brain. Our results indicate that acute MPH treatment significantly increased several rat cerebral metabolites, including amino acid neurotransmitters such as GABA and glutamate, and also upregulated LNAAs such as tyrosine and its precursor phenylalanine. The present study also indicated that a single administration of MPH alters membrane and energy metabolism in brain cells. The acute effects of MPH observed in the present study could be related to the mechanism of action of the drug in the adolescent brain, and in the reduction of ADHD symptoms. It will be important for future studies to investigate the effect of MPH in distinct brain regions that are implicated in the symptoms of ADHD, as well as the persistence of its observed effects following chronic administration.

CHAPTER 5

5 Effect of methylphenidate on neurochemicals and metabolites in the plasma and cerebral regions

5.1 Introduction

MPH reduces the primary ADHD symptoms in approximately 70% of patients (Wilens 2008; Zhang *et al.* 2016). MPH is suggested to exert its therapeutic effects via a blockade of the DAT and the NET, culminating in an increase of synaptic monoaminergic signalling (Berridge *et al.* 2006; Kuczenski and Segal 2002; Volkow *et al.* 1998). In recent times, there appears to be an increased diagnosis of ADHD, as a consequence there is an increased usage of MPH (Dietz *et al.* 2013; Gahr *et al.* 2014; Klein-Schwartz 2003). While MPH is an effective therapeutic drug, its long term effects on brain neurochemicals and metabolites remains unclear.

Several genetic and functional genomic studies have been conducted to determine the aetiology of ADHD and the mechanism of action of anti-ADHD medications, including MPH on the central DA system. However, to our knowledge there are no studies exploring the MPH-induced effects following acute and chronic administration on metabolic changes in the plasma and brain regions implicated in the pathophysiology of ADHD such as the frontal cortex, striatum, and hippocampus. Water-soluble metabolites play crucial roles in metabolic pathways and provide crucial information regarding the biological activities of a particular tissue or fluid. The relative concentration of metabolites in the brain gives useful insights into the functional and structural integrity of astrocytes and neurons (McLoughlin *et al.* 2009). Studying metabolite alterations in brain tissue and biological fluids following MPH treatment could, therefore, provide important information related to the mechanism of action and long-term effects of the drug.

Interestingly, previous studies employing proton magnetic resonance spectroscopy (^{1}H-MRS) to examine ADHD patients have identified some prominent changes in various brain metabolites, particularly in the frontal cortex, basal ganglia and cerebellum. For instance, glutamate and glutamine ratio has been shown to be reduced in the frontal cortex of medication naïve ADHD

patients (Perlov *et al.* 2007) but increased in the cerebellum (Perlov *et al.* 2010). In addition, other studies have shown altered levels of GABA (Bollmann *et al.* 2015), choline (Colla *et al.* 2008), *N*-acetylaspartate (NAA), and *myo*-inositol (Courvoisie *et al.* 2004) in the frontal cortex, striatum and/or hippocampus of some ADHD patients. Given that glutamate and GABA are excitatory and inhibitory neurotransmitters respectively, perturbations in these amino acids suggest a disturbance in the balance between excitatory/inhibitory neurotransmission in ADHD (Bollmann *et al.* 2015; Perlov *et al.* 2007). In terms of stimulant actions, ^{1}H-MRS has been used in some ADHD patients to identify a few metabolites altered by MPH including NAA, glutamate and *myo*-inositol (Carrey *et al.* 2003; Soliva *et al.* 2010). However, due to limited sensitivity, the ^{1}H-MRS is currently unable to detect drug-induced changes in other metabolites with lower-relative abundance, and it also remains difficult to distinctly distinguish the effect caused by drug treatment alone, given that some changes could occur as part of the normal course of a disease. Thus, ^{1}H-NMR spectroscopy was employed to detect the changes caused by MPH treatment in normal (genetically-unmodified) rats in this study.

^{1}H-NMR spectroscopy-based metabolomics could be used to detect a wide array of metabolites in biological samples. ^{1}H-NMR may be used to evaluate changes in a large variety of biofluids and tissues. Compared to ^{1}H-MRS, the ^{1}H-NMR technique has a far greater sensitivity and gives a better spectral resolution. The ^{1}H-NMR technique has been used extensively in studies on several brain disorders including schizophrenia, bipolar disorder, and autism, as well as stimulant and psychotropic drugs (McLoughlin *et al.* 2009; Lan *et al.* 2008; Tsang *et al.* 2006).

In this study, we used high-resolution ^{1}H-NMR spectroscopy to explore and compare the acute and chronic effect of MPH on plasma and brain metabolites. For this purpose we selected, based on their involvements in ADHD symptoms, the following brain regions: frontal cortex, striatum,

and hippocampus. Most of the identified alterations were related to neurotransmission, energy metabolism, and membrane dynamics. The observed treatment duration- and brain region-specific neurochemical alterations induced by MPH are discussed.

5.1.1 Aims

This study was aimed at comparing the effect of acute and chronic MPH treatment on water-soluble metabolites in the plasma and brain regions implicated in the symptoms of ADHD. The objectives of this chapter were:

- To evaluate the effects of MPH on brain regions associated with ADHD symptoms such as striatum, frontal cortex and hippocampus.
- To assess the effects of MPH on water-soluble metabolites in the plasma.
- To compare the acute and chronic effects of MPH on the developing brain.

5.2 Methods

5.2.1 Drug Treatment and sample collection

For a detailed description of the animal housing and MPH treatment procedures see Chapter 2, section 2.1. In brief, the animals were assigned to two treatment groups i.e. acute treatment group (saline-treated controls and drug-treated) and chronic treatment group (saline-treated controls and drug-treated). The animals (180-220 g; post-natal day 40) in the acute treatment group received either a single saline injection (1.0 ml/kg) or a single MPH dose (2.0 mg/kg; n=12 rats/group) intraperitoneally. The animals in the chronic treatment group, on the other hand, received either saline or MPH (2.0 mg/kg) twice-daily for 15 days, with the last injection being on postnatal day 40. One hour after the last injection, the rats were sacrificed by a rapid dislocation of the neck. The brain was removed and trunk blood was collected from each animal. Brain regions

corresponding to the frontal cortex, striatum, and hippocampus were dissected according to the Paxinos and Watson rat brain atlas (see Chapter 2, section 2.13). The dissected tissues were snap-frozen, and then stored at -80°C until ^{1}H-NMR analysis.

5.2.2 Plasma and brain extract preparation and ^{1}H-NMR experiments

The plasma and brain sample preparation, as well as the ^{1}H-NMR experiments were performed as described in Chapter 2, sections 2.2.1, 2.2.2 and 2.2.3.

5.2.3 Pre-processing of NMR spectra

Using ACD/NMR processor (academic edition; Ontario, Canada), the acquired ^{1}H-NMR spectra were phase and baseline-corrected prior to multivariate and univariate data analysis. The ^{1}H-NMR spectra of the brain samples were referenced to the TSP resonance at δ = 0.00 ppm, while the plasma spectra were referenced to the methyl doublet of lactate (1.26-1.33 ppm). The ^{1}H-NMR spectra were then automatically reduced into consecutive integrated spectral regions referred to as the 'intelligent-bucketing' procedure. This procedure yielded a full dataset of 24 rows (samples) and 315 columns (variables) for the frontal cortex of the chronic treatment group. On the other hand, there was a full dataset of 24 rows (samples) and 292 columns (variables) for the plasma samples of the chronic treatment group. To eliminate spectral variations due to differences in the quality of water suppression in each individual spectrum, the region containing residual H_2O/HOD signal (δ = 4.50-5.00 ppm) in both the brain and plasma spectra was not included in the analysis. In addition, spectral regions that did not contain any resonant signals (i.e. noise regions) were also removed from further analysis.

5.2.4 Multivariate and univariate analysis of the plasma and brain extracts

Multivariate and univariate statistical analyses were performed on the TSP-normalised integral values as described in Chapter 2, section 2.2.5. PCA was initially used to visualise the datasets.

OPLS-DA classification (which introduces an orthogonal signal correction filter to the PLS-DA classification method) was also performed along with a 10-fold cross-validation. In addition, a permutation test was also conducted with 2,000 permutations, to ascertain the performance of class discrimination. For the OPLS-DA analysis, while any Q^2 value > 0 has predictive relevance, to ensure comparability and reliability of models across the different brain regions a $Q^2 \geq 0.3$ was used as a cut off for all models as previously described (McLoughlin *et al.* 2009; Worley and Powers 2013). Where models showing a clear difference between the control and drug-treated rats could be constructed and cross-validated (i.e. $Q^2 \geq 0.3$), the discriminating metabolites were identified using the VIP (variable importance in projection) scores.

In addition, the metabolite changes were further confirmed by comparing the mean resonance intensities for the MPH-treated samples and the controls using an ANOVA model (univariate analysis) from the R statistical package. This univariate analysis enabled the verification of the metabolite changes detected from the multivariate analysis, and as well enabled the determination of the level of metabolite changes associated with MPH treatment. The ANOVA *p*-values, fold changes, and multiplicities of the discriminant metabolites for all the plasma and brain samples analysed were presented in Tables 5.2 and 5.3. Bonferroni correction [where p = (0.05/total number of buckets for each sample)] was further applied on those samples that were statistically significant following the univariate analysis but not significant after the multivariate analysis, in order to guard against type I error (false positives).

5.2.5 Metabolic pathway analysis of the brain and plasma datasets

Detailed analysis of the most relevant metabolic pathways altered following MPH treatment was performed using the *MetaboAnalyst 3.0* tool, as described in Chapter 2, section 2.2.7.

5.3 Results

5.3.1 Spectral profiles and statistical analyses of extracts from the rat brain

5.3.1.1 Multivariate and univariate analysis of ^{1}H-NMR datasets from brain tissue extracts

The ^{1}H-NMR datasets were visualised with an S-plot, which demonstrated significant MPH-induced upregulations of some prominent metabolites in the frontal cortex following chronic 2.0 mg/kg MPH treatment compared to controls (Figure 5.1). The plot indicates MPH-induced changes of resonant signals belonging to some notable metabolite categories such as energy and membrane-related metabolites (e.g. lactate, creatine, phosphocholine, taurine etc.), and amino acids (e.g. lysine, aspartate, GABA, glutamate, alanine, tyrosine etc.).

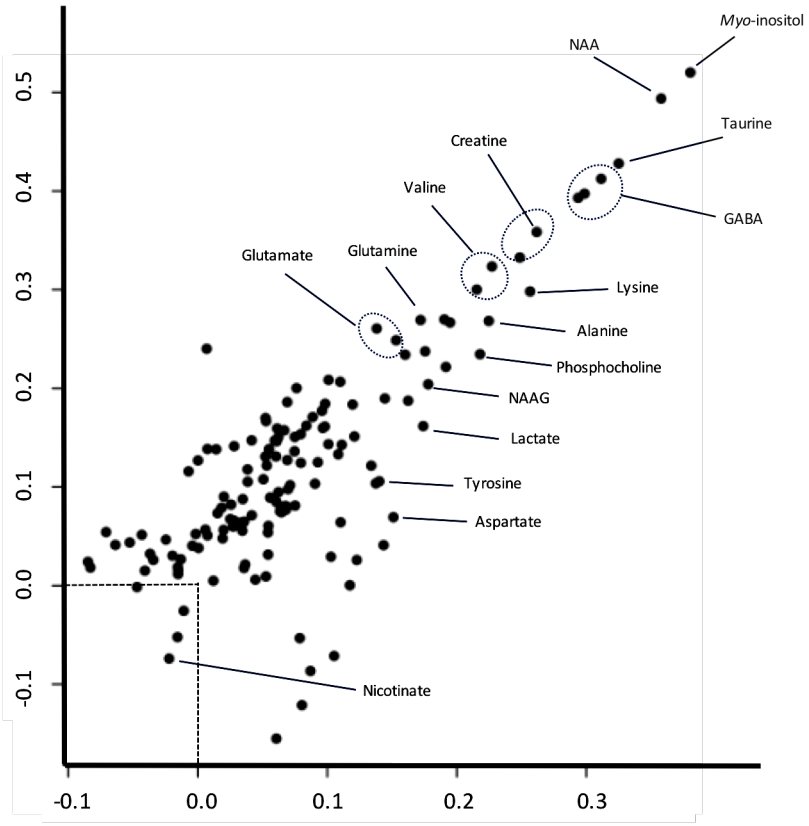

Figure 5.1: S-plot showing the most important discriminant variables in the frontal cortex following chronic 2.0 mg/kg MPH treatment.
Most of the important cortical variables were increased (above 0.0), although there were also a few decreased variables (below 0.0).

To test the statistical significance of the MPH-induced changes in the ^{1}H-NMR datasets, PCA was used for an initial visualisation of the datasets and for identifying potential outliers. The PCA analysis showed a clear separation between the chronic 2.0 mg/kg MPH-treated dataset compared with the corresponding controls in the frontal cortex (Figure 5.2) but not for any of the other investigated brain regions after either acute or chronic treatment. OPLS-DA was then used to analyse the ^{1}H-NMR datasets in order classify the samples based on their treatment status. The OPLS-DA scores plot provided added support for a clear distinction between the chronic MPH-treated and the saline-treated controls in the frontal cortex (Figure 5.2B), but not for the treatment groups in the other examined brain regions when compared with their corresponding controls.

To ensure reliability of models across the different brain regions examined, a Q^2 value ≥ 0.3 was used as a cut off for all models as previously described (McLoughlin *et al.* 2009; Worley and Powers 2013). Here, while the OPLS-DA $Q^2 = 0.30$ (statistically significant) was obtained in the frontal cortex following chronic treatment, the $Q^2 < 0.1$ (non-significant) was obtained for the other examined brain regions following acute and chronic treatment. There was also a corresponding $p < 0.05$ arising from the permutation test (2,000 permutations) for the chronically-treated frontal cortex samples, emphasising a clear separation between the MPH-treated and the control cortical groups.

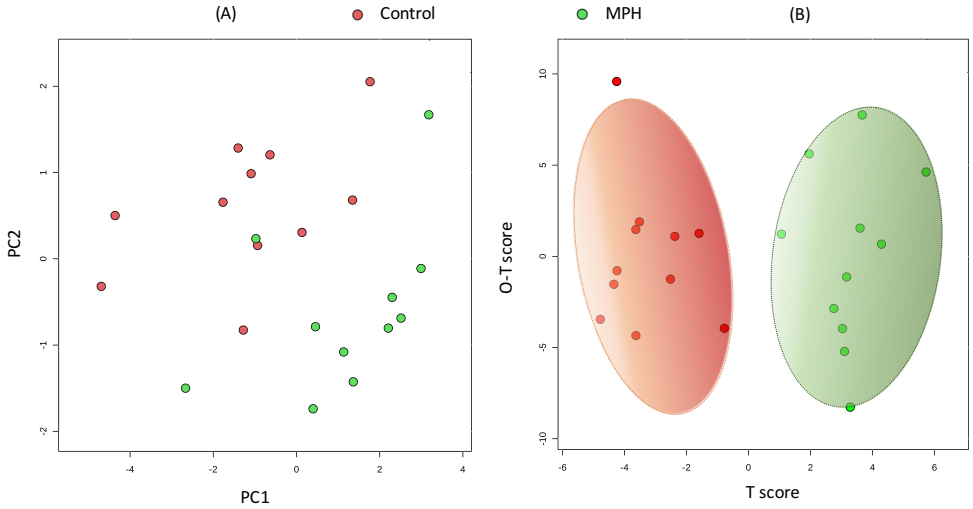

Figure 5.2: PCA and OPLS-DA scores plots of the chronically-treated frontal cortex samples.
(A) PCA scores plot demonstrating a clear separation between the chronic 2.0 mg/kg MPH-treated and saline-treated control groups in the frontal cortex, and (B) OPLS-DA scores plot showing 95% confidence ellipses that further supports the clear distinction between the chronic MPH-treated and saline-treated control groups in the frontal cortex (R^2X = 0.58, Q^2 = 0.30, permutation *p*-value < 0.05).

In addition to the multivariate analysis, further univariate analysis of the ^{1}H-NMR datasets were performed using the ANOVA model previously described (see Chapter 2, section 2.2.5). This analysis revealed statistically significant changes to a number of variables in most of the examined brain regions following either acute or chronic MPH treatment. To guard against false positives in the datasets that did not show statistical significance following multivariate analysis, a correction factor was introduced (Bonferroni correction), where the α-values were adjusted based on the total number of variables (i.e. p = (0.05/total number of bucketed variables for each brain region)) (see Chapter 2, section 2.2.5). The significantly altered variables in the individual brain regions are presented below.

5.3.1.2 Metabolite changes in the frontal cortex following MPH treatment

Acute and chronic MPH treatment increased a number of metabolites in the frontal cortex. However, the changes were more pronounced following chronic treatment (R^2X = 0.58, Q^2 =

0.30, permutation p-value < 0.05; OPLS-DA analysis) compared with the acute treatment group. Figure 5.3 gives the most important metabolite changes in the frontal cortex following acute and chronic treatment. Following acute treatment, four variables were increased (obtained following the ANOVA analysis), with these four variables being assigned to two metabolites (i.e. valine and lysine) (Figure 5.3A). In contrast, chronic treatment increased the levels of twenty variables, which included amino acid transmitters and LNAAs, as well as energy and membrane-related metabolites (see Figure 5.3B).

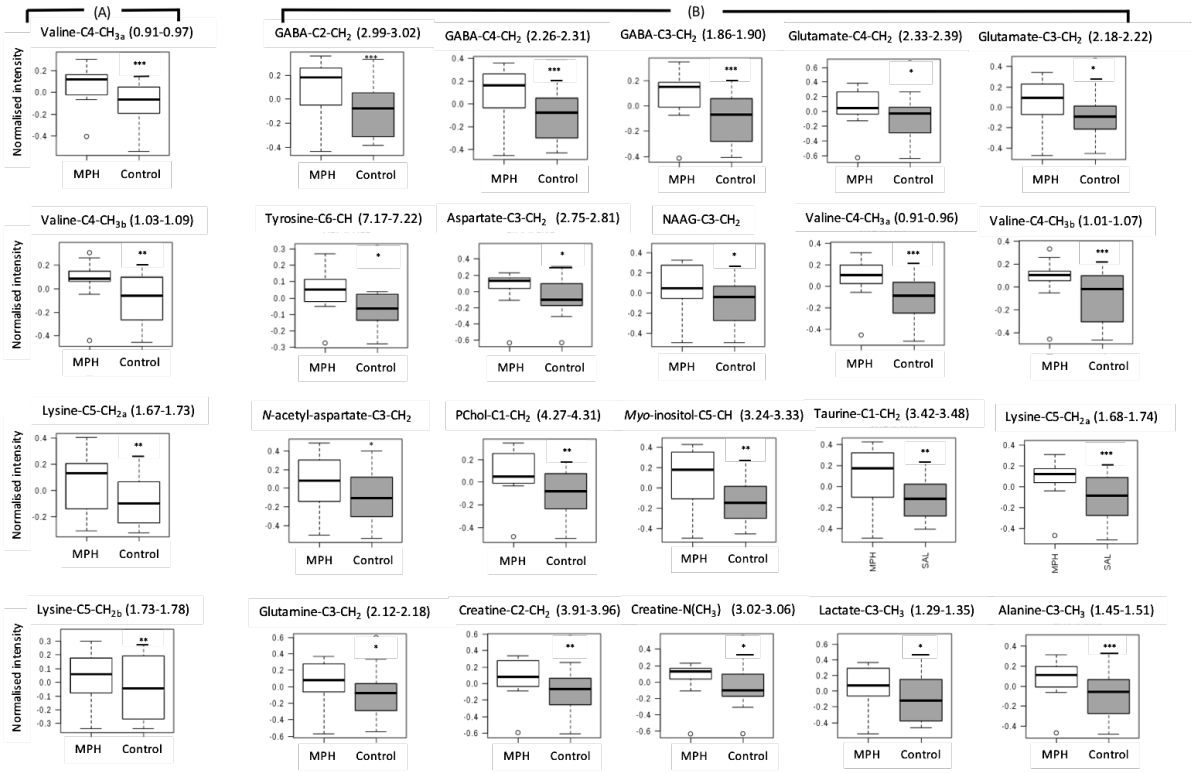

Figure 5.3: Boxplots showing the most important metabolite changes in the frontal cortex. (A) Metabolite changes observed from the ANOVA analysis following acute MPH treatment, (B) Top 20 variables altered following chronic MPH treatment based on both the OPLS-DA and ANOVA analysis. *p < 0.05; **p < 0.01; ***p < 0.001. Abbreviations: NAAG, *N*-acetylaspartylglutamate; PChol, phosphocholine.

5.3.1.3 Quantitative metabolic pathways altered in the frontal cortex

Further, quantitative network pathway analysis was conducted (Xia *et al.* 2015; Xia *et al.* 2012). This analysis revealed statistically significant MPH-induced alterations to a number of metabolic pathways in the frontal cortex following chronic MPH treatment (Table 5.1).

Table 5.1: Quantitative network pathway analysis for the chronic frontal cortical samples. This involves pathway enrichment analysis and pathway impact from pathway topology

Metabolic Pathway	**Total Compounds**	**Hits**	**FDR *p*-value**	**Pathway Impact**
Alanine, aspartate and glutamate metabolism	24	5	0.00021	0.457
Arginine and proline metabolism	44	4	0.00212	0.024
Phenylalanine, tyrosine and tryptophan biosynthesis	4	1	0.00487	0.500
Taurine and hypotaurine metabolism	8	1	0.00624	0.428
Valine, leucine and isoleucine biosynthesis	11	1	0.00697	0.333

5.3.1.4 Metabolite changes in the hippocampus following MPH treatment

Similar to the changes in the frontal cortex, 2.0 mg/kg MPH treatment increased a number of metabolites in the hippocampus following both acute and chronic MPH treatment, although it was acute treatment that had more prominent effect compared to the chronic treatment group (Table 5.2). The ANOVA *p*-values, fold changes, and multiplicities of the most important metabolites separating the MPH-treated samples from the controls are presented in Table 5.2.

Table 5.2: Important metabolites altered in the hippocampus following acute and chronic MPH treatment relative to their corresponding controls

Variable Number	Chemical Shift (ppm)	Assignment	Multiplicity (coupling constants)	Raw ANOVA *p*-values	Fold Change
Acute					
1	0.91-0.97	Valine-C4-CH_{3a}	*m* (3.84)	1.4×10^{-5}	$+1.21^{b}$
2	1.03-1.09	Valine-C4-CH_{3b}	*d* (7.84)	9.9×10^{-8}	$+1.39^{b}$
3	1.46-1.51	Alanine-C3-CH_3	*d* (7.24)	1.3×10^{-3}	+1.33
4	1.67-1.73	Lysine-C5-CH_{2a}	*d* (7.54)	2.3×10^{-5}	$+1.91^{b}$
5	1.73-1.78	Lysine-C5-CH_{2b}	*d* (7.85)	6.6×10^{-6}	$+1.79^{b}$
6	1.88-1.90	GABA-C3-CH_2	*t* (7.39)	1.1×10^{-2}	+1.59
7	1.90-1.96	Acetate-C2-CH_3	s	4.6×10^{-2}	+1.54
8	2.18-2.22	Glutamate-C3-CH_2	*m* (4.88)	3.2×10^{-2}	+1.16
9	2.26-2.31	GABA-C4-CH_2	*t* (7.24)	1.3×10^{-2}	+1.38
10	3.19-3.21	Choline-N$(CH_3)_3$	*s*	4.5×10^{-2}	+1.19
11	3.42-3.48	Taurine-C1-CH_2	*t* (6.65)	3.4×10^{-2}	+1.33
12	3.91-3.96	Creatine-C2-CH_2	*s*	2.3×10^{-2}	+1.68
13	4.03-4.08	*Myo*-inositol-C2-CH	*t* (2.96)	3.4×10^{-2}	+1.55
14	4.11-4.15	Lactate-C2-CH	*d* (6.95)	7.8×10^{-3}	+1.16
15	4.15-4.21	Phosphocholine-C1-CH_2	*m* (2.22)	1.6×10^{-2}	+1.22
16	6.88-6.91	Tyrosine-C3-CH	*d* (8.58)	1.6×10^{-2}	+1.74
17	7.20-7.24	Tyrosine-C6-CH	*d* (8.72)	3.9×10^{-3}	+1.31
18	7.30-7.35	Phenylalanine-C2-CH	*m* (6.36)	2.9×10^{-3}	+1.23
19	8.21-8.26	NAD-N5-CH	*s*	4.5×10^{-3}	+1.17
20	8.44-8.47	Nicotinamide-C5-CH	*s*	5.2×10^{-3}	+1.20
Chronic					
1	0.91-0.96	Valine-C4-CH_{3a}	*m* (3.84)	2.2×10^{-2}	+1.05
2	1.01-1.07	Valine-C4-CH_{3b}	*d* (7.84)	2.3×10^{-3}	+1.10
3	1.45-1.51	Alanine-C3-CH_3	*d* (7.24)	3.1×10^{-2}	+1.08
4	6.87-6.93	Tyrosine-C5-CH	*m* (2.37)	3.2×10^{-2}	+1.24
5	7.28-7.33	Phenylalanine-C2-CH_a	*d* (6.95)	7.2×10^{-5}	$+1.15^{b}$

(^{b}) Significant even after Bonferroni correction

5.3.1.5 Metabolite changes in the striatum following MPH treatment

Unlike the changes in the frontal cortex and hippocampus, MPH decreased several metabolites following acute MPH treatment ($p < 0.05$ for all metabolites based on the ANOVA model) but chronic MPH treatment normalised metabolite levels in this region (with no statistically significant changes observed following chronic MPH treatment; $p > 0.05$) relative to the saline-treated controls (Table 5.3).

Table 5.3: Important metabolites altered in the striatum following acute and chronic MPH treatment relative to corresponding controls

Variable Number	Chemical Shift (ppm)	Assignment	Multiplicity (coupling constants)	Raw ANOVA *p*-values	Fold Change
Acute					
1	0.91-0.97	Valine-C4-CH_{3a}	*m* (3.84)	7.9×10^{-3}	-1.08
2	1.03-1.09	Valine-C4-CH_{3b}	*d* (7.84)	8.2×10^{-3}	-1.17
3	1.67-1.73	Lysine-C5-CH_{2a}	*d* (7.54)	4.0×10^{-5}	-1.23[b]
4	1.73-1.78	Lysine-C5-CH_{2b}	*d* (7.85)	1.9×10^{-4}	-1.25[b]
5	2.00-2.04	*N*-acetyl-aspartate-C2-CH_3	*s*	3.9×10^{-2}	-1.84
6	2.43-2.45	Glutamine-C4-CH_{2a}	*d* (2.37)	2.9×10^{-2}	-1.35
7	2.45-2.51	Glutamine-C4-CH_{2b}	*m* (3.84)	5.1×10^{-2}	-1.10
8	2.98-3.03	GABA-C2-CH_2	*d* (7.69)	4.9×10^{-2}	-1.26
9	3.30-3.33	*Myo*-inositol-C5-CH	*t* (6.21)	3.7×10^{-2}	-1.44
10	3.50-3.53	*Myo*-inositol-C3-CH_2	*dd* (2.96)	3.6×10^{-2}	-1.29
11	3.87-3.91	Glycerol-phosphocholine-C3-CH_3	*d* (3.10)	1.0×10^{-2}	-1.45
12	4.15-4.21	Phosphocholine-C1-CH_2	*m* (4.88)	1.2×10^{-2}	-1.24
13	4.36-4.42	*N*-acetyl-aspartate-C2-CH	*m* (3.99)	1.7×10^{-2}	-1.78
14	6.09-6.13	NAD-N1'-CH	*d* (5.62)	1.1×10^{-2}	-1.59
15	8.33-8.39	NAD-A1'-CH	*s*	2.3×10^{-2}	-1.56
Chronic					
1	2.00-2.04	*N*-acetyl-aspartate-C2-CH_3	s	8.6×10^{-1}	-1.04#
2	2.45-2.51	Glutamine-C4-CH_2	*m* (3.84)	8.2×10^{-1}	+1.04#
3	3.50-3.53	*Myo*-inositol-C3-CH_2	*dd* (2.96)	4.6×10^{-1}	-1.07#
4	3.87-3.91	Glycerol-phosphocholine-C3-CH_3	*d* (3.10)	3.6×10^{-1}	-1.13#
5	6.09-6.13	NAD-N1'-CH	*d* (5.62)	4.9×10^{-1}	+1.07#

([b]) Significant even after Bonferroni correction; # Statistically insignificant. Abbreviation: NAD, Nicotinamide adenine dinucleotide.

5.3.2 Spectral profiles and statistical analyses of plasma samples

5.3.2.1 ^{1}H-NMR profile of rat plasma

The average spectra obtained from the plasma of the control (dark red) and MPH-treated (green) rats is shown in Figure 5.4, spanning the (A) 0.66-4.60 ppm and (B) 5.0-8.56 ppm spectral regions. This plasma spectrum contained several prominent resonant signals including branched chain amino acids (BCAAs), low-density lipoproteins, lipids, glucose, and glutamate, among others (see Figure 5.4).

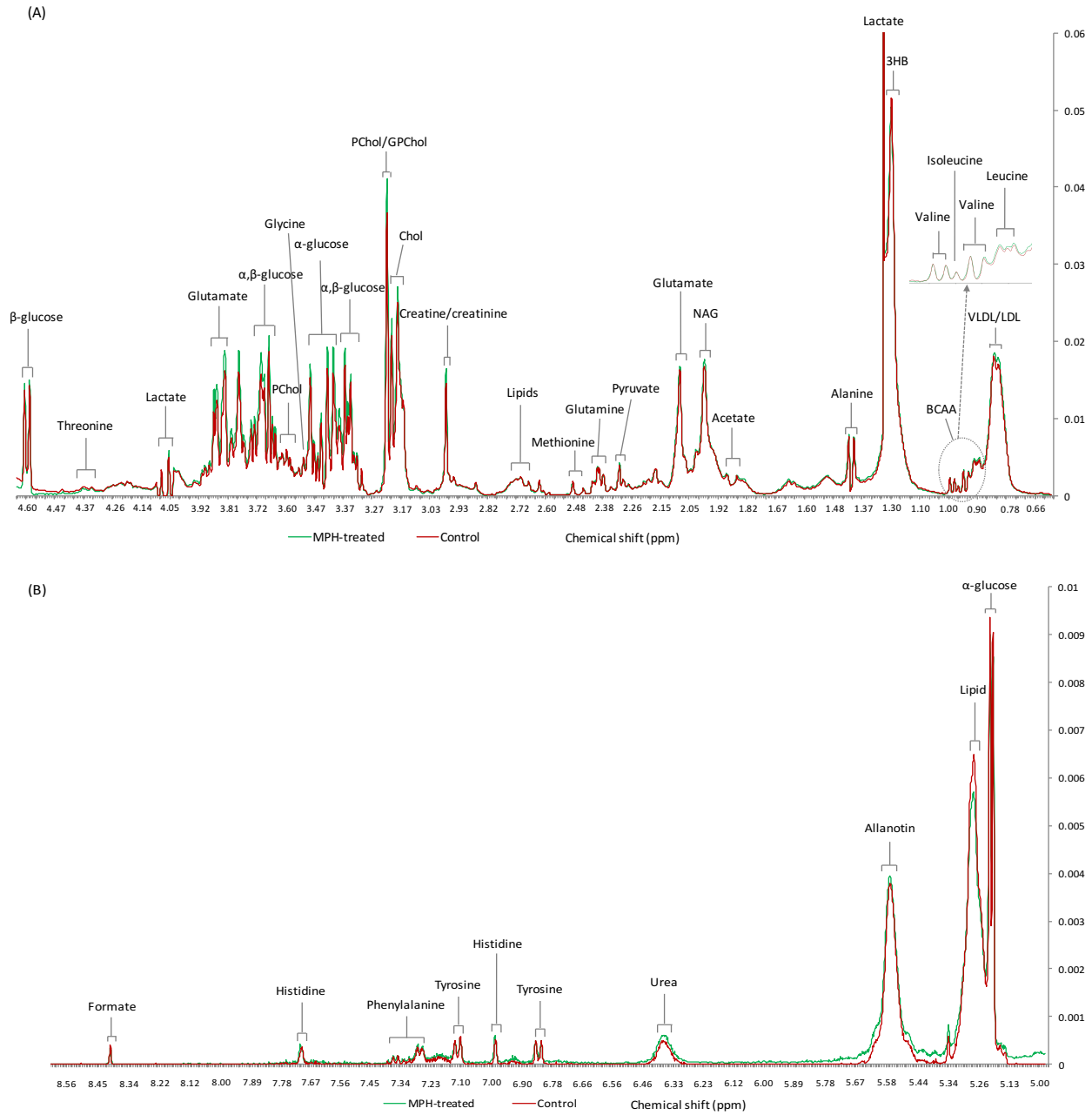

Figure 5.4: Average ^{1}H-NMR spectra from the control and MPH-treated rats.

The spectra display the average of (A) 0.66-4.60 ppm (the expanded BCAA region has been shown in the insert), and (B) 5.0-8.56 ppm spectral regions. Abbreviations: VLDL/LDL, low-density lipoprotein; BCAA, branched chain amino acids; 3HB, 3-hydroxybutyrate; NAG, *N*-acetyl glycoprotein; Lipids, triglycerides and fatty acids; Chol, Choline; PChol, Phosphocholine; GPChol, Glycero-phosphocholine.

5.3.2.2 Multivariate and univariate analysis of the plasma data

Similar to the brain dataset, the integral data from plasma spectra were analysed using both multivariate and univariate statistical parameters. The PCA and OPLS-DA scores plots showed a clear separation between the drug-treated and saline-treated controls following chronic MPH treatment (Figure 5.5) but not acute treatment (i.e. treatment duration-dependent effect). The OPLS-DA analysis yielded a $Q^2 = 0.46$ (statistically significant) and a permutation $p < 0.0005$ (2,000 permutations) for the chronic MPH-treated plasma samples, emphasising a clear separation between the chronic MPH-treated plasma samples and the controls. However, a $Q^2 < 0.1$ (i.e. statistically non-significant effect) was obtained for the acute MPH-treated plasma samples.

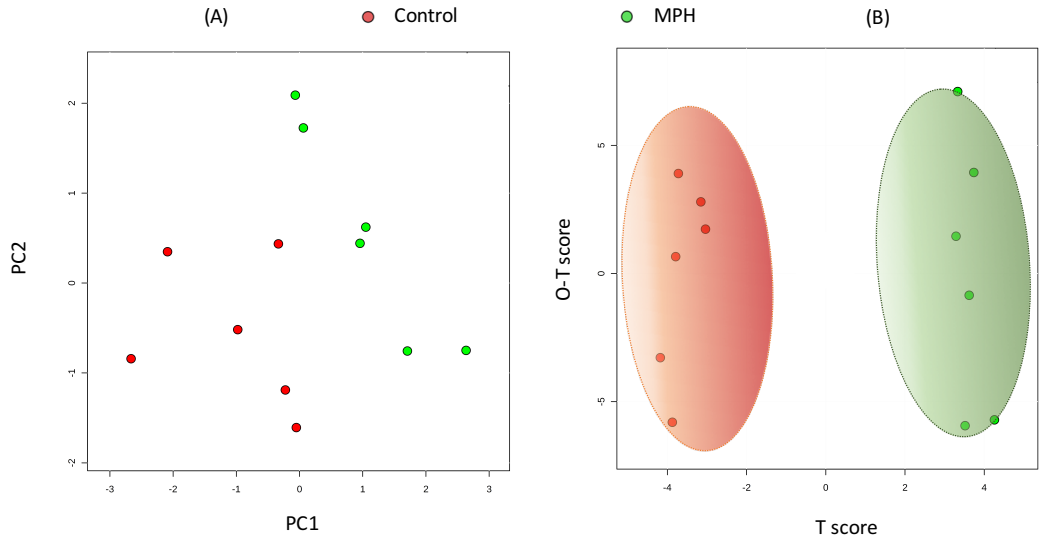

Figure 5.5: PCA and OPLS-DA scores plot of the chronically-treated plasma samples.
(A) PCA scores plot demonstrating a clear separation between the chronic 2.0 mg/kg MPH-treated plasma samples and the corresponding saline-treated controls, and (B) OPLS-DA scores plot showing 95% confidence ellipses that further supports the clear distinction between the chronic MPH-treated plasma samples and the corresponding saline-treated controls ($R^2X = 0.62$, $Q^2 = 0.46$, permutation p-value < 0.0005).

Further, ANOVA was performed (using the R statistical package) to confirm the identities of the variables discriminating the MPH-treated plasma samples from the controls. This ANOVA

analysis showed that indeed none of the metabolites were significantly altered in the plasma samples following acute treatment ($p > 0.05$ for all metabolites) but there were significant alterations to several metabolites following chronic treatment as shown in Figure 5.6. In the chronic treatment group, the increased metabolites included α- and β-glucose, glutamate, and phosphocholine whereas the decreased metabolites included lactate, acetate, threonine, tyrosine, phenylalanine, formate, and 3-methylhistidine (Figure 5.6).

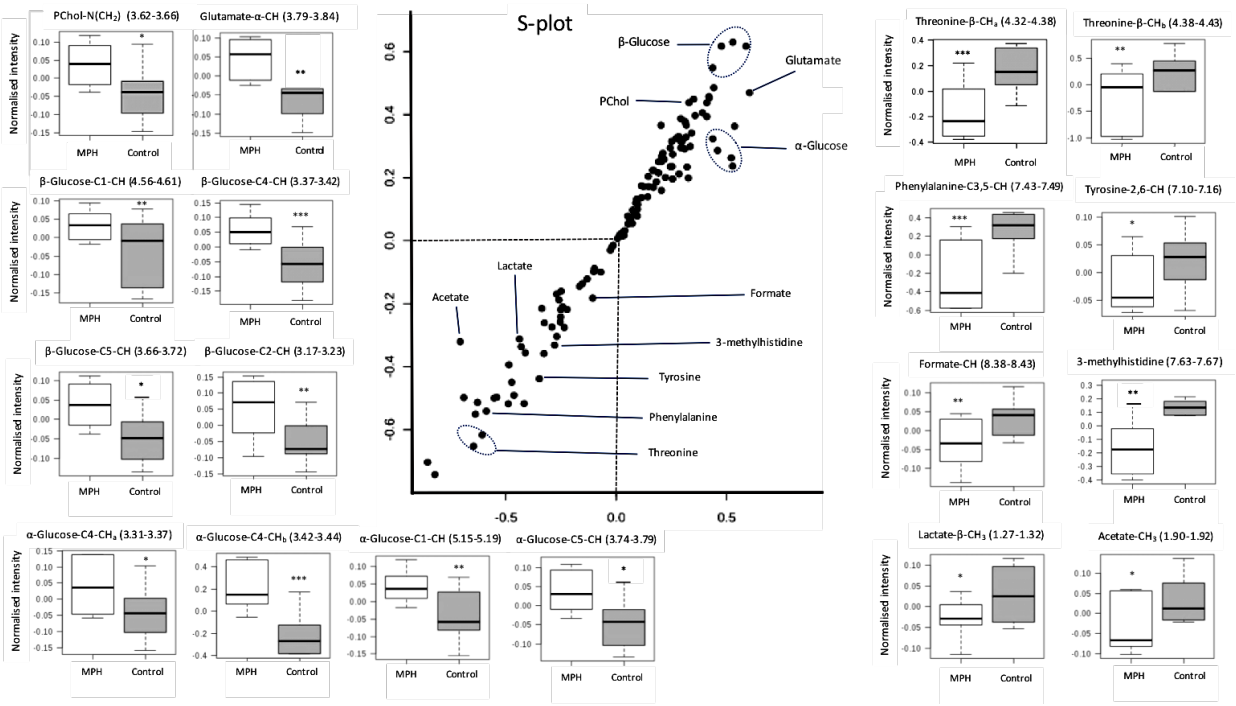

Figure 5.6: S-plot and boxplots displaying the important variables altered in the rat plasma samples following chronic MPH treatment.

The S-plot shows the most important variables that were either increased (upper portion of the plot) or decreased (lower portion of the plot) in rat plasma following chronic 2.0 mg/kg MPH treatment. The discriminating variables in the S-plot are displayed in boxplots along with their significance level from the ANOVA model. *$p < 0.05$; **$p < 0.01$; ***$p < 0.001$.

5.3.2.3 Metabolite set enrichment and metabolic pathway analysis of plasma samples

The quantitative network pathway analysis of the chronically-treated plasma samples revealed statistically significant MPH-induced alterations to a series of metabolic pathways, including

phenylalanine, tyrosine and tryptophan biosynthesis, as well as phenylalanine and tyrosine metabolism, among others (Table 5.4).

Table 5.4: Quantitative network pathway analysis for the chronic plasma samples. This involves pathway enrichment analysis and pathway impact from pathway topology

Metabolic Pathway	Total Compounds	Hits	FDR *p*-value	Pathway Impact
Phenylalanine, tyrosine and tryptophan biosynthesis	4	2	0.000221	1
Phenylalanine metabolism	9	2	0.000434	0.407
Starch and sucrose metabolism	23	1	0.010	0.038
Galactose metabolism	26	1	0.010	0.036
Glycerophospholipid metabolism	30	1	0.010	0.044
Tyrosine metabolism	42	1	0.010	0.140

5.4 Discussion

5.4.1 Principal findings

Here, spectral profiles from rat plasma and three brain regions implicated in the symptoms of ADHD have been examined with regards to metabolic changes induced by MPH, which is the commonest drug prescribed for the treatment of ADHD. The data showed that MPH has both region- and treatment-duration specific effects on plasma and brain metabolites. The drug-related metabolic changes observed following both acute and chronic MPH treatment are likely to provide novel insights into the mechanism of action of the drug.

Specifically, this study revealed that chronic MPH treatment but not acute treatment influenced the metabolic pattern in the plasma samples of the MPH-treated rats when compared to the corresponding control samples (Figure 5.6). In addition, metabolites including those related to amino acid transmission (glutamate, glutamine and GABA), LNAAs (tyrosine, phenylalanine and valine), energy metabolism (lactate, acetate and creatine), and membrane activity (NAA, *myo*-inositol and taurine) were mostly increased in the frontal cortex and hippocampus following both acute and chronic MPH treatment (Figure 5.3 and Table 5.2). In contrast, while no significant

changes were observed in the striatum following chronic treatment, acute MPH treatment decreased some metabolites including the amino-acid neurotransmitters (e.g. GABA and glutamine), energy and membrane-related metabolites (e.g. phosphocholine, glycerol-phosphocholine, NAA, *myo*-inositol and NAD), as well as valine and lysine (Table 5.3).

5.4.2 Metabolic alterations in rat plasma

Chronic but not acute MPH treatment was effective at altering several metabolites in the plasma, with 10 different metabolites (glutamate, lactate, acetate, glucose, phenylalanine, tyrosine, phosphocholine, threonine, formate, and 3-methylhistidine) being significantly altered (Figure 5.6). Three of these metabolites were significantly increased, including the amino acid neurotransmitter glutamate, the membrane metabolite phosphocholine and the energy metabolite glucose (α and β anomers). Given that earlier studies have indicated that MPH enhances excitatory neurotransmission and brain energy metabolites (Berridge *et al.* 2006; Réus *et al.* 2015), the present data suggest that MPH may not only enhance brain levels of these metabolites but that it also elevates these metabolites in the circulatory system. On the other hand, the levels of seven other metabolites were significantly decreased. The decreased metabolites were LNAAs (including phenylalanine and tyrosine) and metabolites related to energy metabolism (including lactate, acetate, formate, 3-methylhistidine and threonine). Threonine can be converted to pyruvate which can also be converted to lactate or formate in some reversible reactions (Buis and Broderick 2005; Leibig *et al.* 2011). The decrease of threonine would imply that chronic MPH treatment may increase the conversion of threonine to lactate and formate in the plasma. The lactate and/or formate formed in the plasma may, however, be carried across the BBB into some brain areas, since a transport system for carrying monocarboxylates across the BBB has been described for which lactate has a high permeability for within young/adolescent animals (Cremer

et al. 1976; Deelchand *et al.* 2009; Waniewski and Martin 1998). Similarly, acetate is also carried across the BBB by this monocarboxylate transport system (Cremer *et al.* 1976; Deelchand *et al.* 2009; Waniewski and Martin 1998).

In the present study, plasma levels of amino acid precursors of catecholamine synthesis, including tyrosine and phenylalanine were also decreased by chronic MPH treatment. Similar to the monocarboxylate system, a transport system (L-amino acid transporter-1; LAT-1) for carrying the polar LNAA compounds across the BBB has also been characterised (Fernström 2013). Therefore, the mechanism of action of MPH could involve an alteration of the balance of plasma LNAAs, favouring the uptake and transport of tyrosine and phenylalanine into the brain where they could be utilised in the synthesis of DA and NA, two catecholamine neurotransmitters implicated in ADHD and the therapeutic action of MPH (Berridge *et al.* 2006; Kuczenski and Segal 2002; Del Campo *et al.* 2011). To determine if indeed brain levels of LNAAs and energy metabolites are enhanced following acute and chronic MPH administration, we examined the metabolic patterns in three brain regions (frontal cortex, striatum, and hippocampus), which are all associated with ADHD and the mechanism of action of MPH.

5.4.3 Metabolic alterations in the frontal cortex

Both acute and chronic MPH treatment significantly increased water-soluble metabolites in the frontal cortex of adolescent rats (Figure 5.3). Acute MPH treatment increased only two metabolites significantly in the frontal cortex (i.e. valine and lysine) based on the ANOVA model. These two metabolites were also increased following chronic MPH treatment, along with 13 other metabolites (Figure 5.3). These 13 increased metabolites include LNAAs (tyrosine and valine), energy metabolites (lactate and creatine), and amino acid-related neurotransmitters (glutamate, glutamine, GABA, NAAG and aspartate), as well as membrane-related metabolites

(NAA, phosphocholine, taurine, and *myo*-inositol). Following chronic MPH administration, the LNAA tyrosine and the energy-related metabolite lactate were significantly increased in the frontal cortex. Given that both of these metabolites were decreased in the corresponding plasma samples it is possible that MPH elevates the levels of these metabolites in the frontal cortex, by enhancing their transport from the plasma into the brain (see Figure 5.6). Enhanced levels of tyrosine in the frontal cortex would potentially enhance the synthesis and storage of DA and NA in this brain region and indeed in Chapter 3, this thesis showed that chronic MPH treatment enhances whole tissue levels of DA in the frontal cortex (Figure 3.7). In this context, tyrosine-rich amino acid mixtures have been shown to reduce ADHD symptoms in young patients, an effect which could also be attributed to enhanced synthesis and storage of catecholamines such as DA (Hinz *et al.* 2011).

Excitatory amino acid transmitters and related metabolites including: glutamate/glutamine, NAAG and aspartate, as well as the main inhibitory amino acid transmitter (GABA) were also found to be increased in this brain region following chronic but not acute MPH treatment. Thus, it is possible that MPH act by ensuring a balance between excitation and inhibition, as abnormal alterations of these glutamatergic and GABAergic metabolites in the frontal cortex have indeed been shown to be involved in the symptoms of ADHD (Bollmann *et al.* 2015; Perlov *et al.* 2007). Further, the glutamate/GABA-glutamine cycle is a metabolite shuttle that determines the release of the neurotransmitters, glutamate and GABA from neurons and their subsequent uptake by astrocytes (i.e. star-shaped glial cells). Astrocytes, in turn, release glutamine that is taken up by neurons for the generation of neurotransmitters (Bak *et al.* 2006; Rowley *et al.* 2012). This cycle between neurons and astrocytes is crucial to the normal functioning of the brain and it is indicative of glutamatergic and GABAergic activity (Bak *et al.* 2006; Rowley *et al.* 2012).

Increases in glutamate/glutamine levels in the frontal cortex of chronically MPH-treated rats in this study may therefore suggest an enhanced but still balanced excitatory/inhibitory transmission. Moreover, the MPH-induced enhancements of metabolite indicators of membrane activity (such as NAA, phosphocholine, taurine and *myo*-inositol) are suggestive of changes in the functional integrity of mitochondria and neuronal energy utilisation (as indicated by the enhanced NAA), membrane integrity (as indicated by the enhanced phosphocholine), and a general protection against glutamate, NAAG, and aspartate mediated excitotoxicity (as indicated by the enhanced taurine and *myo*-inositol).

5.4.4 Metabolic alterations in the hippocampus

Similar to the frontal cortex, both acute and chronic MPH treatment significantly elevated metabolites in the hippocampus based on the ANOVA model (Table 5.2). However, in contrast to the findings in the frontal cortex, acute treatment showed more pronounced effect on metabolite levels compared to chronic MPH treatment. The increased variables in this brain region following acute MPH treatment included 16 different metabolites i.e. LNAAs (phenylalanine, tyrosine, valine), amino acid neurotransmitters (GABA, glutamate), brain energy-related metabolites (lactate, acetate, creatine, nicotinamide adenine dinucleotide (NAD), nicotinamide), and membrane metabolites (taurine, choline, phosphocholine, *myo*-inositol), together with alanine and lysine. Conversely, chronic MPH treatment elevated the levels of only four metabolites compared to the saline-treated controls. These metabolites were the LNAAs (phenylalanine, tyrosine, and valine), as well as alanine (Table 5.2). Thus, in the hippocampus, phenylalanine, tyrosine, valine and alanine are altered by MPH irrespective of treatment-duration (i.e. altered after both acute or chronic treatment). Taken together, the increase of the LNAAs tyrosine and phenylalanine, as well as the energy metabolites lactate and acetate in the hippocampus (and also the frontal cortex) following MPH treatment further indicates that the drug likely acts by increasing the brain pool

of these metabolites, perhaps by increasing their transport across the blood-brain barrier into these two brain regions (i.e. hippocampus and frontal cortex). The hippocampus is a key region involved in cognition and memory, thus MPH-induced increases of these metabolites (e.g. tyrosine and phenylalanine) in this brain region could contribute to the therapeutic action of MPH. Like lactate, acetate is also carried across the blood-brain barrier by the monocarboxylate transport system and this occur at a greater level in young/adolescent animals compared to adults and also serves as an important alternative energy source (Cremer *et al.* 1976; Deelchand *et al.* 2009; Waniewski and Martin 1998). The MPH-induced increase of brain energy-related metabolites such as creatine, NAD, and nicotinamide in the hippocampus is noteworthy. The increase of creatine, a major brain energy source is compatible with previous studies demonstrating that MPH increases creatine kinase activity in the hippocampus, as well as in the frontal cortex of rats (Scaini *et al.* 2008). Similar to the changes in frontal cortex, hippocampal glutamate and GABA were both significantly increased by acute MPH treatment, supporting the idea that MPH may indeed enhance the glutamatergic/GABAergic pathway in these brain regions while also ensuring a balance between excitatory and inhibitory transmission. Moreover, MPH induced an increase of the membrane metabolites (taurine, choline, phosphocholine, *myo*-inositol) that are required for maintaining membrane integrity. For example, taurine is thought to be released in response to toxic concentrations of excitatory transmitters (e.g. glutamate) in hippocampal slices of mice, therefore enhanced levels of taurine by MPH might serve as a general protective mechanism for cell membranes against potential MPH-induced excitotoxicity (Saransaari and Oja 2000).

5.4.5 Metabolic alterations in the striatum

In the striatum, acute MPH treatment but not chronic treatment resulted in significant alterations of metabolites (Table 5.3). Unlike the frontal cortex and hippocampus where increases in

metabolites were recorded, acute MPH treatment resulted in significant reductions of metabolites in the striatum. In total, 9 metabolites were decreased in the striatum including metabolites related to neurotransmission (i.e. GABA and glutamine) and energy/membrane integrity (i.e. phosphocholine, glycerol-phosphocholine, NAA, *myo*-inositol and NAD). The other decreased metabolites were lysine and the BCAA valine (Table 5.3). The mechanism underlying the MPH-induced decreases of metabolites in the striatum remains to be established, but this finding could be specific to the striatum (i.e. region-specific effect). Interestingly, abnormally high glutamate/glutamine levels have been recorded in the striatum of some young medication naïve ADHD patients (Carrey *et al.* 2007), and a previous ^{1}H-MRS (magnetic resonance spectroscopy) study on young ADHD patients treated with MPH reported decreased striatal levels of glutamate/glutamine/GABA compared to the levels before treatment was initiated (Carrey *et al.* 2003), thus these previous clinical studies are consistent with the present findings in the adolescent rat striatum. While both glutamate and DA are implicated in the mechanism of action of MPH, this study shows that the drug acutely changes the striatal levels of these two neurotransmitters in opposite directions. In accordance with our findings some previous studies have shown that such opposite drug induced actions on glutamate and DA is not unique to MPH. For example, Caravaggio *et al.* (2016) concluded that an increase in striatal DA often do not correlate with an increase in striatal glutamate and that a corresponding increase (or decrease) of both neurotransmitters may occur in a treatment-duration dependent manner. Indeed, Holmer *et al.* (2005) used MPTP (1-methyl-4-phenyl-1,2,3,6-tetrahydropyridine) to deplete striatal DA (DA denervation) and observed increased striatal extracellular glutamate two-hours (four 20 mg/kg MPTP doses in this time frame) after treatment (acute effect). However, seven days of MPTP (30 mg/kg) treatment decreased striatal extracellular glutamate (chronic effect), with the decrease of glutamate reversed upon L-DOPA injection (Holmer *et al.* 2005). Kalivas and Duffy (1997)

further showed that the changes in striatal extracellular glutamate may be D2/3 receptor mediated. While extracellular glutamate was not measured in the present study, the increased extracellular DA induced by acute 5.0 mg/kg MPH treatment (Figure 3.8) could result in decreased striatal glutamate/glutamine levels, and may partly support the decreased glutamine levels observed in this study after acute treatment (Table 5.3). In addition, the MPH-induced decrease of striatal GABA levels in this study could be related to the density of glutamate decarboxylase (GAD; responsible for catalysing the decarboxylation of glutamate to GABA). As previously indicated in rodents, MPH treatment elevates the mRNA of glutamate decarboxylase isoenzymes (GAD65 and GAD67) in the frontal cortex, but the drug significantly dampens the transcription of GAD65 in the striatum (Freese *et al.* 2012).

In addition, previous rodent studies have shown that brain NAA, *myo*-inositol and glycerol-phosphocholine levels are related to mitochondrial function and energy metabolism. Indeed, it has been demonstrated that NAA synthesis is reduced when ATP production is decreased (Bates *et al.* 1996; Clark 1998). It is possible that the MPH induced reduction of striatal NAA levels in the present study is related to the decreased NAD levels also detected here. NAD is a coenzyme that exist either in the oxidised (NAD^+) or reduced (NADH) forms. In the mitochondria, NAD (reduced form) is converted to ATP (in the presence of oxygen), which is required to fuel and maintain neuronal function. Thus, NAD loss inhibits cellular respiration, resulting in a decline of mitochondrial ATP production (Kristian *et al.* 2011). Overall, our data suggest that the decreased amino acid neurotransmitters and energy/membrane metabolites in the striatum following acute MPH administration (although normalised following chronic treatment), may be related to altered glutamate decarboxylase density and a possible altered mitochondrial function.

5.4.6 Implications of the duration- and region-specific action of MPH

The observed MPH-induced elevation of metabolite levels in the frontal cortex and hippocampus following both acute and chronic treatment is consistent with our previous findings in the cerebrum following acute 5.0 mg/kg MPH treatment (see Chapter 4). Given that some of the metabolites (such as glutamate and glutamine) identified to be elevated by MPH in the frontal cortex and hippocampus in this study have been previously shown to be decreased in these brain regions in ADHD patients (Perlov *et al.* 2007), the effect of MPH on metabolites in these brain regions and in the plasma may be involved in the therapeutic action of this anti-ADHD medication. Moreover, given that the drug decreased the plasma levels of LNAAs (including tyrosine and phenylalanine) and energy metabolites (including lactate and acetate) and the concurrent increase of these metabolites in the frontal cortex and hippocampus, it appears that the drug alters the balance of plasma levels of these metabolites possibly by favouring their uptake and transport across the blood-brain barrier into the brain (particularly into the frontal cortex and hippocampus) via the LAT-1 and the monocarboxylate transport systems (see Figure 5.7), respectively (Cremer *et al.* 1976; Deelchand *et al.* 2009; Waniewski and Martin 1998; Fernström 2013). In the brain, tyrosine and phenylalanine serve as precursors of catecholamine (i.e. DA and NA) synthesis. In addition, these monoamine systems (i.e. DA and NA) are often reported to be dysfunctional or underactive in ADHD, therefore the MPH-induced increase of their precursors (i.e. tyrosine and phenylalanine) may be important in addressing monoaminergic deficits associated with ADHD. Indeed, it is reported that tyrosine-rich amino acid mixtures can be effective in reducing the symptoms of ADHD in some children (Hinz *et al.* 2011). Primarily, MPH is thought to exert its therapeutic effect via a blockade of the DA and NA transporters (see Figure 5.7). Following transporter blockade, the clinically relevant MPH dose administered in this study is reported to increase the extracellular levels of both DA and NA in some brain

regions including the frontal cortex and hippocampus, hence improving cognition and working memory (Volkow *et al.* 2001; Berridge *et al.* 2006; Kuczenski and Segal 2002; Spencer *et al.* 2012). Given that elevated levels of tyrosine in the brain could result in an enhancement of DA and NA synthesis (Hinz *et al.* 2011), it is possible that the increased levels of tyrosine and its precursor phenylalanine may be an additional mechanism by which MPH elevates DA and NA levels in these brain regions. Therefore, based on the present findings, as well as the previous findings in the cerebrum, we hypothesise that at least in the frontal cortex and hippocampus, MPH may reduce the symptoms of ADHD by: (1) the classical pathway involving DAT and NET blockade, and (2) driving the plasma to brain pool of tyrosine and phenylalanine, as shown in the present study (see Figure 5.7).

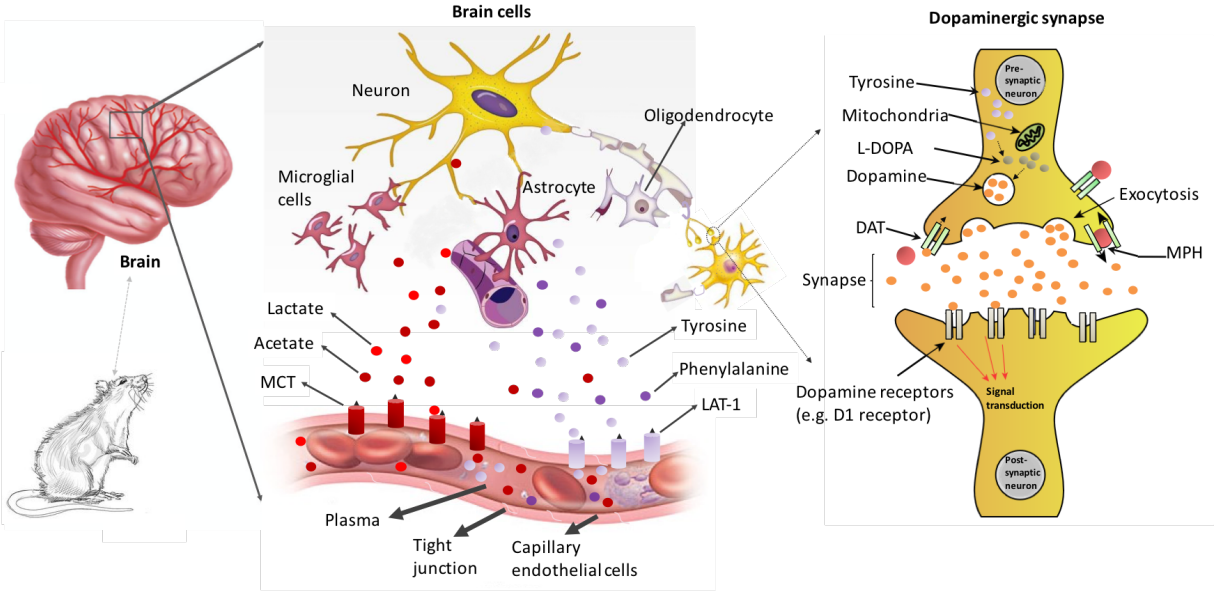

Figure 5.7: MPH-induced transport of some metabolites across the blood-brain barrier.
The blood-brain barrier is a semi-permeable membrane barrier formed by brain endothelial cells which are connected by tight junctions, which separates the circulating blood from extracellular fluid. Metabolites such as tyrosine, phenylalanine, lactate, and acetate, etc., are unable to cross this barrier freely, and therefore rely on transporters such as LAT-1 (L-type amino acid transporter) and MCTs (monocarboxylate transporters) for transport from the plasma into the brain. The present study indicates that MPH may induce an increased transport of these metabolites (i.e. tyrosine, phenylalanine, lactate, and acetate) from the plasma into the brain. Once in the nerve terminals, tyrosine is utilised in the synthesis of dopamine, which subsequently binds to its receptors (e.g. D1 receptor) and trigger a signal cascade.

Consistent with our findings in the cerebrum (see Chapter 4), GABA, glutamate, and/or glutamine were also increased in the frontal cortex and hippocampus following either acute or chronic MPH treatment. Glutamatergic transmission that regulates cortical and hippocampal activity is vital to cognitive function such as working memory (Goldman-Rakic 1995). The enhancement of GABA/glutamate levels following MPH treatment is likely to indicate a general enhancement of inhibitory and excitatory neurotransmission, and is supported by earlier electrophysiological studies which demonstrated that MPH increases GABAergic and glutamatergic neurotransmission in the cortex and hippocampus (Goldman-Rakic 1995). Interestingly, however, GABA and glutamine as well as membrane metabolites (including NAA, *myo*-inositol and phosphocholine) were significantly decreased in the striatum after acute MPH treatment with no major striatal changes observed after chronic drug treatment. The glutamate/GABA-glutamine cycle is an important shuttle between neurons and astrocytes and it is crucial to the normal functioning of the brain, while also providing an indicator of glutamatergic and GABAergic activity (Bak *et al.* 2006; Rowley *et al.* 2012). The MPH-induced decrease of striatal GABA levels in the present study could be related to the density and activity of enzymes involved in this pathway, such as those involved in the conversion of glutamate to GABA (e.g. glutamate decarboxylase). In support of this, the density of the GAD 65 glutamate decarboxylase enzyme is reported to be significantly dampened in the striatum following MPH treatment (Freese *et al.* 2012). Similarly, in support of the present findings, a previous study on young ADHD patients receiving MPH treatment reported decreased levels of glutamate/glutamine/GABA in the striatum (Carrey *et al.* 2003).

Moreover, NAA, *myo*-inositol and phosphocholine are known to play diverse roles in myelin synthesis, neuron-glial signalling, osmoregulation and glutamate/NAAG turnover (Baslow 2003;

Moffett *et al.* 2007). NAA synthesis is closely associated with the functional integrity of mitochondria and neuronal energy utilisation, hence NAA is widely accepted as an indicator of neuronal mitochondrial function and neuronal density (Moffett *et al.* 2007). Indeed, NAA is thought to increase during neurogenesis, and may decrease due to diverse neural pathologies (Maltezos *et al.* 2014; Yao *et al.* 1999). Thus, the increase of NAA in the frontal cortex following MPH therapy could be related to an enhanced energy utilisation in this region, while the reductions of NAA as well as *myo*-inositol and phosphocholine in the striatum observed following acute but not chronic MPH administration in the present study could be related to possible aberrations in mitochondrial function. Similar to our findings, a previous clinical study on young ADHD patients also reported a significantly decreased striatal NAA levels following MPH treatment (Ben Amor 2014).

5.5 Conclusion

In summary, this study shows that acute and chronic MPH treatment alter adolescent rat plasma and brain metabolic profiles. These changes were both treatment duration-dependent and region-specific. Acute MPH significantly decreased striatal amino-acid transmitters, as well as membrane and energy-related metabolite levels, but these effects were not detected after chronic treatment. In contrast, both acute and chronic MPH treatment elevates amino-acid transmitters, LNAAs, energy, and membrane metabolite levels in the frontal cortex and hippocampus. In addition, the present study also suggest that MPH may increase catecholamine synthesis and lactate/acetate levels in the frontal cortex and hippocampus. It was hypothesised that these increases occur via MPH-induced enhancement of tyrosine/phenylalanine and lactate/acetate transport from the plasma into these two brain regions.

CHAPTER 6

6 Methylphenidate and the cerebellum

6.1 Introduction

Current etiological theories of ADHD focus on morphological and functional abnormalities in the fronto-striatal networks (Semrud-Clikeman *et al.* 2000; Castellanos *et al.* 1996; Ashtari *et al.* 2005). However, recent reports indicate that ADHD could also be associated with dysfunctions in neuronal structures beside the fronto-striatal circuitry, including the substantia nigra, thalamus, and cerebellum (Valera *et al.* 2007). In particular, the cerebellum appears to be emerging as one of the important brain structures altered in ADHD, as well as some neuropsychiatric disorders (Ivanov *et al.* 2014). The motor functions of the cerebellum including coordinated voluntary movements have been well established (Fine *et al.* 2002). However, recent findings from neuroanatomical and neuroimaging studies have provided evidence for the involvement of cerebellum in non-motor functions including a variety of linguistic, affective and cognitive processes (De Smet *et al.* 2013). Indeed, the cerebellum is now thought to play crucial roles in cognitive processes such as learning, visuo-spatial processing, emotion, attention shifting, and working memory (Golla *et al.* 2005; Ivry *et al.* 2002; Schmahmann and Sherman 1998; Steinlin 2008; Stoodley *et al.* 2012).

The involvement of the cerebellum in cognitive processes suggests that it could potentially have a role in the cognitive and attentional deficits underlying ADHD. Indeed, research shows that the cortex and the basal ganglia (including the striatum and the nucleus accumbens), which are often reported to be dysfunctional in ADHD, are interconnected with the cerebellum, with outputs of the cerebellum targeting non-motor areas in the posterior parietal and prefrontal cortex as well as the cortical motor areas (Strick *et al.* 2009). The strong connection with the cortex and other cerebral areas, places the cerebellum in a position to influence neural networks in these structures. In addition, neuroimaging studies have provided evidence of consistent cerebellar

morphological abnormalities in ADHD patients (Berquin *et al.* 1998). With regards to this, some structural imaging studies have reported decreased cerebellar volume and abnormal developmental changes of the cerebellum of ADHD patients (Castellanos *et al.* 1996; Castellanos *et al.* 2001; Berquin *et al.* 1998). More specifically, some studies have indicated that the decreased cerebellar volume may be localised to the left anterior and the right posterior cerebellar hemispheres (Ivanov *et al.* 2014). The involvement of the right posterior cerebellar hemisphere in ADHD fits well with studies suggesting a greater involvement of the right hemisphere in ADHD, particularly the right cortex (Voeller and Heilman 1988; Castellanos *et al.* 1996; Semrud-Clikeman *et al.* 2000). The dysfunctional right hemisphere hypothesis in ADHD appears to be supported mostly by functional brain imaging studies, which have linked the cognitive/behavioural abnormalities in ADHD with significant under-activation of the right cortex and right caudate (Vance *et al.* 2007; Rubia *et al.* 1999).

The cerebellum may represent a possible target for anti-ADHD drugs, since deficits in cerebellar grey matter and vermis size associated with ADHD patients have been reported to be normalised following both chronic psychostimulant drug treatment, as well as after cognitive behavioural training programs (Bledsoe *et al.* 2009; Hoekzema *et al.* 2011). Stimulants, such as MPH are often prescribed for individuals with ADHD. The rationale for MPH prescription is based on the assumption that the central catecholamine systems are dysfunctional in ADHD and also based on the known enhancing effect of these drugs on the fronto-striatal dopaminergic and noradrenergic systems (Dougherty *et al.* 1999; Del Campo *et al.* 2011). In rodent studies, MPH use has been linked with changes in the density of DAT (Roessner *et al.* 2010) and DA receptors, as well as the densities of proteins involved in monoamine synthesis and vesicular packaging such as tyrosine hydroxylase (TH) (Panos *et al.* 2014) and vesicular monoamine transporter (VMAT2)

(Simchon *et al.* 2010) in the fronto-striatal circuit, but it is unclear whether these proteins are affected by MPH in the cerebellum.

Interestingly, previous studies using the ^{1}H-MRS technique, a non-invasive technique that permits the quantification of metabolites in ADHD patients *in vivo,* have shown that some neurochemicals including glutamate, glutamine, and creatine exist in abnormally high concentrations in the cerebellum of individuals with ADHD compared to normal controls (Perlov *et al.* 2010). In addition, a previous clinical study has demonstrated that psychostimulant intake by ADHD patients decrease *myo*-inositol and NAA levels (Soliva *et al.* 2010). However, in comparison with the ^{1}H-NMR technique, the ^{1}H-MRS technique is less sensitive and detects fewer brain metabolites (Du *et al.* 2015). Consequently, several studies have utilised ^{1}H-NMR spectroscopy in analysing biofluids and tissue samples from both patients and animal models of various brain disorders (Lan *et al.* 2008; Holmes *et al.* 2001). However, to our knowledge, the effects of MPH on a broad range of neurochemicals and brain metabolites, as well as monoaminergic protein markers in the cerebellum of rats using ^{1}H-NMR and Western blotting respectively have not yet been investigated.

In the present study, we explored the acute and chronic effects of MPH on adolescent rat cerebellar metabolic profiles via ^{1}H-NMR spectroscopy. Further, we investigated the effects of the drug on monoaminergic protein markers implicated in the pathophysiology of ADHD and in the mechanism of action of MPH using Western blotting. We hypothesised that acute and chronic MPH treatment would alter cerebellar metabolites and monoaminergic protein markers.

6.1.1 Aims

This study was aimed at examining the role of the cerebellum in the mechanism of action of MPH. These experiments were set up to test the hypothesis that MPH alters biomolecules and the expression of monoaminergic protein targets in the cerebellum. The experiments specifically examined the following:

- The dose-dependent effects of acute MPH treatment on the cerebellar metabolic pathways using ^{1}H-NMR spectroscopy.
- Treatment duration-dependent effects of the drug on biomolecules in the cerebellum using ^{1}H-NMR spectroscopy.
- The acute and chronic effects of MPH treatment on the protein expression of monoaminergic targets in the cerebellum via Western blotting.
- The effects of MPH treatment on whole tissue levels of DA and its metabolites in the left and right cerebellar hemispheres using HPLC-EC.
- The differences in the effect of MPH in the left and right cerebellum.

6.2 Methods

6.2.1 Drug Treatment and sample collection

Chapter 2, section 2.1 contains a detailed description of the animal housing and MPH treatment procedures. Here, the following animal treatment groups were investigated via:

(a) ^{1}H-NMR analysis: (i) Acute high dose (5.0 mg/kg MPH dose or 1.0 ml/kg saline), n=36 rats (18 MPH-treated and 18 saline-treated controls; cerebellar samples were collected from the left and right sides), (ii) Acute low dose (2.0 mg/kg MPH dose or 1.0 ml/kg saline), n=24 rats (12 MPH-treated and 12 saline-treated controls), (iii) Chronic (2.0 mg/kg MPH or 1.0 ml/kg saline,

twice daily for 15 days), n=24 rats (12 MPH-treated and 12 saline-treated controls). The animals were sacrificed 1 h after the last injection.

(b) Western blot analysis: (i) Acute (2.0 mg/kg MPH dose or 1.0 ml/kg saline), n=12 rats (6 MPH-treated and 6 saline-treated controls), (iii) Chronic (2.0 mg/kg MPH dose or 1.0 ml/kg saline, twice daily for 15 days), n=12 rats (6 MPH-treated and 6 saline-treated controls; samples were collected from the left and right cerebellum). The animals were sacrificed 24 h after the last injection.

(c) HPLC-EC analysis: (i) Acute (2.0 mg/kg MPH dose or 1.0 ml/kg saline), n=12 rats (6 MPH-treated and 6 saline-treated controls), (iii) Chronic (2.0 mg/kg MPH dose or 1.0 ml/kg saline, twice daily for 15 days), n=12 rats (6 MPH-treated and 6 saline-treated controls). The animals were sacrificed 1 h after the last injection.

Animals receiving chronic injections were 20-25 days old (75-90 g) on the first day of treatment and the last injections were given when the animals were 35-40 days old (180-220 g). Following the last injections, the animals were killed by rapid dislocation of the neck and the cerebellum removed and hemi-sected along the midline i.e. through the vermis (for the rats in the Western blot, HPLC-EC, and the acute high dose NMR groups only). The excised cerebellar samples were quickly snap-frozen in isopentane, and then stored at -80°C until analysis.

6.2.2 ^{1}H-NMR Spectroscopic experiments

6.2.2.1 Brain extract preparation and ^{1}H-NMR experiments

The brain sample preparation and the ^{1}H-NMR experiments were performed as described in Chapter 2, sections 2.2.1 and 2.2.3.

6.2.2.2 Pre-processing of NMR spectra

Before multivariate and univariate data analysis, the ACD/NMR processor (academic edition; Ontario, Canada) software was used to correct the ^{1}H-NMR spectra manually for phase and baseline. The ^{1}H-NMR spectra of the tissue samples were referenced to the TSP resonance at δ = 0.00 ppm. The 'intelligent bucketing' procedure was then employed to divide the spectra into integral segments. This yielded a full dataset of 71 rows (samples) and 313 columns (variables) for the acute high dose treatment group and then 24 rows (samples) and 311 columns for the chronic low dose treatment group. The resulting integral intensity values were normalised to the TSP signal (*s*, δ = 0.00 ppm). Subsequently, the spectral regions that did not contain any resonances (i.e. noise regions) and the intense δ = 4.65-5.16 ppm residual H_2O/HOD signal region were removed from all the ^{1}H-NMR datasets. This resulted in a final dataset of 71 (samples/rows) and 119 (variables/columns) for the acute high dose treatment group and then 24 (samples/rows) and 131 (variables/columns) for the chronic treatment group. The integral data was then analysed using multivariate and univariate data analysis strategies.

6.2.3 Multivariate and univariate statistical analysis of the cerebellar datasets

Multivariate and univariate statistical analysis were performed on the TSP-normalised integral values as described in Chapter 2, section 2.2.5. The multivariate analysis performed using *MetaboAnalyst 3.0* tested the performance of the different subsets of the datasets and revealed the discriminatory metabolites selected by OPLS-DA. PCA, OPLS-DA and S-plots were generated for the datasets. In addition, univariate analysis was also performed using an ANOVA model (conducted with the corresponding function in R 3.1.2 statistical software), where 2 factors and 3 primary sources of variation were incorporated: (1) 'treatment status' (Control *vs.* MPH-treated rats, T_i); (2) 'brain hemisphere' (right *vs.* left, H_j) and the (3) 'treatment status' x 'brain

hemisphere' (TH_{ij}) interaction effect. This ANOVA model is represented by equation 1 (Chapter 2, section 2.2.5). In order to ensure a strong performance for multiple comparisons, the FDR (False Discovery Rate) and Bonferroni correction criteria were employed to adjust the significance (*p*-value) of each of the components contributing to the observed variations.

$$Y_{ij} = \mu + T_i + H_j + TH_{ij} + e_{ij} \qquad (1)$$

To determine any significant metabolic patterns arising from each of the experimental factors, including the multivariate TH_{ij} interaction component of variance, simultaneous multivariate analysis of the main variables (i.e. 'brain hemisphere' and 'MPH treatment') was conducted using ASCA (ANOVA simultaneous component analysis), via the two-factor independent samples option available in *MetaboAnalyst 3.0* (which is based on equation 1). Permutation test with 2,000 permutations was used determine the significance of each of the multivariate variance components.

6.2.4 Metabolic pathway analysis of the cerebellar datasets

Detailed analysis of the most relevant cerebral metabolic pathways and networks altered following MPH treatment was performed using the *MetaboAnalyst 3.0* tool, as described in Chapter 2, section 2.2.7.

6.2.5 Immunoblotting

The frozen tissues were thawed, homogenised in RIPA lysis buffer, run on SDS-PAGE and electroblotted as previously described in Chapter 2, section 2.5. The blots were probed with primary antibodies, including anti-DA D1 receptor (1:1000, Millipore, UK), anti-SLC18A2/VMAT2 (1:1000, OriGene, USA), anti-TH (1:1000, Abcam, UK), and anti-β-actin (1:2000, Santa Cruz, USA). The secondary antibodies used were horseradish peroxidase (HRP)

conjugated (1:2000, Santa Cruz, USA). The blots were developed with enhanced chemiluminescent HRP substrate (Amersham Biosciences, UK) and images visualised with an MCID^{TM} core digital imaging system (MCID, UK). Signal intensity was quantified using MCID^{TM} image analysis software (version 7.0). Bands corresponding to VMAT2, TH, and D1 receptor were normalised to β-actin, and all data were expressed as a percentage of the saline-treated controls. The data was analysed with GraphPad Prism (version 5.0, Graph Pad software Inc., La Jolla, CA). Statistical analyses were performed using two-way ANOVA with the factors 'drug' (MPH, saline), 'duration' (acute, chronic) and interactions between 'drug' x 'duration' along with Bonferroni *post-hoc* test. Differences were considered significant if $p < 0.05$. Data are presented as mean ± S.E.M.

6.2.6 Analysis of whole tissue levels of dopamine using HPLC-EC

The effects of both acute and chronic MPH treatment on the whole tissue levels of DA and its metabolites were examined using HPLC-EC. Following the intraperitoneal injections of MPH or saline, the left and right cerebellar hemispheres were quickly dissected out and homogenised in 0.2 M perchloric acid (the amount was based on the tissue weights) until all solid tissue was no longer visible in the solution (approximately 30 s), as previously described in Chapter 2, section 2.4. The whole tissue levels of DA were calculated for each sample (with a correction for the tissue weight). The data from this study was presented as μg/g for each treatment group. The data was analysed using GraphPad Prism (version 5.0, GraphPad Software Inc., La Jolla, CA). Two-way ANOVA with the factors, 'drug' (MPH, saline), and 'hemisphere' (left, right), as well as interactions between 'drug' x 'hemisphere' were carried out on DA concentrations.

6.3 Results

6.3.1 Multivariate analysis of cerebellar ^{1}H-NMR spectroscopic data

The ^{1}H-NMR datasets were initially visualised with PCA, which revealed a clear separation between the acute 5.0 mg/kg MPH-treated (high dose) dataset compared with the controls (Figure 6.1) but not for the acute 2.0 mg/kg (low dose) or the chronic (twice daily 2.0 mg/kg for 15 days) MPH-treated datasets. Subsequently, OPLS-DA was used to analyse the ^{1}H-NMR datasets in order classify the samples based on their treatment status. The OPLS-DA scores plot provided additional support for a clear distinction between the 5.0 mg/kg MPH-treated (high dose) and the saline-treated controls (Figure 6.1B), but not for the acute low dose and the chronic groups when compared with their corresponding controls. To ensure reliability of models across the different treatment regimes, a Q^2 value $\geq$ 0.3 was used as a cut off for all models as previously described (McLoughlin *et al.* 2009; Worley and Powers 2013). The acute high dose yielded $R^2X = 0.6$, $Q^2 = 0.46$, and a permutation *p*-value < 0.0005 (indicating statistical significance following multivariate analysis on this dataset; where R^2X denotes the fraction of the dataset explained by the model; Q^2 denotes the predictive ability of the model). For the acute 2.0 mg/kg and chronic 2.0 mg/kg MPH-treated groups, $Q^2 < 0.1$ were obtained for both (i.e. non-significant following multivariate analysis). However, these datasets were further analysed using the ANOVA model depicted in equation 1 and the results provided in Table 6.2.

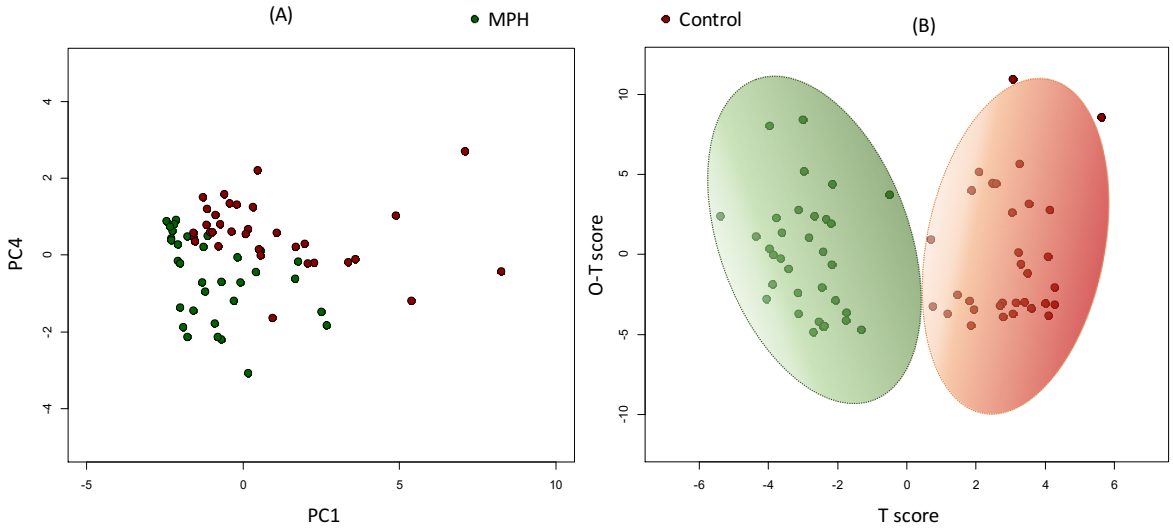

Figure 6.1: PCA and OPLS-DA scores plots of the acute 5.0 mg/kg dose cerebellar samples. (A) PCA scores plot demonstrating a clear separation between the acute high dose (5.0 mg/kg) MPH-treated and saline-treated control groups, and (B) OPLS-DA scores plot showing 95% confidence ellipses that further supporting the clear distinction between the acute high dose MPH-treated and saline-treated control groups (R^2X = 0.6, Q^2 = 0.46, permutation *p*-value < 0.0005).

6.3.2 MPH-induced metabolic alterations in cerebellar samples

Treatment of experimental subjects with MPH resulted in significant metabolic changes in the cerebellum (Table 6.2). The action of MPH was highly dependent on both 'dose' and 'treatment duration', with some of the altered metabolites being decreased and others being increased by acute MPH treatment (i.e. for both low and high doses but more pronounced after high dose). In contrast, most of the metabolites were significantly increased by chronic MPH treatment in comparison with the controls (Table 6.1). The assignments of the most important discriminant metabolites identified from the VIP scores of the OPLS-DA analysis and their *p*-values based on the ANOVA model depicted in equation 1, have been presented in Figure 6.2 (for the acute high dose only) and Table 6.1 (for the acute low 2.0 mg/kg dose and chronic 2.0 mg/kg MPH-treated samples). Table 6.1 also lists the multiplicity, coupling constants, and fold-changes of the identified discriminant metabolites. Negative fold change values (as shown in Table 6.1) indicate

MPH-induced decrease of the specified metabolites relative to the controls. Bonferroni correction [p = (0.05/total number of buckets for each sample)] was further applied on those samples that were statistically significant following the univariate analysis but not significant after the multivariate analysis (i.e. the acute low dose and chronically treated samples) (see Chapter 2, section 2.2.5). All the variables presented in Table 6.1 are statistically significant, but those that were significant following Bonferroni correction are marked using (^{b}).

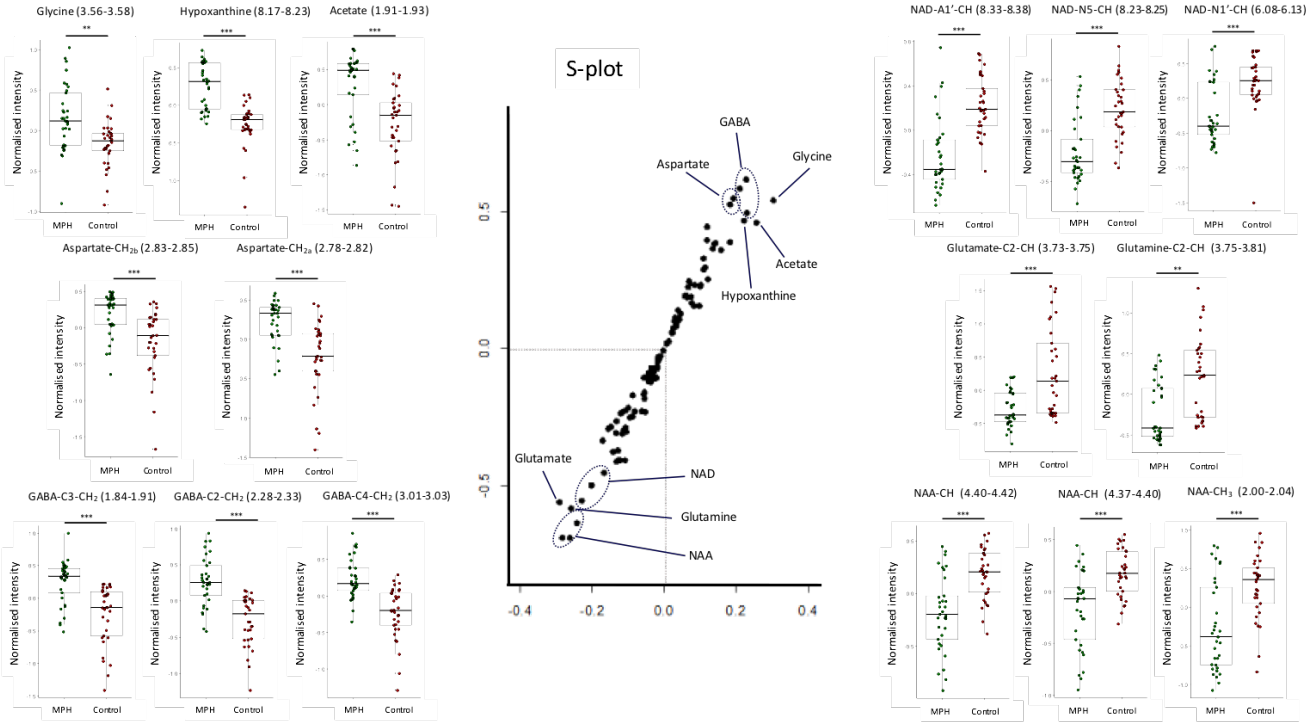

Figure 6.2: S-plot and boxplots revealing the most important discriminant cerebellar metabolites following the acute high MPH dose.

The S-plot shows some increased metabolites (upper portion of the plot) in the cerebellum following acute 5.0 mg/kg MPH treatment (high dose) and some decreased metabolites (lower portion of the plot). The most important discriminating variables in the S-plot are displayed in boxplots together with their significance level from an ANOVA model which included cerebellar 'hemisphere' and 'treatment' as independent variables. *$p < 0.05$; ** $p < 0.005$; ***, $p < 0.001$.

Table 6.1: Variables significantly discriminating the MPH-treated samples from their corresponding controls in the cerebellum obtained based on the ANOVA *p*-values

Variable Ranking	Chemical Shift (ppm)	Assignment	Multiplicity (coupling constants)	Raw ANOVA p-value for 'between treatment status'	Fold Change
Acute treatment, low dose (2.0 mg/kg)					
1	0.91-0.97	Valine-C4-CH_{3a}	*m* (3.84)	3.05×10^{-3}	-1.10
2	1.00-1.06	Valine-C4-CH_{3b}	*m* (3.84)	2.03×10^{-3}	-1.11
3	1.45-1.51	Alanine-C3-CH_3	*d* (7.24)	1.09×10^{-4}	-1.10^{b}
4	1.66-1.78	Lysine-C5-CH_2	*d* (7.69)	4.25×10^{-5}	-1.14^{b}
5	2.00-2.04	*N*-acetyl-aspartate-C3-CH_2	*s*	4.18×10^{-2}	-1.34
6	2.28-2.33	GABA-C4-CH_2	*t* (7.24)	3.55×10^{-2}	+1.10
7	2.43-2.49	Glutamine-C4-CH_2	*m* (4.14, 2.66)	3.69×10^{-2}	-1.11
8	3.01-3.03	GABA-C2-CH_2	*d* (7.69)	3.56×10^{-2}	+1.17
9	4.37-4.40	*N*-acetyl-aspartate-C2-CH_a	*m* (3.99)	8.33×10^{-3}	-1.37
10	4.40-4.42	*N*-acetyl-aspartate-C2-CH_b	*m* (5.32)	2.30×10^{-2}	-1.31
Chronic treatment (2.0 mg/kg)					
1	1.29-1.35	Lactate-C3-CH_3	*d* (6.95)	3.99×10^{-2}	+1.11
2	2.09-2.12	Glutamine-C3-CH_2	*m* (7.54, 2.51)	3.66×10^{-4}	$+1.14^{b}$
3	2.33-2.39	Glutamate-C4-CH_2	*m* (7.39)	9.87×10^{-3}	+1.10
4	3.56-3.58	Glycine-C2-CH_2	*s*	2.22×10^{-4}	$+1.24^{b}$
5	3.94-3.97	Phosphocreatine-C2-(CH_2)	*s*	4.34×10^{-2}	+1.12
6	3.24-3.30	Taurine-C2-CH_2	*t* (5.91)	2.41×10^{-2}	+1.08
7	6.88-6.93	Tyrosine-C5-CH	*m* (2.37)	2.74×10^{-3}	+1.10
8	7.17-7.23	Tyrosine-C6-CH	*m* (2.22)	4.47×10^{-2}	+1.07
9	7.37-7.40	Phenylalanine-C2-CH_b	*d* (6.95)	2.08×10^{-2}	+1.07

(-), Decreased metabolites in the MPH-treated group relative to the controls; (+), Increased metabolites in the MPH-treated group relative to the controls; (^{b}), Statistically significant even after Bonferroni correction.

6.3.3 Exploration of differences between the left and right cerebellar hemispheres via multivariable ASCA analysis

To simultaneously explore the 'treatment status' and 'between-cerebellar hemispheres' variance components for the acute high 5.0 mg/kg dose treatment group only, the ASCA two-factor independent sample analysis option in *MetaboAnalyst 3.0* was used. After performing this analysis, no significant differences (i.e. $p > 0.05$) were recorded for the 'between-cerebellar hemispheres' factor or the 'treatment status' x 'brain hemisphere' interaction effect for the first

two major principal components explored. However, the 'treatment status' factor was indeed significant ($p < 0.05$).

6.3.4 Quantitative network metabolic pathway analysis

The quantitative network pathway analysis (with an integrated enrichment analysis and pathway impact from topology analysis), revealed statistically significant MPH-induced changes to a number of metabolic pathways. The modulated pathways in the acute high dose (5.0 mg/kg) MPH treatment group are listed in Table 6.2. In addition, in order to explore connections between the discriminant metabolites selected by OPLS-DA and those proteins that might be involved in the metabolic changes attributable to MPH treatment, we used Ingenuity Pathway Analysis (IPA). Figure 6.3 shows those connections existing between the important metabolites obtained from the OPLS-DA analysis and the proteins with which they interact, which are mostly glutamatergic and GABAergic receptors. The acute low dose and the chronic groups were left out of this analysis as these datasets did not achieve statistical significance from the multivariate analysis (i.e. the OPLS-DA analysis showed no significant difference for both datasets).

Table 6.2: Quantitative network pathway analysis including pathway impact and pathway enrichment analysis from pathway topology of the acute high dose MPH-treated samples

Metabolic Pathway	Total Compounds	Hits	FDR *p*-value	Pathway Impact
Alanine, aspartate and glutamate metabolism	24	2	0.000532	0.15
Glycine, serine and threonine metabolism	32	2	0.000585	0.24
Taurine and hypotaurine metabolism	8	1	0.000585	0.43
Nicotinate and nicotinamide metabolism	13	1	0.000765	0.24
Starch and sucrose metabolism	23	1	0.00885	0.19
Inositol phosphate metabolism	26	1	0.00938	0.14
Glycerophospholipid metabolism	30	1	0.00966	0.02

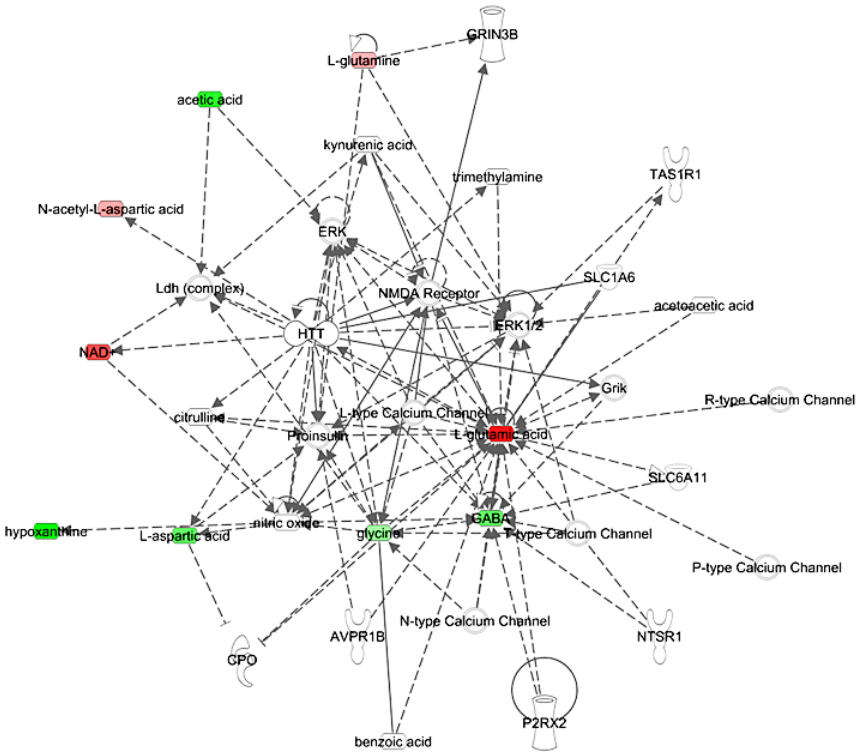

Figure 6.3: Proteomic signalling pathways interconnected with the metabolites altered by acute MPH treatment.

The metabolites that were either increased (green) or decreased (red) following acute 5.0 mg/kg MPH treatment interact with several genes and proteins including: GABA receptors such as *SLC6A11* (encodes GAT3); Lactate dehydrogenase (Ldh); and purinergic receptors (e.g. P2RX2) for ATP; and Glutamate receptors such as *SLC1A6* (encodes EAAT4), *GRIN3B* (encodes NMDA receptor), and Grik (glutamate receptor, ionotropic, kainate 4), as well as calcium channels and NMDA receptors that allow the flow of Ca^{2+} in response to glutamate binding.

6.3.5 MPH-induced modifications of vesicular monoamine transporter density

VMAT2, also known as solute carrier family 18 member 2 (SLC18A2), is a membrane protein that transports neurotransmitters including DA and NA that are implicated in both the pathophysiology and treatment of ADHD (Patel *et al.* 2003). The present study shows that MPH (2.0 mg/kg) alters VMAT2 protein expression in a 'treatment duration' dependent manner. The two-way ANOVA of 'drug' x 'duration' indicated a significant interaction effect between 'drug' and 'duration' ($F_{(1,44)} = 13.9$, $p < 0.0001$) and a significant effect of both 'drug' ($F_{(1,44)} = 8.9$, $p = 0.019$), and 'duration' ($F_{(1,44)} = 10.1$, $p = 0.005$). The *post-hoc* analysis revealed that acute 2.0

mg/kg MPH treatment significantly down-regulated ($p < 0.05$) VMAT2 density, while chronic treatment significantly upregulated ($p < 0.05$) the protein in comparison with the corresponding controls (Figure 6.4). There was, however, no significant effect of MPH on TH and D1 receptor densities in the cerebellum (Figure 6.4).

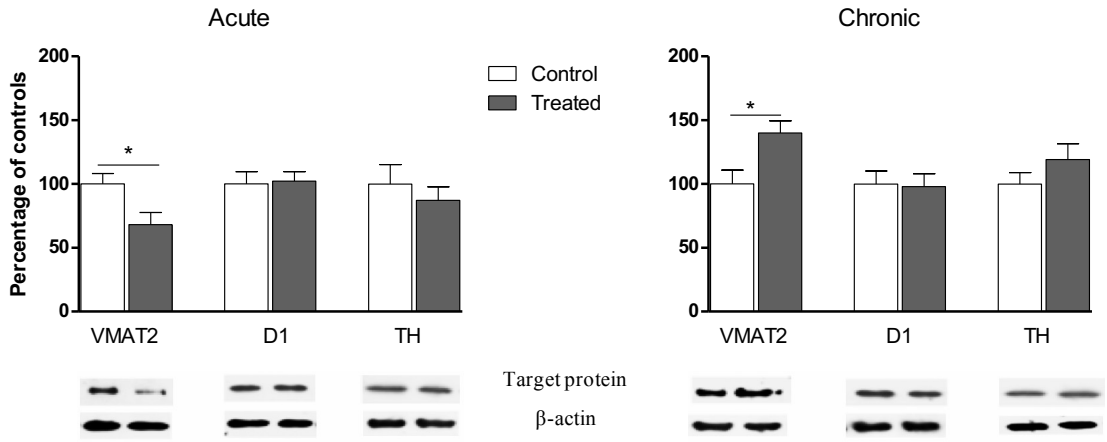

Figure 6.4: Effect of MPH on monoaminergic markers in the cerebellum.
(A) Acute, and (B) Chronic MPH treatment on VMAT2, D1 receptor, and TH protein densities in the cerebellum of adolescent rats. Values represent percentage ± SEM (n=6 rats/group but twelve data points (two from either hemisphere of each animal). *$p < 0.05$ (MPH-treated *vs.* control).

6.3.6 MPH-induced modifications in cerebellar dopamine and its metabolite content

Although DA and its metabolite levels in the cerebellum were very low (lower than the levels in the striatum), they were still detectable (Table 6.3) and somewhat comparable to the levels in the frontal cortex (see Table 6.3; compare with Chapter 3, Table 3.2). Analysis of the whole tissue levels of DA revealed a trend towards decreased DA levels in the acute MPH treated samples compared to the controls, but these did not reach statistical significance ($p > 0.05$). There was also no significant effect of 'hemisphere'. Similarly, chronic MPH treatment did not cause statistically significant changes to the levels of DA in the cerebellum and there was also no significant effect of 'hemisphere' (Figure 6.5).

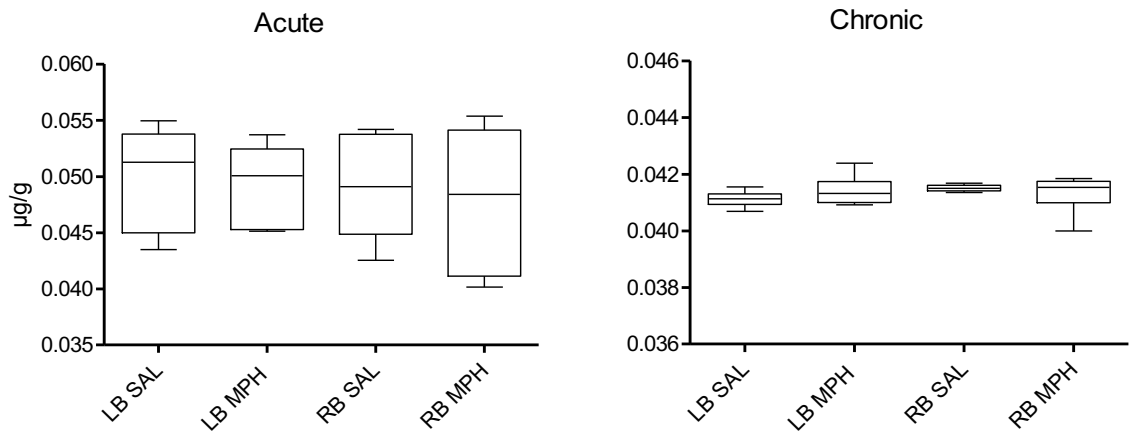

Figure 6.5: MPH-induced whole tissue levels of DA in the cerebellum.
DA levels in the left (LB) and right (RB) cerebellar hemispheres following (A) acute, and (B) chronic 2.0 mg/kg MPH treatment. Values (mean ± SEM, n=6 rats/group) were determined using HPLC coupled with electrochemical detection.

With regards to DOPAC, no significant 'drug' or 'hemisphere' effect was observed after acute treatment (Table 6.3). However, after chronic treatment, there was a significant effect of 'drug' ($F_{(1,20)} = 20.4$, $p < 0.001$) but not 'hemisphere', with the pairwise comparisons indicating higher DOPAC levels in both the left and right MPH-treated groups compared to the controls ($p < 0.05$) (Table 6.3). On the other hand, no significant changes were observed on HVA levels after both acute and chronic treatment. DA turnover as measured by DOPAC/DA ratio was not significantly affected by either 'drug' or 'hemisphere' in the acute samples. However, after chronic treatment, there was a significant effect of both 'drug' ($F_{(1,20)} = 20.6$, $p < 0.001$) and 'hemisphere' ($F_{(1,20)} = 10.3$, $p = 0.004$), with higher DOPAC/DA turnover ratio recorded in both the left ($p < 0.01$) and right ($p < 0.05$) MPH-treated group compared to the controls. No statistically significant effects were observed on the HVA/DA ratio.

Table 6.3: DA and its metabolite levels in the cerebellum following acute and chronic MPH treatment

		Acute		Chronic	
Cerebellum	Brain region	Control	MPH	Control	MPH
DA (μg/g)	Left	0.050 ± 0.002	0.053 ± 0.001	0.0411± 0.0001	0.0414 ± 0.0002
	Right	0.042 ± 0.002	0.048 ± 0.002	0.0415± 0.0001	0.0413 ± 0.0002
DOPAC (μg/g)	Left	0.0029 ± 0.0002	0.0032 ± 0.0001	0.005 ± 0.0005	0.007 ± 0.0003*
	Right	0.0028 ± 0.0001	0.0030 ± 0.0001	0.004 ± 0.0001	0.006 ± 0.0004*
HVA (μg/g)	Left	0.0026 ± 0.0001	0.0027 ± 0.0001	0.0029 ± 0.0004	0.0027 ± 0.0005
	Right	0.0027 ± 0.0001	0.0027 ± 0.0001	0.0033 ± 0.0002	0.0033 ± 0.0003
DOPAC/DA	Left	0.058 ± 0.004	0.059 ± 0.002	0.133 ± 0.01#	0.180 ± 0.08**
	Right	0.069 ± 0.002	0.064 ± 0.005	0.102 ± 0.04	0.147 ± 0.01*
HVA/DA	Left	0.052 ± 0.002	0.051 ± 0.001	0.069 ± 0.01	0.066 ± 0.01
	Right	0.064 ± 0.004	0.056 ± 0.003	0.079 ± 0.005	0.081 ± 0.008

Values (mean ± SEM, n=6 rats/group) were determined using HPLC-EC. *$p < 0.05$, **$p < 0.01$ (significant effect of 'drug' i.e. MPH *vs.* control); #$p < 0.05$ (significant 'hemisphere effect' i.e. left *vs.* right hemisphere).

6.4 Discussion

6.4.1 Principal findings

Cerebellar abnormalities in ADHD patients are frequently detected in magnetic resonance imaging (MRI) studies. In particular, such imaging studies have observed decreased cerebellar volumes in ADHD patients relative to non-ADHD controls (Castellanos *et al.* 1996; Berquin *et al.* 1998). However, to our knowledge, this is the first ^{1}H-NMR spectroscopic study along with Western blotting and HPLC-EC that examines MPH action on adolescent rat cerebellar tissue levels of metabolites and proteins associated with DA and NA function, as well as whole tissue levels of DA and its main metabolites. The data obtained in this study shows 'dose' and 'treatment duration' dependent differences in the action of MPH. Here, while acute MPH 5.0 mg/kg treatment decreased metabolites such as NAA, glutamate, glutamine and NAD, it increased metabolites such as GABA, glycine, aspartate, acetate and hypoxanthine. Similarly, but to a much lesser extent, acute 2.0 mg/kg also increased GABA but decreased membrane-related

metabolites (e.g. NAA) in addition to other metabolites such as glutamine, valine, lysine and alanine. On the other hand, chronic 2.0 mg/kg MPH treatment elevated most metabolites including amino acid transmitters (e.g. glutamate, glutamine and glycine), membrane and energy-related metabolites (e.g. lactate, creatine and taurine), as well as LNAAs (e.g. tyrosine and phenylalanine).

In addition, while acute MPH treatment decreased cerebellar VMAT2 protein density, chronic MPH treatment significantly elevated the expression of VMAT2. However, there were no significant MPH-induced changes in the levels of TH and D1 receptor expression in the cerebellum. Also, although both acute and chronic MPH treatment failed to significantly alter DA levels in the cerebellum, chronic but not acute MPH treatment increased DOPAC and the DOPAC/DA ratio in both the left and right cerebellar hemispheres, suggesting increased cerebellar DA turnover following chronic treatment.

6.4.2 MPH effects on cerebellar dopamine, large neutral amino acids and monoaminergic markers

The present study revealed significant MPH-induced modulations to a number of LNAAs. Here, the branched chain amino acid (BCAA) valine was decreased after acute administration of the 2.0 mg/kg MPH dose (but not the 5.0 mg/kg dose). In contrast, the aromatic amino acids (AAAs) tyrosine and phenylalanine were increased after chronic MPH treatment (Table 6.1). Given that LNAAs are polar compounds and are unable to cross the blood-brain barrier freely, the large neutral amino acid transporter (LAT-1), an active transport system is required for their transport into the brain (Fernström 2013). LNAAs compete for LAT-1 uptake and subsequent transport into the brain; it is therefore possible that MPH modifies the physiological balance of LNAAs in

the plasma (as discussed in Chapter 5), resulting in the increased entry of some LNAAs into the brain over others.

Initially, the cerebellum was not thought to be an area of DA-containing axons, as early investigations found no projections from DA-containing cell groups to the cerebellum (Lindvall and Björklund 1974). However, using more advanced techniques, later studies in rodents revealed a projection from the VTA to the cerebellum (Ikai *et al.* 1992). In addition, results from more recent studies indicate moderate levels of DA and NA in the cerebellum, as well as high densities of TH immunoreactive axons in both rodents and primates (Glaser *et al.* 2006; Melchitzky and Lewis 2000). In this context therefore, the present study measured tissue levels of DA in the cerebellum of MPH-treated and saline-treated rats. Interestingly, the present study has demonstrated significantly increased cerebellar levels of the aromatic amino acid (AAA) tyrosine and its precursor phenylalanine following chronic MPH treatment compared to the corresponding saline-treated control rats (see Table 6.1). These AAAs are involved in the biosynthesis of the catecholamines, DA and NA, which play crucial roles in executive brain functions and motor activity. Given these increased cerebellar AAAs, and the MPH-induced increases of tyrosine and phenylalanine in the cerebral regions such as frontal cortex and hippocampus as described in Chapters 4 and 5, it is possible that MPH alleviates ADHD symptoms not only by DAT and NET blockade but also by elevating the brain pool of precursors to DA and NA synthesis (i.e. tyrosine and phenylalanine). The increased AAAs (i.e. tyrosine and phenylalanine) following chronic 2.0 mg/kg MPH treatment corresponded with an increased DOPAC and dopamine turnover ratio (i.e. DOPAC/dopamine ratio) (Table 6.3) and increased cerebellar VMAT2 density (Figure 6.4), while acute treatment decreased VMAT2 density. However, these MPH-induced alterations to AAAs and VMAT2 density did not result in significant changes of cerebellar DA after either

acute or chronic MPH treatment. This would suggest that, in the cerebellum, over-expression of these AAAs and VMAT2 (induced by chronic 2.0 mg/kg MPH treatment in this thesis) does not lead to increased DA expression, which contrasts our findings in the cerebral areas showing that an increase of these AAAs increase DA levels (see Chapters 3, 4 and 5), as well as a previous report that found increased VMAT2 to be associated with increased DA in mice striatum (Lohr *et al.* 2014). It is possible that in the cerebellum, whole tissue DA represents a substrate for NA synthesis, rather than acting as a neurotransmitter itself. Indeed, a previous study provided some evidence that in the cerebellum, DA may predominantly serve as a substrate for NA synthesis (Glaser *et al.* 2006). Also in support of the present findings, reports from clinical studies indicate that acute MPH treatment does not significantly alter extracellular DA in the cerebellum (Volkow *et al.* 2001).

Further, cerebellar levels of the essential amino acid lysine, the non-essential amino acid alanine, and the BCAA valine, were decreased after acute 2.0 mg/kg MPH treatment but not after 5.0 mg/kg high dose or chronic 2.0 mg/kg MPH treatment. Alanine is involved in glucose production and could be made from the BCAA valine, both of which are decreased following acute 2.0 mg/kg MPH treatment. Moreover, as mentioned above, the cerebellar levels of lysine was also reduced after acute treatment. While lysine's role in the brain remains to be clarified, some studies have suggested that decreased or deficient lysine increases serotonin release (but not DA release) in some brain regions (e.g. amygdala), which results in an enhancement of the levels of anxiety (Smriga *et al.* 2002), a condition which is often comorbid with ADHD and occasionally reported as a side effect of MPH (Mulraney *et al.* 2016).

6.4.3 MPH modulates metabolites in the glutamatergic and GABAergic systems

A major finding of the present study is the acute MPH-induced (2.0 and 5.0 mg/kg) decrease of cerebellar levels of amino acid neurotransmitters involved in the excitatory glutamatergic system (e.g. glutamate and glutamine), and the contrasting elevation of the same metabolites following chronic treatment (2.0 mg/kg, twice daily for 15 days). On the other hand, the inhibitory neurotransmitter metabolite, GABA, was generally increased following acute treatment, with the higher dose of MPH (5.0 mg/kg) showing the most pronounced effect. Glycine, which is also an inhibitory metabolite was significantly enhanced by the higher (5.0 mg/kg) MPH dose but remained unaltered by the lower dose (2.0 mg/kg), but chronic 2.0 mg/kg administration significantly up-regulated glycine. The excitatory AAA aspartate, in contrast to glutamate was increased by acute 5.0 mg/kg MPH, while the lower (2.0 mg/kg) dose failed to alter its levels (Figure 6.2 and Table 6.1).

When glutamine is taken into the cerebellar cells, a mitochondrial associated enzyme (i.e. glutaminase 1) converts it to glutamate (Holten and Gundersen 2008; Marie and Shinjo 2011). Glutamate is also converted to α-ketoglutarate, which enters the tricarboxylic acid cycle in the mitochondria. However, glutamate can also be converted to aspartate that contributes to nucleic acid and serine synthesis. In addition, the inhibitory transmitter GABA is known to be generated from glutamate via glutamate decarboxylase in GABAergic neurons (Holten and Gundersen 2008; Marie and Shinjo 2011). Glutamine, glutamate, and GABA have all been implicated in the pathophysiology of ADHD (Moore *et al.* 2006; Perlov *et al.* 2010; Perlov *et al.* 2007; Bollmann *et al.* 2015). In particular, cerebellar glutamine and glutamate are reported to be abnormally high in ADHD patients compared to matched controls (Perlov *et al.* 2010).

With glutamate and glutamine expressed in both neurons and glial cells, it is uncertain whether the dampened total cerebellar glutamate and glutamine induced by acute 2.0 mg/kg and 5.0 mg/kg MPH treatment is related to altered neuronal excitatory transmission. However, consistent with our findings, previous ^{1}H-MRS studies in young ADHD patients also reported decreased cerebellar glutamate and glutamine levels following acute stimulant medication (Ben Amor 2014; Soliva *et al.* 2010). The findings reported in this study would suggest that acute 2.0 mg/kg and 5.0 mg/kg MPH treatment may enhance the conversion of glutamine to glutamate, and the subsequent conversion of glutamate to aspartate and GABA in the cerebellum, resulting in decreased levels of glutamine and glutamate but increased levels of aspartate and GABA. Indeed, while a previous study has confirmed the existence of GABA and glutamate decarboxylase in the cerebellum (Crook *et al.* 2006), another study has reported that psychostimulant (e.g. cocaine) administration increases the protein levels of the glutamate decarboxylase enzyme relative to controls (Goitia *et al.* 2013), which could potentially increase the conversion of glutamate to GABA and aspartate. Overall, it is possible that the acute MPH-induced decrease of glutamine and glutamate observed in the present study may normalise the levels of these metabolites in the cerebellum of those suffering from ADHD, as a previous study found abnormally high levels of these metabolites in the cerebellum of ADHD patients (Perlov *et al.* 2010).

This dampened cerebellar excitatory amino acid transmitter levels following acute 2.0 mg/kg and 5.0 mg/kg, however, contrasts our previous findings in the cerebral areas, where these MPH doses elevated the excitatory amino acid transmitter glutamate and its precursor glutamine (see Chapters 4 and 5). However, similar contrasting findings in the cerebral areas and the cerebellum have previously been found following MPH treatment in both humans and rodents, with the phenomenon suggested to be mediated by differences between receptor densities (e.g. dopamine

D2 and D4 receptors) in these two brain areas (Volkow *et al.* 1997; Michaelides *et al.* 2010). Also supporting the contrasting findings in the cerebellum and some parts of the cerebrum, some clinical studies on medication naïve ADHD patients found increased excitatory transmitter (glutamate and glutamine) levels in the cerebellum (Perlov *et al.* 2010), but decreased excitatory transmitter (glutamate and glutamine) levels in the frontal cortex relative to their corresponding control groups (Perlov *et al.* 2007). Moreover, previous studies have suggested co-localisation of GABA and glycine in the cerebellum of rats (Crook *et al.* 2006; Ottersen *et al.* 1987). Evidence shows that in the cerebellum of rats, glycine is used as a fast inhibitory neurotransmitter and that it is released together with GABA (Dumoulin *et al.* 2001; Dugué *et al.* 2005). Glycine in the cerebellum is suggested to play important roles in motor control (Avila *et al.* 2013; Rees *et al.* 2003). Thus, an increase of these inhibitory amino acid transmitters (i.e. glycine and GABA) and the decrease of the excitatory transmitter glutamate could have implications on cerebellum-mediated motor activity and may correspond with the effect of MPH in minimising hyperactivity.

6.4.4 MPH regulates cerebellar energy metabolism

Alterations in energy metabolism has been described as a key abnormality in ADHD (Todd and Botteron 2001). In this study, acetate was significantly increased in the cerebellum following acute 5.0 mg/kg MPH treatment compared to controls (Figure 6.2). In addition, lactate and phosphocreatine were also increased following chronic 2.0 mg/kg treatment (Table 6.1). Lactate has emerged as a key player in brain energetics. Converging evidence from *in vitro* and *in vivo* experiments indicate that lactate, a non-glucose fuel, is an efficient energy substrate used preferentially by neurons in maintaining synaptic transmission, especially during periods of intense activity (Larrabee 1995; Smith *et al.* 2003). Lactate is produced locally by astrocytes within the brain in an activity-dependent glutamate-mediated manner (Pellerin and Magistretti 1997). Glycolysis is stimulated within astrocytes by the excitatory neurotransmitter glutamate,

generating and releasing lactate, which is then used by neurons as an anaerobic energy substrate enabling neurons to endure activation (Smith *et al.* 2003). Given that cerebellar glutamate was found in the present study to be increased by chronic MPH administration, it is possible that the increased lactate levels may be related to increased glutamate-mediated stimulation of glycolysis in cerebellar neuronal and astrocytic cells. In support of this, it has been shown in *in vitro* experiments that increased glutamate usage enhances lactate release via the glycolytic pathway (Pellerin and Magistretti 1994). Like lactate, acetate serves as an important alternative energy source (Cremer *et al.* 1976; Deelchand *et al.* 2009; Waniewski and Martin 1998). Therefore, an increase of these metabolites (i.e. acetate and lactate) in the cerebellum may be important for cerebellar neurons in maintaining synaptic transmission during periods of intense activity (Larrabee 1995; Smith *et al.* 2003).

The creatine/phosphocreatine cycle is also linked with brain energy homeostasis, adenosine triphosphate (ATP) production, and functions as an alternative energy source (Rae *et al.* 2003). Similar to lactate, we found that the levels of phosphocreatine were increased following chronic 2.0 mg/kg treatment (Table 6.1). This finding could be related to an earlier study that found no significantly altered cerebellar creatine kinase activity after acute (2.0 and 10.0 mg/kg) MPH treatment but significantly elevated cerebellar creatine kinase activity following chronic (10.0 mg/kg) MPH treatment in both young and adult rats (Scaini *et al.* 2008). In addition to the creatine/phosphocreatine cycle, purine metabolism is also closely linked to ATP production and utilisation. Here, the purine derivative hypoxanthine was increased following acute 5.0 mg/kg MPH treatment relative to the controls (Figure 6.2). Increased hypoxanthine could lead to an increased level of the final metabolic product of purine catabolism, uric acid. In support of this,

d-amphetamine, which also increases synaptic levels of DA (similar to MPH), and is also used in the treatment of ADHD, has been shown to increase brain levels of uric acid (Miele *et al.* 2000).

NAD is another metabolite that plays a crucial role in brain energy metabolism. NAD is a coenzyme that exist either in the oxidised (NAD^+) or reduced (NADH) form. NAD is essential for several mitochondrial enzymatic reactions and cellular bioenergetic metabolism (Kristian *et al.* 2011). In the mitochondria, NAD (reduced form) is converted to ATP (in the presence of oxygen), which is required to fuel and maintain neuronal function. Thus, NAD loss inhibits cellular respiration, resulting in a decline of mitochondrial ATP production and potentially cell death (Kristian *et al.* 2011). NAD loss has been associated with an inability to focus (inattention), chronic fatigue, anxiety, and substance abuse (Castro-Marrero *et al.* 2015; Ieraci and Herrera 2006). Indeed, some recent reports suggest that extracellular NAD may be a candidate neurotransmitter, given its neuronal effects (Durnin *et al.* 2012). In the present study, NAD levels were significantly dampened following acute 5.0 mg/kg (high dose) MPH treatment. Previous studies have indicated that decreased or extremely low levels of NAD predispose both rats and humans to addiction, and that NAD and its precursor, nicotinamide administration protects against ethanol-related addiction and neuronal loss (Ieraci and Herrera 2006; Sauve 2008). This decrease of NAD following the high MPH dose, in the present study, could therefore potentially contribute to the addictive tendencies that may be associated with MPH (Wang *et al.* 2013; Zhu *et al.* 2011). However, considering that this effect was not seen following either acute or chronic 2.0 mg/kg treatment, it is possible that NAD loss may contribute to the addictive tendencies associated with the intake of high (e.g. $\geq$ 5.0 mg/kg) MPH doses (Morton and Stockton 2000).

6.4.5 MPH and the metabolism of membrane components

Impairments in membrane components such as NAA, and taurine are often reported in several psychiatric and behavioural conditions such as schizophrenia and ADHD, respectively (Maltezos *et al.* 2014; Paslakis *et al.* 2014). In the present study, we observed that NAA, an acetylated derivative of aspartate, was decreased following a single injection of both low (2.0 mg/kg) and high (5.0 mg/kg) doses of MPH but unaltered following chronic MPH treatment (Figure 6.2 and Table 6.1). Evidence suggests that NAA is involved in the regulation of neuron-glia signalling, myelin synthesis, and osmoregulation, as well as the turnover of glutamate and NAAG (Baslow 2003; Moffett *et al.* 2007). NAA is synthesised mostly in the mitochondria from aspartate and acetyl-CoA and transported into the neuronal cytoplasm and then eventually transferred to oligodendrocytes for degradation into acetate and aspartate (Baslow 2010). Interestingly, in the present study, the decreased NAA levels following acute MPH treatment coincided with increased levels of both acetate and aspartate (Figure 6.2 and Table 6.1). Possibly suggesting an increased degradation of NAA into these two metabolites (i.e. acetate and aspartate) in the cerebellum following acute MPH treatment. In support of the finding on NAA, other studies on young ADHD patients have also reported that acute MPH treatment decrease NAA levels in the cerebellum (Soliva *et al.* 2010) and striatum (Ben Amor 2014) relative to controls. In addition to the increased breakdown of NAA into acetate and aspartate, the MPH-induced decrease of NAA levels could also be related to impaired energy production, as some studies on rats have shown that NAA levels reduce when energy production (i.e. ATP levels) decreases (Bates *et al.* 1996; Clark 1998). Indeed, in the present study, acute 5.0 mg/kg MPH decreased NAD, which is crucial for the generation of ATP (as discussed above).

Taurine was moderately enhanced following chronic treatment with MPH, this metabolite has a neuromodulatory function as well as a range of important functions in neural tissues including osmoregulation, antioxidation, and neuroprotection (Saransaari and Oja 2000). The release of taurine is evoked in potentially cell damaging conditions such as hypoxia, ischemia, hypoglycemia, free radicals and oxidative stress in cerebellar granule neurons (Saransaari and Oja 2000). Excitotoxic concentrations of glutamate are also reported to potentiate taurine release in mice brain slices (Saransaari and Oja 2000). Therefore, the increased levels of taurine observed following chronic 2.0 mg/kg MPH treatment could be linked to the enhanced excitatory transmission (i.e. the increased glutamate level) observed after chronic MPH treatment. This increased taurine levels could constitute an important protective mechanism preventing (glutamatergic) excitation from reaching neurotoxic levels. Taken together, alterations of NAA and taurine by MPH suggest that the drug alters neuronal mitochondrial/membrane dynamics in the cerebellum.

6.4.6 Comparison of the left and right cerebellar hemispheres

Previous studies have linked ADHD with significantly less activation in the right hemisphere of several brain regions in both young and adult patients during attention and memory related tasks (Vance *et al.* 2007; Rubia *et al.* 1999). To determine if there was a differential action of MPH on the cerebellar hemispheres, we explored the action of the drug in the left and right cerebellar extracts following both acute and chronic MPH treatment. Here, neither the ^{1}H-NMR spectroscopic data or the HPLC-EC data on DA and DOPAC levels revealed any significant differences regarding the action of MPH on the range of metabolites and neurochemicals measured in the left versus the right side of the cerebellum.

6.5 Conclusion

To understand the mechanism of action of MPH, we examined cerebellar neurochemistry and protein marker expression for the monoaminergic system following acute and chronic MPH treatment. Overall, there was a dose- and treatment duration-dependent effect of the drug on cerebellar metabolites. In this regard, acute MPH treatment decreased glutamatergic transmission (i.e. glutamate and glutamine), as well as membrane and energy-related metabolites (e.g. NAA, NAD) but increased GABA, glycine, aspartate, acetate and hypoxanthine levels. However, these effects of acute MPH treatment were mostly more pronounced after the high 5.0 mg/kg dose as compared to the low 2.0 mg/kg dose. On the other hand, chronic 2.0 mg/kg MPH dose increased several metabolites including the AAAs (e.g. tyrosine and phenylalanine), glutamatergic transmitters, energy-related metabolites (e.g. glutamate and glutamine), as well as membrane and energy-related metabolites. In addition, acute MPH treatment significantly decreased VMAT2 levels in the cerebellum, while chronic treatment significantly upregulated the expression of the vesicular transporter. These findings indicate that both drug-dosage and treatment-duration are important factors associated with the action of MPH in the cerebellum.

CHAPTER 7

7 Effect of methylphenidate on neuroplasticity mediating proteins and their corresponding genes

7.1 Introduction

MPH is often prescribed to alleviate the cognitive deficits, impulsivity and hyperactivity symptoms associated with ADHD (Biederman and Faraone 2005). However, the last two decades has witnessed a surge in the prescription of the drug for children and adolescents with the condition, although the long-term effect of the drug still remains largely unknown. Consequently, there are growing concerns over potential long-term adverse effects of the drug, as well as its abuse liability (Swanson and Volkow 2003; Teter *et al.* 2006). Reports indicate that repeated exposure to psychostimulants such as MPH causes complex structural, molecular, and plastic modifications in the brain's reward circuitry (Berman *et al.* 2008; Haydon *et al.* 2009). It is well established that morphological changes of dendrites, particularly at the level of the dendritic spines lead to synaptogenesis (Kang *et al.* 2016). Dendritic spines are small protrusions from a neuron's dendrite and they are at the receiving end of an incoming presynaptic nerve terminal seeking to form a synapse with a postsynaptic target. Dendritic spines are crucial for synaptic strength and help to transmit signals to the cell body of the post synaptic neurons (Kasai *et al.* 2003). Interestingly, a recent study has shown that chronic exposure to MPH and cocaine alter dendritic spine density (Kim *et al.* 2009). Structural and functional changes in spines and synapses are known to be important processes mediating memory and learning, as well as drug-related behaviour (Soria Fregozo and Pérez Vega 2012; Kang *et al.* 2016). Although MPH has been shown to cause morphological changes of dendritic spines, the MPH-induced alterations in genes and proteins involved in plasticity-related pathways have not yet been fully determined.

Alterations of dendritic spine density are often related to the expression patterns of actin-associated genes (Sarowar and Grabrucker 2016). Thus, actin filaments form dendritic spines at the leading edge of cells from their precursors (i.e. filopodia) and the spines cover the surface of

several dendrites (see Figure 7.1), serving as the major contact sites for excitatory synapses in the cortex, striatum, hippocampus, cerebellum and other brain regions (Soria Fregozo and Pérez Vega 2012). Recent studies have increased our understanding of the proteins controlling the formation of dendritic spines, which includes the filament nucleating Arp2/3 complex and its Rho family of GTPase regulators, Cdc42 and Rac, which promote the formation of filopodia (Soria Fregozo and Pérez Vega 2012). Cdc42 and Rac regulate the formation of dendritic spine head by activating the Arp2/3 complex and by inhibiting acting depolymerisation. In addition, Cdc42 serves as one of the main signalling channels that promote branching of dendritic spine heads, while the activation of Arp2/3 polymerises actin and causes an extension of spine heads (Kang *et al.* 2016).

A major actin regulator that has attracted a lot of attention recently is the insulin receptor tyrosine kinase substrate protein 53 (IRSp53), which is also known as brain specific angiogenesis inhibitor 1 associated protein 2 (BAIAP2) (Yeh *et al.* 1996). IRSp53 is a multi-domain adaptor protein that regulates membrane and actin dynamics at actin-rich subcellular structures (see Figure 7.1), such as filopodia and lamellipodia (i.e. broad sheet-like projections containing a network of short branched filaments) (Govind *et al.* 2001; Krugmann *et al.* 2001; Yamagishi *et al.* 2004). This hypothesis is supported by findings demonstrating that IRSp53 localises to the tips of both filopodia and lamellipodia (Nakagawa *et al.* 2003). Although the functions of IRSp53 were initially mainly studied in non-neural cells, recent evidence supports neuronal functions, particularly in the regulation of actin dynamics at excitatory synapses and dendritic spines. Presently, IRSp53/BAIAP2 has been implicated in several brain disorders including ADHD (Liu *et al.* 2013; Ribasés *et al.* 2009), autism spectrum disorders (Levy *et al.* 2011; Toma *et al.* 2011), and schizophrenia (Purcell *et al.* 2014; Fromer *et al.* 2014). Importantly, studies on the

behavioural phenotypes of mice lacking IRSp53 suggest that such mice exhibit social and cognitive deficits, as well as hyperactivity, which are among the core symptoms of ADHD (Kim *et al.* 2009; Sawallisch *et al.* 2009; Chung *et al.* 2015). Thus, these behavioural phenotypes support the usage of IRSp53 knockout mouse models for ADHD and related disorders.

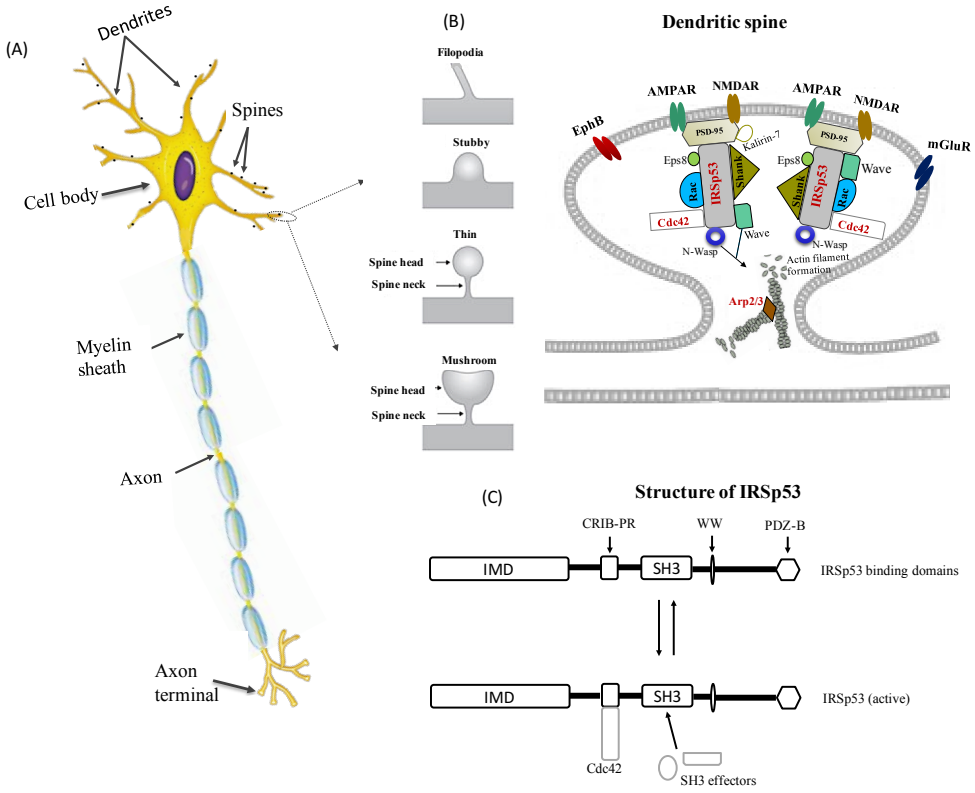

Figure 7.1: Structure and role of IRSp53 in the development of dendritic spines.
(A) Dendritic spines are small protrusions from a neuron's dendrite. (B) Spine formation is mediated by several genes and proteins including IRSp53, Cdc42, and Arp2/3 complex. (C) Binding of activated Cdc42 to the CRIB-PR domain opens up the IRSp53 protein, allowing the SH3 domain to bind downstream effectors, including N-WASP and WAVE2. Abbreviations: NMDAR, NMDA receptor; AMPAR, AMPA receptor; mGluR, metabotropic glutamate receptor; EphB, Ephrin B receptor; Eps8, epidermal growth factor receptor; IMD, IRSp53-MIM homology domain; CRIB-PR, Cdc42/Rac interactive binding-proline rich domain; SH3, Src homology 3 domain; WW, WW domain; and PDZ-B, PSD-95/Dlg/ZO-1 domain-binding motif (Adapted from Kang *et al.* 2016).

The IRSp53 protein has multiple domains for protein-protein interactions, including the CRIB-PR (Cdc42/Rac interactive binding-proline rich) domain, IMD (IRSp53-MIM homology domain;

also called the I-BAR), SH3 (Src homology 3) domain, and the WW domain, as well as the C-terminal PDZ-B (PSD-95/Dlg/ZO-1 domain-binding) motif (see Figure 7.1). Binding of activated Cdc42 to the CRIB-PR domain allows IRSp53 to promote filopodia formation, suggesting that IRSp53 is key for the Cdc42-mediated filopodia and dendritic spine formation (Govind *et al.* 2001; Krugmann *et al.* 2001; Yamagishi *et al.* 2004).

The *Arc* (activity-regulated cytoskeleton-associated) gene is also important for dendritic spine formation, synaptic plasticity, and cognition, as well as being induced following stress (Tzingounis and Nicoll 2006; Banerjee *et al.* 2009). More specifically, the expression of the *Arc* gene and its corresponding protein is induced when synapses are undergoing modification during learning (Steward *et al.* 2015). Our lab recently reported in an *in situ* hybridisation study that acute administration of both MPH and amphetamine significantly decrease *Arc* mRNA in the hippocampus and parietal cortex of young but not adult rats, suggesting that the immature brain respond to MPH differently compared to the adult brain (Banerjee *et al.* 2009).

In the present study, the effect of both acute and chronic MPH exposure to adolescent rats were investigated on the expression of actin dynamics- and plasticity-associated genes and proteins such as IRSp53, Cdc42, Arp2, and Arc. The study provides insights into the plastic changes that might occur in the adolescent brain following early exposure to the anti-ADHD drug, MPH.

7.1.1 Aims

This study was aimed at exploring the effect of MPH on neuroplasticity-related proteins and their corresponding genes some of which have been suggested to be involved in the pathophysiology of ADHD. The experiments tested the hypothesis that MPH treatment influences neuroplasticity-related proteins and that the MPH induced effect varies dependent on length or duration of

treatment. To support the protein findings after chronic MPH administration, expression of the corresponding genes were also measured, this only in selected brain regions previously connected with the symptoms of ADHD and its treatment such as: nucleus accumbens, frontal cortex, dorsal striatum and cerebellum. Specifically, the study evaluated the following:

- The region-specific and treatment duration-dependent effects of MPH treatment on the expression of actin-binding and cytoskeletal-associated proteins using Western blotting.
- The treatment and region-specific effects of MPH treatment on the expression of actin-binding and cytoskeletal-associated genes (i.e. mRNA) such as *Arc*, *IRSp53, Cdc42,* and *Arp2* using polymerase chain reaction.

7.2 Methods

7.2.1 Drug Treatment

For a detailed description of the MPH treatment procedures see Chapter 2, section 2.1. However, in brief, the animals involved in this study were assigned to two treatment groups i.e. acute and chronic groups. The animals in the acute group either received a single 1.0 ml/kg, i.p saline dose (control group; n=6) or 2.0 mg/kg, i.p MPH dose (drug-treated groups; n=6). On the other hand, the animals in the chronic group either received a twice-daily (9 am and 5 pm) 1.0 ml/kg saline dose or 2.0 mg/kg MPH dose for 15 days (n=6 rats/group). The last injection in both treatment groups was administered on postnatal day 40 and the brain regions removed 24 h after this last injection.

7.2.2 Measurements of acute and chronic MPH induced expression of proteins mediating synaptic plasticity

The Western blot technique was employed to examine the acute and chronic effects of MPH treatment on IRSp53/58 (1:2000; OriGene), Cdc42 (1:1000; Santa Cruz Biotechnology), Arp2 (1:1000; Santa Cruz Biotechnology), and Arc (1:1000; Santa Cruz Biotechnology), protein expression in the frontal cortex, parietal cortex, striatum, nucleus accumbens, hippocampus and cerebellum (as previously described in Chapter 2, section 2.5). The proteins were normalised to β-actin (1:2000; Santa Cruz Biotechnology). There were six animals assigned to each treatment group. The animals were sacrificed 24 h after the last drug treatment (post natal day 40) and the brains removed and snap-frozen in isopentane on dry ice and then stored at -80°C until analysis (as previously described in Chapter 2, section 2.1).

7.2.3 Measurements of the mRNA of genes mediating synaptic plasticity following chronic MPH administration

After chronic MPH treatment, the real-time quantitative PCR (RT-qPCR) technique was used to quantify the changes in mRNA levels of *IRSp53/58 (BAIAP2), Cdc42, Arp2,* and *Arc* genes (see Table 2.2). The primers for these genes were selected, designed and verified as previously described (Chapter 2, section 2.6). The animals were sacrificed 24 h after the last drug treatment and the brains removed and snap-frozen in isopentane on dry ice and then stored at -80°C until analysis (as previously described in Chapter 2, section 2.1.3). The RNA extraction procedure, the reverse transcription of RNA to complementary DNA (cDNA), and the RT-qPCR processes have been described in Chapter 2, section 2.6.

7.3 Results

7.3.1 Effect of MPH on the expression of Arc and its corresponding gene

Prolonged MPH exposure has been shown to induce neuroadaptive changes in the brain of young and adolescent rats (Kim *et al.* 2009; Allen *et al.* 2010). The majority of these previous studies are, however, performed following acute rather than repeated administrations of MPH. Hence the effects of both acute and chronic MPH exposure on the expression of the Arc protein (a dendritically located protein strongly associated with neuronal plasticity) were investigated in the present study. Using the Western blot technique, the Arc protein was reliably measured in the nucleus accumbens, frontal cortex, parietal cortex, hippocampus, dorsal striatum, and the cerebellum. The Arc protein showed clear evidence of 'drug' (MPH *vs.* saline) and 'duration' (acute *vs.* chronic) dependent differences in response to MPH treatment. In general, chronic MPH treatment elicited more pronounced effects (significant changes detected in 4/6 brain region) on the Arc protein compared to acute treatment (significant change in only 1/6 brain regions; see Figure 7.2). A similar trend was also clear for the other neuroplasticity-associated proteins measured in this study (Figures 7.4, 7.6 and 7.8). Overall, apart from the cerebellum that responded differently compared to the other regions in the cerebrum, Arc was generally upregulated following chronic treatment while acute treatment failed to have an effect. In contrast, in the cerebellum acute treatment upregulated Arc and down-regulated the protein after chronic treatment (Figure 7.2). The two-way ANOVA revealed a significant 'drug' x 'duration' interaction effect ($F_{(1,20)} = 16.4$, $p < 0.001$) in the parietal cortex, as well as significant effects of 'drug' ($F_{(1,20)} = 5.09$, $p = 0.036$) and 'duration' ($F_{(1,20)} = 18.1$, $p < 0.001$). The *post-hoc* analysis indicated increased cortical Arc protein density in the chronic MPH-treated samples compared to the controls ($p < 0.01$) (Figure 7.2). In the striatum and hippocampus, there were significant effect of 'drug' ($F_{(1,20)} = 4.324$, $p = 0.044$ and $F_{(1,20)} = 4.697$, $p = 0.045$ respectively). The *post-*

hoc analysis showed increased striatal and hippocampal Arc protein expression in the chronic MPH-treated samples compared to the controls. Moreover, in the cerebellum, there was a significant 'drug' x 'duration' interaction effect ($F_{(1,20)} = 10.9$, $p = 0.0033$) and a significant effect of 'drug' ($F_{(1,20)} = 6.9$, $p = 0.034$) and 'duration' ($F_{(1,20)} = 12.9$, $p = 0.0021$). The pairwise analysis showed increased Arc expression in the cerebellum after acute treatment ($p < 0.05$) but decreased expression after chronic MPH treatment ($p < 0.05$) compared to controls (Figure 7.2).

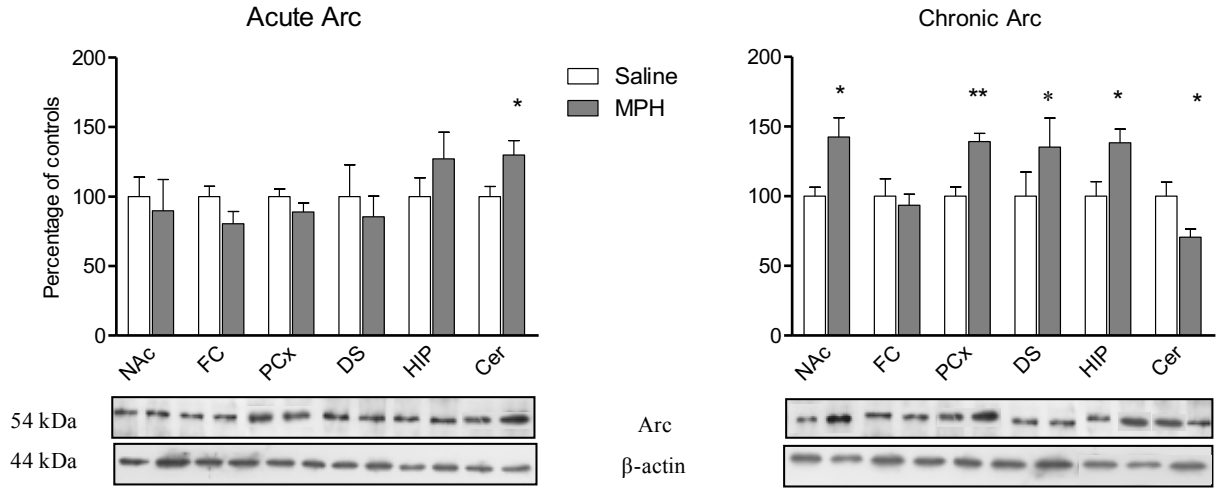

Figure 7.2: Effect of MPH on Arc protein density.
This was measured following (A) Acute, and (B) Chronic 2.0 mg/kg MPH administration. Bars represent percentage ± SEM (n=6 rats/group). *$p < 0.05$, **$p < 0.01$, indicates significant difference as compared to matched saline-treated control groups. Abbreviations: NAc, nucleus accumbens; FC, frontal cortex; PCx, parietal cortex; DS, dorsal striatum; HIP, hippocampus; Cer, cerebellum.

The *Arc* mRNA was measured following chronic MPH administration in the nucleus accumbens, frontal cortex, striatum and cerebellum. Here, similar to the Arc protein, chronic 2.0 mg/kg MPH treatment induced a significant up-regulation of *Arc* mRNA in the striatum ($t_{10} = 2.14$, $p = 0.039$; Student's t-test) but not in any of the other examined brain regions including those that demonstrated increased Arc protein levels after chronic MPH administration (Figure 7.3).

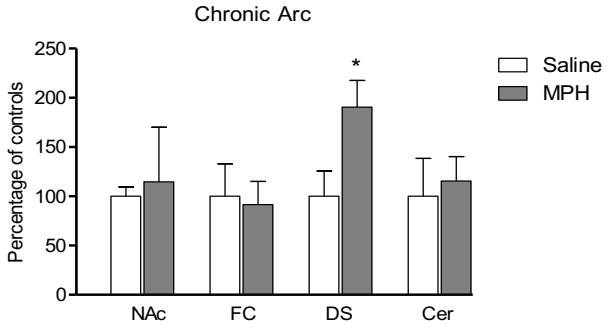

Figure 7.3: Effect of MPH on *Arc* mRNA density.
This was measured following chronic MPH administration. Bars represent mean values ± SEM (n=6 rats/group), data was normalised to both β-actin and GAPDH reference genes. *$p < 0.05$ indicates significant difference as compared to matched saline-treated control groups (Students t-test). Abbreviation: NAc, nucleus accumbens; FC, frontal cortex; DS, striatum; Cer, cerebellum.

7.3.2 Effect of MPH on IRSP53/58 protein and mRNA density

IRSp53/58 (also known BAIAP2) has been implicated in ADHD (Liu *et al.* 2013; Ribasés *et al.* 2009), and it induces extensive actin-containing filopodia and dendritic spine formation, as well as neuronal proliferation (Soria Fregozo and Pérez Vega 2012). Here, the effect of MPH treatment on the expression of IRSp53/58 protein (acute and chronic), as well as the mRNA levels (chronic only) for its corresponding gene was examined. Similar to the trend found regarding the Arc protein, MPH had more pronounced effect on the IRSp53/58 following chronic treatment (Figure 7.4). In this regard, while no significant changes were observed following acute MPH treatment, the two-way ANOVA showed that, in the striatum, there was a significant 'drug' x 'duration' interaction effect ($F_{(1,20)} = 6.36$, $p = 0.021$), as well as a significant effect of both 'drug' ($F_{(1,20)} = 10.6$, $p = 0.0045$) and 'duration' ($F_{(1,20)} = 12.3$, $p = 0.0029$). Further, the Bonferroni *post-hoc* analysis showed increased protein expression in the striatal samples of the MPH-treated rats compared to the corresponding controls ($p < 0.05$) (Figure 7.4). In contrast, in the parietal cortex and cerebellum, chronic MPH induced significant reductions of the IRSp53/58 protein. In the parietal cortex, there was a significant 'drug' x 'duration' interaction effect ($F_{(1,20)} = 6.02$, $p = 0.024$) and a significant effect of 'drug' ($F_{(1,20)} = 7.02$, $p = 0.012$) 'duration' ($F_{(1,20)} =$

6.02, $p = 0.024$). The *post-hoc* analysis showed significantly decreased IRSp53/58 protein in the samples from chronic MPH-treated rats compared to the controls ($p < 0.01$). In comparison, in the cerebellum, there was only a significant effect of 'drug' ($F_{(1,20)} = 5.32$, $p = 0.035$), with the levels being decreased in the chronic MPH-treated sample compared to the controls (Figure 7.4).

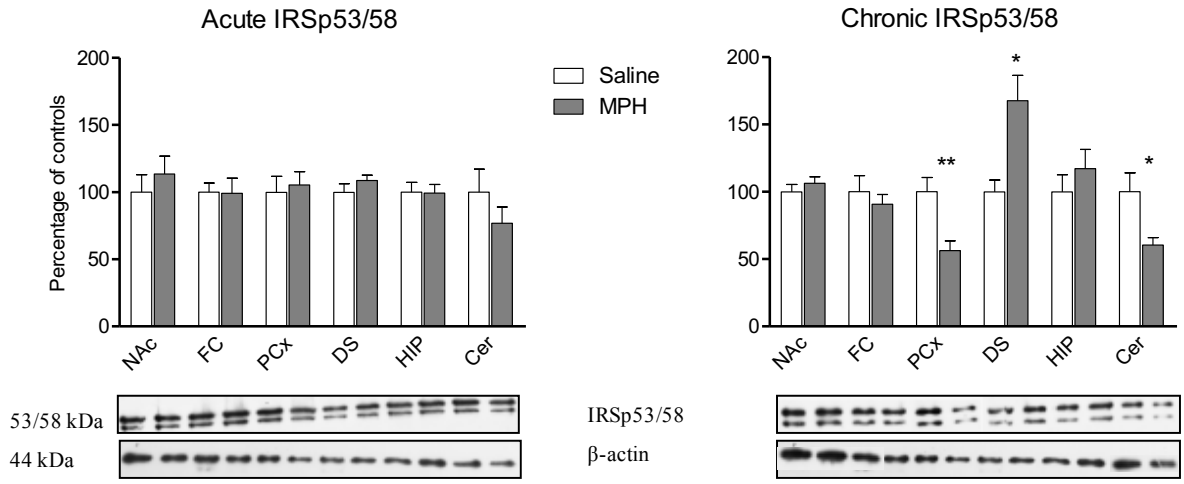

Figure 7.4: Effect of MPH on IRSp53/58 protein density.
This was measured following (A) Acute, and (B) Chronic 2.0 mg/kg MPH administration. Bars represent percentage ± SEM (n=6 rats/group). *$p < 0.05$, **$p < 0.01$ indicates significant difference as compared to matched saline-treated control groups. Abbreviations: NAc, nucleus accumbens; FC, frontal cortex; PCx, parietal cortex; DS, dorsal striatum; HIP, hippocampus; Cer, cerebellum.

The MPH induced up-regulation of IRSp53/58 protein following chronic treatment coincided with increased striatal mRNA levels of the corresponding gene (treatment: $t_{10} = 2.6$, $p = 0.026$) (Figure 7.5). The measured reduction of the IRSp53/58 protein in the cerebellum was, however, not reflected by changes in mRNA levels (Figure 7.5).

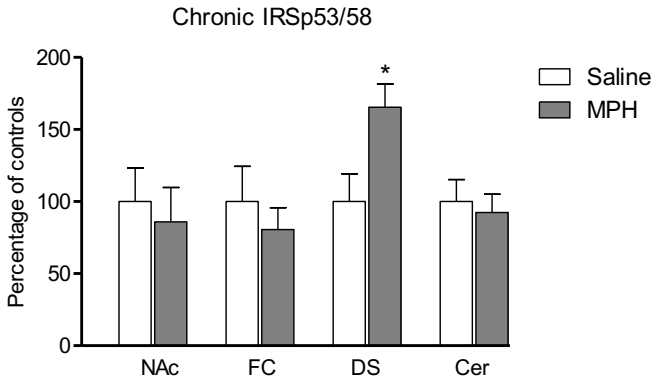

Figure 7.5: Effect of MPH on *IRSp53/58* mRNA density.
This was measured following chronic MPH administration. Bars represent mean values ± SEM (n=6 rats/group), data was normalised to both β-actin and GAPDH reference genes. *$p < 0.05$ indicates significant difference as compared to matched saline-treated control groups (Students t-test). Abbreviation: NAc, nucleus accumbens; FC, frontal cortex; DS, striatum; Cer, cerebellum.

7.3.3 Effect of MPH on Cdc42 protein and mRNA density

The induction of cell protrusions by IRSp53/58 is known to be Cdc42 (and Arp2) dependent (Kang *et al.* 2016). Here, the effects of MPH on Cdc42 protein (acute and chronic) and mRNA levels (chronic only) were examined. In comparison to the Arc and IRSp53/58 proteins, MPH had a less pronounced effect on the Cdc42 protein (Figure 7.6). In the acute group, MPH did not significantly alter the Cdc42 protein expression in any of the brain regions investigated. However, the two-way ANOVA showed a significant effect of 'drug' in the nucleus accumbens ($F_{(1,20)} = 6.82$, $p = 0.018$) but not 'duration'. Specifically, the *post-hoc* analysis indicated that Cdc42 was significantly elevated in the accumbens of chronic MPH-treated rats compared to the controls ($p < 0.05$).

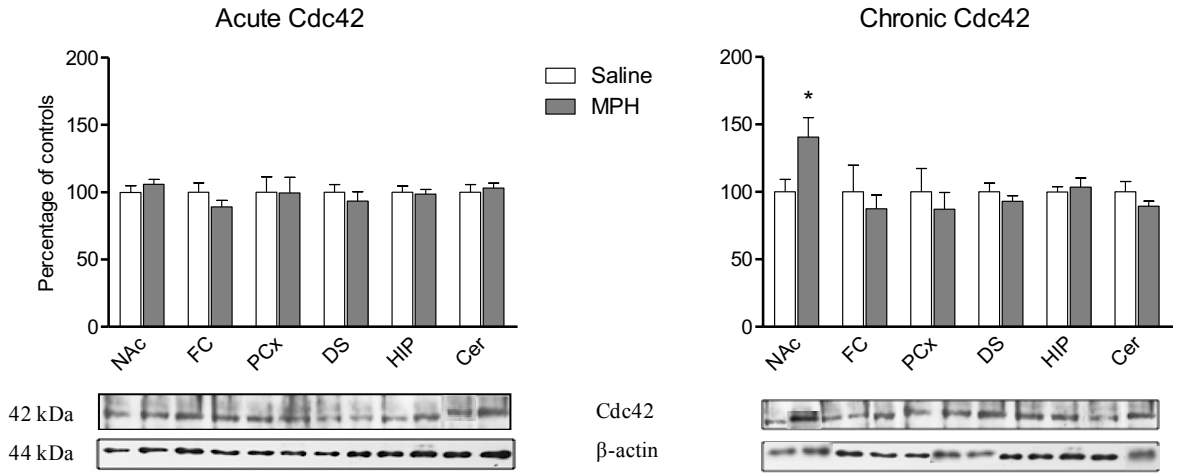

Figure 7.6: Effect of MPH on Cdc42 protein density.
This was measured following (A) Acute, and (B) Chronic 2.0 mg/kg MPH administration. Bars represent percentage ± SEM (n=6 rats/group). $^{*}P < 0.05$ indicates significant difference as compared to matched saline-treated control groups. Abbreviations: NAc, nucleus accumbens; FC, frontal cortex; PCx, parietal cortex; DS, dorsal striatum; HIP, hippocampus; Cer, cerebellum.

The expression of *Cdc42* mRNA levels was also measured in brain samples from chronically treated rats and their controls. The results indicated that chronic MPH treatment does not significantly alter mRNA levels for *Cdc42* in any of the brain regions investigated. There was, however, a trend towards an increased *Cdc42* expression ($p < 0.1$) in both the nucleus accumbens and the frontal cortex, while a decrease of the mRNA was observed in the cerebellum ($p < 0.086$), albeit non-significant (Figure 7.6).

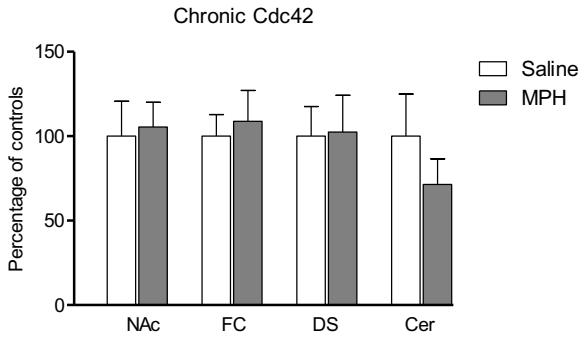

Figure 7.7: Effect of MPH on *Cdc42* mRNA expression.
This was measured following chronic MPH administration. Bars represent mean values ± SEM (n=6 rats/group), data was normalised to both β-actin and GAPDH reference genes. Abbreviation: NAc, nucleus accumbens; FC, frontal cortex; DS, striatum; Cer, cerebellum.

As previously mentioned, the induction of cell protrusions by IRSp53/58 is mediated by both Cdc42 and Arp2 (Kang *et al.* 2016). Thus, the effect of MPH treatment on Arp2 protein expression (acute and chronic) and its corresponding mRNA levels (chronic only) was also examined. The effect of both acute and chronic MPH treatment on Arp2 protein levels is illustrated in Figure 7.8. The two-way ANOVA showed a significant effect of 'drug' ($F_{(1,20)}$ = 4.77, p = 0.043) on Arp2 protein expression in the hippocampus, with the *post-hoc* analysis indicating an increased expression in the acute MPH-treated samples compared to the controls (p < 0.05). Similar to the Cdc42 protein, a significant increase of the Arp2 protein was detected in the nucleus accumbens of the chronic MPH-treated samples compared to the controls (p < 0.05). No significant effect of MPH was, however, observed in the other examined brain regions (Figure 7.8).

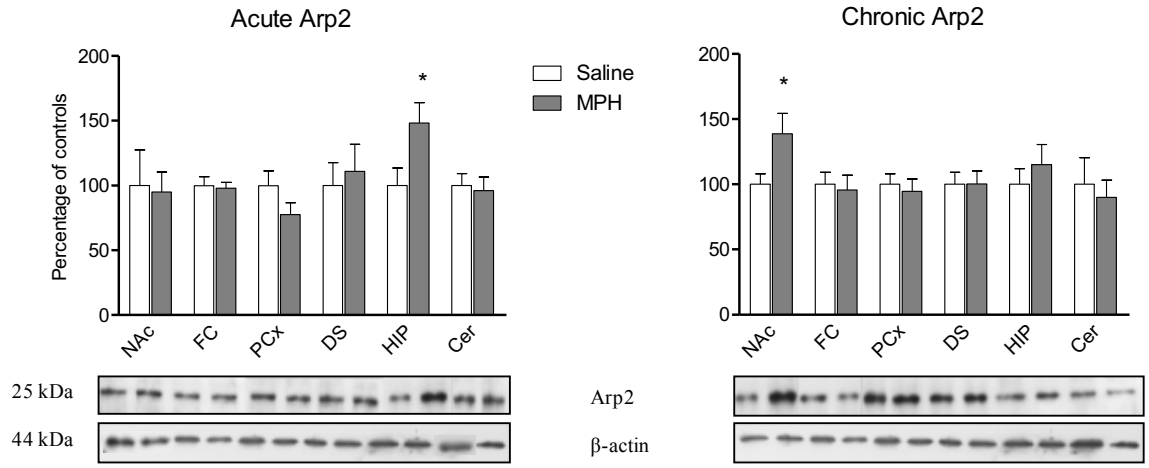

Figure 7.8: Effect of MPH on Arp2 protein density.
This was measured following (A) Acute, and (B) Chronic 2.0 mg/kg MPH administration. Bars represent percentage ± SEM (n=6 rats/group). *$p < 0.05$ indicates significant difference as compared to matched saline-treated control groups. Abbreviations: NAc, nucleus accumbens; FC, frontal cortex; PCx, parietal cortex; DS, dorsal striatum; HIP, hippocampus; Cer, cerebellum.

The analysis of Arp2 mRNA following chronic MPH treatment demonstrated that the enhanced Arp2 protein levels coincided with increased gene expression in the nucleus accumbens ($t_{10} = 2.3$, $p = 0.047$). Similar to the Arp2 protein data, chronic MPH treatment failed to alter mRNA levels for Arp2 in the other brain regions measured (Figure 7.9).

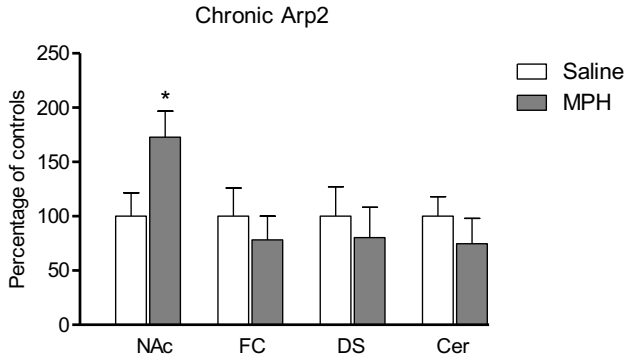

Figure 7.9: Effect of MPH on *Arp2* mRNA expression.
This was measured following chronic MPH administration. Bars represent mean values ± SEM (n=6 rats/group), data was normalised to both β-actin and GAPDH reference genes. *$p < 0.05$ indicates significant difference as compared to matched saline-treated control groups (Students t-test). Abbreviation: NAc, nucleus accumbens; FC, frontal cortex; DS, striatum; Cer, cerebellum.

7.4 Discussion

7.4.1 Principal findings

Prolonged exposure of the maturing brain to psychostimulants such as methylphenidate and amphetamine is known to induce the expression of immediate early genes (IEGs) including *Arc* that are known to be implicated in neuroplastic changes such as dendritic elongation and altered spine density in the immature and adult brain (Kim *et al.* 2009; Allen *et al.* 2010; Chase *et al.* 2007; Banerjee *et al.* 2009). However, to the best of our knowledge, this is the first study that examines MPH-induced changes of the Arc protein and its mRNA simultaneously with proteins and their corresponding genes that are implicated in the insulin receptor (IRSp53/58) signalling pathway. Importantly, the IRSp53/58 protein is a mediator in the formation of both filopodia and dendritic spines (Kang *et al.* 2016).

Here, we report that chronic exposure of adolescent rats to MPH results in significant up-regulation of the Arc mRNA and protein in several areas of the brain some of which are implicated in the symptoms of ADHD (e.g. nucleus accumbens and striatum). The density of *Arc* mRNA did not fully reflect the Arc protein changes indicating that the levels of protein and gene expression, most likely due to different turnover rates, do not always correspond (Vogel and Marcotte 2012; Greenbaum *et al.* 2003). The cerebellum is an area of the brain that has been recently shown to have a proven role in a number of neuropsychiatric and behavioural disorders including ADHD (Ivanov *et al.* 2014). Interestingly, in the present study, this part of the brain reacted to MPH in a very different way in comparison to most parts of the cerebrum. For instance, in the cerebellum, MPH increased Arc expression acutely but chronic treatment decreased the expression of this protein. This suggests that the cerebellum, although altered

differently compared to the regions of the cerebrum, is prone to MPH-induced neuroplastic changes in the adolescent (or maturing) brain.

Similar to the Arc expression, chronic but not acute MPH administration to adolescent rats altered IRSp53/58 protein expression in several brain regions. Notably, chronic MPH increased IRSp53/58 expression in the striatum, a change that coincided with enhanced mRNA density for this protein. In contrast, chronic MPH administration reduced IRSp53/58 protein expression in the parietal cortex and the cerebellum, in the latter region this effect was not reflected in the corresponding gene, as the IRSp53/58 gene remained unaltered in the cerebellum following chronic treatment. In addition, we report that chronic but not acute MPH treatment significantly increased Cdc42 and Arp2 protein expression in the nucleus accumbens, for both Arp2 and Cdc42, this effect coincided with elevated levels of the corresponding mRNA for Arp2 but not Cdc42 (see Figures 7.6-7.9).

7.4.2 Effect of MPH on the expression of Arc

In the present study, we report that chronic MPH treatment increased *Arc* mRNA in the striatum and Arc protein in the nucleus accumbens, parietal cortex, and hippocampus of adolescent rats. Interestingly, while acute MPH increased the expression of cerebellar Arc protein, chronic MPH decreased this protein in the cerebellum. While the mechanism underlying the contrasting findings in the cerebellum remains to be elucidated, MPH-induced enhancement of *Arc* mRNA and protein expression in brain regions such as striatum, cortex (parietal), hippocampus and cerebellum is consistent with some previous reports. For instance, a previous study reported up-regulation of striatal and cortical *Arc* mRNA and protein expression in juvenile rats following both systemic and oral MPH administration (Chase *et al.* 2007). Similarly, a previous study from

our laboratory also reported that acute MPH and amphetamine both increased *Arc* mRNA in the striatum of juvenile and adult rats (Banerjee *et al.* 2009).

It is possible that the MPH-induced changes in the mRNA and protein expression of Arc are related to the levels of glutamate and lactate (see Chapters 4 and 5). In support of this hypothesis, glutamate stimulates *Arc* mRNA expression via NMDA receptor mediated Ca^{2+} influx (Bramham *et al.* 2010). Indeed, this thesis demonstrates that MPH (acute and/or chronic) increases glutamate and its precursor (i.e. glutamine) levels in the hippocampus, striatum, and frontal cortex and cerebellum (see Chapters 4, 5 and 6). Interestingly, lactate has also been shown to increase the expression of the *Arc* gene by acting as a positive modulator of the already activated (by glutamate or glycine) NMDA receptor (Yang *et al.* 2014). Like glutamate, lactate was also increased by MPH (albeit more pronounced after the chronic treatment) in this thesis in the hippocampus, striatum, frontal cortex and cerebellum (see Chapters 4, 5, and 6). Therefore, by increasing glutamate/glutamine or lactate levels in these brain regions, MPH might indirectly modulate the expression of Arc.

Arc gene expression is also well known to be triggered by D1 receptor-induced increase in cAMP levels, and we have shown in this thesis that D1 receptor is enhanced in brain regions such as the nucleus accumbens and parietal cortex (i.e. two regions that also have increased *Arc* expression) following chronic MPH treatment (see Chapter 3). Arc is believed to regulate dendritic spines through actin remodelling, thus mice lacking the *Arc* gene have decreased dendritic spine density (Peebles *et al.* 2010). The *Arc* mRNA, which is induced by an influx of Ca^{2+} through NMDA receptors and voltage-gated Ca^{2+} channels, is trafficked to dendrites and then synthesised at the synaptic sites (Korb and Finkbeiner 2011). In hippocampal neurons, Arc over-expression enhances spine density *in vitro* and a disruption of Arc formation decreases spine density *in vivo*

(Peebles *et al.* 2010). The Arc protein is also known to increase the proportion of the so-called "learning spines" (thin spines) that are more plastic, while it decreases the proportion of the more stable stubby spines (Peebles *et al.* 2010). Therefore, the increased Arc protein expression following the chronic MPH treatment, particularly in the hippocampus may be essential for learning. There are further indications that the Arc protein is essential for modifying cellular responses to activity and therefore crucial for forming new memories and forgetting old ones (Peebles *et al.* 2010). It is also possible that Arc plays important roles in multiple forms of synaptic plasticity, including psychostimulant (MPH and amphetamine)-induced behavioural sensitisation and neurobehavioural adaptations (Koob and Volkow 2010; Chase *et al.* 2007; Korb and Finkbeiner 2011; Moro *et al.* 2007; Bramham *et al.* 2010).

7.4.3 Effect of MPH on the expression of IRSp53, Cdc42, and Arp2

IRSp53/58 is a core component of excitatory (e.g. glutamatergic) synapses (Abbott *et al.* 1999) and it interacts with the membrane bound Cdc42 via the CRIB-PR domain (see Figure 7.1). This allows the SH3 domain of IRSp53/58 to bind its effectors, which mostly converge onto the Arp2/3 complex (Kang *et al.* 2016). The Arp2/3 complex has important cellular functions including initiating the polymerisation of new actin filaments in both presynaptic terminals and postsynaptic spines where they interact with synaptic vesicular movements and the dynamics of dendritic spines respectively (Kim and Lisman 1999).

In this study, we report that while acute MPH treatment had no significant effect on IRSp53/58 protein, chronic treatment increased both the mRNA and protein expression in the dorsal striatum but decreased the protein in the parietal cortex and cerebellum (Figures 7.4 and 7.5). Reports indicate that increasing IRSp53/58 expression in most neuronal cell types induces extensive actin-containing cell protrusions, increased filopodia formation, and dendritic branching and

spine density in a Cdc42 dependent manner as outlined in Figure 7.1 (Krugmann *et al.* 2001; Choi *et al.* 2005). Indeed, Cdc42-IRSp53/58 interaction is known to be crucial for filopodia (a precursor of dendritic spines in neurons) formation and extension (Babitt *et al.* 2005; Oh *et al.* 2013). In this study, we found that chronic MPH treatment significantly increased Cdc42 protein expression in the nucleus accumbens (Figure 7.6). When Cdc42 is expressed in higher concentrations, it promotes F-actin polymerisation, a process that is essential for a microspike (i.e. filopodia) to become long enough to develop into a mature spine (Soria Fregozo and Pérez Vega 2012). Therefore, the observed increase of IRSp53/58 and Cdc42 in the striatum and nucleus accumbens respectively following chronic MPH treatment raises the possibility that prolonged MPH exposure enhances dendritic spine density in these brain areas. In support of this hypothesis, an immunohistochemistry study has shown that chronic exposure to MPH and another psychostimulant (i.e. cocaine) increased dendritic spine density in medium spiny neurons (i.e. GABAergic neurons) in the nucleus accumbens and striatum, respectively (Kim *et al.* 2009). Dendritic spine density or spine plasticity is implicated in learning, long-term memory and motivation (Roberts *et al.* 2010; Xu *et al.* 2009). In particular, the growth of new dendritic spines is thought to partly mediate long-term memory (Roberts *et al.* 2010; Xu *et al.* 2009).

As previously mentioned, the effects of IRSp53/58 and Cdc42 converge on the Arp2/3 complex. Interestingly, in line with the findings on Cdc42, the present study also shows that chronic MPH treatment significantly increased the expression of both the mRNA and protein of Arp2 in the nucleus accumbens, while the acute treatment elevated the expression in the hippocampus (Figures 7.8 and 7.9). Indeed, as mentioned earlier, an activation of the Arp2/3 complex induces polymerisation of new actin filaments that can cause extension of dendritic spine heads (Higgs and Pollard 2001). The hippocampus and nucleus accumbens are key areas in learning/memory

and drug-induced behaviours (Kasai *et al.* 2003). An overexpression of these plasticity-associated proteins in these brain regions might therefore prove critical for memory and learning. However, without microscopic analyses, it is difficult to establish with certainty that increased Arp2, Cdc42 and Arc in the nucleus accumbens may necessarily be accompanied by an increased number of dendritic spines and hence more synapses. Nevertheless, previous electron microscopic analyses have revealed that increases in protein expression and dendritic spines produced by several learning experiences are accompanied by increases in the number of synapses per neuron (Robinson and Kolb 2004). An increased Arp2 expression in the nucleus accumbens as shown in this study fits well with previous studies demonstrating that psychostimulants, such as amphetamine (a drug which similar to MPH increases extracellular levels of DA in the nucleus accumbens) elevates spine density and dendritic branching (Li *et al.* 2003). Further, this effect of amphetamine was shown to be confined to the dendrites of medium spiny neurons in the nucleus accumbens, a primary locus for dopaminergic and glutamatergic inputs into these cells (Robinson and Kolb 2004; Singer *et al.* 2009).

In contrast to the increased IRSp53/58 density in the striatum, chronic MPH treatment decreased this protein in the parietal cortex and cerebellum in the present study (Figure 7.4). Interestingly, previous findings indicate that rodents lacking or having decreased IRSp53/58 display enhanced NMDA receptor function, which is accompanied by social and cognitive deficits and hyperactivity (Kim *et al.* 2009; Sawallisch *et al.* 2009; Chung *et al.* 2015). This suggests that in addition to its potential to dampen neurite growth and spine density, decreased (or lack of) IRSp53/58 could have adverse effects on learning and memory behaviours (Kim *et al.* 2009), particularly in the cortical and cerebellar areas that are known to be involved in cognition and motor activity. The cerebellum is interconnected with aspects of cerebral networks involved in

cognition, hence it sends and receives inputs to and from the cerebral areas making it an important regulator of cognition (Schmahmann and Caplan 2006; Buckner 2013).

7.5 Conclusion

The Arc protein and members of the insulin receptor (IRSp53/58) signalling pathway are all important in the regulation of actin filament, dendritic spine formation, and plastic changes that mediate memory, learning and drug-related behaviours in the maturing brain. In this study, we demonstrate that MPH alters the expression of Arc and other proteins involved in the IRSp53/58 signalling pathway (i.e. Cdc42 and Arp2), as well as their corresponding mRNAs in the adolescent rat brain. Overall, the effects were more pronounced after chronic MPH treatment indicating that long-term treatment of the widely prescribed anti-ADHD drug, MPH, causes neuroadaptive changes in the maturing brain. This study investigated simultaneously the action of MPH in specific regions of the cerebrum, in addition to the cerebellum, a brain region suggested to be involved in the symptoms of ADHD but rarely explored regarding the action of psychostimulants. Interestingly, we found that MPH altered the cerebellum differently compared to most regions of the cerebrum including the action of the drug on the Arc protein, emphasising the distinct roles of these two large brain areas. In the cerebrum, particularly marked changes by chronic MPH were detected in the striatum and nucleus accumbens that are known targets for MPH. These marked changes included: up-regulation of Arc (protein and mRNA), IRSp53/58 (protein and mRNA), Cdc42 (protein only) and Arp2 (protein and mRNA). No significant MPH induced changes of these proteins or their corresponding genes were recorded in frontal cortex (a region that has an increased noradrenergic function), possibly suggesting that NA does not mediate these neuroplasticity-related changes. An increase of these proteins in the striatum and nucleus accumbens could have implications in the formation of new dendritic spines in these

brain regions, and may also have implications on memory, learning, and drug-related behaviour (i.e. addiction). The functional consequence of the contrasting reduction of Arc and IRSp53/58 deserves further investigations.

CHAPTER 8

8 Concluding remarks and future perspectives

The overall aim of this study was to examine the mechanisms of action of the commonly prescribed anti-ADHD drug MPH and the long-term consequences, if any, of chronic exposure to this drug on the maturing brain. It is worth noting that global consumption of MPH has increased rapidly (~269% between 1995 and 2006), with the estimates indicating that the amount of MPH consumed even exceeds the prescriptions of the drug per year (Gahr *et al.* 2014; Dietz *et al.* 2013). Additional reports indicate that the drug is becoming increasingly popular among young people and students who use it as either a performance enhancer or study aid (Gahr *et al.* 2014; Dietz *et al.* 2013; Lakhan and Kirchgessner 2012; Swanson and Volkow 2003). This thesis has hopefully made a significant contribution to our understanding of the mechanisms of action of this drug in the adolescent brain.

In general, abnormalities in monoaminergic systems such as the dopaminergic and noradrenergic systems, as well as alterations in metabolic pathways (including glutamatergic and GABAergic pathways) within the cortico-striato-cerebellar circuitry have been implicated in the pathophysiology of ADHD (Del Campo *et al.* 2011; Perlov *et al.* 2007; Volkow *et al.* 1998) and in the mechanism of several anti-ADHD drugs including MPH (Volkow *et al.* 1998; Del Campo *et al.* 2011). Dopaminergic function is believed to be impaired in ADHD due to an abnormal cortical and striatal DAT expression (Dougherty *et al.* 1999; Spencer *et al.* 2005). In addition, several studies have suggested that hemispheric abnormalities contribute to ADHD pathology. Indeed, observations from several neuroanatomical studies have suggested that ADHD may be associated with a right hemisphere dysfunction (Castellanos *et al.* 1996; Makris *et al.* 2007; Rubia *et al.* 1999). Therefore, to explore the possible existence of a lateralised MPH action, we investigated the effect of the drug on dopaminergic and metabolic markers in the left and right hemispheres of brain regions within the cortico-striato-cerebellar circuitry. Moreover, to study

the effect of MPH on the developing brain, we tested two MPH doses (2.0 and 5.0 mg/kg, i.p.). Both of these doses in different settings have previously been shown to achieve clinically relevant plasma concentrations (8-40 ng/ml) in rats, and have not been shown to cause any visible signs of acute toxicity (Balcioglu *et al.* 2009; Kuczenski and Segal 2002; Kuczenski and Segal 2005).

A major finding from Chapter 3 of this thesis is the significant up-regulation of the dopamine transporter (i.e. DAT) in the striatum and nucleus accumbens, particularly after chronic MPH administration. So far, findings on DAT expression in studies on ADHD patients have been inconsistent, with some initial studies suggesting upregulated striatal DAT density in people diagnosed with ADHD (Dougherty *et al.* 1999; Spencer *et al.* 2007), and others reporting either no significant changes or significant decreases of the transporter (Volkow *et al.* 2009; Volkow *et al.* 2007a; Volkow *et al.* 2007b). The data reported in this thesis suggest that it is chronic MPH exposure that upregulate DAT density in the striatum and accumbens. This finding is consistent with recent clinical study that also showed that chronic MPH treatment elevates DAT density significantly in the nucleus accumbens (Wang *et al.* 2013). Interestingly, this thesis shows that not only DAT density is increased by chronic MPH treatment in the accumbens, as noradrenaline transporter (i.e. NET) density, which is also targeted by MPH, was significantly upregulated in the nucleus accumbens, as well as in the parietal cortex, an effect which to our knowledge, is reported for the first time in this thesis. It is known that the levels of DAT (and perhaps NET) expressed on neuronal membranes are regulated by the extracellular concentrations of DA (and/or NA), with DAT levels decreasing when extracellular DA levels are low and increasing when extracellular DA levels are high (Wang *et al.* 2013). From the findings reported in this study and the evidence in literature, the increased DAT and NET densities in the nucleus

accumbens, striatum and parietal cortex following prolonged exposure to MPH, appear to be consistent with an adaptational response in order to compensate for the prolonged increases in extracellular DA (and/or NA). Such upregulation of DAT and NET levels following chronic MPH treatment may limit the long-term efficacy of the drug and could increase drug-seeking behaviour as larger doses of the drug may be required by individuals taking the medication to obtain clinical efficacy (Hazell 2011; Wang *et al.* 2013).

Another significant finding from Chapter 3 is that MPH increases whole tissue levels of DA in the frontal cortex, as well as both whole tissue and extracellular levels of DA in the striatum. The increased whole tissue levels of DA in the frontal cortex, following both acute and chronic MPH administration, indicates enhanced vesicular storage of DA induced by the drug, and together with DAT blockade will contribute to the known effect of MPH, which has to do with the increase of extracellular levels of DA (Berridge *et al.* 2006; Kuczenski and Segal 2002). Such enhanced concentration of extracellular DA will increase stimulation of D1 receptors in the frontal cortex and ultimately improve working memory and help to sustain attention for longer periods. This finding in the frontal cortex could be of particular importance as previous functional imaging studies have found an under-activation of several areas of the cortex including the frontal and parietal areas in ADHD patients during tasks related to attention (Dickstein *et al.* 2006; Rubia *et al.* 1999; Vance *et al.* 2007). This under-activation in ADHD is suggested to be more prominent in the right cortex, based on this ADHD has been tagged as a right hemisphere disorder (Vance *et al.* 2007; Rubia *et al.* 1999). Despite this, our findings indicate that the MPH-induced upregulation of DA in the frontal cortex was more pronounced in the left frontal cortex, a finding that has not previously been reported. Further, following chronic administration, the MPH-induced increase of whole tissue DA levels in the frontal cortex, is unlikely to be driven by

enhanced expression of the rate-limiting enzyme for DA synthesis (i.e. TH), as the expression of this protein remained unaltered in the frontal cortex. Given that the expression of the vesicular protein VMAT2 was increased by chronic MPH in the frontal cortex, increased tissue levels of DA in this brain region is probably a reflection of increased DA vesicular storage capacity. In a similar vein, the increased whole tissue and extracellular DA levels in the striatum were more pronounced in the left side, further reinforcing the hypothesis that MPH exerts more pronounced effects on monoaminergic markers in the left side of the adolescent rat brain. Consistent with the present findings, a previous clinical study also showed that MPH may have a more pronounced effect on neurochemicals in the left frontal cortex and left striatum compared to the corresponding right sides of these brain areas (Ben Amor 2014). In contrast to the importance of the right frontal cortex in ADHD, a dysfunction of the left striatum is considered to be a core abnormality in ADHD, as some studies have reported that individuals suffering from left striatal lesions have deficits in attention and executive function (Vaidya *et al.* 2005; Benke *et al.* 2003). Therefore, an MPH-induced increase of whole tissue and extracellular DA levels in the left striatum may be critical to the normalisation of striatal functions in those suffering from ADHD.

Results from Chapters 4 and 5 depict, perhaps, the most novel aspect of the work presented in this thesis. The findings in Chapters 4 and 5 show that the MPH alters the LNAAs, tyrosine and phenylalanine, as well as several metabolic pathways in the cerebrum. Given that the MPH-induced increase of whole tissue and extracellular DA levels in the striatum and frontal cortex reported in Chapter 3 of this thesis did not correspond with increased TH densities, we sought to determine alternative mechanisms by which MPH elevates DA levels in these brain regions. Currently, increased extracellular DA levels (in the frontal cortex and striatum as well as other brain regions) following MPH administration is attributed to the blockade of DAT (and NET) by

MPH and very few studies, if any, have examined other possible mechanisms that may mediate this effect of MPH on DA levels. The data presented in this thesis indicate that along with blocking DAT and NET, MPH may increase DA and NA by increasing the levels of tyrosine and phenylalanine (that act as substrates for catecholamine synthesis) in the cerebrum. This finding resulted in our novel hypothesis that MPH may alleviate ADHD symptoms in two ways: (1) by a blockade of DAT and NET, and (2) by enhancing the brain pool of tyrosine and phenylalanine. To further confirm this finding and to also determine in which specific cerebral areas that MPH alters these LNAAs, we examined the effects of the drug in three brain areas, including the frontal cortex, hippocampus and striatum in Chapter 5. The data suggested that indeed MPH increases the brain pool of tyrosine and phenylalanine and that the effect was restricted to the frontal cortex and the hippocampus but not the striatum of adolescent rats (region-specific effect) after either acute or chronic drug treatment. With the finding on these LNAAs confirmed, there was still the question of the source and mechanism by which MPH increases tyrosine and phenylalanine in the frontal cortex and the hippocampus. Thus, we further examined the the effect of MPH on plasma levels (Chapter 5). In this regard, this thesis reveals that chronic but not acute MPH treatment (treatment duration-dependent effect) alters the balance of these LNAAs in the plasma, possibly favouring the competitive uptake of plasma tyrosine and phenylalanine and their subsequent transport across the blood-brain-barrier into the frontal cortex and hippocampus via the LAT-1 transport system (Fernström 2013), which for example, resulted in decreased plasma levels of tyrosine and phenylalanine in the chronically treated rats compared to the corresponding controls. Although increased levels of tyrosine and phenylalanine do not directly imply an enhanced DA synthesis as TH is a rate-limiting enzyme that can get saturated at high brain levels of tyrosine, there are studies demonstrating that administration of a tyrosine-rich amino acid mixture effectively reduces ADHD symptoms in some children (Hinz *et al.* 2011),

and also that tyrosine potentiates MPH-induced increase of extracellular DA in rats when co-administered (Woods and Meyer 1991). Given the present findings, therefore, this thesis offers an additional explanation beyond what currently exist in literature and may shape our understanding of the therapeutic action of MPH in the treatment of ADHD and possibly initiate an enhanced use of dietary supplement with high levels of tyrosine and phenylalanine for the treatment of ADHD symptoms.

Results from Chapters 4, 5 and 6, further demonstrate that MPH alters a number of metabolic pathways. In particular, data from this thesis reveals that metabolites related to the glutamatergic/GABAergic pathway (including glutamate, glutamine and GABA) and those related to brain energy metabolism (e.g. lactate, acetate, creatine and NAD) may contribute to the mechanism of action of MPH. These metabolites are altered by MPH treatment in both the cerebral and cerebellar areas. Over the years, the dopaminergic and noradrenergic systems have received much attention in studies examining ADHD pathology and stimulant treatment (Del Campo *et al.* 2011). However, while these two catecholaminergic systems may be very important systems in ADHD, together with the findings presented in this thesis, a number of recent reports suggest that the glutamatergic/GABAergic system and brain energy metabolites are also critical. Indeed, converging evidence shows that glutamate, glutamine and GABA, as well as lactate, acetate and creatine have abnormal concentrations in multiple brain regions of both young and adult drug naïve ADHD patients (Carrey *et al.* 2007; Jin *et al.* 2001; Maltezos *et al.* 2014; Perlov *et al.* 2007; Perlov *et al.* 2010), and data from this thesis suggests that some of these brain metabolic abnormalities could indeed be normalised following MPH therapy. Like tyrosine and phenylalanine, this thesis also shows that chronic MPH treatment alters the balance of plasma lactate and acetate, favouring the competitive uptake of these energy-related metabolites by the

monocarboxylate transport system, which transports them across the blood-brain barrier into brain areas such as the frontal cortex (Cremer *et al.* 1976; Deelchand *et al.* 2009; Waniewski and Martin 1998). Thus, the findings on the metabolites presented in this thesis indicate that more attention needs to be paid to the brain energy-related and the glutamatergic/GABAergic pathways in research on ADHD.

Further research is required to understand the role of the L-type amino acid transporter (LAT) system in the mechanism of action of psychostimulants, particularly following chronic MPH therapy. LATs are responsible for the transport of LNAAs such as tyrosine and phenylalanine. Most of these transporters possess two subunits, a light chain, which includes LAT1 and LAT2 and a heavy chain (CD98/4F2hc), and are located in the cell membrane (Ohtsuki *et al.* 2010). Given its expression within the BBB, LAT-1 is particularly important in studies on brain disorders, as abnormalities in its density or activity may influence amino acid transport, with far-reaching effects on dopaminergic neuronal function and drug therapy (Ohtsuki *et al.* 2010). For instance, LAT-1 has been shown to participate in L-DOPA (a medication for Parkinson's disease) transport across the BBB (Pinho *et al.* 2004). Unfortunately, time constraints did not permit us to investigate the effect of MPH treatment on the mRNA and protein expression of this transport system, although we put forward the hypothesis that the LAT-1 system may facilitate an increased transport of LNAAs (e.g. tyrosine and phenylalanine) across the BBB, based on the previous observation that substrate availability influences the uptake of these LNAAs by this transport system into the brain (Fernström 2013). It is, however, uncertain whether MPH only alters the physiological balance of tyrosine and phenylalanine in the plasma favouring their uptake into the brain or whether MPH treatment also alters the protein expression and the activity of the LAT-1 system. As already mentioned, we also found that MPH treatment alters the

physiological balance of lactate and acetate in the plasma, which are also transported across the BBB by another transport system, the monocarboxylate transport system. In particular, in young/adolescent animals, lactate and acetate are suggested to have a high affinity for and high permeability to the monocarboxylate transport system (Cremer *et al.* 1976; Deelchand *et al.* 2009; Waniewski and Martin 1998). Thus, the examination of possible MPH induced changes of the mRNA and protein expression patterns for the monocarboxylate transport system, as well as the LAT-1, and the LAT-2 transport systems deserve future investigations.

Our in-depth investigation regarding the mechanism of action of MPH in the cerebellum is also of interest and reported in Chapter 6. In recent times, the cerebellum and its potential role in ADHD and cognition is the subject of intense research (Schmahmann and Caplan 2006; Buckner 2013; Ivanov *et al.* 2014). Indeed, recent studies have demonstrated that along with its traditional role in motor activity, the cerebellum plays important roles in cognition, mostly due to its dense connection with the cerebral cortex and the previously unknown presence of dopaminergic and noradrenergic markers in this region (Schmahmann and Caplan 2006; Buckner 2013). In this thesis, contrasting findings were recorded following acute and chronic MPH treatment. Here, acute MPH treatment decreased some examined biomarkers (e.g. VMAT2, as well as glutamate, glutamine, NAA and NAD) but increased other biomarkers (e.g. GABA, glycine, aspartate, acetate and hypoxanthine) in a dose-dependent manner. In contrast, chronic treatment generally enhanced several biomarkers (e.g. VMAT2, glutamate, glutamine, phenylalanine, tyrosine, lactate, glycine, taurine, and creatine), suggesting treatment duration-dependent effects of MPH on the cerebellum. The increased VMAT2 following chronic MPH treatment corresponded with increased tyrosine and phenylalanine. However, this did not correlate with increased cerebellar DA, which would suggest that perhaps in the cerebellum, the increased LNAAs may elevate the

synthesis of NA rather than DA (i.e. whole tissue DA in the cerebellum serves mostly as a substrate for NA synthesis), as previously suggested (Glaser *et al.* 2006). Further, although the mechanisms underlying the MPH-induced contrasting findings in the cerebellum after acute and chronic treatment are not yet clear, the findings following acute treatment are consistent with previous studies that found decreased NAA levels compared to corresponding controls, as well as decreased glutamate and glutamine levels in young ADHD patients that had received MPH treatment (Ben Amor 2014; Soliva *et al.* 2010). Interestingly, the MPH-induced decrease of some cerebellar metabolites (e.g. glutamate and glutamine) following acute treatment are in sharp contrast to the MPH-induced increase of these metabolites in the cerebrum following acute treatment. However, similar to our findings, reports from both human and rodent studies have also indicated contrasting findings between the MPH-induced metabolic changes in the cerebral areas and the cerebellum (Michaelides *et al.* 2010; Volkow *et al.* 1997).

Chronic exposure to psychostimulants such as MPH has been previously suggested to cause complex structural and plastic modifications in the reward circuitry of the developing brain, involving changes to actin cytoskeleton and dendritic spine morphology (Berman *et al.* 2008; Haydon *et al.* 2009). Dendritic spines are crucial for synaptic strength and help to transmit signals to the cell body of the post-synaptic neurons (Kasai *et al.* 2003). Structural and functional changes in spines and synapses are known to be important processes mediating memory and learning, as well as drug-related behaviour (Soria Fregozo and Pérez Vega 2012; Kang *et al.* 2016). Interestingly, a recent study has shown that chronic exposure to MPH and cocaine alter dendritic spine density (Kim *et al.* 2009). Therefore, we sought to determine the mechanisms underlying the MPH-induced alterations to dendritic spines by evaluating signalling pathways (including Arc and IRSp53 pathways) that are associated with spine formation. Indeed, the Arc

and insulin receptor (IRSp53/58) pathways have been been implicated in the pathophysiology of ADHD and in the modulation of human memory strength (Liu *et al.* 2013; Ribasés *et al.* 2009).

We found that while acute MPH treatment has minimal effects on plasticity-related proteins within the Arc and IRSp53 pathways, chronic MPH treatment has a much more pronounced effect. For instance, chronic MPH treatment induced an increase of *Arc* gene in the striatum and the Arc protein in the parietal cortex and hippocampus. The MPH-induced increase of Arc may be linked to glutamate and lactate levels as well as D1 receptor density, since glutamate and lactate stimulate *Arc* mRNA expression via NMDA receptor mediated Ca^{2+} influx (Bramham *et al.* 2010) and *Arc* gene expression is also stimulated by D1 receptor-induced increase of cAMP. Interestingly, this thesis has demonstrated that chronic MPH increases the levels of glutamate and its precursor glutamine in the hippocampus, striatum and frontal cortex, as well as increased D1 receptor in the accumbens and parietal cortex. The Arc protein increases the proportion of the so-called "learning spines" (Peebles *et al.* 2010). Therefore, the increased Arc protein expression following the chronic MPH treatment, particularly in the hippocampus may be essential for learning. On the other hand, chronic but not acute MPH treatment also enhanced the densities of IRSp53/58, Cdc42, and Arp2 in the striatum and the nucleus accumbens. Reports indicate that IRSp53/58 localises at synapses and mediate filopodia (a precursor of dendritic spine) formation, and that increasing IRSp53/58 expression in most cell types often induces extensive actin-containing cell protrusions, which may be Cdc42 dependent (Krugmann *et al.* 2001). Similarly, higher expressions of Cdc42 and its downstream signalling molecules including the Arp2/3 complex promotes F-actin polymerisation, a process that is essential for a filopodia to become long enough to develop into a mature spine (Soria Fregozo and Pérez Vega 2012). Therefore, the observed increase of IRSp53/58, Cdc42 and Arp2 in the striatum and nucleus accumbens

following chronic MPH treatment (as shown in Chapter 7 of this thesis) raises the possibility that prolonged MPH exposure enhances dendritic spine density in these brain areas. Consistent with this finding, MPH and cocaine have both been shown to increase dendritic spine density in the striatum and nucleus accumbens (Kim *et al.* 2009). The MPH-induced changes in dendritic spine density and these plasticity-associated genes and proteins could be related to learning and memory consolidation, as well as drug-seeking behaviour (Everitt and Robbins 2005; Kalivas and O'Brien 2008). In addition, given that IRSp53 co-localises with insulin receptors at the synapse and insulin has been detected in the brain (although the source still remains unknown), it cannot be excluded that the IRSp53 pathway may be involved in insulin signalling that mediates glucose homeostasis, feeding behaviour and cognitive processes (Blázquez *et al.* 2014).

In summary, this thesis will contribute to an enhanced understanding of the mechanism of action of MPH in the developing brain. The data presented in this thesis show an upregulation of both DAT and NET following chronic MPH treatment, which could potentially limit the long-term efficacy of the drug. In addition, the data also show a potential new mechanism of action of MPH involving enhanced transport of plasma LNAAs such as tyrosine and phenylalanine into the brain, beside the already established DAT blocking mechanism of the drug. This finding could be instrumental for the development of new treatment paradigms for ADHD management including modified diets that are rich in phenylalanine and tyrosine and therapeutic drugs targeting transporters for these LNAAs.

APPENDIX 1

Principal Component Analysis (PCA) was conducted on the cerebral datasets (see Chapter 4). This demonstrated a clear separation between the acute 5.0 mg/kg MPH-treated and the control groups (Figure A1).

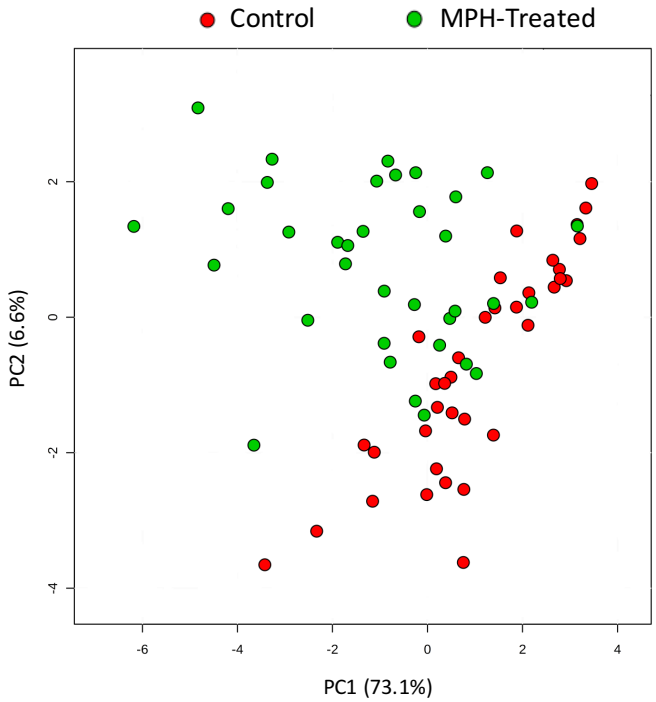

Figure A1: PCA scores plot showing a clear separation between the acute 5.0 mg/kg MPH-treated (green) and the saline-treated control (red) groups, comprising both the left and right cerebral hemispheres.

BIBLIOGRAPHY

Abbas R., Palumbo D., Walters F., Belden H., Berry S. A. (2016) Single-dose Pharmacokinetic Properties and Relative Bioavailability of a Novel Methylphenidate Extended-release Chewable Tablet Compared With Immediate-release Methylphenidate Chewable Tablet. *Clin. Ther.* **38**, 1151–1157.

Abbott M.-A., Wells D. G., Fallon J. R. (1999) The Insulin Receptor Tyrosine Kinase Substrate p58/53 and the Insulin Receptor Are Components of CNS Synapses. *J. Neurosci.* **19**, 7300–7308.

Acworth I., Nicholass J., Morgan B., Newsholme E. A. (1986) Effect of sustained exercise on concentrations of plasma aromatic and branched-chain amino acids and brain amines. *Biochem. Biophys. Res. Commun.* **137**, 149–153.

Adler L. A., Kroon R. A., Stein M., Shahid M., Tarazi F. I., Szegedi A., Schipper J., Cazorla P. (2012) A translational approach to evaluate the efficacy and safety of the novel AMPA receptor positive allosteric modulator org 26576 in adult attention-deficit/hyperactivity disorder. *Biol. Psychiatry* **72**, 971–977.

Aittokallio T., Schwikowski B. (2006) Graph-based methods for analysing networks in cell biology. *Brief. Bioinform.* **7**, 243–255.

Albin R. L., Young A. B., Penney J. B. (1989) The functional anatomy of basal ganglia disorders. *Trends Neurosci.* **12**, 366–375.

Albin R. L., Young A. B., Penney J. B. (1995) The functional anatomy of disorders of the basal ganglia. *Trends Neurosci.* **18**, 63–64.

Allen J. K., Wilkinson M., Soo E. C., Hui J. P. M., Chase T. D., Carrey N. (2010) Chronic low dose Adderall XR down-regulates cfos expression in infantile and prepubertal rat striatum and cortex. *Neuroscience* **169**, 1901–1912.

Altarelli I., Leroy F., Monzalvo K., Fluss J., Billard C., Dehaene-Lambertz G., Galaburda A. M., Ramus F. (2014) Planum temporale asymmetry in developmental dyslexia: Revisiting an old question. *Hum. Brain Mapp.* **35**, 5717–5735.

American Psychiatric Association (2013) *Diagnostic and Statistical Manual of Mental Disorders*. American Psychiatric Association.

Amiri A., Torabi Parizi G., Kousha M., Saadat F., Modabbernia M.-J., Najafi K., Atrkar Roushan Z. (2013) Changes in plasma Brain-derived neurotrophic factor (BDNF) levels induced by methylphenidate in children with Attention deficit-hyperactivity disorder (ADHD). *Prog. Neuropsychopharmacol. Biol. Psychiatry* **47**, 20–24.

Andersen S. L., Navalta C. P. (2011) New frontiers in developmental neuropharmacology: Can long-term therapeutic effects of drugs be optimized through carefully timed early intervention? *J. Child Psychol. Psychiatry* **52**, 476–503.

Arcos-Burgos M., Castellanos F. X., Konecki D., Lopera F., Pineda D., Palacio J. D., Rapoport J. L., Berg K., Bailey-Wilson J., Muenke M. (2004) Pedigree disequilibrium test (PDT) replicates association and linkage between DRD4 and ADHD in multigenerational and extended pedigrees from a genetic isolate. *Mol. Psychiatry* **9**, 252–259.

Ariyannur P. S., Moffett J. R., Manickam P., Pattabiraman N., Arun P., Nitta A., Nabeshima T., Madhavarao C. N., Namboodiri A. M. A. (2010) Methamphetamine-induced neuronal protein NAT8L is the NAA biosynthetic enzyme: Implications for specialized acetyl coenzyme A metabolism in the CNS. *Brain Res.* **1335**, 1–13.

Arning L., Ocklenburg S., Schulz S., Ness V., Gerding W. M., Hengstler J. G., Falkenstein M., Epplen J. T., Güntürkün O., Beste C. (2013) PCSK6 VNTR Polymorphism Is Associated with Degree of Handedness but Not Direction of Handedness. *PLoS ONE* **8**.

Arnsten A. F. T. (2009) Toward a new understanding of attention-deficit hyperactivity disorder pathophysiology: an important role for prefrontal cortex dysfunction. *CNS Drugs* **23 Suppl 1**, 33–41.

Arnsten A. F. T. (2011) Catecholamine Influences on Dorsolateral Prefrontal Cortical Networks. *Biol. Psychiatry* **69**, e89–e99.

Arnsten A. F. T., Li B.-M. (2005) Neurobiology of executive functions: catecholamine influences on prefrontal cortical functions. *Biol. Psychiatry* **57**, 1377–1384.

Arnsten A. F. T., Rubia K. (2012) Neurobiological circuits regulating attention, cognitive control, motivation, and emotion: disruptions in neurodevelopmental psychiatric disorders. *J. Am. Acad. Child Adolesc. Psychiatry* **51**, 356–367.

Arthur A. D., Terri S. L. (2001) *Assessing Attention-Deficit/Hyperactivity Disorder*. Kluwer Academic/Plenum Publishers. Springer., New York, NY, USA.

Ashtari M., Kumra S., Bhaskar S. L., Clarke T., Thaden E., Cervellione K. L., Rhinewine J., et al. (2005) Attention-deficit/hyperactivity disorder: a preliminary diffusion tensor imaging study. *Biol. Psychiatry* **57**, 448–455.

Assis L. C., Scaini G., Di-Pietro P. B., Castro A. A., Comim C. M., Streck E. L., Quevedo J. (2007) Effect of Antipsychotics on Creatine Kinase Activity in Rat Brain. *Basic Clin. Pharmacol. Toxicol.* **101**, 315–319.

Avila A., Nguyen L., Rigo J.-M. (2013) Glycine receptors and brain development. *Front. Cell. Neurosci.* **7**.

Babitt J. L., Zhang Y., Samad T. A., Xia Y., Tang J., Campagna J. A., Schneyer A. L., Woolf C. J., Lin H. Y. (2005) Repulsive guidance molecule (RGMa), a DRAGON homologue, is a bone morphogenetic protein co-receptor. *J. Biol. Chem.* **280**, 29820–29827.

Bak L. K., Schousboe A., Waagepetersen H. S. (2006) The glutamate/GABA-glutamine cycle: aspects of transport, neurotransmitter homeostasis and ammonia transfer. *J. Neurochem.* **98**, 641–653.

Bakhshayesh A. R., Hänsch S., Wyschkon A., Rezai M. J., Esser G. (2011) Neurofeedback in ADHD: a single-blind randomized controlled trial. *Eur. Child Adolesc. Psychiatry* **20**, 481–491.

Bakker S. C., Meulen E. M. van der, Buitelaar J. K., Sandkuijl L. A., Pauls D. L., Monsuur A. J., Slot R. van 't, et al. (2003) A Whole-Genome Scan in 164 Dutch Sib Pairs with Attention-Deficit/Hyperactivity Disorder: Suggestive Evidence for Linkage on Chromosomes 7p and 15q. *Am. J. Hum. Genet.* **72**, 1251–1260.

Balcioglu A., Ren J.-Q., McCarthy D., Spencer T. J., Biederman J., Bhide P. G. (2009) Plasma and brain concentrations of oral therapeutic doses of methylphenidate and their impact on brain monoamine content in mice. *Neuropharmacology* **57**, 687–693.

Banerjee E., Nandagopal K. (2015) Does serotonin deficit mediate susceptibility to ADHD? *Neurochem. Int.* **82**, 52–68.

Banerjee P. S., Aston J., Khundakar A. A., Zetterström T. S. C. (2009) Differential regulation of psychostimulant-induced gene expression of brain derived neurotrophic factor and the immediate-early gene Arc in the juvenile and adult brain. *Eur. J. Neurosci.* **29**, 465–476.

Barkley R. A. (1997) Behavioral inhibition, sustained attention, and executive functions: constructing a unifying theory of ADHD. *Psychol. Bull.* **121**, 65–94.

Barr C. L., Feng Y., Wigg K., Bloom S., Roberts W., Malone M., Schachar R., Tannock R., Kennedy J. L. (2000) Identification of DNA variants in the SNAP-25 gene and linkage study of these polymorphisms and attention-deficit hyperactivity disorder. *Mol. Psychiatry* **5**, 405–409.

Baslow M. H. (2002) Evidence supporting a role for N-acetyl-L-aspartate as a molecular water pump in myelinated neurons in the central nervous system: An analytical review. *Neurochem. Int.* **40**, 295–300.

Baslow M. H. (2003) N-Acetylaspartate in the Vertebrate Brain: Metabolism and Function. *Neurochem. Res.* **28**, 941–953.

Baslow M. H. (2010) Evidence that the tri-cellular metabolism of N-acetylaspartate functions as the brain's "operating system": How NAA metabolism supports meaningful intercellular frequency-encoded communications. *Amino Acids* **39**, 1139–1145.

Bates T. E., Strangward M., Keelan J., Davey G. P., Munro P. M., Clark J. B. (1996) Inhibition of N-acetylaspartate production: implications for 1H MRS studies in vivo. *Neuroreport* **7**, 1397–1400.

Beaulieu J.-M., Gainetdinov R. R. (2011) The Physiology, Signaling, and Pharmacology of Dopamine Receptors. *Pharmacol. Rev.* **63**, 182–217.

Beckonert O., Keun H. C., Ebbels T. M. D., Bundy J., Holmes E., Lindon J. C., Nicholson J. K. (2007) Metabolic profiling, metabolomic and metabonomic procedures for NMR spectroscopy of urine, plasma, serum and tissue extracts. *Nat. Protoc.* **2**, 2692–2703.

Bélanger S. A., Vanasse M., Spahis S., Sylvestre M.-P., Lippé S., L'heureux F., Ghadirian P., Vanasse C.-M., Levy E. (2009) Omega-3 fatty acid treatment of children with attention-deficit hyperactivity disorder: A randomized, double-blind, placebo-controlled study. *Paediatr. Child Health* **14**, 89–98.

Belousov A. B., Pol A. N. V. D. (1997) Dopamine Inhibition: Enhancement of GABA Activity and Potassium Channel Activation in Hypothalamic and Arcuate Nucleus Neurons. *J. Neurophysiol.* **78**, 674–688.

Ben Amor L. (2014) 1H-Magnetic resonance spectroscopy study of stimulant medication effect on brain metabolites in French Canadian children with attention deficit hyperactivity disorder. *Neuropsychiatr. Dis. Treat.*, 47.

Ben-Jonathan N., Hnasko R. (2001) Dopamine as a Prolactin (PRL) Inhibitor. *Endocr. Rev.* **22**, 724–763.

Benke T., Delazer M., Bartha L., Auer A. (2003) Basal ganglia lesions and the theory of fronto-subcortical loops: neuropsychological findings in two patients with left caudate lesions. *Neurocase* **9**, 70–85.

Berger A. (1999) Ritalin may influence serotonin balance in hyperactive children. *BMJ* **318**, 212.

Berman S., O'Neill J., Fears S., Bartzokis G., London E. D. (2008) Abuse of amphetamines and structural abnormalities in the brain. *Ann. N. Y. Acad. Sci.* **1141**, 195–220.

Berquin P. C., Giedd J. N., Jacobsen L. K., Hamburger S. D., Krain A. L., Rapoport J. L., Castellanos F. X. (1998) Cerebellum in attention-deficit hyperactivity disorder A morphometric MRI study. *Neurology* **50**, 1087–1093.

Berridge C. W., Devilbiss D. M., Andrzejewski M. E., Arnsten A. F. T., Kelley A. E., Schmeichel B., Hamilton C., Spencer R. C. (2006) Methylphenidate Preferentially Increases Catecholamine Neurotransmission within the Prefrontal Cortex at Low Doses that Enhance Cognitive Function. *Biol. Psychiatry* **60**, 1111–1120.

Bertler Å., Rosengren E. (1959) Occurrence and distribution of dopamine in brain and other tissues. *Experientia* **15**, 10–11.

Beveridge T. J. R., Smith H. R., Nader M. A., Porrino L. J. (2005) Effects of chronic cocaine self-administration on norepinephrine transporters in the nonhuman primate brain. *Psychopharmacology (Berl.)* **180**, 781–788.

Bhattacharya S. B., Datta A. G. (1993) Is brain a gluconeogenic organ? *Mol. Cell. Biochem.* **125**, 51–57.

Biederman J. (2005) Attention-deficit/hyperactivity disorder: a selective overview. *Biol. Psychiatry* **57**, 1215–1220.

Biederman J., Faraone S. V. (2005) Attention-deficit hyperactivity disorder. *Lancet Lond. Engl.* **366**, 237–248.

Biederman J., Faraone S. V., Keenan K., Knee D., Tsuang M. T. (1990) Family-Genetic and Psychosocial Risk Factors in DSM-III Attention Deficit Disorder. *J. Am. Acad. Child Adolesc. Psychiatry* **29**, 526–533.

Birnbaum S. G., Yuan P. X., Wang M., Vijayraghavan S., Bloom A. K., Davis D. J., Gobeske K. T., Sweatt J. D., Manji H. K., Arnsten A. F. T. (2004) Protein kinase C overactivity impairs prefrontal cortical regulation of working memory. *Science* **306**, 882–884.

Bjork J. M., Grant S. J., Chen G., Hommer D. W. (2014) Dietary tyrosine/phenylalanine depletion effects on behavioral and brain signatures of human motivational processing. *Neuropsychopharmacol. Off. Publ. Am. Coll. Neuropsychopharmacol.* **39**, 595–604.

Björklund A., Dunnett S. B. (2007) Dopamine neuron systems in the brain: an update. *Trends Neurosci.* **30**, 194–202.

Blaschko H. (1942) The activity of l(—)-dopa decarboxylase. *J. Physiol.* **101**, 337–349.

Blázquez E., Velázquez E., Hurtado-Carneiro V., Ruiz-Albusac J. M. (2014) Insulin in the Brain: Its Pathophysiological Implications for States Related with Central Insulin Resistance, Type 2 Diabetes and Alzheimer's Disease. *Front. Endocrinol.* **5**.

Bledsoe J., Semrud-Clikeman M., Pliszka S. R. (2009) A magnetic resonance imaging study of the cerebellar vermis in chronically treated and treatment-naïve children with attention-deficit/hyperactivity disorder combined type. *Biol. Psychiatry* **65**, 620–624.

Bollmann S., Ghisleni C., Poil S.-S., Martin E., Ball J., Eich-Höchli D., Edden R. A. E., et al. (2015) Developmental changes in gamma-aminobutyric acid levels in attention-deficit/hyperactivity disorder. *Transl. Psychiatry* **5**, e589.

Boris M., Mandel F. S. (1994) Foods and additives are common causes of the attention deficit hyperactive disorder in children. *Ann. Allergy* **72**, 462–468.

Borycz J., Zapata A., Quiroz C., Volkow N. D., Ferré S. (2008) 5-HT 1B receptor-mediated serotoninergic modulation of methylphenidate-induced locomotor activation in rats. *Neuropsychopharmacol. Off. Publ. Am. Coll. Neuropsychopharmacol.* **33**, 619–626.

Brambilla P., Stanley J. A., Nicoletti M. A., Sassi R. B., Mallinger A. G., Frank E., Kupfer D., Keshavan M. S., Soares J. C. (2005) 1H magnetic resonance spectroscopy investigation of the dorsolateral prefrontal cortex in bipolar disorder patients. *J. Affect. Disord.* **86**, 61–67.

Bramham C. R., Alme M. N., Bittins M., Kuipers S. D., Nair R. R., Pai B., Panja D., et al. (2010) The Arc of synaptic memory. *Exp. Brain Res. Exp. Hirnforsch. Exp. Cerebrale* **200**, 125–140.

Brand A., Richter-Landsberg C., Leibfritz D. (1993) Multinuclear NMR studies on the energy metabolism of glial and neuronal cells. *Dev. Neurosci.* **15**, 289–298.

Brigman J. L., Mathur P., Harvey-White J., Izquierdo A., Saksida L. M., Bussey T. J., Fox S., Deneris E., Murphy D. L., Holmes A. (2010) Pharmacological or genetic inactivation of the serotonin transporter improves reversal learning in mice. *Cereb. Cortex N. Y. N 1991* **20**, 1955–1963.

Brookes K., Xu X., Chen W., Zhou K., Neale B., Lowe N., Anney R., et al. (2006) The analysis of 51 genes in DSM-IV combined type attention deficit hyperactivity disorder: association signals in DRD4, DAT1 and 16 other genes. *Mol. Psychiatry* **11**, 934–953.

Brunner D., Hen R. (1997) Insights into the neurobiology of impulsive behavior from serotonin receptor knockout mice. *Ann. N. Y. Acad. Sci.* **836**, 81–105.

Bu Q., Lv L., Yan G., Deng P., Wang Y., Zhou J., Yang Y., Li Y., Cen X. (2013) NMR-based metabonomic in hippocampus, nucleus accumbens and prefrontal cortex of methamphetamine-sensitized rats. *Neurotoxicology* **36**, 17–23.

Buckner R. L. (2013) The Cerebellum and Cognitive Function: 25 Years of Insight from Anatomy and Neuroimaging. *Neuron* **80**, 807–815.

Buis J. M., Broderick J. B. (2005) Pyruvate formate-lyase activating enzyme: elucidation of a novel mechanism for glycyl radical formation. *Arch. Biochem. Biophys.* **433**, 288–296.

Butini S., Nikolic K., Kassel S., Brückmann H., Filipic S., Agbaba D., Gemma S., et al. (2016) Polypharmacology of dopamine receptor ligands. *Prog. Neurobiol.* **142**, 68–103.

Bymaster F. P., Katner J. S., Nelson D. L., Hemrick-Luecke S. K., Threlkeld P. G., Heiligenstein J. H., Morin S. M., Gehlert D. R., Perry K. W. (2002) Atomoxetine increases extracellular levels of norepinephrine and dopamine in prefrontal cortex of rat: a potential mechanism for efficacy in attention deficit/hyperactivity disorder. *Neuropsychopharmacol. Off. Publ. Am. Coll. Neuropsychopharmacol.* **27**, 699–711.

Calipari E. S., Ferris M. J., Melchior J. R., Bermejo K., Salahpour A., Roberts D. C. S., Jones S. R. (2014) Methylphenidate and cocaine self-administration produce distinct dopamine terminal alterations. *Addict. Biol.* **19**, 145–155.

Calipari E. S., Jones S. R. (2014) Sensitized Nucleus Accumbens Dopamine Terminal Responses to Methylphenidate and Dopamine Transporter Releasers after Intermittent-Access Self-Administration. *Neuropharmacology* **82**, 1–10.

Cano-Cebrián M. J., Zornoza-Sabina T., Guerri C., Polache A., Granero L. (2003) Local acamprosate modulates dopamine release in the rat nucleus accumbens through NMDA receptors: An in vivo microdialysis study. *Naunyn. Schmiedebergs Arch. Pharmacol.* **367**, 119–125.

Caravaggio F., Nakajima S., Plitman E., Gerretsen P., Chung J. K., Iwata Y., Graff-Guerrero A. (2016) The effect of striatal dopamine depletion on striatal and cortical glutamate: A mini-review. *Prog. Neuropsychopharmacol. Biol. Psychiatry* **65**, 49–53.

Carlson C. L., Shin M., Booth J. (1999) The case for DSM-IV subtypes in ADHD. *Ment. Retard. Dev. Disabil. Res. Rev.* **5**, 199–206.

Carrey N. J., MacMaster F. P., Gaudet L., Schmidt M. H. (2007) Striatal creatine and glutamate/glutamine in attention-deficit/hyperactivity disorder. *J. Child Adolesc. Psychopharmacol.* **17**, 11–17.

Carrey N., MacMaster F. P., Fogel J., Sparkes S., Waschbusch D., Sullivan S., Schmidt M. (2003) Metabolite changes resulting from treatment in children with ADHD: a 1H-MRS study. *Clin. Neuropharmacol.* **26**, 218–221.

Carrey N., MacMaster F. P., Sparkes S. J., Khan S. C., Kusumakar V. (2002) Glutamatergic changes with treatment in attention deficit hyperactivity disorder: a preliminary case series. *J. Child Adolesc. Psychopharmacol.* **12**, 331–336.

Carter C. S., Krener P., Chaderjian M., Northcutt C., Wolfe V. (1995) Asymmetrical visual-spatial attentional performance in ADHD: evidence for a right hemispheric deficit. *Biol. Psychiatry* **37**, 789–797.

Cartier E. A., Parra L. A., Baust T. B., Quiroz M., Salazar G., Faundez V., Egaña L., Torres G. E. (2010) A Biochemical and Functional Protein Complex Involving Dopamine Synthesis and Transport into Synaptic Vesicles. *J. Biol. Chem.* **285**, 1957–1966.

Casey B. J., Castellanos F. X., Giedd J. N., Marsh W. L., Hamburger S. D., Schubert A. B., Vauss Y. C., et al. (1997) Implication of right frontostriatal circuitry in response inhibition and attention-deficit/hyperactivity disorder. *J. Am. Acad. Child Adolesc. Psychiatry* **36**, 374–383.

Castellanos F. X., Giedd J. N., Berquin P. C., Walter J. M., Sharp W., Tran T., Vaituzis A. C., et al. (2001) Quantitative brain magnetic resonance imaging in girls with attention-deficit/hyperactivity disorder. *Arch. Gen. Psychiatry* **58**, 289–295.

Castellanos F. X., Giedd J. N., Marsh W. L., Hamburger S. D., Vaituzis A. C., Dickstein D. P., Sarfatti S. E., et al. (1996) Quantitative brain magnetic resonance imaging in attention-deficit hyperactivity disorder. *Arch. Gen. Psychiatry* **53**, 607–616.

Castro-Marrero J., Cordero M. D., Segundo M. J., Sáez-Francàs N., Calvo N., Román-Malo L., Aliste L., Fernández de Sevilla T., Alegre J. (2015) Does Oral Coenzyme Q10 Plus NADH Supplementation Improve Fatigue and Biochemical Parameters in Chronic Fatigue Syndrome? *Antioxid. Redox Signal.* **22**, 679–685.

Chan C. Y., Sun H. S., Shah S. M., Agovic M. S., Friedman E., Banerjee S. P. (2014) Modes of direct modulation by taurine of the glutamate NMDA receptor in rat cortex. *Eur. J. Pharmacol.* **728**, 167–175.

Charlety P. J., Grenhoff J., Chergui K., De la Chapelle B., Buda M., Svensson T. H., Chouvet G. (1991) Burst firing of mesencephalic dopamine neurons is inhibited by somatodendritic application of kynurenate. *Acta Physiol. Scand.* **142**, 105–112.

Chase T., Carrey N., Soo E., Wilkinson M. (2007) Methylphenidate regulates activity regulated cytoskeletal associated but not brain-derived neurotrophic factor gene expression in the developing rat striatum. *Neuroscience* **144**, 969–984.

Chefer V. I., Thompson A. C., Zapata A., Shippenberg T. S. (2009) Overview of Brain Microdialysis. *Curr. Protoc. Neurosci. Editor. Board Jacqueline N Crawley Al*, Chapter, Unit7.1.

Chen J., Shi B., Xiang H., Hou W., Qin X., Tian J., Du G. (2015) 1H NMR-based metabolic profiling of liver in chronic unpredictable mild stress rats with genipin treatment. *J. Pharm. Biomed. Anal.* **115**, 150–158.

Cheng J., Xiong Z., Duffney L. J., Wei J., Liu A., Liu S., Chen G.-J., Yan Z. (2014) Methylphenidate Exerts Dose-Dependent Effects on Glutamate Receptors and Behaviors. *Biol. Psychiatry* **76**, 953–962.

Cheon K.-A., Ryu Y. H., Kim Y.-K., Namkoong K., Kim C.-H., Lee J. D. (2003) Dopamine transporter density in the basal ganglia assessed with [123I]IPT SPET in children with attention deficit hyperactivity disorder. *Eur. J. Nucl. Med. Mol. Imaging* **30**, 306–311.

Chergui K., Charléty P. J., Akaoka H., Saunier C. F., Brunet J. L., Buda M., Svensson T. H., Chouvet G. (1993) Tonic activation of NMDA receptors causes spontaneous burst discharge of rat midbrain dopamine neurons in vivo. *Eur. J. Neurosci.* **5**, 137–144.

Chio C. L., Lajiness M. E., Huff R. M. (1994) Activation of heterologously expressed D3 dopamine receptors: comparison with D2 dopamine receptors. *Mol. Pharmacol.* **45**, 51–60.

Choi J., Ko J., Racz B., Burette A., Lee J.-R., Kim S., Na M., et al. (2005) Regulation of Dendritic Spine Morphogenesis by Insulin Receptor Substrate 53, a Downstream Effector of Rac1 and Cdc42 Small GTPases. *J. Neurosci.* **25**, 869–879.

Choi J. W., Han D. H., Kang K. D., Jung H. Y., Renshaw P. F. (2015) Aerobic exercise and attention deficit hyperactivity disorder: brain research. *Med. Sci. Sports Exerc.* **47**, 33–39.
Chung W., Choi S. Y., Lee E., Park H., Kang J., Park H., Choi Y., et al. (2015) Social deficits in IRSp53 mutant mice improved by NMDAR and mGluR5 suppression. *Nat. Neurosci.* **18**, 435–443.
Clark J. B. (1998) N-acetyl aspartate: a marker for neuronal loss or mitochondrial dysfunction. *Dev. Neurosci.* **20**, 271–276.
Clarke H. F., Walker S. C., Dalley J. W., Robbins T. W., Roberts A. C. (2007) Cognitive inflexibility after prefrontal serotonin depletion is behaviorally and neurochemically specific. *Cereb. Cortex N. Y. N 1991* **17**, 18–27.
Cloarec O., Dumas M.-E., Craig A., Barton R. H., Trygg J., Hudson J., Blancher C., et al. (2005) Statistical Total Correlation Spectroscopy: An Exploratory Approach for Latent Biomarker Identification from Metabolic ^{1} H NMR Data Sets. *Anal. Chem.* **77**, 1282–1289.
Cohen A. I., Todd R. D., Harmon S., O'Malley K. L. (1992) Photoreceptors of mouse retinas possess D4 receptors coupled to adenylate cyclase. *Proc. Natl. Acad. Sci. U. S. A.* **89**, 12093–12097.
Colla M., Ende G., Alm B., Deuschle M., Heuser I., Kronenberg G. (2008) Cognitive MR spectroscopy of anterior cingulate cortex in ADHD: Elevated choline signal correlates with slowed hit reaction times. *J. Psychiatr. Res.* **42**, 587–595.
Colquhoun I., Bunday S. (1981) A lack of essential fatty acids as a possible cause of hyperactivity in children. *Med. Hypotheses* **7**, 673–679.
Connor D. F., Fletcher K. E., Swanson J. M. (1999) A meta-analysis of clonidine for symptoms of attention-deficit hyperactivity disorder. *J. Am. Acad. Child Adolesc. Psychiatry* **38**, 1551–1559.
Corballis M. C. (2009) The evolution and genetics of cerebral asymmetry. *Philos. Trans. R. Soc. Lond. B. Biol. Sci.* **364**, 867–879.
Corominas-Roso M., Ramos-Quiroga J. A., Ribases M., Sanchez-Mora C., Palomar G., Valero S., Bosch R., Casas M. (2013) Decreased serum levels of brain-derived neurotrophic factor in adults with attention-deficit hyperactivity disorder. *Int. J. Neuropsychopharmacol. Off. Sci. J. Coll. Int. Neuropsychopharmacol. CINP*, 1–9.
Cortese S., Holtmann M., Banaschewski T., Buitelaar J., Coghill D., Danckaerts M., Dittmann R. W., et al. (2013) Practitioner review: current best practice in the management of adverse events during treatment with ADHD medications in children and adolescents. *J. Child Psychol. Psychiatry* **54**, 227–246.
Corvol J. C., Studler J. M., Schonn J. S., Girault J. A., Hervé D. (2001) Galpha(olf) is necessary for coupling D1 and A2a receptors to adenylyl cyclase in the striatum. *J. Neurochem.* **76**, 1585–1588.
Coull J. T., Hwang H. J., Leyton M., Dagher A. (2012) Dopamine Precursor Depletion Impairs Timing in Healthy Volunteers by Attenuating Activity in Putamen and Supplementary Motor Area. *J. Neurosci.* **32**, 16704–16715.
Courvoisie H., Hooper S. R., Fine C., Kwock L., Castillo M. (2004) Neurometabolic Functioning and Neuropsychological Correlates in Children with ADHD-H: Preliminary Findings. *J. Neuropsychiatry Clin. Neurosci.* **16**, 63–69.
Cremer J. E., Braun L. D., Oldendorf W. H. (1976) Changes during development in transport processes of the blood-brain barrier. *BBA - Biomembr.* **448**, 633–637.

Crook J., Hendrickson A., Robinson F. R. (2006) Co-localization of glycine and gaba immunoreactivity in interneurons in Macaca monkey cerebellar cortex. *Neuroscience* **141**, 1951–1959.

Dahlström A., Fuxe K. (1964) Evidence for the existence of monoamine-containing neurons in the central nervous system. I, Demonstration of monoamines in the cell bodies of brain stem neurons. *Acta Physiol. Scand. Suppl.*, SUPPL 232:1-55.

Danbolt N. C. (2001) Glutamate uptake. *Prog. Neurobiol.* **65**, 1–105.

Darvesh A. S., Carroll R. T., Geldenhuys W. J., Gudelsky G. A., Klein J., Meshul C. K., Van der Schyf C. J. (2011) In vivo brain microdialysis: advances in neuropsychopharmacology and drug discovery. *Expert Opin. Drug Discov.* **6**, 109–127.

Daubner S. C., Le T., Wang S. (2011) Tyrosine Hydroxylase and Regulation of Dopamine Synthesis. *Arch. Biochem. Biophys.* **508**, 1–12.

De Mei C., Ramos M., Iitaka C., Borrelli E. (2009) Getting specialized: presynaptic and postsynaptic dopamine D2 receptors. *Curr. Opin. Pharmacol.* **9**, 53–58.

De Smet H. J., Paquier P., Verhoeven J., Mariën P. (2013) The cerebellum: Its role in language and related cognitive and affective functions. *Brain Lang.* **127**, 334–342.

Deelchand D. K., Shestov A. A., Koski D. M., Uğurbil K., Henry P.-G. (2009) Acetate Transport and Utilization in the Rat Brain. *J. Neurochem.* **109**, 46–54.

Del Arco A., Mora F. (2005) Glutamate-dopamine in vivo interaction in the prefrontal cortex modulates the release of dopamine and acetylcholine in the nucleus accumbens of the awake rat. *J. Neural Transm.* **112**, 97–109.

Del Campo N., Chamberlain S. R., Sahakian B. J., Robbins T. W. (2011) The Roles of Dopamine and Noradrenaline in the Pathophysiology and Treatment of Attention-Deficit/Hyperactivity Disorder. *Biol. Psychiatry* **69**, e145–e157.

Derflinger S., Gaser C., Myers N., Arsic M., Kurz A., Zimmer C., Wohlschläger A., Mühlau M. (2011) Grey-matter atrophy in Alzheimer's disease is asymmetric but not lateralized. *J. Alzheimers Dis.* **25**, 347–357.

Di Miceli M., Gronier B. (2015) Psychostimulants and atomoxetine alter the electrophysiological activity of prefrontal cortex neurons, interaction with catecholamine and glutamate NMDA receptors. *Psychopharmacology (Berl.)* **232**, 2191–2205.

Dickstein S. G., Bannon K., Castellanos F. X., Milham M. P. (2006) The neural correlates of attention deficit hyperactivity disorder: an ALE meta-analysis. *J. Child Psychol. Psychiatry* **47**, 1051–1062.

Dietz P., Striegel H., Franke A. G., Lieb K., Simon P., Ulrich R. (2013) Randomized response estimates for the 12-month prevalence of cognitive-enhancing drug use in university students. *Pharmacotherapy* **33**, 44–50.

Dona A. C., Kyriakides M., Scott F., Shephard E. A., Varshavi D., Veselkov K., Everett J. R. (2016) A guide to the identification of metabolites in NMR-based metabonomics/metabolomics experiments. *Comput. Struct. Biotechnol. J.* **14**, 135–153.

Dorval K. M., Wigg K. G., Crosbie J., Tannock R., Kennedy J. L., Ickowicz A., Pathare T., Malone M., Schachar R., Barr C. L. (2007) Association of the glutamate receptor subunit gene GRIN2B with attention-deficit/hyperactivity disorder. *Genes Brain Behav.* **6**, 444–452.

Dougherty D. D., Bonab A. A., Spencer T. J., Rauch S. L., Madras B. K., Fischman A. J. (1999) Dopamine transporter density in patients with attention deficit hyperactivity disorder. *Lancet Lond. Engl.* **354**, 2132–2133.

Dramsdahl M., Ersland L., Plessen K. J., Haavik J., Hugdahl K., Specht K. (2011) Adults with Attention-Deficit/Hyperactivity Disorder – A Brain Magnetic Resonance Spectroscopy Study. *Front. Psychiatry* **2**.

Drui G., Carnicella S., Carcenac C., Favier M., Bertrand A., Boulet S., Savasta M. (2014) Loss of dopaminergic nigrostriatal neurons accounts for the motivational and affective deficits in Parkinson's disease. *Mol. Psychiatry* **19**, 358–367.

Du C., Shao X., Zhu R., Li Y., Zhao Q., Fu D., Gu H., et al. (2015) NMR-Based Metabolic Profiling Reveals Neurochemical Alterations in the Brain of Rats Treated with Sorafenib. *Neurotox. Res.*

Dudman J. T., Eaton M. E., Rajadhyaksha A., Macías W., Taher M., Barczak A., Kameyama K., Huganir R., Konradi C. (2003) Dopamine D1 receptors mediate CREB phosphorylation via phosphorylation of the NMDA receptor at Ser897–NR1. *J. Neurochem.* **87**, 922–934.

Dugué G. P., Dumoulin A., Triller A., Dieudonné S. (2005) Target-dependent use of coreleased inhibitory transmitters at central synapses. *J. Neurosci.* **25**, 6490–6498.

Dumoulin A., Triller A., Dieudonné S. (2001) IPSC kinetics at identified GABAergic and mixed GABAergic and glycinergic synapses onto cerebellar Golgi cells. *J. Neurosci.* **21**, 6045–6057.

Duncan N. W., Wiebking C., Northoff G. (2014) Associations of regional GABA and glutamate with intrinsic and extrinsic neural activity in humans—A review of multimodal imaging studies. *Neurosci. Biobehav. Rev.* **47**, 36–52.

Durnin L., Dai Y., Aiba I., Shuttleworth C. W., Yamboliev I. A., Mutafova-Yambolieva V. N. (2012) Release, neuronal effects and removal of extracellular β-nicotinamide adenine dinucleotide (β-NAD^+) in the rat brain. *Eur. J. Neurosci.* **35**, 423–435.

Durston S., Zeeuw P. de, Staal W. G. (2009) Imaging genetics in ADHD: A focus on cognitive control. *Neurosci. Biobehav. Rev.* **33**, 674–689.

Edden R. A. E., Crocetti D., Zhu H., Gilbert D. L., Mostofsky S. H. (2012) Reduced GABA concentration in attention-deficit/hyperactivity disorder. *Arch. Gen. Psychiatry* **69**, 750–753.

Engert V., Pruessner J. C. (2008) Dopaminergic and Noradrenergic Contributions to Functionality in ADHD: The Role of Methylphenidate. *Curr. Neuropharmacol.* **6**, 322–328.

Everitt B. J., Robbins T. W. (2005) Neural systems of reinforcement for drug addiction: from actions to habits to compulsion. *Nat. Neurosci.* **8**, 1481–1489.

Fair D. A., Posner J., Nagel B. J., Bathula D., Dias T. G. C., Mills K. L., Blythe M. S., Giwa A., Schmitt C. F., Nigg J. T. (2010) Atypical default network connectivity in youth with attention-deficit/ hyperactivity disorder. *Biol. Psychiatry* **68**, 1084–1091.

Faraone S. V., Biederman J., Spencer T., Michelson D., Adler L., Reimherr F., Glatt S. J. (2005a) Efficacy of atomoxetine in adult attention-Deficit/Hyperactivity Disorder: a drug-placebo response curve analysis. *Behav. Brain Funct. BBF* **1**, 16.

Faraone S. V., Mick E. (2010) Molecular Genetics of Attention Deficit Hyperactivity Disorder. *Psychiatr. Clin. North Am.* **33**, 159–180.

Faraone S. V., Perlis R. H., Doyle A. E., Smoller J. W., Goralnick J. J., Holmgren M. A., Sklar P. (2005b) Molecular Genetics of Attention-Deficit/Hyperactivity Disorder. *Biol. Psychiatry* **57**, 1313–1323.

Feenstra M. G. P., van der W., Botterblom M. H. A. (1995) Concentration-dependent dual action of locally applied N-methyl-d-aspartate on extracellular dopamine in the rat prefrontal cortex in vivo. *Neurosci. Lett.* **201**, 175–178.

Fekete M. I., Szentendrei T., Herman J. P., Kanyicska B. (1980) Effects of reserpine and antidepressants on dopamine and DOPAC (3,4-dihydroxyphenylacetic acid) concentrations in the striatum, olfactory tubercle and median eminence of rats. *Eur. J. Pharmacol.* **64**, 231–238.

Fernando J. C., Curzon G. (1978) Effect of d-amphetamine on tryptophan and other aromatic amino acids in brain. *Eur. J. Pharmacol.* **49**, 339–349.

Fernström J. D. (2013) Large neutral amino acids: dietary effects on brain neurochemistry and function. *Amino Acids* **45**, 419–430.

Fernström J. D., Fernström M. H. (2007) Tyrosine, phenylalanine, and catecholamine synthesis and function in the brain. *J. Nutr.* **137**, 1539S–1547S; discussion 1548S.

Filipek P. A., Semrud-Clikeman M., Steingard R. J., Renshaw P. F., Kennedy D. N., Biederman J. (1997) Volumetric MRI analysis comparing subjects having attention-deficit hyperactivity disorder with normal controls. *Neurology* **48**, 589–601.

Fine E. J., Ionita C. C., Lohr L. (2002) The history of the development of the cerebellar examination. *Semin. Neurol.* **22**, 375–384.

Fisher S. E., Francks C., McCracken J. T., McGough J. J., Marlow A. J., MacPhie I. L., Newbury D. F., et al. (2002) A Genomewide Scan for Loci Involved in Attention-Deficit/Hyperactivity Disorder. *Am. J. Hum. Genet.* **70**, 1183–1196.

Fleckenstein A. E., Volz T. J., Hanson G. R. (2009) Psychostimulant-induced alterations in vesicular monoamine transporter-2 function: Neurotoxic and therapeutic implications. *Neuropharmacology* **56**, **Supplement 1**, 133–138.

Ford C. P., Gantz S. C., Phillips P. E. M., Williams J. T. (2010) Control of extracellular dopamine at dendrite and axon terminals. *J. Neurosci. Off. J. Soc. Neurosci.* **30**, 6975–6983.

Fornstedt B., Carlsson A. (1989) A marked rise in 5-S-cysteinyl-dopamine levels in guinea-pig striatum following reserpine treatment. *J. Neural Transm.* **76**, 155–161.

Fossbakk A., Kleppe R., Knappskog P. M., Martinez A., Haavik J. (2014) Functional Studies of Tyrosine Hydroxylase Missense Variants Reveal Distinct Patterns of Molecular Defects in Dopa-Responsive Dystonia. *Hum. Mutat.* **35**, 880–890.

Freese L., Muller E. J., Souza M. F., Couto-Pereira N. S., Tosca C. F., Ferigolo M., Barros H. M. T. (2012) GABA system changes in methylphenidate sensitized female rats. *Behav. Brain Res.* **231**, 181–186.

Fricks-Gleason A. N., Marshall J. F. (2011) Role of Dopamine D1 Receptors in the Activation of Nucleus Accumbens Extracellular Signal-Regulated Kinase (ERK) by Cocaine-Paired Contextual Cues. *Neuropsychopharmacology* **36**, 434–444.

Fromer M., Pocklington A. J., Kavanagh D. H., Williams H. J., Dwyer S., Gormley P., Georgieva L., et al. (2014) De novo mutations in schizophrenia implicate synaptic networks. *Nature* **506**, 179–184.

Fry J. M. (1998) Treatment modalities for narcolepsy. *Neurology* **50**, S43-48.

Fusar-Poli P., Rubia K., Rossi G., Sartori G., Balottin U. (2012) Striatal dopamine transporter alterations in ADHD: pathophysiology or adaptation to psychostimulants? A meta-analysis. *Am. J. Psychiatry* **169**, 264–272.

Gadow K. D., DeVincent C. J., Siegal V. I., Olvet D. M., Kibria S., Kirsch S. F., Hatchwell E. (2013) Allele-specific associations of 5-HTTLPR/rs25531 with ADHD and autism spectrum disorder. *Prog. Neuropsychopharmacol. Biol. Psychiatry* **40**, 292–297.

Gahr M., Freudenmann R. W., Hiemke C., Kölle M. A., Schönfeldt-Lecuona C. (2014) Abuse of methylphenidate in Germany: Data from spontaneous reports of adverse drug reactions. *Psychiatry Res.* **215**, 252–254.

Gainetdinov R. R., Jones S. R., Caron M. G. (1999) Functional hyperdopaminergia in dopamine transporter knock-out mice. *Biol. Psychiatry* **46**, 303–311.

Gallagher T. A., Nemeth A. J., Hacein-Bey L. (2008) An Introduction to the Fourier Transform: Relationship to MRI. *Am. J. Roentgenol.* **190**, 1396–1405.

Gamo N. J., Wang M., Arnsten A. F. T. (2010) Methylphenidate and atomoxetine enhance prefrontal function through α2-adrenergic and dopamine D1 receptors. *J. Am. Acad. Child Adolesc. Psychiatry* **49**, 1011–1023.

Gao H.-C., Zhu H., Song C.-Y., Lin L., Xiang Y., Yan Z.-H., Bai G.-H., Ye F.-Q., Li X.-K. (2012) Metabolic Changes Detected by Ex Vivo High Resolution 1H NMR Spectroscopy in the Striatum of 6-OHDA-Induced Parkinson's Rat. *Mol. Neurobiol.* **47**, 123–130.

García-Sánchez C., Estévez-González A., Suárez-Romero E., Junqué C. (1997) Right hemisphere dysfunction in subjects with attention-deficit disorder with and without hyperactivity. *J. Child Neurol.* **12**, 107–115.

Garibyan L., Avashia N. (2013) Research Techniques Made Simple: Polymerase Chain Reaction (PCR). *J. Invest. Dermatol.* **133**, e6.

Gaude E., Chignola F., Spiliotopoulos D., Spitaleri A., Ghitti M., M Garcia-Manteiga J., Mari S., Musco G. (2013) muma, An R Package for Metabolomics Univariate and Multivariate Statistical Analysis. *Curr. Metabolomics* **1**, 180–189.

Georges F., Aston-Jones G. (2002) Activation of ventral tegmental area cells by the bed nucleus of the stria terminalis: a novel excitatory amino acid input to midbrain dopamine neurons. *J. Neurosci. Off. J. Soc. Neurosci.* **22**, 5173–5187.

Geurts H. M., Verté S., Oosterlaan J., Roeyers H., Sergeant J. A. (2005) ADHD subtypes: do they differ in their executive functioning profile? *Arch. Clin. Neuropsychol.* **20**, 457–477.

Glaser P. E. A., Surgener S. P., Grondin R., Gash C. R., Palmer M., Castellanos F. X., Gerhardt G. A. (2006) Cerebellar neurotransmission in attention-deficit/hyperactivity disorder: does dopamine neurotransmission occur in the cerebellar vermis? *J. Neurosci. Methods* **151**, 62–67.

Glick S. D., Ross D. A. (1981) Lateralization of function in the rat brain: Basic mechanisms may be operative in humans. *Trends Neurosci.* **4**, 196–199.

Goitia B., Raineri M., González L. E., Rozas J. L., Garcia-Rill E., Bisagno V., Urbano F. J. (2013) Differential effects of methylphenidate and cocaine on GABA transmission in sensory thalamic nuclei. *J. Neurochem.* **124**, 602–612.

Goldman-Rakic P. S. (1995) Cellular basis of working memory. *Neuron* **14**, 477–485.

Goldman-Rakic P. S., Castner S. A., Svensson T. H., Siever L. J., Williams G. V. (2004) Targeting the dopamine D1 receptor in schizophrenia: insights for cognitive dysfunction. *Psychopharmacology (Berl.)* **174**, 3–16.

Golla H., Thier P., Haarmeier T. (2005) Disturbed overt but normal covert shifts of attention in adult cerebellar patients. *Brain J. Neurol.* **128**, 1525–1535.

Gong W., Neill D. B., Lynn M., Justice J. B. (1999) Dopamine D1/D2 agonists injected into nucleus accumbens and ventral pallidum differentially affect locomotor activity depending on site. *Neuroscience* **93**, 1349–1358.

Govind S., Kozma R., Monfries C., Lim L., Ahmed S. (2001) Cdc42Hs facilitates cytoskeletal reorganization and neurite outgrowth by localizing the 58-kD insulin receptor substrate to filamentous actin. *J. Cell Biol.* **152**, 579–594.

Govindaraju V., Young K., Maudsley A. A. (2000) Proton NMR chemical shifts and coupling constants for brain metabolites. *NMR Biomed.* **13**, 129–153.
Greenbaum D., Colangelo C., Williams K., Gerstein M. (2003) Comparing protein abundance and mRNA expression levels on a genomic scale. *Genome Biol.* **4**, 117.
Greenhill L., Beyer D. H., Finkleson J., Shaffer D., Biederman J., Conners C. K., Gillberg C., et al. (2002) Guidelines and algorithms for the use of methylphenidate in children with Attention-Deficit/ Hyperactivity Disorder. *J. Atten. Disord.* **6 Suppl 1**, S89-100.
Grenhoff J., Nisell M., Ferré S., Aston-Jones G., Svensson T. H. (1993) Noradrenergic modulation of midbrain dopamine cell firing elicited by stimulation of the locus coeruleus in the rat. *J. Neural Transm. Gen. Sect.* **93**, 11–25.
Grenhoff J., Svensson T. H. (1993) Prazosin modulates the firing pattern of dopamine neurons in rat ventral tegmental area. *Eur. J. Pharmacol.* **233**, 79–84.
Gronier B., Aston J., James A., Liauzun C., Claire L., Zetterström T. (2010) Age-dependent effects of methylphenidate in the prefrontal cortex: evidence from electrophysiological and Arc gene expression measurements. *J. Psychopharmacol. Oxf. Engl.* **24**, 1819–1827.
Habib R., Nyberg L., Tulving E. (2003) Hemispheric asymmetries of memory: the HERA model revisited. *Trends Cogn. Sci.* **7**, 241–245.
Hannestad J., Gallezot J.-D., Planeta-Wilson B., Lin S.-F., Williams W. A., Dyck C. H. van, Malison R. T., Carson R. E., Ding Y.-S. (2010) Clinically Relevant Doses of Methylphenidate Significantly Occupy the Norepinephrine Transporter in Humans In Vivo. *Biol. Psychiatry* **68**, 854–860.
Harris J. J., Attwell D. (2012) The energetics of CNS white matter. *J. Neurosci.* **32**, 356–371.
Haydon P. G., Blendy J., Moss S. J., Rob Jackson F. (2009) Astrocytic control of synaptic transmission and plasticity: a target for drugs of abuse? *Neuropharmacology* **56 Suppl 1**, 83–90.
Hazell P. (2011) The challenges to demonstrating long-term effects of psychostimulant treatment for attention-deficit/hyperactivity disorder. *Curr. Opin. Psychiatry* **24**, 286–290.
H'Doubler P. B., Peterson M., Shek W., Auchincloss H., Abbott W. M., Orkin R. W. (1991) Spontaneously hypertensive and Wistar Kyoto rats are genetically disparate. *Lab. Anim. Sci.* **41**, 471–473.
Heal D. J., Pierce D. M. (2006) Methylphenidate and its isomers: their role in the treatment of attention-deficit hyperactivity disorder using a transdermal delivery system. *CNS Drugs* **20**, 713–738.
Hebebrand J., Dempfle A., Saar K., Thiele H., Herpertz-Dahlmann B., Linder M., Kiefl H., et al. (2006) A genome-wide scan for attention-deficit/hyperactivity disorder in 155 German sib-pairs. *Mol. Psychiatry* **11**, 196–205.
Heilman K. M., Bowers D., Valenstein E., Watson R. T. (1986) The right hemisphere: neuropsychological functions. *J. Neurosurg.* **64**, 693–704.
Heilman K. M., Van Den Abell T. (1980) Right hemisphere dominance for attention: the mechanism underlying hemispheric asymmetries of inattention (neglect). *Neurology* **30**, 327–330.
Hernández L. F., Segovia G., Mora F. (2003) Effects of Activation of NMDA and AMPA Glutamate Receptors on the Extracellular Concentrations of Dopamine, Acetylcholine, and GABA in Striatum of the Awake Rat: A Microdialysis Study. *Neurochem. Res.* **28**, 1819–1827.
Herring B. E., Silm K., Edwards R. H., Nicoll R. A. (2015) Is Aspartate an Excitatory Neurotransmitter? *J. Neurosci.* **35**, 10168–10171.

Hervé D. (2011) Identification of a Specific Assembly of the G Protein Golf as a Critical and Regulated Module of Dopamine and Adenosine-Activated cAMP Pathways in the Striatum. *Front. Neuroanat.* **5**.

Hetzler B. E., Meckel K. R., Stickle B. A. (2014) Methylphenidate alters flash-evoked potentials, body temperature, and behavior in Long-Evans rats. *Pharmacol. Biochem. Behav.* **116**, 75–83.

Higgs H. N., Pollard T. D. (2001) Regulation of actin filament network formation through ARP2/3 complex: activation by a diverse array of proteins. *Annu. Rev. Biochem.* **70**, 649–676.

Hinz M., Stein A., Neff R., Weinberg R., Uncini T. (2011) Treatment of attention deficit hyperactivity disorder with monoamine amino acid precursors and organic cation transporter assay interpretation. *Neuropsychiatr. Dis. Treat.* **7**, 31–38.

Hoekzema E., Carmona S., Ramos-Quiroga J. A., Barba E., Bielsa A., Tremols V., Rovira M., et al. (2011) Training-induced neuroanatomical plasticity in ADHD: a tensor-based morphometric study. *Hum. Brain Mapp.* **32**, 1741–1749.

Holmer H. K., Keyghobadi M., Moore C., Meshul C. K. (2005) l-dopa-induced reversal in striatal glutamate following partial depletion of nigrostriatal dopamine with 1-methyl-4-phenyl-1,2,3,6-tetrahydropyridine. *Neuroscience* **136**, 333–341.

Holmes E., Tsang T. M., Huang J. T.-J., Leweke F. M., Koethe D., Gerth C. W., Nolden B. M., et al. (2006) Metabolic profiling of CSF: evidence that early intervention may impact on disease progression and outcome in schizophrenia. *PLoS Med.* **3**, e327.

Holmes S. E., O'Hearn E., Rosenblatt A., Callahan C., Hwang H. S., Ingersoll-Ashworth R. G., Fleisher A., et al. (2001) A repeat expansion in the gene encoding junctophilin-3 is associated with Huntington disease-like 2. *Nat. Genet.* **29**, 377–378.

Holten A. T., Gundersen V. (2008) Glutamine as a precursor for transmitter glutamate, aspartate and GABA in the cerebellum: a role for phosphate-activated glutaminase. *J. Neurochem.* **104**, 1032–1042.

Hori K., Yasuda H., Konno D., Maruoka H., Tsumoto T., Sobue K. (2005) NMDA Receptor-Dependent Synaptic Translocation of Insulin Receptor Substrate p53 via Protein Kinase C Signaling. *J. Neurosci.* **25**, 2670–2681.

Hornykiewicz O. (2002) Dopamine miracle: From brain homogenate to dopamine replacement. *Mov. Disord.* **17**, 501–508.

Hynd G. W., Hern K. L., Novey E. S., Eliopulos D., Marshall R., Gonzalez J. J., Voeller K. K. (1993) Attention deficit-hyperactivity disorder and asymmetry of the caudate nucleus. *J. Child Neurol.* **8**, 339–347.

Ieraci A., Herrera D. G. (2006) Nicotinamide Protects against Ethanol-Induced Apoptotic Neurodegeneration in the Developing Mouse Brain. *PLOS Med.* **3**, e101.

Ikai Y., Takada M., Shinonaga Y., Mizuno N. (1992) Dopaminergic and non-dopaminergic neurons in the ventral tegmental area of the rat project, respectively, to the cerebellar cortex and deep cerebellar nuclei. *Neuroscience* **51**, 719–728.

Ivanov I., Murrough J. W., Bansal R., Hao X., Peterson B. S. (2014) Cerebellar Morphology and the Effects of Stimulant Medications in Youths with Attention Deficit-Hyperactivity Disorder. *Neuropsychopharmacology* **39**, 718–726.

Iversen S. D., Iversen L. L. (2007) Dopamine: 50 years in perspective. *Trends Neurosci.* **30**, 188–193.

Ivry R. B., Spencer R. M., Zelaznik H. N., Diedrichsen J. (2002) The cerebellum and event timing. *Ann. N. Y. Acad. Sci.* **978**, 302–317.

Jaanus S. D. (1992) Ocular side effects of selected systemic drugs. *Optom. Clin. Off. Publ. Prentice Soc.* **2**, 73–96.
Jenson D., Yang K., Acevedo-Rodriguez A., Levine A., Broussard J. I., Tang J., Dani J. A. (2015) Dopamine and norepinephrine receptors participate in methylphenidate enhancement of in vivo hippocampal synaptic plasticity. *Neuropharmacology* **90**, 23–32.
Jin Z., Zang Y. F., Zeng Y. W., Zhang L., Wang Y. F. (2001) Striatal neuronal loss or dysfunction and choline rise in children with attention-deficit hyperactivity disorder: a 1H-magnetic resonance spectroscopy study. *Neurosci. Lett.* **315**, 45–48.
Jones S. (2011) *Dopamine – Glutamate Interactions in the Basal Ganglia. https://www.crcpress.com/Dopamine--Glutamate-Interactions-in-the-Basal-Ganglia/Jones/9781420088793*.
Jones S. R., Gainetdinov R. R., Jaber M., Giros B., Wightman R. M., Caron M. G. (1998) Profound neuronal plasticity in response to inactivation of the dopamine transporter. *Proc. Natl. Acad. Sci. U. S. A.* **95**, 4029–4034.
Kalivas P. W., Duffy P. (1997) Dopamine regulation of extracellular glutamate in the nucleus accumbens. *Brain Res.* **761**, 173–177.
Kalivas P. W., O'Brien C. (2008) Drug addiction as a pathology of staged neuroplasticity. *Neuropsychopharmacol. Off. Publ. Am. Coll. Neuropsychopharmacol.* **33**, 166–180.
Kang J., Park H., Kim E. (2016) IRSp53/BAIAP2 in dendritic spine development, NMDA receptor regulation, and psychiatric disorders. *Neuropharmacology* **100**, 27–39.
Kapur S., Remington G. (1996) Serotonin-dopamine interaction and its relevance to schizophrenia. *Am. J. Psychiatry* **153**, 466–476.
Karreman M., Moghaddam B. (1996) The prefrontal cortex regulates the basal release of dopamine in the limbic striatum: an effect mediated by ventral tegmental area. *J. Neurochem.* **66**, 589–598.
Kasai H., Matsuzaki M., Noguchi J., Yasumatsu N., Nakahara H. (2003) Structure-stability-function relationships of dendritic spines. *Trends Neurosci.* **26**, 360–368.
Kendrick K. M., Guevara-Guzman R., De L. R., Christensen J., Østergaard K., Emson P. C. (1996) NMDA and kainate-evoked release of nitric oxide and classical transmitters in the rat striatum: In vivo evidence that nitric oxide may play a neuroprotective role. *Eur. J. Neurosci.* **8**, 2619–2634.
Kennard M., Spencer S., Fountain J. (1941) Hyperactivity in monkeys following lesions of the frontal lobes. *J Neuro- Physiol.* **4**, 512–524.
Kessler R. C., Adler L., Berkley R., Biederman J., Conners C. K., Demler O., Faraone S. V., et al. (2006) The prevalence and correlates of adult ADHD in the United States: Results from the National Comorbidity Survey Replication. *Am. J. Psychiatry* **163**, 716–723.
Killeen P. R., Russell V. A., Sergeant J. A. (2013) A behavioral neuroenergetics theory of ADHD. *Neurosci. Biobehav. Rev.* **37**, 625–657.
Kim C. H., Lisman J. E. (1999) A role of actin filament in synaptic transmission and long-term potentiation. *J. Neurosci. Off. J. Soc. Neurosci.* **19**, 4314–4324.
Kim Y., Teylan M. A., Baron M., Sands A., Nairn A. C., Greengard P. (2009) Methylphenidate-induced dendritic spine formation and DeltaFosB expression in nucleus accumbens. *Proc. Natl. Acad. Sci. U. S. A.* **106**, 2915–2920.
Klein-Schwartz W. (2003) Pediatric methylphenidate exposures: 7-Year experience of poison centers in the United States. *Clin. Pediatr. (Phila.)* **42**, 159–164.
Koda K., Ago Y., Cong Y., Kita Y., Takuma K., Matsuda T. (2010) Effects of acute and chronic administration of atomoxetine and methylphenidate on extracellular levels of

noradrenaline, dopamine and serotonin in the prefrontal cortex and striatum of mice. *J. Neurochem.* **114**, 259–270.
Kolar D., Keller A., Golfinopoulos M., Cumyn L., Syer C., Hechtman L. (2008) Treatment of adults with attention-deficit/hyperactivity disorder. *Neuropsychiatr. Dis. Treat.* **4**, 389–403.
Konradi C., Leveque J. C., Hyman S. E. (1996) Amphetamine and dopamine-induced immediate early gene expression in striatal neurons depends on postsynaptic NMDA receptors and calcium. *J. Neurosci. Off. J. Soc. Neurosci.* **16**, 4231–4239.
Kontro P., Oja S. S. (1990) Interactions of taurine with GABAB binding sites in mouse brain. *Neuropharmacology* **29**, 243–247.
Koob G. F., Volkow N. D. (2010) Neurocircuitry of Addiction. *Neuropsychopharmacology* **35**, 217–238.
Korb E., Finkbeiner S. (2011) Arc in synaptic plasticity: from gene to behavior. *Trends Neurosci.* **34**, 591–598.
Kraemer M., Uekermann J., Wiltfang J., Kis B. (2010) Methylphenidate-induced psychosis in adult attention-deficit/hyperactivity disorder: report of 3 new cases and review of the literature. *Clin. Neuropharmacol.* **33**, 204–206.
Krapacher F. A., Mlewski E. C., Ferreras S., Pisano V., Paolorossi M., Hansen C., Paglini G. (2010) Mice lacking p35 display hyperactivity and paradoxical response to psychostimulants. *J. Neurochem.* **114**, 203–214.
Kristian T., Balan I., Schuh R., Onken M. (2011) Mitochondrial dysfunction and nicotinamide dinucleotide catabolism as mechanisms of cell death and promising targets for neuroprotection. *J. Neurosci. Res.* **89**, 1946–1955.
Kristofiková Z., Rícný J., Ort M., Rípová D. (2010) Aging and lateralization of the rat brain on a biochemical level. *Neurochem. Res.* **35**, 1138–1146.
Kronenberg G., Ende G., Alm B., Deuschle M., Heuser I., Colla M. (2008) Increased NAA and reduced choline levels in the anterior cingulum following chronic methylphenidate: A spectroscopic test-retest study in adult ADHD. *Eur. Arch. Psychiatry Clin. Neurosci.* **258**, 446–450.
Krugmann S., Jordens I., Gevaert K., Driessens M., Vandekerckhove J., Hall A. (2001) Cdc42 induces filopodia by promoting the formation of an IRSp53:Mena complex. *Curr. Biol. CB* **11**, 1645–1655.
Kuczenski R., Segal D. S. (2002) Exposure of adolescent rats to oral methylphenidate: preferential effects on extracellular norepinephrine and absence of sensitization and cross-sensitization to methamphetamine. *J. Neurosci. Off. J. Soc. Neurosci.* **22**, 7264–7271.
Kuczenski R., Segal D. S. (2005) Stimulant actions in rodents: implications for attention-deficit/hyperactivity disorder treatment and potential substance abuse. *Biol. Psychiatry* **57**, 1391–1396.
Kuntsi J., Eley T. C., Taylor A., Hughes C., Asherson P., Caspi A., Moffitt T. E. (2004) Co-occurrence of ADHD and low IQ has genetic origins. *Am. J. Med. Genet. Part B Neuropsychiatr. Genet. Off. Publ. Int. Soc. Psychiatr. Genet.* **124B**, 41–47.
Kurien B. T., Scofield R. H. (2006) Western blotting. *Methods* **38**, 283–293.
Laatikainen L. M., Sharp T., Harrison P. J., Tunbridge E. M. (2013) Sexually Dimorphic Effects of Catechol-O-Methyltransferase (COMT) Inhibition on Dopamine Metabolism in Multiple Brain Regions. *PLOS ONE* **8**, e61839.

Lakhan S. E., Kirchgessner A. (2012) Prescription stimulants in individuals with and without attention deficit hyperactivity disorder: misuse, cognitive impact, and adverse effects. *Brain Behav.* **2**, 661–677.

Lan M. J., McLoughlin G. A., Griffin J. L., Tsang T. M., Huang J. T. J., Yuan P., Manji H., Holmes E., Bahn S. (2008) Metabonomic analysis identifies molecular changes associated with the pathophysiology and drug treatment of bipolar disorder. *Mol. Psychiatry* **14**, 269–279.

Larrabee M. G. (1995) Lactate metabolism and its effects on glucose metabolism in an excised neural tissue. *J. Neurochem.* **64**, 1734–1741.

Lavielle S., Tassin J.-P., Thierry A.-M., Blanc G., Herve D., Barthelemy C., Glowinski J. (1979) Blockade by benzodiazepines of the selective high increase in dopamine turnover induced by stress in mesocortical dopaminergic neurons of the rat. *Brain Res.* **168**, 585–594.

Le Masurier M., Zetterström T., Cowen P., Sharp T. (2013) Tyrosine-free amino acid mixtures reduce physiologically-evoked release of dopamine in a selective and activity-dependent manner. *J. Psychopharmacol. Oxf. Engl.* **28**, 561–569.

Leibig M., Liebeke M., Mader D., Lalk M., Peschel A., Götz F. (2011) Pyruvate Formate Lyase Acts as a Formate Supplier for Metabolic Processes during Anaerobiosis in Staphylococcus aureus. *J. Bacteriol.* **193**, 952–962.

Lepelletier F.-X., Tauber C., Nicolas C., Solinas M., Castelnau P., Belzung C., Emond P., et al. (2015) Prenatal Exposure to Methylphenidate Affects the Dopamine System and the Reactivity to Natural Reward in Adulthood in Rats. *Int. J. Neuropsychopharmacol.* **18**.

Lesch K. P., Merker S., Reif A., Novak M. (2013) Dances with black widow spiders: Dysregulation of glutamate signalling enters centre stage in ADHD. *Eur. Neuropsychopharmacol.* **23**, 479–491.

Levy D., Ronemus M., Yamrom B., Lee Y., Leotta A., Kendall J., Marks S., et al. (2011) Rare de novo and transmitted copy-number variation in autistic spectrum disorders. *Neuron* **70**, 886–897.

Li Y., Kolb B., Robinson T. E. (2003) The location of persistent amphetamine-induced changes in the density of dendritic spines on medium spiny neurons in the nucleus accumbens and caudate-putamen. *Neuropsychopharmacol. Off. Publ. Am. Coll. Neuropsychopharmacol.* **28**, 1082–1085.

Lindvall O., Björklund A. (1974) The organization of the ascending catecholamine neuron systems in the rat brain as revealed by the glyoxylic acid fluorescence method. *Acta Physiol. Scand. Suppl.* **412**, 1–48.

Lister J. P., Tonkiss J., Blatt G. J., Kemper T. L., DeBassio W. A., Galler J. R., Rosene D. L. (2006) Asymmetry of neuron numbers in the hippocampal formation of prenatally malnourished and normally nourished rats: a stereological investigation. *Hippocampus* **16**, 946–958.

Little K. Y., Zhang L., Desmond T., Frey K. A., Dalack G. W., Cassin B. J. (1999) Striatal dopaminergic abnormalities in human cocaine users. *Am. J. Psychiatry* **156**, 238–245.

Liu G., Xiao L., Fang T., Cai Y., Jia G., Zhao H., Wang J., Chen X., Wu C. (2014) Pea Fiber and Wheat Bran Fiber Show Distinct Metabolic Profiles in Rats as Investigated by a 1H NMR-Based Metabolomic Approach. *PLoS ONE* **9**, e115561.

Liu L., Sun L., Li Z.-H., Li H.-M., Wei L.-P., Wang Y.-F., Qian Q.-J. (2013) BAIAP2 exhibits association to childhood ADHD especially predominantly inattentive subtype in Chinese Han subjects. *Behav. Brain Funct. BBF* **9**, 48.

Lohr K. M., Bernstein A. I., Stout K. A., Dunn A. R., Lazo C. R., Alter S. P., Wang M., et al. (2014) Increased vesicular monoamine transporter enhances dopamine release and opposes Parkinson disease-related neurodegeneration in vivo. *Proc. Natl. Acad. Sci.* **111**, 9977–9982.

Lu C.-K., Kuang T.-M., Chou J. C.-K. (2006) Methylphenidate (Ritalin)-associated cataract and glaucoma. *J. Chin. Med. Assoc. JCMA* **69**, 589–590.

Ma C.-L., Arnsten A. F. T., Li B.-M. (2005) Locomotor hyperactivity induced by blockade of prefrontal cortical alpha2-adrenoceptors in monkeys. *Biol. Psychiatry* **57**, 192–195.

Macey D. J., Smith H. R., Nader M. A., Porrino L. J. (2003) Chronic cocaine self-administration upregulates the norepinephrine transporter and alters functional activity in the bed nucleus of the stria terminalis of the rhesus monkey. *J. Neurosci. Off. J. Soc. Neurosci.* **23**, 12–16.

Mahmood T., Yang P.-C. (2012) Western Blot: Technique, Theory, and Trouble Shooting. *North Am. J. Med. Sci.* **4**, 429–434.

Maiti P., Manna J., Ilavazhagan G., Rossignol J., Dunbar G. L. (2015) Molecular regulation of dendritic spine dynamics and their potential impact on synaptic plasticity and neurological diseases. *Neurosci. Biobehav. Rev.* **59**, 208–237.

Makris N., Biederman J., Valera E. M., Bush G., Kaiser J., Kennedy D. N., Caviness V. S., Faraone S. V., Seidman L. J. (2007) Cortical thinning of the attention and executive function networks in adults with attention-deficit/hyperactivity disorder. *Cereb. Cortex N. Y. N 1991* **17**, 1364–1375.

Maltezos S., Horder J., Coghlan S., Skirrow C., O'Gorman R., Lavender T. J., Mendez M. A., et al. (2014) Glutamate/glutamine and neuronal integrity in adults with ADHD: a proton MRS study. *Transl. Psychiatry* **4**, e373.

Marie S. K. N., Shinjo S. M. O. (2011) Metabolism and Brain Cancer. *Clinics* **66**, 33–43.

Marsman A., Mandl R. C. W., Klomp D. W. J., Bohlken M. M., Boer V. O., Andreychenko A., Cahn W., Kahn R. S., Luijten P. R., Hulshoff Pol H. E. (2014) GABA and glutamate in schizophrenia: A 7 T 1H-MRS study. *NeuroImage Clin.* **6**, 398–407.

McCarthy S., Wilton L., Murray M. L., Hodgkins P., Asherson P., Wong I. C. (2012) The epidemiology of pharmacologically treated attention deficit hyperactivity disorder (ADHD) in children, adolescents and adults in UK primary care. *BMC Pediatr.* **12**, 78.

McLoughlin G. A., Ma D., Tsang T. M., Jones D. N. C., Cilia J., Hill M. D., Robbins M. J., et al. (2009) Analyzing the effects of psychotropic drugs on metabolite profiles in rat brain using 1H NMR spectroscopy. *J. Proteome Res.* **8**, 1943–1952.

McLoughlin G., Ronald A., Kuntsi J., Asherson P., Plomin R. (2007) Genetic support for the dual nature of attention deficit hyperactivity disorder: substantial genetic overlap between the inattentive and hyperactive-impulsive components. *J. Abnorm. Child Psychol.* **35**, 999–1008.

McTavish S. F. B., Raumann B., Cowen P. J., Sharp T. (2001) Tyrosine depletion attenuates the behavioural stimulant effects of amphetamine and cocaine in rats. *Eur. J. Pharmacol.* **424**, 115–119.

Meiser J., Weindl D., Hiller K. (2013) Complexity of dopamine metabolism. *Cell Commun. Signal. CCS* **11**, 34.

Melchitzky D. S., Lewis D. A. (2000) Tyrosine hydroxylase- and dopamine transporter-immunoreactive axons in the primate cerebellum. Evidence for a lobular- and laminar-specific dopamine innervation. *Neuropsychopharmacol. Off. Publ. Am. Coll. Neuropsychopharmacol.* **22**, 466–472.

Miao J., Fan Q., Cui Q., Zhang H., Chen L., Wang S., Guan N., Guan Y., Ding J. (2009) Newly identified cytoskeletal components are associated with dynamic changes of podocyte foot processes. *Nephrol. Dial. Transplant.* **24**, 3297–3305.

Michaelides M., Pascau J., Gispert J.-D., Delis F., Grandy D. K., Wang G.-J., Desco M., Rubinstein M., Volkow N. D., Thanos P. K. (2010) Dopamine D4 Receptors Modulate Brain Metabolic Activity in the Prefrontal Cortex and Cerebellum at Rest and in Response to Methylphenidate. *Eur. J. Neurosci.* **32**, 668–676.

Middleton F. A., Strick P. L. (1994) Anatomical evidence for cerebellar and basal ganglia involvement in higher cognitive function. *Science* **266**, 458–461.

Miele M., Mura M. A., Enrico P., Esposito G., Serra P. A., Migheli R., Zangani D., Miele E., Desole M. S. (2000) On the mechanism of d-amphetamine-induced changes in glutamate, ascorbic acid and uric acid release in the striatum of freely moving rats. *Br. J. Pharmacol.* **129**, 582–588.

Milich R., Balentine A. C., Lynam D. R. (2001) ADHD Combined Type and ADHD Predominantly Inattentive Type Are Distinct and Unrelated Disorders. *Clin. Psychol. Sci. Pract.* **8**, 463–488.

Miller E. (2014) Dopamine and Glutamate Dysfunction in a Rodent Model of Attention-Deficit/Hyperactivity Disorder: Implications for Future Neuropharmacology. *Theses Diss.--Anat. Neurobiol.*

Milner B., Klein D. (2016) Loss of recent memory after bilateral hippocampal lesions: memory and memories-looking back and looking forward. *J. Neurol. Neurosurg. Psychiatry* **87**, 230.

Missale C., Nash S. R., Robinson S. W., Jaber M., Caron M. G. (1998) Dopamine receptors: from structure to function. *Physiol. Rev.* **78**, 189–225.

Moffett J. R., Ross B., Arun P., Madhavarao C. N., Namboodiri M. A. A. (2007) N-Acetylaspartate in the CNS: From Neurodiagnostics to Neurobiology. *Prog. Neurobiol.* **81**, 89–131.

Moghaddam B., Berridge C. W., Goldman-Rakic P. S., Bunney B. S., Roth R. H. (1993) In vivo assessment of basal and drug-induced dopamine release in cortical and subcortical regions of the anesthetized primate. *Synap. N. Y. N* **13**, 215–222.

Moghaddam B., Bunney B. S. (1989) Differential effect of cocaine on extracellular dopamine levels in rat medial prefrontal cortex and nucleus accumbens: comparison to amphetamine. *Synap. N. Y. N* **4**, 156–161.

Money K. M., Stanwood G. D. (2013) Developmental origins of brain disorders: roles for dopamine. *Front. Cell. Neurosci.* **7**, 260.

Monsma F. J., Mahan L. C., McVittie L. D., Gerfen C. R., Sibley D. R. (1990) Molecular cloning and expression of a D1 dopamine receptor linked to adenylyl cyclase activation. *Proc. Natl. Acad. Sci. U. S. A.* **87**, 6723–6727.

Moore C. M., Biederman J., Wozniak J., Mick E., Aleardi M., Wardrop M., Dougherty M., et al. (2006) Differences in brain chemistry in children and adolescents with attention deficit hyperactivity disorder with and without comorbid bipolar disorder: A proton magnetic resonance spectroscopy study. *Am. J. Psychiatry* **163**, 316–318.

Mora F., Segovia G., Arco A. del (2008) Glutamate–dopamine–GABA interactions in the aging basal ganglia. *Brain Res. Rev.* **58**, 340–353.

Morland C., Nordengen K., Larsson M., Prolo L. M., Farzampour Z., Reimer R. J., Gundersen V. (2013) Vesicular uptake and exocytosis of L-aspartate is independent of sialin. *FASEB J. Off. Publ. Fed. Am. Soc. Exp. Biol.* **27**, 1264–1274.

Moro H., Sato H., Ida I., Oshima A., Sakurai N., Shihara N., Horikawa Y., Mikuni M. (2007) Effects of SKF-38393, a dopamine D1 receptor agonist on expression of amphetamine-induced behavioral sensitization and expression of immediate early gene arc in prefrontal cortex of rats. *Pharmacol. Biochem. Behav.* **87**, 56–64.

Morris M. E., Iansek R., Matyas T. A., Summers J. J. (1994) The pathogenesis of gait hypokinesia in Parkinson's disease. *Brain J. Neurol.* **117 (Pt 5)**, 1169–1181.

Morton W. A., Stockton G. G. (2000) Methylphenidate Abuse and Psychiatric Side Effects. *Prim. Care Companion J. Clin. Psychiatry* **2**, 159–164.

Mullis K. B. (1990) The unusual origin of the polymerase chain reaction. *Sci. Am.* **262**, 56–61, 64–65.

Mulraney M., Schilpzand E. J., Anderson V., Nicholson J. M., Efron D., Hazell P., Sciberras E. (2016) Correlates of Anxiety in 6- to 8-Year-Old Children With ADHD: A Community-Based Study. *J. Atten. Disord.*

Nagel B. J., Bathula D., Herting M., Schmitt C., Kroenke C. D., Fair D., Nigg J. T. (2011) Altered white matter microstructure in children with attention-deficit/ hyperactivity disorder. *J. Am. Acad. Child Adolesc. Psychiatry* **50**, 283–292.

Nakagawa H., Miki H., Nozumi M., Takenawa T., Miyamoto S., Wehland J., Small J. V. (2003) IRSp53 is colocalised with WAVE2 at the tips of protruding lamellipodia and filopodia independently of Mena. *J. Cell Sci.* **116**, 2577–2583.

Narendran R., Jedema H. P., Lopresti B. J., Mason N. S., Himes M. L., Bradberry C. W. (2015) Decreased vesicular monoamine transporter type 2 availability in the striatum following chronic cocaine self-administration in nonhuman primates. *Biol. Psychiatry* **77**, 488–492.

Nielsen J. A., Chapin D. S., Moore K. E. (1983) Differential effects of d-amphetamine, beta-phenylethylamine, cocaine and methylphenidate on the rate of dopamine synthesis in terminals of nigrostriatal and mesolimbic neurons and on the efflux of dopamine metabolites into cerebroventricular perfusates of rats. *Life Sci.* **33**, 1899–1907.

Nielsen J. A., Zielinski B. A., Ferguson M. A., Lainhart J. E., Anderson J. S. (2013) An Evaluation of the Left-Brain vs. Right-Brain Hypothesis with Resting State Functional Connectivity Magnetic Resonance Imaging. *PLoS ONE* **8**, e71275.

Nigg J. T., Swanson J. M., Hinshaw S. P. (1997) Covert visual spatial attention in boys with attention deficit hyperactivity disorder: lateral effects, methylphenidate response and results for parents. *Neuropsychologia* **35**, 165–176.

Ning Y., Sun Q., Dong Y., Xu W., Zhang W., Huang H., Li Q. (2011) Slit2-N inhibits PDGF-induced migration in rat airway smooth muscle cells: WASP and Arp2/3 involved. *Toxicology* **283**, 32–40.

Niswender C. M., Conn P. J. (2010) Metabotropic Glutamate Receptors: Physiology, Pharmacology, and Disease. *Annu. Rev. Pharmacol. Toxicol.* **50**, 295–322.

Nonkes L. J. P., Vondervoort I. I. G. M. van de, Leeuw M. J. C. de, Wijlaars L. P., Maes J. H. R., Homberg J. R. (2012) Serotonin transporter knockout rats show improved strategy set-shifting and reduced latent inhibition. *Learn. Mem. Cold Spring Harb. N* **19**, 190–193.

Nottebohm F. (1971) Neural lateralization of vocal control in a passerine bird. I. Song. *J. Exp. Zool.* **177**, 229–261.

Obeso J. A., Marin C., Rodriguez-Oroz C., Blesa J., Benitez-Temiño B., Mena-Segovia J., Rodríguez M., Olanow C. W. (2008) The basal ganglia in Parkinson's disease: Current concepts and unexplained observations. *Ann. Neurol.* **64**, S30–S46.

Oh S. Y., Knelson E. H., Blobe G. C., Mythreye K. (2013) The type III TGFβ receptor regulates filopodia formation via a Cdc42-mediated IRSp53-N-WASP interaction in epithelial cells. *Biochem. J.* **454**, 79–89.

Ohtsuki S., Yamaguchi H., Kang Y.-S., Hori S., Terasaki T. (2010) Reduction of L-type amino acid transporter 1 mRNA expression in brain capillaries in a mouse model of Parkinson's disease. *Biol. Pharm. Bull.* **33**, 1250–1252.

Onal-Hartmann C., Pauli P., Ocklenburg S., Güntürkün O. (2012) The motor side of emotions: investigating the relationship between hemispheres, motor reactions and emotional stimuli. *Psychol. Res.* **76**, 311–316.

Ottersen O. P., Davanger S., Storm-Mathisen J. (1987) Glycine-like immunoreactivity in the cerebellum of rat and Senegalese baboon, Papio papio: a comparison with the distribution of GABA-like immunoreactivity and with [3H]glycine and [3H]GABA uptake. *Exp. Brain Res.* **66**, 211–221.

Panos J. J., Law C. D., Ferguson S. A. (2014) Effects of perinatal methylphenidate (MPH) treatment in male and female Sprague-Dawley offspring. *Neurotoxicol. Teratol.* **42**, 9–16.

Paoletti L., Elena C., Domizi P., Banchio C. (2011) Role of phosphatidylcholine during neuronal differentiation. *IUBMB Life* **63**, 714–720.

Pasini A., Paloscia C., Alessandrelli R., Porfirio M. C., Curatolo P. (2007) Attention and executive functions profile in drug naive ADHD subtypes. *Brain Dev.* **29**, 400–408.

Paslakis G., Träber F., Roberz J., Block W., Jessen F. (2014) N-acetyl-aspartate (NAA) as a correlate of pharmacological treatment in psychiatric disorders: A systematic review. *Eur. Neuropsychopharmacol.* **24**, 1659–1675.

Patel J., Mooslehner K. A., Chan P. M., Emson P. C., Stamford J. A. (2003) Presynaptic control of striatal dopamine neurotransmission in adult vesicular monoamine transporter 2 (VMAT2) mutant mice. *J. Neurochem.* **85**, 898–910.

Patneau D. K., Mayer M. L. (1990) Structure-activity relationships for amino acid transmitter candidates acting at N-methyl-D-aspartate and quisqualate receptors. *J. Neurosci. Off. J. Soc. Neurosci.* **10**, 2385–2399.

Paxinos G., Watson C. (2006) *The Rat Brain in Stereotaxic Coordinates: Hard Cover Edition*. Academic Press.

Peebles C. L., Yoo J., Thwin M. T., Palop J. J., Noebels J. L., Finkbeiner S. (2010) Arc regulates spine morphology and maintains network stability in vivo. *Proc. Natl. Acad. Sci.* **107**, 18173–18178.

Pellerin L., Magistretti P. J. (1994) Glutamate uptake into astrocytes stimulates aerobic glycolysis: a mechanism coupling neuronal activity to glucose utilization. *Proc. Natl. Acad. Sci.* **91**, 10625–10629.

Pellerin L., Magistretti P. J. (1997) Glutamate uptake stimulates Na+,K+-ATPase activity in astrocytes via activation of a distinct subunit highly sensitive to ouabain. *J. Neurochem.* **69**, 2132–2137.

Perlov E., Philipsen A., Hesslinger B., Buechert M., Ahrendts J., Feige B., Bubl E., Hennig J., Ebert D., Tebartz van Elst L. (2007) Reduced cingulate glutamate/glutamine-to-creatine ratios in adult patients with attention deficit/hyperactivity disorder – A magnet resonance spectroscopy study. *J. Psychiatr. Res.* **41**, 934–941.

Perlov E., Philipsen A., Matthies S., Drieling T., Maier S., Bubl E., Hesslinger B., et al. (2009) Spectroscopic findings in attention-deficit/hyperactivity disorder: Review and meta-analysis. *World J. Biol. Psychiatry* **10**, 355–365.

Perlov E., Tebarzt van Elst L., Buechert M., Maier S., Matthies S., Ebert D., Hesslinger B., Philipsen A. (2010) H1-MR-spectroscopy of cerebellum in adult attention deficit/hyperactivity disorder. *J. Psychiatr. Res.* **44**, 938–943.

Petersen M. R., Beecher M. D., Zoloth, Moody D. B., Stebbins W. C. (1978) Neural lateralization of species-specific vocalizations by Japanese macaques (Macaca fuscata). *Science* **202**, 324–327.

Pettit H. O., Ettenberg A., Bloom F. E., Koob G. F. (1984) Destruction of dopamine in the nucleus accumbens selectively attenuates cocaine but not heroin self-administration in rats. *Psychopharmacology (Berl.)* **84**, 167–173.

Pierce R. C., Kumaresan V. (2006) The mesolimbic dopamine system: The final common pathway for the reinforcing effect of drugs of abuse? *Neurosci. Biobehav. Rev.* **30**, 215–238.

Pifl C., Rajput A., Reither H., Blesa J., Cavada C., Obeso J. A., Rajput A. H., Hornykiewicz O. (2014) Is Parkinson's Disease a Vesicular Dopamine Storage Disorder? Evidence from a Study in Isolated Synaptic Vesicles of Human and Nonhuman Primate Striatum. *J. Neurosci.* **34**, 8210–8218.

Pinho M. J., Serrão M. P., Gomes P., Hopfer U., Jose P. A., Soares-da-Silva P. (2004) Over-expression of renal LAT1 and LAT2 and enhanced L-DOPA uptake in SHR immortalized renal proximal tubular cells. *Kidney Int.* **66**, 216–226.

Polanczyk G. V., Salum G. A., Sugaya L. S., Caye A., Rohde L. A. (2015) Annual research review: A meta-analysis of the worldwide prevalence of mental disorders in children and adolescents. *J. Child Psychol. Psychiatry* **56**, 345–365.

Porrino L. J., Lucignani G. (1987) Different patterns of local brain energy metabolism associated with high and low doses of methylphenidate. Relevance to its action in hyperactive children. *Biol. Psychiatry* **22**, 126–138.

Posner J., Siciliano F., Wang Z., Liu J., Sonuga-Barke E., Greenhill L. (2014) A multimodal MRI study of the hippocampus in medication-naive children with ADHD: What connects ADHD and depression? *Psychiatry Res. Neuroimaging* **224**, 112–118.

Prabakaran S., Swatton J. E., Ryan M. M., Huffaker S. J., Huang J. T.-J., Griffin J. L., Wayland M., et al. (2004) Mitochondrial dysfunction in schizophrenia: evidence for compromised brain metabolism and oxidative stress. *Mol. Psychiatry* **9**, 684–697, 643.

Purcell S. M., Moran J. L., Fromer M., Ruderfer D., Solovieff N., Roussos P., O'Dushlaine C., et al. (2014) A polygenic burden of rare disruptive mutations in schizophrenia. *Nature* **506**, 185–190.

Purves D., Augustine G. J., Fitzpatrick D., Katz L. C., LaMantia A.-S., McNamara J. O., Williams S. M. (2001) Glutamate Receptors.

Quansah E., Karikari T. K. (2016) Potential role of metabolomics in the improvement of research on traditional African medicine. *Phytochem. Lett.* **17**, 270–277.

Quist J. F., Kennedy J. L. (2001) Genetics of Childhood Disorders: XXIII. ADHD, Part 7: The Serotonin System. *J. Am. Acad. Child Adolesc. Psychiatry* **40**, 253–256.

Rabiner D. L. (2013) Stimulant prescription cautions: addressing misuse, diversion and malingering. *Curr. Psychiatry Rep.* **15**, 375.

Rae C., Digney A. L., McEwan S. R., Bates T. C. (2003) Oral creatine monohydrate supplementation improves brain performance: a double-blind, placebo-controlled, cross-over trial. *Proc. R. Soc. B Biol. Sci.* **270**, 2147–2150.

Rees M. I., Harvey K., Ward H., White J. H., Evans L., Duguid I. C., Hsu C. C.-H., et al. (2003) Isoform heterogeneity of the human gephyrin gene (GPHN), binding domains to the

glycine receptor, and mutation analysis in hyperekplexia. *J. Biol. Chem.* **278**, 24688–24696.
Réus G. Z., Scaini G., Jeremias G. C., Furlanetto C. B., Morais M. O. S., Mello-Santos L. M., Quevedo J., Streck E. L. (2014) Brain apoptosis signaling pathways are regulated by methylphenidate treatment in young and adult rats. *Brain Res.* **1583**, 269–276.
Réus G. Z., Scaini G., Titus S. E., Furlanetto C. B., Wessler L. B., Ferreira G. K., Gonçalves C. L., Jeremias G. C., Quevedo J., Streck E. L. (2015) Methylphenidate increases glucose uptake in the brain of young and adult rats. *Pharmacol. Rep. PR* **67**, 1033–1040.
Ribasés M., Bosch R., Hervás A., Ramos-Quiroga J. A., Sánchez-Mora C., Bielsa A., Gastaminza X., et al. (2009) Case-control study of six genes asymmetrically expressed in the two cerebral hemispheres: association of BAIAP2 with attention-deficit/hyperactivity disorder. *Biol. Psychiatry* **66**, 926–934.
Ricciardi L., Ricciardi D., Lena F., Plotnik M., Petracca M., Barricella S., Bentivoglio A. R., Modugno N., Bernabei R., Fasano A. (2015) Working on asymmetry in Parkinson's disease: randomized, controlled pilot study. *Neurol. Sci. Off. J. Ital. Neurol. Soc. Ital. Soc. Clin. Neurophysiol.*
Ripps H., Shen W. (2012) Review: taurine: a "very essential" amino acid. *Mol. Vis.* **18**, 2673–2686.
Robbins T. W., Arnsten A. F. T. (2009) The neuropsychopharmacology of fronto-executive function: monoaminergic modulation. *Annu. Rev. Neurosci.* **32**, 267–287.
Roberts T. F., Tschida K. A., Klein M. E., Mooney R. (2010) Rapid spine stabilization and synaptic enhancement at the onset of behavioural learning. *Nature* **463**, 948–952.
Robinson T. E., Kolb B. (2004) Structural plasticity associated with exposure to drugs of abuse. *Neuropharmacology* **47 Suppl 1**, 33–46.
Rodriguez A., Kaakinen M., Moilanen I., Taanila A., McGough J. J., Loo S., Järvelin M.-R. (2010) Mixed-handedness is linked to mental health problems in children and adolescents. *Pediatrics* **125**, e340-348.
Roessner V., Sagvolden T., Dasbanerjee T., Middleton F. A., Faraone S. V., Walaas S. I., Becker A., Rothenberger A., Bock N. (2010) Methylphenidate normalizes elevated dopamine transporter densities in an animal model of the attention-deficit/hyperactivity disorder combined type, but not to the same extent in one of the attention-deficit/hyperactivity disorder inattentive type. *Neuroscience* **167**, 1183–1191.
Rowley N. M., Madsen K. K., Schousboe A., Steve White H. (2012) Glutamate and GABA synthesis, release, transport and metabolism as targets for seizure control. *Neurochem. Int.* **61**, 546–558.
Rozas C., Carvallo C., Contreras D., Carreño M., Ugarte G., Delgado R., Zeise M. L., Morales B. (2015) Methylphenidate amplifies long-term potentiation in rat hippocampus CA1 area involving the insertion of AMPA receptors by activation of β-adrenergic and D1/D5 receptors. *Neuropharmacology* **99**, 15–27.
Rubia K., Overmeyer S., Taylor E., Brammer M., Williams S. C., Simmons A., Bullmore E. T. (1999) Hypofrontality in attention deficit hyperactivity disorder during higher-order motor control: a study with functional MRI. *Am. J. Psychiatry* **156**, 891–896.
Ruocco L. A., Gironi Carnevale U. A., Treno C., Sadile A. G., Melisi D., Arra C., Ibba M., Schirru C., Carboni E. (2010) Prepuberal subchronic methylphenidate and atomoxetine induce different long-term effects on adult behaviour and forebrain dopamine, norepinephrine and serotonin in Naples High-Excitability rats. *Behav. Brain Res.* **210**, 99–106.

Russell V. A., Oades R. D., Tannock R., Killeen P. R., Auerbach J. G., Johansen E. B., Sagvolden T. (2006) Response variability in Attention-Deficit/Hyperactivity Disorder: a neuronal and glial energetics hypothesis. *Behav. Brain Funct.* **2**, 30.

Russell V. A., Sagvolden T., Johansen E. B. (2005) Animal models of attention-deficit hyperactivity disorder. *Behav. Brain Funct. BBF* **1**, 9.

Russo S. J., Nestler E. J. (2013) The brain reward circuitry in mood disorders. *Nat. Rev. Neurosci.* **14**, 609–625.

Sagvolden T., Russell V. A., Aase H., Johansen E. B., Farshbaf M. (2005) Rodent models of attention-deficit/hyperactivity disorder. *Biol. Psychiatry* **57**, 1239–1247.

Sala C., Segal M. (2014) Dendritic spines: The locus of structural and functional plasticity. *Physiol. Rev.* **94**, 141–188.

Salimäki J., Scriba G., Piepponen T. P., Rautolahti N., Ahtee L. (2003) The effects of systemically administered taurine and N-pivaloyltaurine on striatal extracellular dopamine and taurine in freely moving rats. *Naunyn. Schmiedebergs Arch. Pharmacol.* **368**, 134–141.

Sandoval V., Riddle E. L., Hanson G. R., Fleckenstein A. E. (2002) Methylphenidate redistributes vesicular monoamine transporter-2: role of dopamine receptors. *J. Neurosci. Off. J. Soc. Neurosci.* **22**, 8705–8710.

Sano I., Gamo T., Kakimoto Y., Taniguchi K., Takesada M., Nishinuma K. (1959) Distribution of catechol compounds in human brain. *Biochim. Biophys. Acta* **32**, 586–587.

Saransaari P., Oja S. S. (2000) Taurine and neural cell damage. *Amino Acids* **19**, 509–526.

Sarowar T., Grabrucker A. M. (2016) Actin-Dependent Alterations of Dendritic Spine Morphology in Shankopathies. *Neural Plast.* **2016**.

Sarramea Crespo F., Luque R., Prieto D., Sau P., Albert C., Leal I., Luxan A. de, et al. (2008) Biochemical changes in the cingulum in patients with schizophrenia and chronic bipolar disorder. *Eur. Arch. Psychiatry Clin. Neurosci.* **258**, 394–401.

Sauve A. A. (2008) NAD+ and Vitamin B3: From Metabolism to Therapies. *J. Pharmacol. Exp. Ther.* **324**, 883–893.

Sawallisch C., Berhörster K., Disanza A., Mantoani S., Kintscher M., Stoenica L., Dityatev A., et al. (2009) The insulin receptor substrate of 53 kDa (IRSp53) limits hippocampal synaptic plasticity. *J. Biol. Chem.* **284**, 9225–9236.

Scaini G., Fagundes A. O., Rezin G. T., Gomes K. M., Zugno A. I., Quevedo J., Streck E. L. (2008) Methylphenidate increases creatine kinase activity in the brain of young and adult rats. *Life Sci.* **83**, 795–800.

Schaefer T. L., Ehrman L. A., Gudelsky G. A., Vorhees C. V., Williams M. T. (2006) Comparison of monoamine and corticosterone levels 24 h following (+)methamphetamine, (+/−)3,4-methylenedioxymethamphetamine, cocaine, (+)fenfluramine or (+/−)methylphenidate administration in the neonatal rat. *J. Neurochem.* **98**, 1369–1378.

Schiffer W. K., Volkow N. D., Fowler J. S., Alexoff D. L., Logan J., Dewey S. L. (2006) Therapeutic doses of amphetamine or methylphenidate differentially increase synaptic and extracellular dopamine. *Synap. N. Y. N* **59**, 243–251.

Schmahmann J. D., Caplan D. (2006) Cognition, emotion and the cerebellum. *Brain* **129**, 290–292.

Schmahmann J. D., Sherman J. C. (1998) The cerebellar cognitive affective syndrome. *Brain J. Neurol.* **121 (Pt 4)**, 561–579.

Schmitz F., Pierozan P., Rodrigues A. F., Biasibetti H., Coelho D. M., Mussulini B. H., Pereira M. S. L., et al. (2016) Chronic Treatment with a Clinically Relevant Dose of Methylphenidate Increases Glutamate Levels in Cerebrospinal Fluid and Impairs Glutamatergic Homeostasis in Prefrontal Cortex of Juvenile Rats. *Mol. Neurobiol.* **53**, 2384–2396.

Schrimsher G. W., Billingsley R. L., Jackson E. F., Moore B. D. (2002) Caudate nucleus volume asymmetry predicts attention-deficit hyperactivity disorder (ADHD) symptomatology in children. *J. Child Neurol.* **17**, 877–884.

Seeman P., Madras B. (2002) Methylphenidate elevates resting dopamine which lowers the impulse-triggered release of dopamine: a hypothesis. *Behav. Brain Res.* **130**, 79–83.

Seeman P., Madras B. K. (1998) Anti-hyperactivity medication: methylphenidate and amphetamine. *Mol. Psychiatry* **3**, 386–396.

Semrud-Clikeman M., Steingard R. J., Filipek P., Biederman J., Bekken K., Renshaw P. F. (2000) Using MRI to examine brain-behavior relationships in males with attention deficit disorder with hyperactivity. *J. Am. Acad. Child Adolesc. Psychiatry* **39**, 477–484.

Seneca N., Gulyás B., Varrone A., Schou M., Airaksinen A., Tauscher J., Vandenhende F., et al. (2006) Atomoxetine occupies the norepinephrine transporter in a dose-dependent fashion: a PET study in nonhuman primate brain using (S,S)-[18F]FMeNER-D2. *Psychopharmacology (Berl.)* **188**, 119–127.

Sgamma T., Pape J., Massiah A., Jackson S. (2016) Selection of reference genes for diurnal and developmental time-course real-time PCR expression analyses in lettuce. *Plant Methods* **12**.

Sharp T., Zetterström T., Ungerstedt U. (1986) An In Vivo Study of Dopamine Release and Metabolism in Rat Brain Regions Using Intracerebral Dialysis. *J. Neurochem.* **47**, 113–122.

Shaw G. A., Brown G. (1991) Laterality, Implicit Memory and Attention Disorder. *Educ. Stud.* **17**, 15–23.

Shaw P., Eckstrand K., Sharp W., Blumenthal J., Lerch J. P., Greenstein D., Clasen L., Evans A., Giedd J., Rapoport J. L. (2007) Attention-deficit/hyperactivity disorder is characterized by a delay in cortical maturation. *Proc. Natl. Acad. Sci. U. S. A.* **104**, 19649–19654.

Shaw P., Lalonde F., Lepage C., Rabin C., Eckstrand K., Sharp W., Greenstein D., Evans A., Giedd J. N., Rapoport J. (2009) Development of cortical asymmetry in typically developing children and its disruption in attention-deficit/hyperactivity disorder. *Arch. Gen. Psychiatry* **66**, 888–896.

Shen K. Z., Johnson S. W. (1997) A slow excitatory postsynaptic current mediated by G-protein-coupled metabotropic glutamate receptors in rat ventral tegmental dopamine neurons. *Eur. J. Neurosci.* **9**, 48–54.

Simchon Y., Weizman A., Rehavi M. (2010) The effect of chronic methylphenidate administration on presynaptic dopaminergic parameters in a rat model for ADHD. *Eur. Neuropsychopharmacol. J. Eur. Coll. Neuropsychopharmacol.* **20**, 714–720.

Singer B. F., Tanabe L. M., Gorny G., Jake-Matthews C., Li Y., Kolb B., Vezina P. (2009) Amphetamine-induced changes in dendritic morphology in rat forebrain correspond to associative drug conditioning rather than non-associative drug sensitization. *Biol. Psychiatry* **65**, 835–840.

Smith D., Pernet A., Hallett W. A., Bingham E., Marsden P. K., Amiel S. A. (2003) Lactate: A Preferred Fuel for Human Brain Metabolism In Vivo. *J. Cereb. Blood Flow Metab.* **23**, 658–664.

Smriga M., Kameishi M., Uneyama H., Torii K. (2002) Dietary L-lysine deficiency increases stress-induced anxiety and fecal excretion in rats. *J. Nutr.* **132**, 3744–3746.
Sokoloff P., Giros B., Martres M. P., Bouthenet M. L., Schwartz J. C. (1990) Molecular cloning and characterization of a novel dopamine receptor (D3) as a target for neuroleptics. *Nature* **347**, 146–151.
Solanto M. V. (1998) Neuropsychopharmacological mechanisms of stimulant drug action in attention-deficit hyperactivity disorder: A review and integration. *Behav. Brain Res.* **94**, 127–152.
Soliva J. C., Moreno A., Fauquet J., Bielsa A., Carmona S., Gispert J. D., Rovira M., Bulbena A., Vilarroya O. (2010) Cerebellar neurometabolite abnormalities in pediatric attention/deficit hyperactivity disorder: A proton MR spectroscopic study. *Neurosci. Lett.* **470**, 60–64.
Sonuga-Barke E. J. S., Brandeis D., Cortese S., Daley D., Ferrin M., Holtmann M., Stevenson J., et al. (2013) Nonpharmacological Interventions for ADHD: Systematic Review and Meta-Analyses of Randomized Controlled Trials of Dietary and Psychological Treatments. *Am. J. Psychiatry* **170**, 275–289.
Soria Fregozo C., Pérez Vega M. I. (2012) Actin-binding proteins and signalling pathways associated with the formation and maintenance of dendritic spines. *Neurol. Engl. Ed.* **27**, 421–431.
Spencer R. C., Devilbiss D. M., Berridge C. W. (2015) The cognition-enhancing effects of psychostimulants involve direct action in the prefrontal cortex. *Biol. Psychiatry* **77**, 940–950.
Spencer R. C., Klein R. M., Berridge C. W. (2012) Psychostimulants Act Within the Prefrontal Cortex to Improve Cognitive Function. *Biol. Psychiatry* **72**, 221–227.
Spencer T. J., Biederman J., Madras B. K., Dougherty D. D., Bonab A. A., Livni E., Meltzer P. C., Martin J., Rauch S., Fischman A. J. (2007) Further evidence of dopamine transporter dysregulation in ADHD: a controlled PET imaging study using altropane. *Biol. Psychiatry* **62**, 1059–1061.
Spencer T. J., Biederman J., Madras B. K., Faraone S. V., Dougherty D. D., Bonab A. A., Fischman A. J. (2005) In Vivo Neuroreceptor Imaging in Attention-Deficit/Hyperactivity Disorder: A Focus on The Dopamine Transporter. *Biol. Psychiatry* **57**, 1293–1300.
Spivak B., Vered Y., Yoran-Hegesh R., Averbuch E., Mester R., Graf E., Weizman A. (1999) Circulatory levels of catecholamines, serotonin and lipids in attention deficit hyperactivity disorder. *Acta Psychiatr. Scand.* **99**, 300–304.
Sprich S., Biederman J., Crawford M. H., Mundy E., Faraone S. V. (2000) Adoptive and Biological Families of Children and Adolescents With ADHD. *J. Am. Acad. Child Adolesc. Psychiatry* **39**, 1432–1437.
Squire L. R., Bloom F. E., Spitzer N. C., eds (2008) *Fundamental Neuroscience*. Academic Press.
Steele M., Jensen P. S., Quinn D. M. P. (2006) Remission versus response as the goal of therapy in ADHD: A new standard for the field? *Clin. Ther.* **28**, 1892–1908.
Stefanatos G. A., Wasserstein J. (2001) Attention deficit/hyperactivity disorder as a right hemisphere syndrome. Selective literature review and detailed neuropsychological case studies. *Ann. N. Y. Acad. Sci.* **931**, 172–195.
Steiner N. J., Sheldrick R. C., Gotthelf D., Perrin E. C. (2011) Computer-based attention training in the schools for children with attention deficit/hyperactivity disorder: a preliminary trial. *Clin. Pediatr. (Phila.)* **50**, 615–622.
Steinlin M. (2008) Cerebellar disorders in childhood: cognitive problems. *Cerebellum Lond. Engl.* **7**, 607–610.

Steward O., Farris S., Pirbhoy P. S., Darnell J., Driesche S. J. V. (2015) Localization and local translation of Arc/Arg3.1 mRNA at synapses: some observations and paradoxes. *Front. Mol. Neurosci.* **7**.

Stoodley C. J., Valera E. M., Schmahmann J. D. (2012) Functional topography of the cerebellum for motor and cognitive tasks: an fMRI study. *NeuroImage* **59**, 1560–1570.

Strick P. L., Dum R. P., Fiez J. A. (2009) Cerebellum and nonmotor function. *Annu. Rev. Neurosci.* **32**, 413–434.

Suárez L. M., Bustamante J., Orensanz L. M., Martín del Río R., Solís J. M. (2014) Cooperation of taurine uptake and dopamine D1 receptor activation facilitates the induction of protein synthesis-dependent late LTP. *Neuropharmacology* **79**, 101–111.

Sulzer D., Cragg S. J., Rice M. E. (2016) Striatal dopamine neurotransmission: regulation of release and uptake. *Basal Ganglia* **6**, 123–148.

Swanson J. M., Volkow N. D. (2003) Serum and brain concentrations of methylphenidate: implications for use and abuse. *Neurosci. Biobehav. Rev.* **27**, 615–621.

Tafazoli S., O'Neill J., Bejjani A., Ly R., Salamon N., McCracken J. T., Alger J. R., Levitt J. G. (2013) 1H MRSI of middle frontal gyrus in pediatric ADHD. *J. Psychiatr. Res.* **47**, 505–512.

Teter C. J., McCabe S. E., LaGrange K., Cranford J. A., Boyd C. J. (2006) Illicit use of specific prescription stimulants among college students: prevalence, motives, and routes of administration. *Pharmacotherapy* **26**, 1501–1510.

Thakur G. A., Sengupta S. M., Grizenko N., Choudhry Z., Joober R. (2012) Comprehensive Phenotype/Genotype Analyses of the Norepinephrine Transporter Gene (SLC6A2) in ADHD: Relation to Maternal Smoking during Pregnancy. *PLOS ONE* **7**, e49616.

Thoma P., Soria Bauser D., Norra C., Brüne M., Juckel G., Suchan B. (2014) Do you see what I feel?--Electrophysiological correlates of emotional face and body perception in schizophrenia. *Clin. Neurophysiol. Off. J. Int. Fed. Clin. Neurophysiol.* **125**, 1152–1163.

Todd R. D., Botteron K. N. (2001) Is attention-deficit/hyperactivity disorder an energy deficiency syndrome? *Biol. Psychiatry* **50**, 151–158.

Todd R. D., Lobos E. A., Sun L.-W., Neuman R. J. (2003) Mutational analysis of the nicotinic acetylcholine receptor alpha 4 subunit gene in attention deficit/hyperactivity disorder: evidence for association of an intronic polymorphism with attention problems. *Mol. Psychiatry* **8**, 103–108.

Toga A. W., Thompson P. M. (2003) Mapping brain asymmetry. *Nat. Rev. Neurosci.* **4**, 37–48.

Toma C., Hervás A., Balmaña N., Vilella E., Aguilera F., Cuscó I., Campo M. del, et al. (2011) Association study of six candidate genes asymmetrically expressed in the two cerebral hemispheres suggests the involvement of BAIAP2 in autism. *J. Psychiatr. Res.* **45**, 280–282.

Tran A. H., Tamura R., Uwano T., Kobayashi T., Katsuki M., Ono T. (2005) Dopamine D1 receptors involved in locomotor activity and accumbens neural responses to prediction of reward associated with place. *Proc. Natl. Acad. Sci. U. S. A.* **102**, 2117–2122.

Tsang T. M., Huang J. T.-J., Holmes E., Bahn S. (2006) Metabolic profiling of plasma from discordant schizophrenia twins: correlation between lipid signals and global functioning in female schizophrenia patients. *J. Proteome Res.* **5**, 756–760.

Tzingounis A. V., Nicoll R. A. (2006) Arc/Arg3.1: linking gene expression to synaptic plasticity and memory. *Neuron* **52**, 403–407.

Ungerstedt U., Herrera-Marchintz M., Jungnelius U., Stahle L., Tossman U., Zetterström T. (1982) *Dopamine synaptic mechanisms reflected in studies combining behavioral*

recordings and brain dialysis, In: Kotisaka M, Editor. Advances in Dopamine Research. Pergamon Press; Elmsford, N.Y.

Vaidya C. J., Bunge S. A., Dudukovic N. M., Zalecki C. A., Elliott G. R., Gabrieli J. D. E. (2005) Altered neural substrates of cognitive control in childhood ADHD: evidence from functional magnetic resonance imaging. *Am. J. Psychiatry* **162**, 1605–1613.

Valera E. M., Faraone S. V., Murray K. E., Seidman L. J. (2007) Meta-analysis of structural imaging findings in attention-deficit/hyperactivity disorder. *Biol. Psychiatry* **61**, 1361–1369.

Vance A., Silk T. J., Casey M., Rinehart N. J., Bradshaw J. L., Bellgrove M. A., Cunnington R. (2007) Right parietal dysfunction in children with attention deficit hyperactivity disorder, combined type: a functional MRI study. *Mol. Psychiatry* **12**, 826–832, 793.

VanGuilder H. D., Vrana K. E., Freeman W. M. (2008) Twenty-five years of quantitative PCR for gene expression analysis. *BioTechniques* **44**, 619–626.

Vles J. S. H., Feron F. J. M., Hendriksen J. G. M., Jolles J., Kroonenburgh M. J. P. G. van, Weber W. E. J. (2003) Methylphenidate down-regulates the dopamine receptor and transporter system in children with attention deficit hyperkinetic disorder (ADHD). *Neuropediatrics* **34**, 77–80.

Voeller K. K., Heilman K. M. (1988) Attention deficit disorder in children: a neglect syndrome? *Neurology* **38**, 806–808.

Vogel C., Marcotte E. M. (2012) Insights into the regulation of protein abundance from proteomic and transcriptomic analyses. *Nat. Rev. Genet.* **13**, 227–232.

Volkow N. D. (2006) Stimulant medications: how to minimize their reinforcing effects? *Am. J. Psychiatry* **163**, 359–361.

Volkow N. D., Fowler J. S., Wang G.-J., Telang F., Logan J., Wong C., Ma J., Pradhan K., Benveniste H., Swanson J. M. (2008) Methylphenidate Decreased the Amount of Glucose Needed by the Brain to Perform a Cognitive Task. *PLoS ONE* **3**, e2017.

Volkow N. D., Wang G., Fowler J. S., Logan J., Gerasimov M., Maynard L., Ding Y., Gatley S. J., Gifford A., Franceschi D. (2001) Therapeutic doses of oral methylphenidate significantly increase extracellular dopamine in the human brain. *J. Neurosci. Off. J. Soc. Neurosci.* **21**, RC121.

Volkow N. D., Wang G. J., Fowler J. S., Gatley S. J., Logan J., Ding Y. S., Hitzemann R., Pappas N. (1998) Dopamine transporter occupancies in the human brain induced by therapeutic doses of oral methylphenidate. *Am. J. Psychiatry* **155**, 1325–1331.

Volkow N. D., Wang G. J., Fowler J. S., Logan J., Angrist B., Hitzemann R., Lieberman J., Pappas N. (1997) Effects of methylphenidate on regional brain glucose metabolism in humans: relationship to dopamine D2 receptors. *Am. J. Psychiatry* **154**, 50–55.

Volkow N. D., Wang G.-J., Fowler J. S., Ding Y.-S. (2005) Imaging the effects of methylphenidate on brain dopamine: new model on its therapeutic actions for attention-deficit/hyperactivity disorder. *Biol. Psychiatry* **57**, 1410–1415.

Volkow N. D., Wang G.-J., Kollins S. H., Wigal T. L., Newcorn J. H., Telang F., Fowler J. S., et al. (2009) Evaluating Dopamine Reward Pathway in ADHD. *JAMA J. Am. Med. Assoc.* **302**, 1084–1091.

Volkow N. D., Wang G.-J., Newcorn J., Fowler J. S., Telang F., Solanto M. V., Logan J., et al. (2007a) Brain dopamine transporter levels in treatment and drug naïve adults with ADHD. *NeuroImage* **34**, 1182–1190.

Volkow N. D., Wang G.-J., Newcorn J., Telang F., Solanto M. V., Fowler J. S., Logan J., et al. (2007b) Depressed dopamine activity in caudate and preliminary evidence of limbic

involvement in adults with attention-deficit/hyperactivity disorder. *Arch. Gen. Psychiatry* **64**, 932–940.
Wagner A., Drewencki L., Chen X., Santos F., Khan A., Harun R., Torres G., Michael A., Dixon C. (2009) Chronic Methylphenidate Treatment Enhances Striatal Dopamine Neurotransmission After Experimental Traumatic Brain Injury. *J. Neurochem.* **108**, 986–997.
Wahlström D., White T., Luciana M. (2010) Neurobehavioral evidence for changes in dopamine system activity during adolescence. *Neurosci. Biobehav. Rev.* **34**, 631–648.
Waldie K. E., Hausmann M. (2010) Right fronto-parietal dysfunction in children with ADHD and developmental dyslexia as determined by line bisection judgements. *Neuropsychologia* **48**, 3650–3656.
Wallace J., Jackson R. K., Shotton T. L., Munjal I., McQuade R., Gartside S. E. (2014) Characterization of electrically evoked field potentials in the medial prefrontal cortex and orbitofrontal cortex of the rat: Modulation by monoamines. *Eur. Neuropsychopharmacol.* **24**, 321–332.
Wang G.-J., Volkow N. D., Wigal T., Kollins S. H., Newcorn J. H., Telang F., Logan J., et al. (2013) Long-Term Stimulant Treatment Affects Brain Dopamine Transporter Level in Patients with Attention Deficit Hyperactive Disorder. *PLoS ONE* **8**.
Wang J., Yang Q. X., Sun X., Vesek J., Mosher Z., Vasavada M., Chu J., et al. (2015) MRI evaluation of asymmetry of nigrostriatal damage in the early stage of early-onset Parkinson's disease. *Parkinsonism Relat. Disord.* **21**, 590–596.
Wang Y., Xu R., Sasaoka T., Tonegawa S., Kung M. P., Sankoorikal E. B. (2000) Dopamine D2 long receptor-deficient mice display alterations in striatum-dependent functions. *J. Neurosci. Off. J. Soc. Neurosci.* **20**, 8305–8314.
Waniewski R. A., Martin D. L. (1998) Preferential utilization of acetate by astrocytes is attributable to transport. *J. Neurosci. Off. J. Soc. Neurosci.* **18**, 5225–5233.
Warrer P., Thomsen P. H., Dalsgaard S., Hansen E. H., Aagaard L., Wallach Kildemoes H., Rasmussen H. B. (2016) Switch in Therapy from Methylphenidate to Atomoxetine in Children and Adolescents with Attention-Deficit/Hyperactivity Disorder: An Analysis of Patient Records. *J. Child Adolesc. Psychopharmacol.*
Waters N. J., Holmes E., Waterfield C. J., Farrant R. D., Nicholson J. K. (2002) NMR and pattern recognition studies on liver extracts and intact livers from rats treated with α-naphthylisothiocyanate. *Biochem. Pharmacol.* **64**, 67–77.
Westerink B. H. (1985) Sequence and significance of dopamine metabolism in the rat brain. *Neurochem. Int.* **7**, 221–227.
White F. J., Bednarz L. M., Wachtel S. R., Hjorth S., Brooderson R. J. (1988) Is stimulation of both D1 and D2 receptors necessary for the expression of dopamine-mediated behaviors? *Pharmacol. Biochem. Behav.* **30**, 189–193.
Wiguna T., Guerrero A. P. S., Wibisono S., Sastroasmoro S. (2012) Effect of 12-week administration of 20-mg long-acting methylphenidate on Glu/Cr, NAA/Cr, Cho/Cr, and mI/Cr ratios in the prefrontal cortices of school-age children in Indonesia: A study using 1H Magnetic Resonance Spectroscopy (MRS). *Clin. Neuropharmacol.* **35**, 81–85.
Wilens T. E. (2008) Effects of methylphenidate on the catecholaminergic system in attention-deficit/hyperactivity disorder. *J. Clin. Psychopharmacol.* **28**, S46–S53.
Wilens T. E., Biederman J., Lerner M., Concerta Study Group (2004) Effects of once-daily osmotic-release methylphenidate on blood pressure and heart rate in children with

attention-deficit/hyperactivity disorder: results from a one-year follow-up study. *J. Clin. Psychopharmacol.* **24**, 36–41.
Williams M. A., Li C., Kash T. L., Matthews R. T., Winder D. G. (2014) Excitatory drive onto dopaminergic neurons in the rostral linear nucleus is enhanced by norepinephrine in an α1 adrenergic receptor-dependent manner. *Neuropharmacology* **86**, 116–124.
Wingo A. P., Ghaemi S. N. (2008) Frequency of stimulant treatment and of stimulant-associated mania/hypomania in bipolar disorder patients. *Psychopharmacol. Bull.* **41**, 37–47.
Wise R. A. (2004) Dopamine, learning and motivation. *Nat. Rev. Neurosci.* **5**, 483–494.
Wishart D. S., Jewison T., Guo A. C., Wilson M., Knox C., Liu Y., Djoumbou Y., et al. (2013) HMDB 3.0—The Human Metabolome Database in 2013. *Nucleic Acids Res.* **41**, D801–D807.
Wolf M. E., Roth R. H. (1990) Autoreceptor regulation of dopamine synthesis. *Ann. N. Y. Acad. Sci.* **604**, 323–343.
Woods S. K., Meyer J. S. (1991) Exogenous tyrosine potentiates the methylphenidate-induced increase in extracellular dopamine in the nucleus accumbens: a microdialysis study. *Brain Res.* **560**, 97–105.
Worley B., Powers R. (2013) Multivariate Analysis in Metabolomics. *Curr. Metabolomics* **1**, 92–107.
Xia J., Mandal R., Sinelnikov I. V., Broadhurst D., Wishart D. S. (2012) MetaboAnalyst 2.0—a comprehensive server for metabolomic data analysis. *Nucleic Acids Res.* **40**, W127–W133.
Xia J., Sinelnikov I. V., Han B., Wishart D. S. (2015) MetaboAnalyst 3.0--making metabolomics more meaningful. *Nucleic Acids Res.* **43**, W251-257.
Xing B., Li Y.-C., Gao W.-J. (2016) Norepinephrine versus dopamine and their interaction in modulating synaptic function in the prefrontal cortex. *Brain Res.* **1641**, **Part B**, 217–233.
Xu T., Yu X., Perlik A. J., Tobin W. F., Zweig J. A., Tennant K., Jones T., Zuo Y. (2009) Rapid formation and selective stabilization of synapses for enduring motor memories. *Nature* **462**, 915–919.
Yamagishi A., Masuda M., Ohki T., Onishi H., Mochizuki N. (2004) A novel actin bundling/filopodium-forming domain conserved in insulin receptor tyrosine kinase substrate p53 and missing in metastasis protein. *J. Biol. Chem.* **279**, 14929–14936.
Yamamoto M., Hatta T. (1982) Handedness and imbalance lateralization on the tapping test in MBD children. *Int. J. Neurosci.* **17**, 215–218.
Yang J., Ruchti E., Petit J.-M., Jourdain P., Grenningloh G., Allaman I., Magistretti P. J. (2014) Lactate promotes plasticity gene expression by potentiating NMDA signaling in neurons. *Proc. Natl. Acad. Sci. U. S. A.* **111**, 12228–12233.
Yang L., Qian Q., Liu L., Li H., Faraone S. V., Wang Y. (2013) Adrenergic neurotransmitter system transporter and receptor genes associated with atomoxetine response in attention-deficit hyperactivity disorder children. *J. Neural Transm. Vienna Austria 1996* **120**, 1127–1133.
Yang P., Wu M.-T., Dung S.-S., Ko C.-W. (2010) Short-TE proton magnetic resonance spectroscopy investigation in adolescents with attention-deficit hyperactivity disorder. *Psychiatry Res. Neuroimaging* **181**, 199–203.
Yano M., Steiner H. (2007) Methylphenidate and cocaine: the same effects on gene regulation? *Trends Pharmacol. Sci.* **28**, 588–596.

Yao F. S., Caserta M. T., Wyrwicz A. M. (1999) In vitro proton and phosphorus NMR spectroscopic analysis of murine (C57Bl/6J) brain development. *NMR Biomed.* **12**, 463–470.

Yeh T. C., Ogawa W., Danielsen A. G., Roth R. A. (1996) Characterization and Cloning of a 58/53-kDa Substrate of the Insulin Receptor Tyrosine Kinase. *J. Biol. Chem.* **271**, 2921–2928.

Zahniser N. R., Sorkin A. (2004) Rapid regulation of the dopamine transporter: role in stimulant addiction? *Neuropharmacology* **47**, **Supplement 1**, 80–91.

Zetterström T., Sharp T., Collin A. K., Ungerstedt U. (1988) In vivo measurement of extracellular dopamine and DOPAC in rat striatum after various dopamine-releasing drugs implications for the origin of extracellular DOPAC. *Eur. J. Pharmacol.* **148**, 327–334.

Zhang X., Newport G. D., Callicott R., Liu S., Thompson J., Berridge M. S., Apana S. M., Slikker Jr. W., Wang C., Paule M. G. (2016) MicroPET/CT assessment of FDG uptake in brain after long-term methylphenidate treatment in nonhuman primates. *Neurotoxicol. Teratol.* **56**, 68–74.

Zhu J., Spencer T. J., Liu-Chen L.-Y., Biederman J., Bhide P. G. (2011) Methylphenidate and μ opioid receptor interactions: A pharmacological target for prevention of stimulant abuse. *Neuropharmacology* **61**, 283–292.